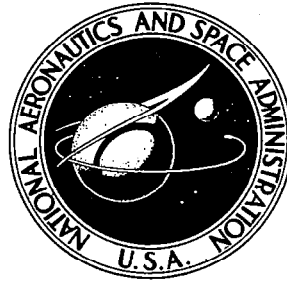


**NASA CONTRACTOR
REPORT**



NASA CR

C.1

0060108

TECH LIBRARY KAFB, NM

NASA CR-742

KIRTLAND

DAMPING OF STRUCTURAL COMPOSITES WITH VISCOELASTIC SHEAR-DAMPING MECHANISMS

*by Jerome E. Ruzicka, Thomas F. Derby, Dale W. Schubert,
and Jerome S. Pepi*

Prepared by

BARRY WRIGHT CORPORATION

Watertown, Mass.

for Langley Research Center

NATIONAL AERONAUTICS AND SPACE ADMINISTRATION • WASHINGTON, D. C. • MARCH 1967



0060108

NASA CR-'42

DAMPING OF STRUCTURAL COMPOSITES WITH VISCOELASTIC
SHEAR-DAMPING MECHANISMS

By Jerome E. Ruzicka, Thomas F. Derby,
Dale W. Schubert, and Jerome S. Pepi

Distribution of this report is provided in the interest of
information exchange. Responsibility for the contents
resides in the author or organization that prepared it.

Prepared under Contract No. NAS 1-5640 by
BARRY WRIGHT CORPORATION
Watertown, Mass.

for Langley Research Center

NATIONAL AERONAUTICS AND SPACE ADMINISTRATION

For sale by the Clearinghouse for Federal Scientific and Technical Information
Springfield, Virginia 22151 - CFSTI price \$3.00

DAMPING OF STRUCTURAL COMPOSITES
WITH VISCOELASTIC SHEAR-DAMPING MECHANISMS

By Jerome E. Ruzicka, Thomas F. Derby,
Dale W. Schubert and Jerome S. Pepi

ABSTRACT

An investigation is conducted to evaluate the so-called geometrical parameter of structural composites with viscoelastic shear-damping mechanisms. Design equations and graphs are developed for the geometrical parameter of a wide range of viscoelastic shear-damped structural composite designs. Using existing theory, manual and automated procedures are developed for the prediction of the structure loss factor of structural composites comprised of two elastic elements separated by a thin viscoelastic damping layer. Laboratory experiments are performed to verify the basic theory and design procedures developed. A comparison of theoretical predictions and experimental measurements of the structure loss factor is made for two-elastic-element structural composites fabricated from various combinations of structural materials including aluminum, steel and fibre-glass.

CONTENTS

	Page
SUMMARY	1
SECTION 1: INTRODUCTION	2
SECTION 2: ANALYSIS AND DESIGN DATA FOR GEOMETRICAL PARAMETER	7
Geometrical Parameter Analyses	8
Two-elastic-element structural composites	9
Three-elastic-element structural composites	10
Cell-insert structural composites	11
Orthogonally symmetric cross-sections	12
Effect of symmetrical sheathing addition	13
Formulation of Design Parameters	14
Effect of viscoelastic damping layer thickness	15
Equivalent modulus concept	18
Geometrical Parameter Design Data	22
Laminated structural sheets	22
Constrained honeycomb sheets	24
Laminated honeycomb sheets	25
Box-beam and I-beam constructions	25
Structural bar designs	26
Structural tube designs	28
Structural shape beams	30
Dumbbell model	31
Geometrical Parameter Design Considerations	31
SECTION 3: DESIGN OF TWO-ELASTIC-ELEMENT STRUCTURAL COMPOSITES	34
Fundamental Equations for Damping Parameters	34
Basic assumptions of theory	36
Typical structural composite designs	36
Development of Design Equations and Graphs	37
Coupling parameter Z	38
Resonant frequency ratio f_r/f_o	39
Shear parameter X	40
Generalized shear parameter equation	41
Optimum shear parameter X_{op}	41
Maximum structure loss factor η_{max}	42
Loss factor ratio η/η_{max}	42
Optimum frequency parameter Ω_{op}	43
Manual Design Procedure	44
Automated Design Procedure	48
Temperature Effects	49
Other Design Considerations	50
Static stiffness	50
Weight	51
Static load distribution	52

	Page
SECTION 4: EXPERIMENTAL VERIFICATION OF DESIGN PROCEDURE FOR TWO-ELASTIC-ELEMENT STRUCTURAL COMPOSITES	53
Design Procedure Application Example	53
Measurement of Structure Loss Factor	58
Theoretical and Experimental Structure Loss Factor Data	61
Sources of errors	62
Statistical analysis of experimental data	64
CONCLUSIONS	66
REFERENCES	68
FIGURES	70-176

DAMPING OF STRUCTURAL COMPOSITES WITH VISCOELASTIC SHEAR-DAMPING MECHANISMS

By Jerome E. Ruzicka, Thomas F. Derby,
Dale W. Schubert and Jerome S. Pepi

Barry Controls
Division of Barry Wright Corporation
Watertown, Massachusetts

SUMMARY

An investigation of parameters important in the design of structural composites with viscoelastic shear-damping mechanisms has been conducted. Design equations and graphs are developed for the so-called geometrical parameter of a wide range of viscoelastic shear-damped structural composites, which include: laminated beams and plates (comprised of solid and/or honeycomb structural sheets), box-beam constructions, bars of various cross-sections, square and circular tubes, structural shape beams including angle, channel, T- and I-sections, and a dumbbell model (which frequently provides a simplified representation of a more complex structural assembly).

Using existing theory, manual and automated design procedures for the prediction of structure loss factor are developed for viscoelastic shear-damped structural composites comprised of two elastic elements separated by a thin viscoelastic damping layer. The design procedures which apply for any cross-section geometry and arbitrary structural and viscoelastic material properties, are used to predict the damping characteristics of a wide range of two-elastic-element structural composite beams employed in an experimental verification program. As a design example, the details of the numerical calculations for a typical structural composite beam are presented.

Laboratory experiments have been performed to verify the theoretical predictions and to provide insight into practical design considerations. A comparison of theoretical predictions and experimental measurements of the structure loss factor is made for two-elastic-element structural composites fabricated from various combinations of structural materials including aluminum, steel and fibre-glass. Structural specimens include laminated beams comprised of solid sheets, solid and honeycomb sheets, honeycomb sheets, and structural channels. A total of 118 loss factor measurements were made for various free-free bending modes of 27 different beam specimens. A statistical analysis of this data compared to the theoretical values of loss factor indicated that the difference had a mean value of 0.6 per cent and a standard deviation of approximately 30 per cent. Consequently, it is concluded that the existing theory and the procedures developed for the prediction of the loss factor of two-elastic element viscoelastic shear-damped structural composites is satisfactory within accepted engineering accuracy.

SECTION 1: INTRODUCTION

The damping properties of structural fabrications can be considerably enhanced by the incorporation of viscoelastic shear-damping mechanisms in structural members and joints [Ref. 1]. Special design configurations incorporating distributed viscoelastic shear-damping mechanisms have been devised which consist of a combination of elastic beam or plate elements separated by layers of a viscoelastic damping material [Ref. 2-8]. The elastic elements are made from common structural materials and the damping materials are generally polymers exhibiting high loss factors and relatively low values of stiffness. When structural composites with constrained viscoelastic layers undergo flexural vibrations, the layers of viscoelastic damping material are subjected to cyclic shear strains, which cause energy of mechanical motion to be converted into thermal energy. Because of this energy conversion process, viscoelastic shear-damped structural composites are capable of exhibiting extremely high degrees of damping.

Techniques for fabricating structural composites with viscoelastic shear-damping mechanisms include the use of adhesively bonded intermediate damping layers and self-bonding adhesive damping layers [Ref. 2]. The structural composites with adhesively bonded damping layers offer the advantage of being able to provide any thickness of viscoelastic damping material in the structural composite, since the damping layer can be produced in sheet form to the desired thickness prior to bonding between the elastic structural elements. The thickness of the self-bonding adhesive viscoelastic damping layer is limited; however, its use offers an advantage with regard to the relative simplicity of production and workability of the composite structure.

Early investigations of distributed viscoelastic shear-damping mechanisms were concerned with the damping effectiveness of a viscoelastic damping layer constrained between two structural sheets, where one sheet was very thin relative to the other [Ref. 3]. This damped structural configuration was intended to represent the application of a damping tape (consisting of a thin metal foil with adhesive backing) to a structural beam requiring

additional damping. An evaluation was also made of the damping performance obtained by the application of a multiplicity of damping tapes to a structural beam [Ref. 4].

It was found that multiple damping tapes offered no significant improvement in damping at high frequencies (greater than 1000Hz), but provided a substantial increase in damping for lower frequencies. Furthermore, the damping provided by multiple damping tapes was essentially equal to that of a single damping tape having a foil thickness which equals the sum of the foil thicknesses of the multiple damping tape treatment and a viscoelastic damping layer thickness equal to that of only one of the multiple damping tapes. The same maximum degree of damping was obtained whether the damping tapes were applied to one or both sides of the structural beam being damped; however, the frequency at which the maximum damping occurred differed for these two cases. These analyses applied for the case where the total foil thickness is considerably less than the structural beam thickness. Experiments indicated that the measured and theoretically predicted damping were in reasonably good agreement, with values of the structure loss factor being generally less than 0.05 for practical damping tape treatments.

An analysis was subsequently performed to predict the damping properties of structural composites incorporating distributed viscoelastic shear-damping mechanisms for the case where the structural composites consisted of two elastic elements of arbitrary material and size with an intervening viscoelastic damping layer [Ref. 5, 6]. For geometrical configurations incorporating a thin layer of viscoelastic damping material that is soft compared to the stiffness of structural materials employed in the structural composite, the structure loss factor η may be expressed in terms of three parameters, as follows:

$$\eta = \eta(\beta, X, Y) \quad (1)$$

where β is the loss factor of the viscoelastic shear-damping material, X is defined as the shear parameter, and Y is defined as the geometrical parameter.

The damping material loss factor β is the ratio of the imaginary and real components of the complex shear modulus $G^* = G' + jG''$, as follows:

$$\beta = G''/G' \quad (2)$$

where G'' and G' are the loss modulus and storage modulus of the viscoelastic material, respectively. The shear parameter X depends on the storage modulus and amount of viscoelastic material employed, the weight loading on the structural member, the flexural rigidity, the geometry of the cross-section, and the frequency of vibration. The geometrical parameter Y , which is a function only of the geometry of the cross-section and the modulus of elasticity of the elastic elements comprising the structural composite, may be expressed mathematically as follows [Ref. 5, 7, 8]:

$$Y = \frac{(EI)_{\infty}}{(EI)_0} - 1 \quad (3)$$

where $(EI)_0$ is the flexural rigidity of the structural composite when its elastic members are uncoupled and $(EI)_{\infty}$ is the flexural rigidity of the structural composite when its elastic members are completely coupled.

Theoretical and experimental evidence indicates that high values of the geometrical parameter are required for a structural composite to exhibit a high degree of damping. Based on (1) the theory of viscoelastically damped beams with two elastic elements [Ref. 5], (2) the application of a lumped parameter model as a simplified representation of a viscoelastic shear-damped structural composite [Ref. 7], and (3) experimental data acquired on various structural composites [Ref. 8], it is concluded that the geometrical parameter Y is a fundamental design parameter which plays a significant role in the performance of all structural composite designs which incorporate viscoelastic shear-damping mechanisms. Consequently even if the equivalent of the shear parameter X is not defined for a more complex structural composite, the value of the geometrical parameter in itself provides a guide for arriving at a suitable design, especially when this information is coupled with previous practical experience of designing and evaluating viscoelastic shear-damped structural composites.

In general, the problem of designing structural composites with viscoelastic shear-damping mechanisms involves the selection of a viscoelastic damping material having a high loss factor β and arranging the cross-section geometry of the elastic elements to produce a high value of the geometrical parameter Y . Maximization of damping at a specified frequency or temperature, however, will require the optimization of the shear parameter X for two-elastic-element structural composites or an equivalent parameter for more complex structural composite designs. Alternately, subsequent to the selection of a viscoelastic damping material having a high value of loss factor β and the determination of the geometrical parameter Y , a trial and error procedure can be employed to arrive at a damping material thickness which provides the degree of damping required in the frequency and temperature ranges of interest. Naturally, other design considerations such as static stiffness, weight, stress, structure resonant frequency, and size, enter into the design process and must be evaluated with structural damping as joint design criteria. For most practical structural designs, it is generally desirable for the geometrical parameter Y to have a value between 0.5 and 5.

The present investigation is concerned with the development of data useful in the design of viscoelastic shear-damped structural composites and the experimental verification of theoretical predictions of structure loss factor. Specifically, the investigation encompasses the following studies:

- (1) Mathematical analysis of the geometrical parameter Y for a wide range of viscoelastic shear-damped structural composite designs.
- (2) Development of simplified procedures for predicting the loss factor of viscoelastic shear-damped structural composites comprised of two elastic elements.
- (3) Performance of laboratory experiments on two-elastic-element viscoelastic shear-damped beams to evaluate the adequacy of the existing theory and design procedures developed.

These three studies are discussed, respectively, in the following sections of this report. Particular emphasis has been placed on design configurations

which have potential application in air-borne and aerospace structural assemblies. Furthermore, analyses and experiments have been limited to structural composite designs which incorporate thin layers of relatively soft viscoelastic damping material; consequently, the results of the studies are particularly applicable to structural composites which incorporate self-bonding adhesive damping layers as a distributed shear-damping mechanism.

SECTION 2: ANALYSIS AND DESIGN DATA FOR GEOMETRICAL PARAMETER

This section of the report presents various mathematical methods by which the geometrical parameter of viscoelastic shear-damped structural composites may be analyzed. These analyses are employed to develop design equations and graphs for the geometrical parameter of a wide variety of structural composite designs including: laminated beams and plates (comprised of solid and/or honeycomb structural sheets), box-beam constructions, bars of various cross-sections, square and circular tubes, structural shape beams (angle, channel, T- and I-sections), and a dumbbell model. Cross-sections of these structural composite designs are presented in Figures 2.1 to 2.8. In evaluating the geometrical parameter of these structural composite designs, the viscoelastic damping layer thickness and the number, modulus, and size of elastic elements are kept arbitrary whenever possible. In some cases, however, it is necessary to impose some restrictions to allow the development of useful graphical design data.

Cross-sections of damped structural plates are presented in Figures 2.1 to 2.4. The plate designs shown in Figure 2.1 consist of laminated solid sheets, whereas the designs shown in Figures 2.2 and 2.3 consist of honeycomb sheets constrained by solid sheets, and laminated honeycomb sheets, respectively. The plate designs shown in Figure 2.4 consist of box-beam or I-beam constructions constrained symmetrically by solid sheets.

Cross-sections of damped structural bars are presented in Figure 2.5. The designs may be employed to produce square and round cross-section bars, as well as bars having cross-sections intermediate to these shapes. Cross-sections of damped tubes, both square and round, are presented in Figure 2.6.

Cross-sections of damped structural shape beams are presented in Figures 2.7 and 2.8. Shown in Figure 2.7 are designs for damped angle, channel, and T- and I-sections. The dumbbell model shown in Figure 2.8 may be employed as a simple representation of more complex structural

assemblies and is frequently useful in obtaining a first-order approximation of the mechanical characteristics of structural members such as box-beam and truss constructions.

Cross-sections of other viscoelastic shear-damped structural composites, which are of a more complicated nature, are presented in Figures 2.9 and 2.10. Figure 2.9 shows structural beams of multilaminate construction; Figure 2.10 shows structural beams of cell-insert construction [Ref. 7]. Since these structural configurations involve too many parameters to develop specific design data, more generalized equations for the geometrical parameter must be employed for design purposes.

Geometrical Parameter Analyses

The fundamental equation for the geometrical parameter stated by Equation (3) can be written in the following equivalent form:

$$Y = \frac{(EI)_{\infty}}{(EI)_o} - 1 = \frac{(EI)_t}{(EI)_o} \quad (4)$$

where $(EI)_o$ and $(EI)_{\infty}$ represent the uncoupled and coupled flexural rigidities, respectively, and $(EI)_t = (EI)_{\infty} - (EI)_o$ is the transfer flexural rigidity for the composite structure.

The uncoupled condition corresponds to that wherein the elastic elements of the structural composite experience the same flexural deformations but act independent of each other with regard to their resistance to bending. Consequently, for the case where the viscoelastic shear-damping material is soft compared to the stiffness of the elastic elements used in the structural composite, the uncoupled flexural rigidity $(EI)_o$ represents the "static" flexural rigidity (corresponding to the flexural stiffness exhibited for static loading), which is equal to the sum of the flexural rigidities of each elastic element about its own neutral axis. The coupled condition corresponds to that wherein the elastic and viscoelastic elements experience the same flexural deformations and act as a single unit with regard to resistance to bending. The coupled flexural rigidity $(EI)_{\infty}$, therefore, corresponds to the sum of the flexural rigidities of each elastic element about the composite neutral axis.

The relationships for geometrical parameter expressed by Equation (4) can be applied to calculate the geometrical parameter of any continuous composite structure by determining the location of the neutral axes and the flexural rigidities applicable for the uncoupled and coupled conditions. The neutral axes for the uncoupled condition are those axes passing through the center of the area elements comprising the structural composite. The composite neutral axis for the coupled condition is defined as that axis about which the total moment of the extensional stiffnesses EA is zero. Defining $\bar{\delta}$ as the distance between the composite neutral axis and an arbitrary reference axis, the location of the composite neutral axis is specified by

$$\bar{\delta} = \frac{\sum E_i A_i \delta_i}{\sum E_i A_i} \quad (5)$$

where δ_i is the distance from the center of area A_i to the reference axis.

Certain simplifications can be made when restrictions are placed on the geometry of the structural composite; three specific geometrical configurations in this category which are of considerable practical importance are structural composites consisting of two elastic elements, three elastic elements, and cell-insert constructions. Other practical configurations which result in design simplifications include orthogonally symmetric cross-sections and sheathing additions to cross-sections having an axis of symmetry. Discussions of these special cases follow.

Two-elastic-element structural composites. - In using Equation (3) to determine the geometrical parameter of two-elastic-element structural composites, it is necessary to determine the location of the composite neutral axis as defined by Equation (5) in order to evaluate $(EI)_{\infty}$; this frequently results in a laborious analysis. By selecting the composite neutral axis as the arbitrary reference axis for taking the extensional stiffness moment, an equation for geometrical parameter can be developed for two-elastic-element structural composites which does not require knowledge of the location of the composite neutral axis. In this case, the geometrical parameter is given by

$$Y = \frac{M A_1 A_2 d^2}{(M A_1 + A_2) (M I_1 + I_2)} \quad (6)$$

where $M = E_1/E_2$ is the modulus ratio, A_1 and A_2 are the cross-section areas of the two elastic elements, I_1 and I_2 are the moments of inertia of the two areas, and d is the distance between the neutral axes of the two elastic elements. The requirement of determining the location of the composite neutral axis is replaced by that of determining the distance between the neutral axes of the two elastic elements. This determination is relatively easy to make thereby simplifying the analysis of structural composites comprised of two elastic elements.

Three-elastic-element structural composites. - Simplified equations for the geometrical parameter of three-elastic-element structural composites can be developed when two of the three elements are identical. In this case, the geometrical parameter is given by

$$Y = \frac{E_1 A_1 [E_1 A_1 (d_1 - d_2)^2 + E_2 A_2 (d_1^2 + d_2^2)]}{(2E_1 A_1 + E_2 A_2) (2E_1 I_1 + E_2 I_2)} \quad (7)$$

This equation requires the determination of d_1 and d_2 , which are the distances between the neutral axes of the two identical elements and the third element; these distances have the same sign when the two identical elements are located on the same side of the third element and are of opposite sign when they are located on opposite sides of the third element. This determination is easily made compared to the difficulty generally encountered in establishing the location of the composite neutral axis by use of Equation (5).

If the three elements are arranged to produce a symmetrical cross-section ($d_1 = -d_2 \equiv d$), the geometrical parameter is given by

$$Y = \frac{2M A_1 d^2}{2M I_1 + I_2} \quad (8)$$

where d is the distance between the neutral axes of the two outer (identical) elements and the neutral axis of the inner element (which is also the composite neutral axis since the inner element must be symmetrical for this case).

Cell-insert structural composites. - Cell-insert composite structures consist of a cellular structural member in which structural insert members are separated from the hollow cells by a layer of viscoelastic shear-damping material, as illustrated in Figure 2.10. The geometrical parameter for cell-insert constructions is evaluated by application of Equation (4) to obtain

$$Y = \frac{E_c A_c \bar{e}_c^2 + \sum E_i A_i \bar{e}_i^2}{E_c I_c + \sum E_i I_i} \quad (9)$$

where \bar{e} represents the distance from the neutral axis of a given area element to the composite neutral axis, and the subscripts c and i refer to cell and insert, respectively. This equation applies both for symmetrical and unsymmetrical cross-section configurations and requires the determination of the composite neutral axis location by use of Equation (5). Furthermore, it is assumed that the cell-member is constructed from only one material, while the inserts are of arbitrary shape, size, and material.

The equation for geometrical parameter can be simplified for the case of a symmetrical cross-section. This implies that the neutral axis of the cell-structure coincides with the composite neutral axis, thereby requiring the distance \bar{e}_c to be zero. Hence, the geometrical parameter is given by

$$Y = \frac{\sum E_i A_i \bar{e}_i^2}{E_c I_c + \sum E_i I_i} \quad (10)$$

This equation applies for example, to the square tube, rectangular bar, and I-section cell-insert constructions shown in Figure 2.10(a), (d) and (e), respectively.

A further simplification can be made by requiring the inserts to be of the same size and material, and be located at the same distance \bar{e}_i from the composite neutral axis. Designating N_i as the total number of inserts

($N_i = 2, 4, 6 \dots$), the geometrical parameter is given by

$$Y = \frac{\left(\frac{\epsilon_i}{r_i}\right)^2}{1 + \frac{1}{N_i} \left(\frac{E_c}{E_i}\right) \left(\frac{I_c}{I_i}\right)} \quad (N_i = 2, 4, 6 \dots) \quad (11)$$

where $r_i = \sqrt{I_i/A_i}$. This equation applies, for example, to the rectangular bar cell-insert construction shown in Figure 2.10(d), and would also apply to the I-section construction shown in Figure 2.10(e) if the inserts were identical in size, material and orientation relative to the composite neutral axis.

There are a number of practical cell-insert symmetrical design configurations for which $E_c I_c \gg N_i E_i I_i$. For these cases, the geometrical parameter is given approximately by

$$Y \approx N_i \left(\frac{E_i}{E_c}\right) \left(\frac{I_i}{I_c}\right) \left(\frac{\epsilon_i}{r_i}\right)^2 \quad (N_i = 2, 4, 6 \dots) \quad (12)$$

This equation, for example, provides a means of rapidly determining the geometrical parameter of the cell-insert I-beam shown in Figure 2.10(e) when identical inserts having a relatively low value of flexural rigidity are employed.

Orthogonally symmetric cross-sections. - When evaluating the geometrical parameter of a structural composite, the plane in which flexural vibrations occur must be specified. For cross-sections of arbitrary shape, a different geometrical parameter may apply for each plane of vibration considered. However, under certain circumstances, the geometrical parameter will be invariant with the plane of vibration and the direction of the neutral axis is immaterial.

An example of this situation is a cross-section which has orthogonal symmetry. This type of symmetry requires that the cross-section

geometry be symmetrical about a given axis and also be identical to the geometry relative to an orthogonal axis. For this case, it can be shown that the geometrical parameter has the same value regardless of the direction of the neutral axis. Typical structural composites which satisfy this requirement include all the bar designs shown in Figure 2.5 with the exception of the design of Figure 2.5(e). Also satisfying the orthogonal symmetry requirement are the tube designs shown in Figure 2.6(a, b, c) and in Figure 2.10(a).

Effect of symmetrical sheathing addition. - In some instances, it may be desirable to provide a longitudinal elastic sheathing around the periphery of a viscoelastic shear-damped beam for use as an element positioning device, to offer protection from various environments, to improve the physical appearance of the structural member, etc. The effect of such an addition on the geometrical parameter may be easily evaluated for the case wherein a constant thickness sheathing is added to a symmetrical cross-section such that its neutral axis coincides with the composite neutral axis of the beam. The addition of the sheathing increases the flexural rigidity for the uncoupled and coupled conditions by the same amount and, using Equation (4), the modified geometrical parameter Y' may be shown to be

$$Y' = \left(\frac{1}{1 + \frac{(EI)_s}{(EI)_o}} \right) Y \quad (13)$$

where $(EI)_s$ is the flexural rigidity of the sheathing, and Y and $(EI)_o$ are the geometrical parameter and static flexural rigidity, respectively, of the composite beam prior to the addition of the sheathing. Hence, with the determination of the sheathing flexural rigidity and using the values of geometrical parameter and static flexural rigidity previously developed for the beam, the decrease in geometrical parameter caused by the addition of the sheathing is readily evaluated. The modified static flexural rigidity of the new composite beam is given by $(EI)_o' = (EI)_o + (EI)_s$.

Examples of composite beams to which a sheathing may be added for the reasons given above are the bars shown in Figure 2.5 (a, b, c, d, f) and tubes shown in Figure 2.6(a, d). Since the addition of the sheathing reduces

the geometrical parameter of the composite beam, consideration should be given to the use of a thin sheathing made from a low-modulus material which performs its intended function without providing a significant increase in the static flexural rigidity of the beam.

Formulation of Design Parameters

By using either the generalized or appropriate simplified version of the equation for geometrical parameter previously presented, specific design relationships for the geometrical parameter Y of the viscoelastic shear-damped structural composites shown in Figures 2.1 to 2.8 can be developed in the following form:

$$Y = Y_0 (M, R, T, D, S, N) [Y/Y_0] \quad (14)$$

where Y_0 is the value of the geometrical parameter for zero thickness of the viscoelastic damping layer and Y/Y_0 is a geometrical parameter correction factor specifying the effect which the thickness of the viscoelastic damping layer H_v has on the value of the geometrical parameter. To keep the design equations for geometrical parameter as general as possible, the following dimensionless parameters are employed:

$$M = E_1/E_2 = \text{ratio of moduli of elasticity}$$

$$R = H_1/H_2 = \text{thickness ratio}$$

$$T = H_s/H_c = \text{thickness ratio}$$

$$D = B/A = \text{dimension ratio}$$

$$S = H/A = \text{dimension ratio}$$

$$N = \text{number of elastic elements}$$

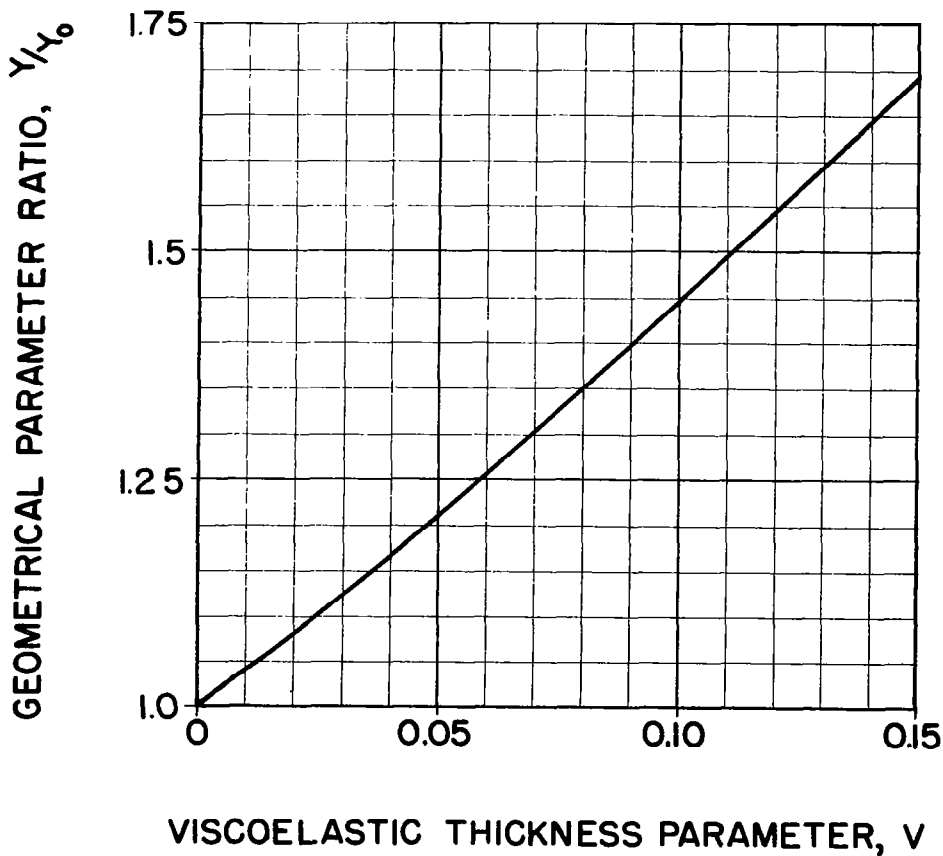
where E represents modulus of elasticity, H represents thickness, and B and A (with no subscript) represent overall size dimensions. In some cases, A (with identifying subscript) is also employed to represent cross-section area; this distinction is made quite obvious for the various structural composite design cross-sections considered. Figures 2.1 to 2.8 define

the dimensional parameters for each specific structural composite design. Any consistent set of units may be used for these parameters and, for maximum generalization, only dimensionless design graphs are developed for the geometrical parameter.

Effect of viscoelastic damping layer thickness. - For the structural composite designs which have geometrical parameters described by Equation (14), the geometrical parameter correction factor may be written

$$Y/Y_0 = (1+2V)^2 \quad (15)$$

where the viscoelastic thickness parameter V represents the ratio of the viscoelastic damping layer thickness H_v to a reference thickness. This equation is shown in the graph below, which indicates that the geometrical parameter is increased by a correction factor ranging from one to 1.7 for



values of the viscoelastic thickness parameter ranging from 0 to 0.15. The viscoelastic thickness parameter is limited to small values in accordance with the assumption that the viscoelastic damping material layers incorporated in the structural composite are thin compared to the thicknesses of the elastic elements of the structural composite.

Increasing the thickness of the viscoelastic damping layer has its greatest effect on the geometrical parameter when it results in a significant increase in the distance between the neutral axes of the elastic elements of the structural composite. This is the case, for example, for the composite structural plates and beams shown in Figures 2.1 to 2.4 and 2.7. For the composite structural bars, tubes and dumbbell model having a fixed overall size shown in Figures 2.5, 2.6 and 2.8, however, an increase in the viscoelastic damping material thickness has a less significant effect and, in certain instances, would cause a decrease in the static flexural rigidity $(EI)_0$ because of the resulting reduction of cross-section area of some elastic elements. The bar design shown in Figure 2.5(i) and the tube design shown in Figure 2.6(e) are examples of this situation.

For a number of practical cases, the reference thickness employed in the definition of the viscoelastic thickness parameter V can be defined solely in terms of thicknesses of elastic elements comprising the structural composite. In more complicated cases, the reference thickness definition may contain some of the thickness or dimension ratios previously defined in addition to the thicknesses of the elastic elements. For the composite structural plates and shapes shown in Figures 2.1 to 2.4 and 2.7, the general form of the viscoelastic thickness parameter V is

$$V = \frac{H_v}{H_1 + \lambda H_2} \quad (16)$$

where the thickness H_v of the viscoelastic damping layer is assumed constant throughout the composite structure, H_1 and H_2 are thicknesses of the elastic elements of the structural composites, and λ is a factor which may be either purely numeric or a function of other dimensionless parameters.

With the exception of the unsymmetrical three-laminate plate designs and the plate designs consisting of N identical structural sheets, the factor λ for the composite plate designs is unity; this includes the design configurations shown in Figures 2.1 (a, c), 2.2(a, b), 2.3(a, c), and 2.4(a, b).

For the unsymmetrical three-laminate plate designs, it can be shown that the geometrical parameter correction factor Y/Y_0 is greater than that indicated by Equation (15) for values of the thickness ratio H_1/H_2 less than unity, where the viscoelastic thickness parameter V is defined by Equation (16) with $\lambda = 1$. For values of the thickness ratio H_1/H_2 greater than unity, the correction factor Y/Y_0 is less than that indicated by Equation (15). Finally, the correction factor Y/Y_0 is given exactly by Equation (15) when the thickness ratio H_1/H_2 is equal to unity. Hence, the effect of the viscoelastic damping layer thickness on the value of the geometrical parameter of unsymmetrical three-laminate plate designs can be stated qualitatively as follows:

$$\begin{aligned} Y/Y_0 &\geq (1+2V)^2 & (H_1/H_2 \leq 1.0) \\ Y/Y_0 &\leq (1+2V)^2 & (H_1/H_2 \geq 1.0) \end{aligned} \quad (17)$$

To obtain a quantitative evaluation of this effect, the geometrical parameter Y can be determined directly for specified values of the viscoelastic thickness parameter V ; however, the results cannot be expressed as a correction factor in the form indicated by Equation (14).

For the plate designs comprised of a lamination of N identical structural sheets, as shown in Figure 2.1(b) and 2.3(b), the viscoelastic-thickness parameter V is given by

$$V = \frac{H_v}{2H} \quad (18)$$

where H is the thickness of the structural sheets (solid or honeycomb) employed in the composite structural plate designs.

More complex forms of the viscoelastic thickness parameter V apply for the composite beam design configurations shown in Figure 2.7. The factor λ for the composite angle, channel, T-section and I-section designs shown in Figure 2.7 is given by

$$\text{Angle: } \lambda_1 = \frac{3+S^2}{2-S}; \lambda_2 = \frac{1}{S} \quad (19)$$

$$\text{Channel: } \lambda = \frac{SD+2(1-S^2)}{S[D+2(1-S)]} \quad (20)$$

$$\text{T-Section: } \lambda = \frac{SD+(1-S^2)}{S[D+(1-S)]} \quad (21)$$

$$\text{I-Section: } \lambda = \frac{1}{S} \quad (22)$$

where the dimension ratios S and D are as previously defined. Two values of the factor λ are given for the angle design: λ_1 applies for the neutral axis at 45 degrees to and intersecting the sides of the angle, whereas λ_2 applies for the neutral axis at 45 degrees to the sides of the angle passing through the apex of the angle construction. For specific values of the dimension ratios S and D for a given composite structural design configuration, the factor λ may be calculated and the effect of the viscoelastic damping layer thickness evaluated by application of Equations (15) and (16).

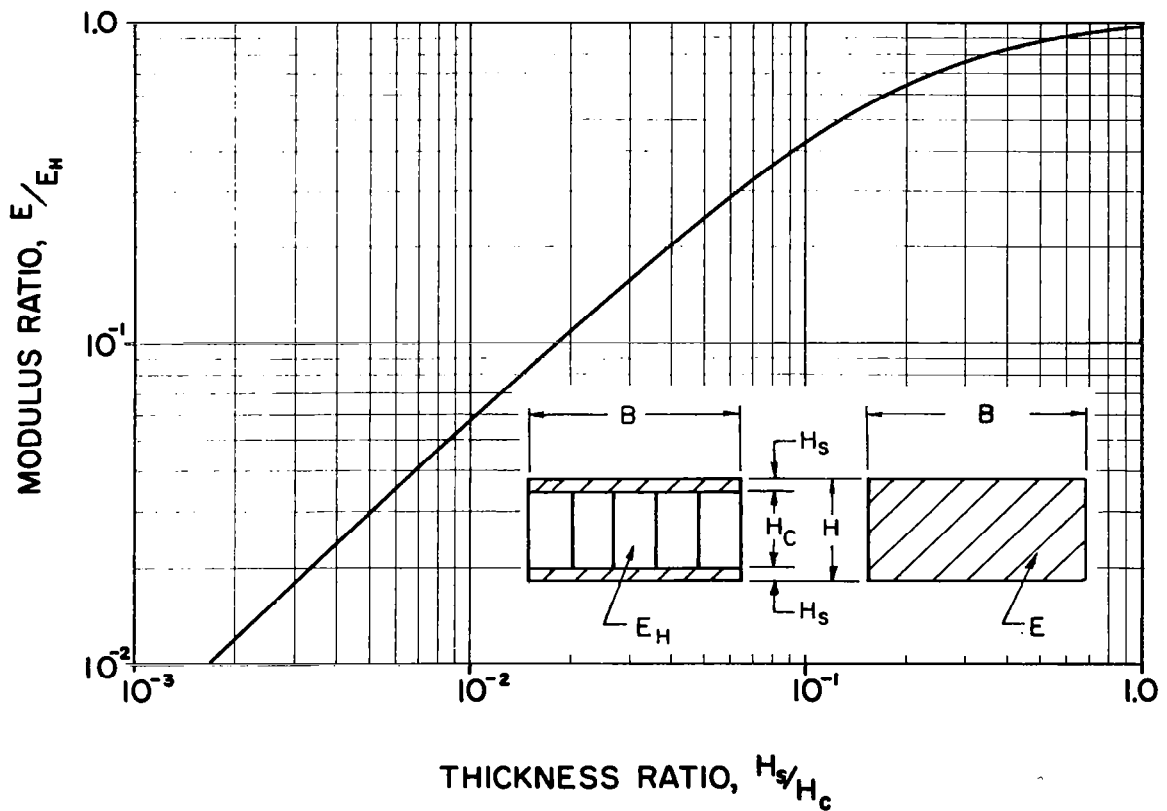
Equivalent modulus concept. - A simplification in the analysis and development of design data for structural composites involving honeycomb sheets, box-beam or I-beam constructions can be introduced by use of the concept of equivalent modulus. By equating the flexural rigidity of a solid rectangular sheet to that of a honeycomb sheet, box-beam, or I-beam construction of equal thickness and width, an "equivalent" modulus of the solid sheet can be determined.

For example, for a honeycomb sheet comprised of two skin members of thickness H_s bonded to a core of thickness H_c as shown in Figures 2.2 and 2.3, the equivalent modulus E of a solid structural sheet, which has a

rectangular cross-section and a thickness $H = 2H_s + H_c$, is given by

$$\frac{E}{E_H} = \frac{(2T+1)^3 - 1}{(2T+1)^3} \quad (23)$$

where E_H is the modulus of the honeycomb sheet skin material and $T = H_s/H_c$ is the ratio of the skin thickness to the core thickness of the honeycomb sheet. This equation, which is shown in the graph below, indicates that the modulus ratio is given approximately by $E/E_H \approx 6T$ for



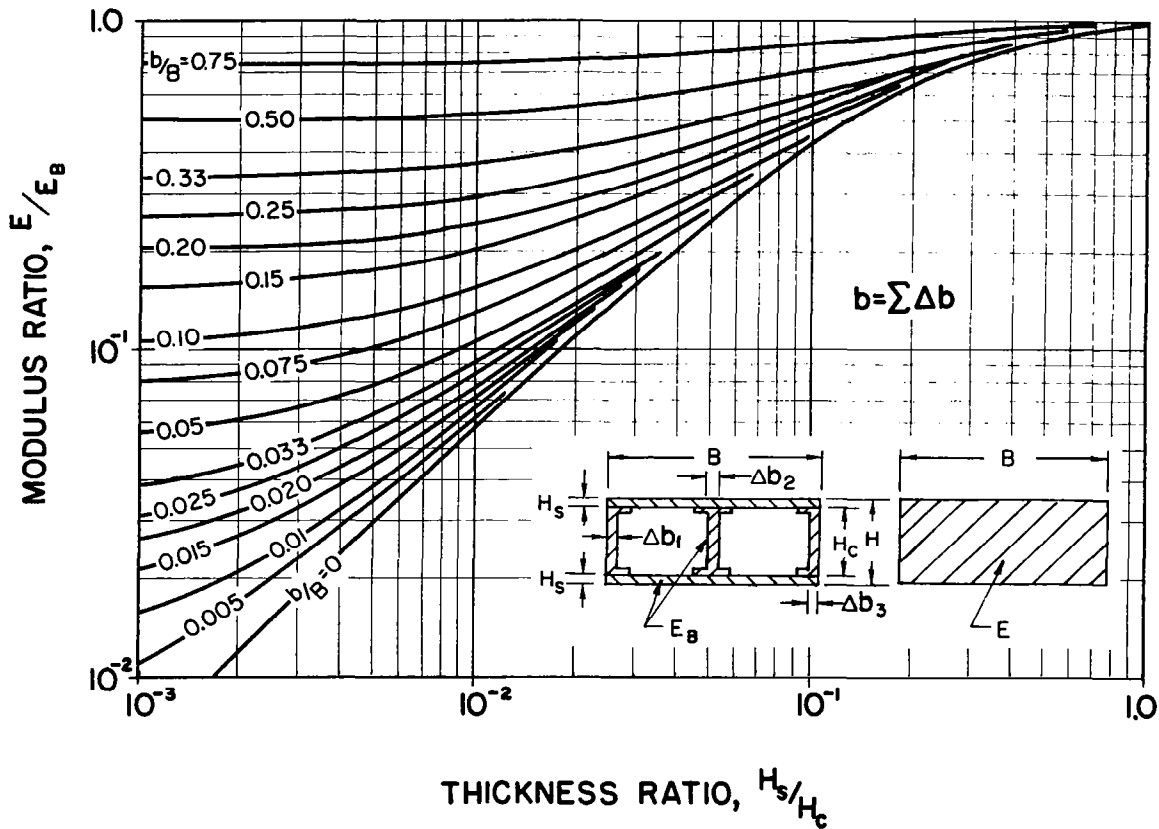
values of the thickness ratio $H_s/H_c < 0.04$. It is significant that when $H_s/H_c \geq 0.5$, the effective modulus E very nearly equals the modulus of the honeycomb skins E_H .

A similar analysis applied to box-beam and I-beam constructions of the type shown in Figure 2.4 results in the following relation for the

modulus E of a solid structural sheet having an equivalent bending stiffness

$$\frac{E}{E_B} = \frac{(2T+1)^3 + b/B - 1}{(2T+1)^3} \quad (24)$$

where E_B is the modulus of the box-beam material, $T = H_s/H_c$ is the ratio of the skin (or flange) thickness to the core (or web) thickness of the box-beam (or I-beam) construction, and b/B is the ratio of the total effective core (or web) width to the width of the beam. This equation, which is shown in the graph below, indicates that the modulus ratio E/E_B approaches the



value b/B as the thickness ratio H_s/H_c approaches zero. For values of the thickness ratio $H_s/H_c \geq 0.5$, the effective modulus E very nearly equals the modulus of the beam E_B , especially for larger values of the width ratio b/B . When $b/B \approx 1$, the modulus ratio E/E_B approaches unity since the box- or I-beam essentially becomes a solid rectangular beam.

Finally, for the case of $b/B = 0$, the box-beam and I-beam constructions degenerate into an idealized honeycomb sheet and the relation for the modulus ratio E/E_B reduces the relation for the modulus ratio E/E_H for the honeycomb sheet.

The graphs for the equivalent modulus ratios provide a rapid means of determining the bending stiffness of a honeycomb sheet and box-beam or I-beam constructions since the effective flexural rigidity is given simply by $(EI) = EB(2H_s + H_c)^3/12$, where E and B are the equivalent modulus and the width of the structural member, respectively.

While the equivalent modulus concept may be applied directly to determine the modulus of a solid rectangular cross-section sheet having the same thickness, width and bending stiffness as a honeycomb, box-beam, or I-beam construction, care is required with regard to its use in the development of mathematical expressions for geometrical parameter. Since the transfer flexural rigidity $(EI)_t$ of this type of construction is not reproduced by the "equivalent" solid sheet, this concept can only be employed for purposes of simplification of geometrical parameter analyses when the overall geometry of the composite structure is such that the neutral axis of the structural member for which an equivalence is sought is identical for the uncoupled and coupled conditions. This requirement essentially stipulates that the transfer flexural rigidity of the honeycomb, box-beam or I-beam construction is zero and the transfer flexural rigidity of all other structural elements are unchanged by substitution of the "equivalent" solid structural sheet. Consequently, the equivalent modulus concept provides a simplification in the determination of the geometrical parameter of the symmetrical double-constrained honeycomb, box-beam, and I-beam structural composites shown in Figures 2.2(b), 2.4(a) and 2.4(b), respectively. For these structural composites, the structural member to be replaced by an equivalent solid sheet is oriented in a manner such that its neutral axis of flexure is located identically for the uncoupled and coupled conditions.

Geometrical Parameter Design Data

The specific structural composites which have been evaluated for geometrical properties important in the design for high damping are shown in Figures 2.1 to 2.8. Equations and graphical presentations are developed for the geometrical parameter Y_0 in terms of the modulus, thickness and dimension ratios previously defined. An indication is made with regard to the applicability of the geometrical parameter correction factor Y/Y_0 for determining the value of the geometrical parameter Y . A wide variation in the values of the modulus and size parameters, keeping within the realm of practicality of design, is included in the design graphs to provide flexibility in the selection of cross-section configurations which have a satisfactory value of the geometrical parameter. Equations are provided for the static flexural rigidity $(EI)_0$ and the structure weight per unit length w in terms of cross-section dimensional characteristics, modulus of elasticity E , and the weight density γ (weight per unit volume). For designs involving two elastic elements, the mean length of the viscoelastic damping layer in the cross-section plane B_v and the distance between the neutral planes of the two elastic elements d are also provided.

Laminated structural sheets. - Cross-section configurations and design equations for damped structural plates consisting of laminated solid structural sheets are presented in Figure 2.11(A). Included are designs comprised of two, three (symmetrical and unsymmetrical) and N identical solid structural sheets. The geometrical parameter Y_0 for these damped plate designs is presented graphically in Figures 2.11(B)-(D) for parametric variations of the modulus ratio E_1/E_2 and the thickness ratio H_1/H_2 . Since the geometrical parameter correction factor stated by Equation (15) is not directly applicable to the unsymmetrical three solid sheet plate design, graphs of the geometrical parameter Y are presented in Figure 2.11(E) for values of the viscoelastic thickness parameter V equal to (a) 0.05, (b) 0.10, (c) 0.15 and (d) 0.20, where V is given by Equation (16) with λ equal to unity.

To evaluate the relative merits of the symmetrical and unsymmetrical three-elastic-element plate designs with regard to the value of geometrical parameter Y_0 , the ratio Y_s/Y_u is presented graphically in Figure 2.11(F), where Y_s and Y_u are the geometrical parameters Y_0 for the symmetrical and unsymmetrical designs, respectively. The symmetrical design has a larger geometrical parameter for modulus ratios E_1/E_2 greater than unity, for all values of the thickness ratio H_1/H_2 . For modulus ratios less than unity, the unsymmetrical design has the larger geometrical parameter. Finally, the symmetrical and unsymmetrical designs have the same value of geometrical parameter for a modulus ratio of unity.

Geometrical parameter design graphs are not presented for the plate design comprised of N identical solid sheets since the governing equation is simple enough to allow mental calculation. Very large values of the geometrical parameter Y_0 are attained as the number of equal thickness and stiffness sheets is increased.

The values of modulus and thickness ratios which maximize the geometrical parameter Y_0 may be determined in concept by determining the conditions for which $dY_0/dR = 0$. For the two solid sheet design, the thickness ratio at which the maximum geometrical parameter $(Y_0)_{\max} = 3.0$ occurs is given by

$$\left(H_1/H_2\right)_{Y_{\max}} = \sqrt{E_2/E_1} \quad (25)$$

For the three solid sheet designs, the conditions for maximization of geometrical parameter may be obtained numerically in lieu of the differential calculus technique which does not provide a convenient closed form solution.

The results of a maximization analysis are shown in Figure 2.11(G), where the thickness ratio for maximizing Y_0 is shown at (a) and the value $(Y_0)_{\max}$ is shown at (b) as a function of the modulus ratio. For modulus ratios greater than unity, the thickness ratio for maximum geometrical parameter is less than unity; conversely, for modulus ratios less than unity, the thickness ratio for maximum geometrical parameter is greater than unity. The thickness ratio for which the geometrical parameter is maximized is

different depending upon whether two or three laminates are employed; however, the same thickness ratio maximizes the geometrical parameter for the symmetrical and unsymmetrical three laminate design.

The curves presented in Figure 2.11(G) indicate that very large values of the geometrical parameter can be attained with the three laminate design, especially for the symmetrical configuration. For modulus ratios greater than unity, the symmetrical configuration provides a higher maximum geometrical parameter whereas, for modulus ratios less than unity, the unsymmetrical configuration provides higher values of the maximum geometrical parameter.

Constrained honeycomb sheets. - Cross-section configurations and design equations for damped structural plates consisting of constrained honeycomb structural sheets are presented in Figure 2.12(A). Included are single-constrained and double-constrained (symmetrical and unsymmetrical) designs comprised of laminated honeycomb and solid structural sheets. The geometrical parameter Y_0 is presented graphically in Figures 2.12(B) and (D) for the single-constrained and unsymmetrical double-constrained honeycomb plate designs. Parametric variations of the thickness ratios H_S/H_C and H_1/H_2 are presented, with specific values of the modulus ratio E_1/E_H equal to (a) 1/3, (b) 1.0, (c) 3, and (d) 10.

Graphs of the equivalent modulus ratio E_2/E_H and geometrical parameter Y_0 are presented in Figure 2.12(C) for the symmetrical double-constrained honeycomb design. Broad parametric variations of the modulus ratio E_1/E_2 and thickness ratio H_1/H_2 can be presented graphically in this case by use of the equivalent modulus concept for the central honeycomb structural element. Equation (23) or its graphical equivalent provides a means of determining the values of the equivalent modulus ratio E_2/E_H in terms of the thickness ratio H_S/H_C . Using this information, the effective modulus ratio E_1/E_2 is calculated and the graphical solution for the symmetrical three solid sheet design may be applied directly to determine the geometrical parameter in terms of the modulus ratio E_1/E_2 and the thickness ratio H_1/H_2 . This procedure can be carried out in its entirety by use of the graphical data presented in Figure 2.12(C).

Laminated honeycomb sheets. - Cross-section configurations and design equations for damped structural plates consisting of laminated honeycomb structural sheets are presented in Figure 2.13(A). Included are designs comprised of two, three (symmetrical and unsymmetrical) and N identical honeycomb structural sheets. Determination of the geometrical parameter Y_0 is considerably simplified when the thickness ratios H_{S1}/H_{C1} and H_{S2}/H_{C2} (or H_S/H_C for the plate design comprised of N identical sheets) approach zero. In this case, the geometrical parameter approaches one-third of the value which would exist if the structural sheets were solid; hence, the geometrical parameter Y_0 can be determined by use of Figures 2.11(B)-(D) in terms of the modulus ratio E_1/E_2 and thickness ratio H_1/H_2 .

The geometrical parameter Y_0 is presented graphically in Figures 2.13(B)-(F) for parametric variations of the thickness ratios H_{S1}/H_{C1} and H_{S2}/H_{C2} , with various specific values of the modulus ratio E_1/E_2 and thickness ratio H_1/H_2 . Design graphs for values of the modulus ratio $E_1/E_2 = 1$ and thickness ratio H_1/H_2 equal to (a) 1.0, (b) 1.5, (c) 2 and (d) 4 are provided in Figure 2.13(B) for the two honeycomb sheet design. For the three honeycomb sheet designs having values of the thickness ratio H_1/H_2 equal to (a) 0.25, (b) 0.5, (c) 1.0 and (d) 2, the geometrical parameter Y_0 is shown graphically in Figures 2.13(C) and (E) for the modulus ratio $E_1/E_2 = 1$, and Figures 2.13(D) and (F) for the modulus ratio $E_1/E_2 = 3$.

A graph of the geometrical parameter Y_0 is presented in Figure 2.13(G) for the damped structural plate comprised of N identical honeycomb sheets. As the number of identical honeycomb sheets is increased, the value of the geometrical parameter is increased. For low values of the thickness ratios H_S/H_C , the geometrical parameter is given approximately by $Y_0 \approx \frac{1}{3} (N^2 - 1)$; this approximation is applicable, for example, for $H_S/H_C < 0.1$ when $N = 2$, $H_S/H_C < 0.05$ when $N = 3$, and $H_S/H_C < 0.02$ when $N = 4$.

Box-beam and I-beam constructions. - Cross-section configurations, design equations, and graphs of the equivalent modulus ratio E_2/E_B and geometrical parameter Y_0 for damped symmetrical double-constrained plates incorporating box-beam and I-beam constructions are presented in Figure 2.14. Broad parametric variations of the modulus ratio E_1/E_2 and thickness

ratio H_1/H_2 can be presented graphically in this case by use of the equivalent modulus concept for the central structural element. Equation (24) or its graphical equivalent provides a means of determining the equivalent value of the modulus ratio E_2/E_B in terms of the thickness ratio H_S/H_C . Using this information, the effective modulus ratio E_1/E_2 is calculated and the graphical solutions presented for solid sheet designs are applied directly to determine the geometrical parameter in terms of the modulus ratio E_1/E_2 and the thickness ratio H_1/H_2 . This procedure can be carried out in its entirety by use of the graphical data presented in Figure 2.14. When the width ratio b/B becomes very small, the geometrical parameter becomes approximately equal to that for a double-constrained honeycomb sheet as shown graphically in Figure 2.12 (C).

Structural bar designs. - Cross-section configurations and design equations for damped structural bars consisting of a multiplicity of longitudinal elastic elements arranged to produce various cross-section shapes are presented in Figure 2.15 (A). Included are designs for square and round cross-section bars, as well as bars having cross-sections intermediate to these shapes. The geometrical parameter Y_0 is presented graphically in Figures 2.15 (B)-(L).

Graphs of the geometrical parameter Y_0 are presented in Figure 2.15 (B)-(E) for composite structural bar designs comprised of a central elastic element in the shape of a cross and a symmetrical set of four elastic elements with square, quarter-round or triangular shapes. Data are presented for parametric variations of the modulus ratio E_1/E_2 and dimension ratio B/A . These bar designs have orthogonally symmetric cross-sections; hence, the value of the geometrical parameter Y_0 given in the design graphs applies for any plane of flexural vibration.

Graphs of the geometrical parameter Y_0 are presented in Figure 2.15 (F)-(H) for composite structural bar designs comprised of N identical insert members of rectangular cross-section placed in each of four rectangular grooves located on the faces of a square bar. Data are presented for parametric variations of the modulus ratio E_1/E_2 and dimension ratio B/A . Values of the dimension ratio H/A equal to 0.05 and

0.1 are specified in Figures 2.15(F) and (G), respectively, and values of this ratio equal to 0.15 and 0.2 are specified in Figure 2.15(H). Specific values of the number of elastic insert elements N range from one to infinity, with the final graph for each value of the specified dimension ratio H/A being applicable for the indicated range of N values. For the case of the dimension ratio H/A equal to 0.2, one design graph provides a good approximation for the geometrical parameter Y_0 for all values of the number of elastic insert elements N , as presented in Figure 2.15(H); consequently, for this value of H/A , there is no advantage to employ a large number of insert elements since the geometrical parameter provided by the insertion of a single rectangular member in each groove cannot be significantly increased. This composite structural bar design has an orthogonally symmetric cross-section; hence, the value of the geometrical parameter Y_0 given in the design graphs applies for any plane of flexural bending.

Graphs of the geometrical parameter Y_0 are presented in Figures 2.15 (I) and (J) for a composite structural bar design comprised of N thin solid sheets laminated to a central square bar element. Data are presented for parametric variations of the modulus ratio E_1/E_2 and dimension ratio H/A , with the number of laminated solid sheets N equal to (a) 1, (b) 2, (c) 3 and (d) 6. Since the cross-section of this bar design is not orthogonally symmetric, the design graphs in Figures 2.15(I) and (J) are presented for the two principal planes of flexural bending.

A graph of the modified geometrical parameter $Y (A_C/A_i)$ is presented in Figure 2.15(K) for square and round composite structural bar designs comprised of a large number of elastic insert elements placed within square and round structural tubes. Data are presented for parametric variations of the modulus ratio E_1/E_2 and the dimension ratio B/A . The geometrical parameter Y is given by the product of the modified geometrical parameter obtained from Figure 2.15(K) and the ratio of the total area of inserts A_i to the area of the hollow cell A_C , where $A_C = B^2$ for the square bar and $A_C = \pi B^2/4$ for the circular bar. This composite structural bar design has an orthogonally symmetric cross-section; hence, the value of the geometrical parameter Y obtained by use of the design graph applies for any plane of flexural vibration.

A graph of the geometrical parameter Y_0 is presented in Figure 2.15(L) for a round structural composite bar comprised of four quarter-round elastic insert elements placed within a round structural tube. Design data are presented for parametric variations of the modulus ratio E_1/E_2 and the dimension ratio B/A . Since this composite structural bar design has an orthogonally symmetric cross-section, the geometrical parameter Y_0 given by the design graph applies for any plane of flexural vibration.

Structural tube designs. - Cross-section configurations and design equations for damped structural tubes consisting of a combination of solid structural tubes and longitudinal elastic constraining elements are presented in Figure 2.16(A). Included are designs for square and round cross-section tubes, for which the geometrical parameter Y_0 are presented graphically in Figures 2.16(B)-(M).

Graphs of the geometrical parameter Y_0 are presented in Figure 2.15(B)-(E) for a composite structural tube design comprised of N identical rectangular strips placed on the four outer faces of a square tube. Data are presented for parametric variations of the modulus ratio E_1/E_2 and thickness ratio H_1/H_2 . The number of rectangular strips N is equal to (a) 1, (b) 2, (c) 4, and (d) $10 - \infty$ in the design graphs for specific values of the dimension ratio H_2/A equal to 0.05, 0.1, 0.15 and 0.2 in Figures 2.16(B), (C), (D) and (E), respectively. For each value of the dimension ratio H_2/A considered, a single design graph suffices for values of N ranging from ten to infinity. Since this composite structural tube design has an orthogonally symmetric cross-section, the value of the geometrical parameter Y_0 given in the design graphs applies for any plane of flexural bending.

A graph of the geometrical parameter Y_0 is presented in Figure 2.16(F) for a composite structural tube design comprised of four structural angles placed on the outside corners of a square tube. Data are presented for parametric variations of the modulus ratio E_1/E_2 and thickness ratio H_1/H_2 , with specific values of the dimension ratio H_2/A equal to (a) 0.05, (b) 0.1, (c) 0.15 and (d) 0.2. Since this composite structural tube design has an orthogonally symmetric cross-section, the value of the geometrical

parameter Y_0 given in the design graph applies for any plane of flexural bending.

A graph of the geometrical parameter Y_0 is presented in Figure 2.16(G) for a composite structural tube design comprised of four structural angles placed on the outside corners of a square tube, with four rectangular sheets placed on the four faces formed by the angle members. Data are presented for parametric variations of the modulus ratio E_1/E_2 and thickness ratio H_1/H_2 , with specific values of the dimension ratio H_2/A equal to (a) 0.05, (b) 0.1, (c) 0.15 and (d) 0.2. For this design, the structural angle and sheets laminated to the central tube element have the same thickness H_1 and modulus E_1 . Since this composite structural tube design has an orthogonally symmetric cross-section, the value of the geometrical parameter Y_0 given in the design graph applies for any plane of flexural bending.

Graphs of the geometrical parameter Y_0 are presented in Figure 2.16(H) and (I) for a composite structural tube design comprised of N identical tube segments placed around the outer circumference of a circular tube. Data are presented for parametric variations of the modulus ratio E_1/E_2 and the thickness ratio H_1/H_2 . The number of tube segments N is equal to (a) 3, (b) 4, (c) 6 and (d) infinity in the design graphs for specific values of the dimension ratio H_2/A equal to 0.05 and 0.1 in Figures 2.16(H) and (I), respectively. It can be shown that, for values of N greater than 2, the value of the geometrical parameter Y_0 given in the design graphs applies for any plane of flexural bending, even though there may not be orthogonal symmetry (e.g., $N = 3$).

Graphs of the geometrical parameter Y_0 are presented in Figure 2.16(J)-(M) for a composite structural tube design comprised of N identical tube segments placed between two concentric circular tubes. Data are presented for parametric variations of the thickness ratios H_3/H_2 and H_1/H_2 , with the modulus ratio $E_3/E_2 = 1.0$. The number of tube segments N is equal to (a) 3, (b) 4, (c) 6 and (d) infinity in the design graphs. Values of modulus ratio E_1/E_2 equal to 1.0 and dimension ratio H_2/A equal to 0.05 and 0.1 are considered in Figures 2.16(J) and (K), respectively.

Similarly, values of the modulus ratio E_1/E_2 equal to 3.0 and dimension ratio H_2/A equal to 0.05 and 0.1 are considered in Figures 2.16(L) and (M), respectively. For values of N greater than 2, the value of the geometrical parameter Y_0 given in the design graphs applies for any plane of flexural bending.

Structural shape beams. - Cross-section configurations and design equations for damped angle, channel, T-section and I-section beams, which consist of solid rectangular sheets laminated to the outside of conventional structural shape beams, are presented in Figure 2.17(A). It should be noted that the value of the geometrical parameter is much less (and in some cases could become zero) when the rectangular sheets are laminated on the inside surface of the structural shape beams. For example, consider the channel and T-section beams. If the thickness of the rectangular sheets were such that their neutral axes coincided with those of the channel or T-sections, the transfer flexural rigidity would be zero and, in accordance with Equation (4), the geometrical parameter would be zero. Hence, only designs providing desirable values of the geometrical parameter are considered.

Graphs of the geometrical parameter Y_0 are presented in Figure 2.17(B)-(E) for the angle, channel, T-section and I-section beams, respectively. Data are presented for parametric variations of the modulus ratio E_1/E_2 and thickness ratio H_1/H_2 .

Since the cross-section of the composite structural angle design is not orthogonally symmetric, the design graphs in Figure 2.17(B) present the geometrical parameter Y_0 for the two principal planes of flexural bending. Values of the dimension ratio H_2/A equal to 0.1 and 0.2 are specified for the design graphs and the value of the factor λ is indicated which may be used with Equations (15) and (16) to evaluate the effect of the viscoelastic damping layer thickness on the geometrical parameter.

Practical values of the dimension ratios B/A and H_2/A are specified in the design graphs for the channel, T-section and I-section beams. In each case, the value of the factor λ is indicated which allows the effect of the viscoelastic damping layer thickness on the geometrical parameter to be evaluated by use of Equations (15) and (16). The geometrical parameter

design graphs for the channel and T-sections which are presented in Figure 2.17 (C) and (D), respectively, indicate that a general decrease in the geometrical parameter occurs for an increase in the dimension ratio B/A . This is a somewhat unexpected result since there is a general trend for the geometrical parameter to increase with increasing dimension ratio B/A and to approach the value of the geometrical parameter for solid plates as B/A approaches infinity. However, in the region of greatest interest ($2 < B/A < 4$ for the channel and $1 < B/A < 2$ for the T-section) the opposite is true. An alternate method of obtaining the geometrical parameter of the double-constrained I-section beam presented in Figure 2.17 (E) is to employ the previous analysis of this type of construction based on the use of the equivalent modulus concept, as presented graphically in Figure 2.14.

Dumbbell model. - A cross-section configuration, design equations and a graph of the geometrical parameter Y_0 for a damped dumbbell model is presented in Figure 2.18. The cross-section areas A_1 and A_2 may be of any shape and it is assumed that the distance H between the symmetrically located areas is substantially greater than the square root of the cross-section areas. Data are presented for parametric variations of the modulus ratio E_1/E_2 and the area ratio A_1/A_2 . This design graph provides a first-order approximation of the geometrical parameter Y_0 of complex structural assemblies such as truss constructions.

Geometrical Parameter Design Considerations

From the point of view of producing structural composites with high damping, it is desirable to design structure cross-sections having high values of the geometrical parameter Y . The design data presented for the various viscoelastic shear-damped structural composites allow the selection of modulus and geometry to attain a desired value of the geometrical parameter. For a given selection of structural materials, the dimensional properties of the cross-section can frequently be selected to maximize the value of the geometrical parameter.

A value of the geometrical parameter Y ranging from 0.5 to 5.0 is generally required to design highly damped structures which satisfy other

performance requirements such as static stiffness, weight, stress, structure resonant frequency and size. The structure loss factor η may not be sufficiently high for values of the geometrical parameter less than 0.5, whereas a substantial increase in values of the geometrical parameter greater than 5 may provide only a slight increase in the structure loss factor [Ref. 8]. Each application must be evaluated on its own merits, however, since particular design and performance requirements may justify the selection of a value of geometrical parameter out of this range.

The design graphs indicate that it may be advantageous, with regard to attaining a high value of the geometrical parameter Y_0 , to employ materials having different moduli of elasticity in the structural composite. This is the case, for example, for the constrained honeycomb sheets and the structural bar and tube designs considered. However, for designs such as the damped plate in the form of two laminated solid sheets, the use of different materials for the two elastic elements does not provide any advantage with regard to the maximum obtainable value of the geometrical parameter Y_0 ; however, it does provide flexibility in the selection of the thicknesses of the solid sheets.

The choice of materials in the fabrication of a structural composite depends on many considerations other than structural damping. For example, protection from hostile environments, thermal conduction, electrical conduction, radiation shielding, strength, weight, etc., all represent broader design implications which may suggest the use of a specific combination of structural materials.

Certain structural composite designs involve a number of elastic elements N which generally should be made large to obtain high values of the geometrical parameter. However, the rate of change of the geometrical parameter with N frequently decreases for higher numbers of elastic elements, and the design graphs can be employed to determine the most advantageous number of elastic elements from the point of view of structural performance and fabrication.

The design data presented herein allows the evaluation of the geometrical parameter, static flexural rigidity, and structure weight for changes made in modulus, size and number of elastic elements comprising

the structural composite. Hence, by judicious variation of the modulus and geometry parameters, a compromise between all design and performance requirements can be attained.

SECTION 3: DESIGN OF TWO-ELASTIC-ELEMENT STRUCTURAL COMPOSITES

This section of the report presents the development of design procedures for two-elastic-element structural composites based on fundamental equations previously developed for the loss factor and related parameters for viscoelastically damped beam structures. The assumptions employed in the derivation of the fundamental equations are reviewed and typical structural composite designs for which the theory applies are identified. Both a manual design procedure using graphical design data and an automated procedure employing digital computer techniques are developed. The implications of other design considerations such as temperature, static stiffness, weight and static load distribution are also discussed. An example of the use of these procedures is presented in Section 4 of this report.

Fundamental Equations for Damping Parameters

The structure loss factor η is defined as the ratio of the imaginary and real parts of the complex flexural rigidity $(EI)^* = (EI)(-i\eta)$. For viscoelastic shear-damped structural composites comprised of two elastic elements and an intervening viscoelastic damping layer, the complex flexural rigidity $(EI)^*$ is given by [Ref. 5] :

$$(EI)^* = (EI)_0 \left[1 + \frac{X^*}{1+X^*} Y \right] \quad (26)$$

where the complex shear parameter $X^* = X(1-i\beta)$. Evaluation of the complex flexural rigidity for the uncoupled condition ($X = 0$) and the coupled condition ($X = \infty$) provides the fundamental relationship for geometrical parameter Y given by Equation (3). By expanding Equation (26) into a basic complex form, the following equation for the structure loss factor is obtained [Ref. 5] :

$$\eta = \frac{\beta XY}{1+X(Y+2)+(1+\beta^2)X^2(Y+1)} \quad (27)$$

where the loss factor β of the viscoelastic damping material defined by Equation (2) is in general a function of frequency and temperature and the geometrical parameter Y is defined generally by Equation (4) and more explicitly by Equation (6).

The ratio d^2/Y from Equation (6) is independent of the viscoelastic damping layer thickness H_v and, therefore, is equal to d_o^2/Y_o , where d_o and Y_o are the distance between the neutral planes of the two elastic elements and the geometrical parameter, respectively, for $H_v = 0$. Consequently, the shear parameter X is given by [Ref. 5, 8]

$$X = \frac{G' B_v d_o^2}{p^2 H_v Y_o (EI)_o} \quad (28)$$

where G' is the storage modulus of the viscoelastic shear-damping material, B_v is the mean length of the viscoelastic damping layer in the cross-section plane, $(EI)_o$ is the static flexural rigidity of the structural composite corresponding to the uncoupled condition (i. e. , $(EI)_o = E_1 I_1 + E_2 I_2$), and p is the wave number for flexural vibrations. The flexural vibration wave number p is given by

$$p = 2\pi/\lambda \quad (29)$$

where λ is the wavelength of a flexural wave. Alternately, the wave number p may be related to the circular frequency ω and the cyclic frequency f as follows

$$p^2 = \omega \sqrt{\frac{w}{g(EI)_r}} = 2\pi f \sqrt{\frac{w}{g(EI)_r}} \quad (30)$$

where w is the weight per unit length of the composite structure, g is the gravitational acceleration constant, and $(EI)_r$ is the effective flexural rigidity of the structure for the resonant mode of vibration being considered.

The following are presentations of the basic assumptions made in the development of the fundamental theory for the damping of two-elastic-element

viscoelastic shear-damped structural composites undergoing flexural vibration and typical structural composite designs for which the theory applies.

Basic assumptions of theory. - In the development of the fundamental equations for complex flexural rigidity, loss factor, and shear parameter, the following assumptions have been employed:

- (1) The structural composite beam is comprised of two elastic elements of arbitrary modulus and cross-section area between which is constrained a viscoelastic shear-damping layer.
- (2) The mode shape of the vibrating beam is sinusoidal.
- (3) The effects imposed by boundary constraints are negligible.
- (4) Shear and torsional distortions of the elastic elements are neglected.
- (5) The cross-section dimensions of the elastic and viscoelastic elements remain unchanged during vibration.
- (6) Contact without slippage is maintained at all interfaces.
- (7) Linear stress-strain relations apply for the viscoelastic and elastic materials employed in the structural composite.
- (8) Axial inertial forces are negligible.
- (9) The elastic elements have zero extensional and shear loss factors.
- (10) The elastic elements are considerably stiffer in extension than the viscoelastic material.
- (11) The viscoelastic layer is thin compared to the thickness of the elastic elements.
- (12) The viscoelastic layer is of approximately constant thickness throughout the structural composite.

Additional assumptions are delineated in the development of design equations and graphs for predicting the structure loss factor of two-elastic-element viscoelastic shear-damped structural composites.

Typical structural composite designs. - Cross-section configurations of typical two-elastic-element structural composite designs are presented in

Figure 3.1. Included are laminated (a) solid sheets, (b) honeycomb sheets, (c) solid and honeycomb sheets, (d) T-section, (e) channel section, and (f) angle section designs. The composite angle section design shown in Figure 3.1(f) actually is comprised of three elastic elements. However, for vibrations about the neutral axis which is at 45 degrees to and intersecting the sides of the angle, each of the two rectangular elastic elements of modulus E_1 may be considered as representing one-half the stiffness of a single effective elastic element because of the physical orientation and identical flexural bending properties of the elements. Hence, the angle section design can be considered as a two-elastic-element structural composite.

Specification of the moduli E_1 and E_2 of the two elastic elements and the cross-section dimensional characteristics of the two elastic elements allows relevant geometrical properties to be calculated by use of the design data previously presented for these cross-section configurations. Specifically, data in the form of design equations and graphs for the geometrical properties of two-elastic-element structural composites are presented in Section 2 of this report as follows: laminated solid sheets, Figure 2.11 (A,B); laminated honeycomb sheets, Figure 2.13 (A,B); single-constrained honeycomb sheet, Figure 2.12 (A,B); and laminated T-section, channel and angle sections, Figure 2.17 (A-D). In the following discussion of design equations, graphs and procedures, it shall be assumed that the geometrical parameter Y , the static flexural rigidity $(EI)_0$, the weight per unit length w , the distance between the neutral planes of the two elastic elements d , and the mean length of the viscoelastic damping layer in the cross-section plane B_v have been determined by direct calculation or by use of the graphical design aids provided in Section 2 of the report.

Development of Design Equations and Graphs

If the wavelength of the flexural vibration wave λ is known, the wave number p is simply determined by Equation (29). However, the structural designer is frequently interested in predicting the variation of the structure loss factor η as a function of the frequency of vibration $f = \omega/2\pi$ so that

the degree of damping at the various structural resonances can be established. Hence, Equation (30) is the appropriate equation to be employed to determine the wave number. This requires the evaluation of the effective flexural rigidity $(EI)_r$ for which no precise definition exists. Based on analyses of the dynamic stiffness characteristics of a lumped parameter model representation of viscoelastic shear-damped structural composites [Ref. 7] and subsequent experimental confirmation of the design procedures developed, there appears to be considerable justification for assuming that the effective flexural rigidity $(EI)_r$ is the real part of the complex flexural rigidity $(EI)^*$.

Coupling parameter Z. - By use of Equation (26) and assuming that the effective flexural rigidity $(EI)_r$ is the real part of the complex flexural rigidity $(EI)^*$, the following relationship for effective flexural rigidity is obtained

$$(EI)_r = (EI)_o (1 + ZY) \quad (31)$$

where the coupling parameter Z given by

$$Z = \frac{(1 + 1/X) + \beta^2}{(1 + 1/X)^2 + \beta^2} \quad (32)$$

is shown graphically in Figure 3.2 for parametric variations of the shear parameter X and the damping material loss factor β . It should be recognized that, since the shear parameter X and the loss factor β depend on frequency in general, the coupling parameter Z is also frequency dependent.

As indicated by Equations (31) and (32) and Figure 3.2, the value of the coupling parameter Z defines the degree of dynamic coupling between the two-elastic elements of the structural composite. For values of the coupling parameter Z approaching zero (low values of X), the effective flexural rigidity $(EI)_r$ essentially equals the static or uncoupled flexural rigidity $(EI)_o$. For values of the coupling parameter Z approaching one (high values of X), the effective flexural rigidity $(EI)_r$ essentially equals the coupled flexural rigidity $(EI)_\infty = (EI)_o(Y+1)$. Values of the effective flexural

rigidity $(EI)_r$ range between $(EI)_o$ and $(EI)_\infty$ for intermediate values of the shear parameter X , with higher values of the loss factor β causing the degree of dynamic coupling to be increased.

Resonant frequency ratio f_r/f_o . - Assuming that the resonant frequencies of the composite structural beam or plate are the same as a solid beam or plate having the same static loading and a flexural rigidity equal to $(EI)_r$, the standard natural frequency equations available in the technical literature [Ref. 9, 10] can be employed for resonant frequency prediction purposes with the value of $(EI)_r$ given by Equation (31). It is convenient to employ the uncoupled resonant frequency f_o , which is determined by the beam or plate natural frequency equation in terms of the static flexural rigidity $(EI)_o$, as a reference frequency for purposes of developing a dimensionless resonant frequency ratio. For flexural vibrations of beams and plates, the natural frequency varies as the square root of the flexural rigidity, where the constant of proportionality is a function of the mode of vibration, size, and static loading conditions. Consequently, for a given mode of vibration with the assumption that the same constant of proportionality applies for solid and damped beams and plates having comparable size, boundary, and static loading conditions, the resonant frequency ratio f_r/f_o may be written

$$\frac{f_r}{f_o} = \sqrt{\frac{(EI)_r}{(EI)_o}} \quad (33)$$

Using Equation (31), the resonant frequency ratio is given by

$$\frac{f_r}{f_o} = \sqrt{1 + ZY} \quad (34)$$

which is shown graphically in Figure 3.3 for parametric variations of the geometrical parameter Y and the coupling parameter Z . Since the coupling parameter Z is frequency dependent and solutions being developed for structure loss factor are applicable only for resonant conditions, the value of the coupling parameter Z is a function of the resonant frequency f_r ;

consequently, the determination of the resonant frequency ratio by use of Equation (34) requires an iterative process.

Referring to Equation (34) and Figure 3.3, the coupling parameter Z determines (for a specified value of geometrical parameter Y) the ratio of the resonant frequency f_r to the uncoupled natural frequency f_o for a given mode of vibration. For low values of Z and all values of Y , there is little dynamic coupling and the resonant frequency f_r is essentially the uncoupled natural frequency f_o . For values of Z approaching one, the resonant frequency f_r approaches a value $\sqrt{Y+1} f_o$ for all values of Y . Defining the coupled natural frequency f_∞ as follows

$$f_\infty = \sqrt{Y+1} f_o \quad (35)$$

the geometrical parameter Y can be written

$$Y = \left(\frac{f_\infty}{f_o} \right)^2 - 1 \quad (36)$$

which represents an additional alternate form of the relationship for geometrical parameter given by Equation (4). It is concluded that, for each flexural mode of vibration, the appropriate uncoupled natural frequency f_o and coupled natural frequency f_∞ represent lower and upper bounds on the structural composite resonant frequency f_r .

Shear parameter X . - By substituting Equations (30), (31), and (34) into Equation (28), the following form of the equation for the shear parameter X is developed:

$$X = C \left(\frac{G'}{f} \right) \left(\frac{f_r}{f_o} \right) \quad (37)$$

where the shear parameter coefficient C given by

$$C = \frac{\sqrt{g}}{2\pi} \frac{B_v d_o^2}{H_v Y_o \sqrt{w(EI)_o}} \quad (38)$$

is independent of frequency and readily evaluated for a specified structural composite cross-section design configuration by use of the design data for geometrical properties presented in Section 2 of the report.

The shear parameter X is a complicated function of frequency. In addition to its direct dependence on the reciprocal of frequency, there is an indirect dependence on frequency since the viscoelastic material storage modulus G' is generally a function of frequency, and determination of the resonant frequency ratio f_r/f_0 requires an iterative process with frequency as the iteration variable.

Generalized shear parameter equation. - Since the structure loss factor η and the resonant frequency ratio f_r/f_0 are mathematically continuous functions of frequency through their dependence on the shear parameter X and the viscoelastic damping material loss factor β , it is desirable to combine the previously defined frequency-dependent parameters to arrive at an equation for shear parameter which does not require an iteration process for its solution. By substitution of Equations (32) and (34) into Equation (37), the following fourth-order equation with the shear parameter X as the variable is obtained:

$$(1 + \beta^2)X^4 + 2X^3 + \left[1 - C^2 \left(\frac{G'}{f}\right)^2 (Y + 1)(1 + \beta^2)\right] X^2 - C^2 \left(\frac{G'}{f}\right)^2 (Y + 2)X - C^2 \left(\frac{G'}{f}\right)^2 = 0 \quad (39)$$

Solution of this equation for the single positive real root provides a value of the shear parameter for each value of frequency selected. Obviously, it is necessary that dynamic elastic data for the viscoelastic damping material be available so that the appropriate values of the storage modulus G' and the loss factor β may be inserted in the generalized shear parameter equation.

Optimum shear parameter X_{op} . - Inspection of the relationship for structure loss factor η given by Equation (27) reveals that an optimization of design parameters is required to maximize the degree of structural damping. For values of the shear parameter X equal to zero or infinity, the structure loss factor η is zero. For intermediate values of X , the structure loss factor η is finite and achieves a maximum value when a specific relationship exists between the shear parameter X , the loss factor β , and the geometrical parameter Y . Based on the procedure of establishing the geometrical parameter Y and selecting a viscoelastic damping material having specified storage modulus G' and loss factor β characteristics, the value of the

optimum shear parameter X_{op} may be determined by evaluating $d\eta/dX = 0$ to obtain [Ref. 6]

$$X_{op} = \frac{1}{\sqrt{(Y+1)(1+\beta^2)}} \quad (40)$$

which is shown graphically in Figure 3.4 for parametric variations of the geometrical parameter Y and viscoelastic material loss factor β . The value of the optimum shear parameter varies between zero and one. For the most common designs having values of the geometrical parameter Y between 0.5 and 5, the value of the optimum shear parameter ranges from 0.2 to 0.8.

Maximum structure loss factor η_{max} . The value of the maximum structure loss factor η_{max} which results when the shear parameter achieves its optimum value is determined by substitution of the relation for X_{op} given by Equation (40) into the general structure loss factor relationship given by Equation (27) to obtain [Ref. 6]

$$\eta_{max} = \frac{\beta Y}{Y+2+2\sqrt{(Y+1)(1+\beta^2)}} \quad (41)$$

which is shown graphically in Figure 3.5 for parametric variations of the geometrical parameter Y and the viscoelastic material loss factor β . This design graph clearly demonstrates the desirability of selecting a viscoelastic damping material having a relatively large loss factor β over the frequency and temperature ranges of interest. The curve for $\beta = \infty$ is an upper-bound curve for the maximum structure loss factor based on the use of a pure viscous shear-damping mechanism.

Loss factor ratio η/η_{max} . - The structure loss factor for non-optimum damping conditions can be evaluated in terms of the loss factor ratio η/η_{max} obtained by dividing Equation (27) by Equation (41) and employing the definition of the optimum shear parameter X_{op} given by Equation (40), to obtain

$$\eta/\eta_{max} = \frac{[2 + (Y+2)X_{op}] (X/X_{op})}{1 + [(Y+2)X_{op}] (X/X_{op}) + (X/X_{op})^2} \quad (42)$$

which is shown graphically in Figure 3.6 for parametric variations of the shear parameter ratio X/X_{op} and the parameter $(Y+2)X_{op}$. Consequently, for a value of the shear parameter X other than optimum, Equation (42) or Figure 3.6 can be employed to determine the fraction of maximum loss factor which will be obtained at each frequency for which the value of X has been determined. This design graph indicates that, for practical values of the geometrical parameter Y and optimum shear parameter X_{op} , the structure loss factor η is within 15 per cent of the maximum structure loss factor η_{max} when the shear parameter is one-half or twice its optimum value. Even when the shear parameter is less than four times and greater than one-fourth its optimum value, the structure loss factor η is greater than one-half its maximum value. The noncritical nature of the shear parameter optimization is of considerable practical significance because of the flexibility it introduces into the design process with regard to eliminating the necessity of exactness in designing for optimum conditions.

Optimum frequency parameter Ω_{op} . - When the structure loss factor η is displayed graphically as a function of frequency on log-log coordinates, the curve is approximately symmetrical about the frequency at which the loss factor is a maximum. In certain cases, it may be desirable to optimize the design of a structural composite at the logarithmic midpoint of the frequency range of interest. For the optimum value of the shear parameter, the resonant frequency ratio f_r/f_o defined by Equation (34) becomes

$$\frac{f_{op}}{f_o} = \sqrt{1 + Z_{op} Y} \quad (43)$$

where the optimum coupling parameter Z_{op} is given by Equation (32) with X replaced by X_{op} . From Equations (37) and (43), the optimum structure resonant frequency f_{op} is given by

$$f_{op} = C G' \Omega_{op} \quad (44)$$

where the optimum frequency parameter Ω_{op} defined as

$$\Omega_{op} = \frac{\sqrt{1 + Z_{op} Y}}{X_{op}} \quad (45)$$

is shown graphically in Figure 3.7 for parametric variations of the geometrical parameter Y and the viscoelastic material loss factor β . Since the viscoelastic material storage modulus G' and the optimum frequency parameter Ω_{op} are both frequency dependent, determination of the optimum resonant frequency through an iteration process using Equation (44) is considerably aided by the graphical presentation of Ω_{op} in Figure 3.7.

The thickness of the viscoelastic damping layer H_v required for the structure loss factor η to achieve a maximum value may be determined from Equations (38) and (44) as follows

$$(H_v)_{op} = C_o \left(\frac{G'}{f} \right)_{op} (\Omega_{op}) \quad (46)$$

where the ratio $\left(\frac{G'}{f} \right)_{op}$ is determined at the frequency f_{op} , the optimum frequency parameter Ω_{op} is given by Equation (45) and Figure 3.7, and the damping layer thickness coefficient C_o is given by

$$C_o = \frac{\sqrt{g}}{2\pi} \frac{B_v d_o^2}{Y_o \sqrt{w(EI)_o}} \quad (47)$$

which is equal to the product of the viscoelastic damping layer thickness H_v and the shear parameter coefficient C defined by Equation (38).

Manual Design Procedure

A manual design procedure for the prediction of the loss factor of two-elastic-element viscoelastic shear-damped structural composites may be formulated based on the use of the equations and graphs for design parameters previously presented. Of particular interest to structural design engineers is the variation of the structure loss factor η with frequency. This information provides a rapid means of establishing the degree of damping for the various

structural resonances of interest. The following procedure is based on the assumption that a particular viscoelastic material is employed for which the ratio (G'/f) and the loss factor β are known as a function of frequency for the temperature of interest:

(1) For the cross-section and structural material properties of the structural composite, determine the value of the geometrical parameter Y , the static flexural rigidity $(EI)_0$, the weight per unit length w , the distance between the two neutral planes d , and the length of viscoelastic damping layer B_v in the cross-section plane. The design equations and graphs presented in Section 2 of this report can be used for this purpose.

(2) Calculate the value of the shear parameter coefficient C expressed by Equation (38).

(3) From data for the dynamic elastic characteristics of the viscoelastic damping material, determine the values of the ratio (G'/f) and the loss factor β for a number of frequencies which span the frequency range of interest.

(4) Calculate the resonant frequency ratio f_r/f_0 and the shear parameter X for each frequency selected. A different value of f_r/f_0 will exist in general for each frequency selected since the dynamic coupling between the two elastic elements comprising the structural composite (as determined by the coupling parameter Z) is a function of frequency. As an initial estimate, assume $Z = 0$ and, therefore, $f_r/f_0 = 1$; hence, from Equation (37), the initial estimate of the shear parameter X for each frequency selected for analysis is $X_0 = C(G'/f)$. By entering Figure 3.2 with this value of X and using the appropriate value of β for each frequency, a revised estimate of the value of the coupling parameter $Z = Z_1$ is obtained. With this revised value of Z and the value of the geometrical parameter Y previously calculated, Figure 3.3 is used to determine the resonant frequency ratio $(f_r/f_0)_1$. This value of the resonant frequency ratio is used to calculate the first frequency-dependent estimate of the shear parameter $X_1 = C(G'/f)(f_r/f_0)_1$. This new value of the shear parameter X is used to obtain a revised estimate of the coupling parameter Z_2 and resonant frequency ratio $(f_r/f_0)_2$ to provide a second estimate of the shear parameter X_2 .

This iteration process is repeated until the value of the shear parameter X so determined does not change with a new iteration cycle to within the desired degree of accuracy. In general, three iterations should suffice in determining the value of the shear parameter X at each frequency selected. To determine the uncoupled natural frequency f_0 corresponding to each frequency selected, divide each frequency by its corresponding frequency ratio f_r/f_0 .

(5) Using the value of the geometrical parameter Y and the values of the shear parameter X and the loss factor β for each frequency selected for analysis, the structure loss factor η is calculated by use of Equation (27). Alternately, the structure loss factor η can be determined with the aid of the design graphs presented in Figures 3.4-3.6. Using Figure 3.4, the optimum shear parameter X_{op} is determined for the value of β which applies for each frequency; hence, the value of the shear parameter ratio X/X_{op} can be tabulated. Figure 3.5 is employed to obtain the maximum value of the structure loss factor η_{max} which would occur if $X = X_{op}$. For each value of the ratio X/X_{op} previously determined, Figure 3.6 is used to obtain the value of the loss factor ratio η/η_{max} which, in turn, is multiplied by η_{max} to obtain the value of the structure loss factor η at each frequency selected for analysis.

(6) The frequency at which the maximum structure loss factor given by Figure 3.5 will occur can be calculated by determining the value of the optimum frequency parameter Ω_{op} from Figure 3.7. This determines the value of the ratio $(G'/f)_{op} = 1/C\Omega_{op}$ which is located on the graph of (G'/f) versus frequency for the viscoelastic material being employed to provide the value of the optimum resonant frequency f_{op} . This procedure may require an iteration process since, in general, the loss factor β is dependent upon frequency. For the particular structural composite design being evaluated, the optimum resonant frequency f_{op} may be far removed from the frequency range of interest and, consequently, would be of academic interest only, as it adds little to the understanding of the damping performance of the structural composite.

This manual design procedure will result in a tabulation of values of structure loss factor η and uncoupled natural frequencies f_0 for each frequency used in the iteration process. Since η and f_0 are mathematically continuous

functions of frequency, curves can be passed through the discrete calculated data points to obtain continuous functions of frequency $f = f_r$ versus the uncoupled natural frequency f_o , and structure loss factor η versus frequency $f = f_r$.

It may be desired to obtain the maximum value of structure loss factor η_{\max} at a specific frequency. The optimum design procedure for this requirement is as follows:

(1) For the specified frequency $f = f_{op}$, determine the values of the viscoelastic material storage modulus G' and loss factor β .

(2) With this value of β and an initial assumption that $Y = Y_o$, Figure 3.7 is used to determine the initial estimate of the optimum frequency parameter Ω_{op} .

(3) Calculate the value of the damping layer thickness coefficient C_o using Equation (47).

(4) Using the values of C_o , G' and Ω_{op} determined, calculate the initial estimate of the optimum damping layer thickness $(H_v)_{op}$ using Equation (46).

(5) For greater accuracy in determining $(H_v)_{op}$, the initial estimate of its value can be used to determine a more accurate estimate of the geometrical parameter Y by use of Equations (14) and (15). This new value of Y is then used to recalculate the value of the optimum frequency parameter Ω_{op} and the optimum damping layer thickness $(H_v)_{op}$. Generally, one iteration is sufficient because of the weak dependence of the geometrical parameter on the viscoelastic damping layer thickness.

(6) Using the value of the optimum viscoelastic damping layer thickness $(H_v)_{op}$ determined, the value of the shear parameter coefficient $C = C_o/H_v$ is calculated and a prediction of the resonant frequency versus the uncoupled natural frequency and the structure loss factor versus the resonant frequency is made following the general procedure previously outlined.

Use of the optimum design procedure allows maximum damping to be attained in the region of a specific structural resonance at which excessive vibration

excitation is anticipated and a very high degree of vibration reduction is required. However, it is possible that the value of $(H_V)_{op}$ for a particular structural composite design is impractical from a fabrication point of view or does not satisfy the analytical requirement that H_V be small compared to the thickness of the elastic elements comprising the structural composite. This may preclude design optimization at the desired frequency; however, determination of $(H_V)_{op}$ provides an indication of how close a practical non-optimum design can be to the optimum design. Therefore, within the practical limitations of fabrication and performance prediction capabilities, the possibility exists to tailor viscoelastic shear-damped structural composite designs to maximize damping at particularly troublesome frequencies.

Automated Design Procedure

The necessity for using a manual iteration process to predict the structure loss factor versus frequency characteristics of two-elastic-element viscoelastic shear-damped structural composites can be eliminated by programming the generalized shear parameter relation given by Equation (39) on a digital computer to determine the single positive real root of the equation for each frequency selected, which gives the values of the shear parameter X required. Alternately, the manual design procedure can be programmed, which involves using Equations (32), (34) and (37) in an automated iteration process to determine the shear parameter X for each frequency selected. The second method has been found to be the more rapid one. The value of the shear parameter coefficient C is determined by use of Equation (38) and, for each frequency f specified, the values of the storage modulus G' and loss factor β are obtained from the dynamic elastic data for the viscoelastic damping material employed. The values of shear parameter X determined by one of the methods described above for each frequency may be stored in the computer for subsequent insertion into the relation for structure loss factor η given by Equation (27). Also, the values of the shear parameter X , along with values of C , (G'/f) , and the frequency $f = f_r$, can be inserted into Equation (37) to obtain values of the uncoupled natural frequency f_o corresponding to each frequency.

A curve passed through the discrete data points provides continuous functions of frequency $f = f_r$ versus the uncoupled natural frequency f_o , and structure loss factor η versus frequency $f = f_r$. Since inaccuracies associated with graphical solutions and approximations resulting from iteration processes are avoided, the automated design procedure provides a more accurate prediction of the damping and frequency characteristics than the manual design procedure previously outlined. Perhaps more important is the fact that the automated design procedure provides a more rapid means of calculating the damping and frequency characteristics.

In a similar manner, a digital program can be written to perform the iteration required (as outlined in the manual design procedure) to determine the optimum viscoelastic damping layer thickness $(H_v)_{op}$ required to obtain the maximum value of structure loss factor η_{max} at a specific frequency. With each cycle of iteration, a more accurate estimate of the geometrical parameter Y is obtained which provides greater accuracy in the prediction of $(H_v)_{op}$. The iteration process can be continued until values of $(H_v)_{op}$ are determined to within a specified degree of accuracy. Having determined the value of $(H_v)_{op}$, the automated design procedure previously described may be employed to predict the structure loss factor versus frequency and uncoupled natural frequency characteristics.

Temperature Effects

The effect that temperature has on the viscoelastic damping material loss factor β and the storage modulus G' is much the same as that of frequency except that increasing temperature corresponds to decreasing frequency and decreasing temperature corresponds to increasing frequency. For very high environmental temperatures, the damping material operates in its "rubbery" region, and since little energy is dissipated, the structure loss factor is small. For very low environmental temperatures, the damping material operates in its "glassy" region, and again since little energy is dissipated, the structure loss factor is small. In the design procedures previously outlined, the temperature was considered constant. To cover a temperature range of interest, loss factor versus frequency curves can be

made for various temperatures throughout the temperature range of interest. Of course, it is also possible to construct loss factor versus temperature curves for various frequencies of interest. These curves will have shapes similar to the loss factor versus frequency curves and, in fact, the frequency and temperature dependence of the viscoelastic properties of high polymer damping materials are interrelated by physical laws [Ref. 11, 12].

Other Design Considerations

By applying the viscoelastic damping techniques described, structural composites having large loss factors can be constructed. However, there are other design considerations that are frequently as important as the energy dissipation capability of the structure. The following are discussions of the static stiffness, weight and static load distribution characteristics of viscoelastic shear-damped structural composites.

Static stiffness. - When compared on the basis of equal weight, the static stiffness of a viscoelastic shear damped structural composite is less than that of a conventional structural member. Consequently, if a conventional structural member having a relatively low loss factor is to be replaced by a viscoelastic shear-damped structural composite of equal weight, a reduction in static stiffness of the structural member can be expected. However, due to the coupling between the individual elastic elements of the structural composite, as determined by the coupling parameter Z , the dynamic stiffness of the structural composite will always be greater than its static stiffness.

The variation of the static stiffness K_0 of a viscoelastic shear-damped structural composite with the value of the geometrical parameter Y_0 is shown graphically in Figure 3.8, and is given by [Ref. 8]

$$\frac{K_0}{K_\infty} = \frac{1}{Y_0 + 1} \quad (48)$$

where K_∞ is the stiffness of the structure when the individual elastic elements of the structural composite are completely coupled. It is assumed that the

viscoelastic damping material is soft compared to the stiffness of the structural materials employed in the structural composite and, therefore, the static stiffness of the structure is determined by the static flexural rigidity $(EI)_0$. Since the stiffness K_∞ represents the stiffness of the structural member prior to adapting its cross-section to accommodate a viscoelastic shear-damping mechanism, Figure 3.8 provides a comparison between the static stiffness properties of conventional and viscoelastic shear-damped structural members having the same weight.

A substantial decrease in the static stiffness of the structure results even for relatively low values of the geometrical parameter Y_0 . The static stiffness of the viscoelastic shear-damped structural composite is one-half that of the equal-weight conventional structural member when the geometrical parameter $Y_0 = 1$. For values of the geometrical parameter $Y_0 = 2$ and $Y_0 = 3$, the static stiffness is one-third and one-fourth that of the conventional structural member, respectively. The geometrical parameter Y should have a high value to obtain a large structure loss factor η and a low value to maintain a relatively high static stiffness K_0 for a specified weight of structure; therefore, selection of the value of the geometrical parameter should be based on the relative importance of damping and static stiffness as design requirements.

Weight. - When compared on the basis of equal static stiffness, the weight of a viscoelastic shear-damped structural composite is greater than that of a conventional structural member. Consequently, if a conventional structural member is to be replaced by a viscoelastic shear-damped structural composite of equal static stiffness, an increase in weight can be expected. In general, there is no direct relationship between weight and the geometrical parameter Y . However, for a composite structural beam or plate comprised of a lamination of two solid sheets of the same material, the following relation can be developed

$$\frac{W_d}{W_s} = \sqrt[3]{Y_0 + 1} \quad (49)$$

where W_d is the weight of a viscoelastic shear-damped structural composite and W_s is the weight of a solid plate of the same material having a stiffness equal to the static stiffness of the damped plate. This relation is shown graphically in Figure 3.9.

For a value of the geometrical parameter $Y_0 = 1$, there is a 26 per cent increase in weight. The rate of increase in weight drops off as Y_0 increases so that for $Y_0 = 3$ (sandwich beams), the weight increase is 59 per cent and does not become 100 per cent until a value of $Y_0 = 7$ is reached. Here again, the geometrical parameter Y should have a high value to obtain a large structure loss factor η and a low value to maintain a relatively light structure weight W_d for a specified static stiffness. Consequently, structure weight, stiffness and damping must be considered as joint design criteria.

Static load distribution. - The static load distribution specifies the fraction of the total statically applied load which is carried by each of the elastic structural elements comprising the structural composite and, therefore, is useful in performing stress analyses for static loading. Each elastic element in the viscoelastic shear-damped structural composite undergoes the same transverse deflection under bending; therefore, the load carried by each elastic element is in proportion to its flexural rigidity, as follows

$$\frac{P_i}{P} = \frac{E_i I_i}{(EI)_0} \quad (50)$$

where P_i is the load carried by an elastic element, $E_i I_i$ is the flexural rigidity of that elastic element, P is the total applied static load, and $(EI)_0$ is the static flexural rigidity of the structural composite. For example, the relations for static load distribution for a composite structural beam or plate comprised of a lamination of two solid sheets of arbitrary material given by

$$\frac{P_1}{P} = \frac{MR^3}{MR^3 + 1} ; \frac{P_2}{P} = \frac{1}{MR^3 + 1} \quad (51)$$

are presented graphically in Figure 3.10 for parametric variations of the modulus ratio $M = E_1/E_2$ and the thickness ratio $R = H_1/H_2$.

SECTION 4: EXPERIMENTAL VERIFICATION OF DESIGN

PROCEDURE FOR TWO-ELASTIC-ELEMENT STRUCTURAL COMPOSITES

This section of the report presents a comparison of the theoretical predictions and experimental measurements of the structure loss factor of two-elastic-element viscoelastic shear-damped structural composite beams. Cross-sections of the experimental structural specimens, which included laminated beams comprised of solid sheets, solid and honeycomb sheets, honeycomb sheets, and channel sections, are presented in Figure 4.1. The structural composites were fabricated from various combinations of structural materials including aluminum, steel, and fibre-glass. The thickness of the viscoelastic damping layer H_v was maintained reasonably constant during the experiments which were performed at temperatures ranging between 75° and 90°F.

The following are discussions of the prediction and measurement techniques for the structure loss factor, followed by a comparison of the theoretical and experimental values for beam specimens having designs indicated in Figure 4.1.

Design Procedure Application Example

The design procedures presented in Section 3 of this report have been used to predict the loss factor versus frequency characteristics of 27 different beam specimens. As an example of the application of the manual and automated design procedure, the numerical details of one of the beam designs will be delineated.

Consider a structural composite cross-section comprised of two solid rectangular sheets laminated with a thin layer of viscoelastic damping material, as shown in Figure 4.1(a). The modulus, weight density, and dimension characteristics are as follows:

$$(A) \quad E_1 = E_2 = 10.3 \times 10^6 \text{ psi}; \quad \gamma_1 = \gamma_2 = 0.098 \text{ lb./in.}^3$$

$$(B) \quad H_1 = 0.0628 \text{ in.}; \quad H_2 = 0.0629 \text{ in.}$$

$$(C) H_v = 0.0055 \text{ in.}$$

$$(D) B = 3.0 \text{ in.}$$

From these characteristics, the following modulus and dimension ratios are calculated:

$$(A) M = E_1/E_2 = 1.0$$

$$(B) R = H_1/H_2 \approx 1.0$$

$$(C) V = H_v/(H_1 + H_2) = 0.0435$$

The following represents the calculations performed in accordance with the various steps in the manual design procedure outlined in Section 3 of the report:

(1) Using the modulus and dimension data determined and the design information presented in Figures 2.11(A) and (B), the following geometrical properties are calculated:

$$(A) Y_o = 3.0; Y/Y_o = 1.18; Y = 3.54$$

$$(B) (EI)_o = 1,287.5 \text{ lb.} - \text{in.}^2$$

$$(C) w = 0.037 \text{ lb./in.}$$

$$(D) d = 0.068 \text{ in.}; d_o = 0.0625 \text{ in.}$$

$$(E) B_v = 3.0 \text{ in.}$$

(2) The value of the shear parameter coefficient C is calculated using Equation (38) to obtain $C = 0.327$.

(3) The value of the ratio (G'/f) and loss factor β for a number of frequencies which span the frequency range of interest (10 to 1000 Hz) and for the temperature of interest are determined from a graph of the dynamic elastic characteristics of the viscoelastic material, such as that presented in Figure 4.2 for the viscoelastic damping material employed in the structural composite (3M No. 466 adhesive transfer tape). The data for the viscoelastic shear damping material presented in Figure 4.2 indicates that the loss factor β has a reasonably constant value over the frequency range of interest, whereas the G' and G'/f characteristics vary as a power function of frequency. Temperature variations in the neighborhood of room temperature have a minor

effect on the value of the loss factor and a substantial effect on the G and G'/f characteristics. This graph clearly demonstrates the significant effect which temperature may have on the dynamic elastic characteristics of visco-elastic damping materials and consequently on the loss factor characteristics of a structural composite incorporating the material in a shear-damping mechanism. For the discrete frequencies selected for analysis, which are indicated in the design example data chart presented in Figure 4.3, and a specified temperature of 75°F , a relatively constant value of $\beta = 1.4$ and the values of G'/f indicated in Figure 4.3, are obtained from Figure 4.2.

(4) The resonant frequency ratio f_r/f_o and the shear parameter X for each discrete frequency is determined by an iteration process using Figures 3.2 and 3.3. As an initial estimate for each frequency, choose the values $Z = 0$ and hence, $f_r/f_o = 1$. For example, for $f = 10$ Hz, $X_o = C(G'/f) = 1.52$. Enter Figure 3.2 with $\beta = 1.4$ and $X = 1.52$ to obtain a value $Z_1 = 0.77$. Enter Figure 3.3 with $Z = 0.77$ and $Y = 3.54$ to obtain a revised estimate of the resonant frequency ratio $(f_r/f_o)_1 = 1.95$; this value is used in Equation (37) to calculate $X_1 = 2.96$. With this new value of the shear parameter, values of $Z_2 = 0.88$ and $(f_r/f_o)_2 = 2.03$ are obtained from Figures 3.2 and 3.3, respectively, which give a value $X_3 = 3.08$ using Equation (37). An additional iteration cycle results in $Z_3 = 0.88$ indicating that further iterations are not required for the degree of accuracy associated with reading the design graphs. Hence, values of $f_r/f_o = 2.03$ and $X = 3.08$ are inserted in the chart of Figure 4.3 for a frequency of 10 Hz. Since the discrete frequency $f = 10$ Hz actually represents a possible resonant frequency of the structural composite beam, the value of the uncoupled natural frequency is obtained by dividing the selected frequency $f = f_r$ by the resonant frequency ratio f_r/f_o to obtain a value of $f_o = 4.93$ Hz.

(5) For values of $\beta = 1.4$ and $Y = 3.54$, Figures 3.4 and 3.5 indicate that $X_{op} = 0.27$ and $\eta_{max} = 0.385$, respectively. Calculating $X/X_{op} = 11.4$, Figure 3.6 with $(Y+2)X_{op} = 1.5$ indicates that $\eta/\eta_{max} = 0.28$. Hence, the structure loss factor $\eta = 0.108$. This procedure is repeated for each frequency selected for analysis in the frequency range of interest, and the results are recorded in the chart of Figure 4.3. A curve is passed through discrete data points to develop the continuous functions for loss factor η versus frequency

and resonant frequency f_r versus uncoupled natural frequency f_o presented graphically in Figure 4.4. In this example, the viscoelastic damping material loss factor β was considered essentially independent of frequency so that the optimum shear parameter X_{op} and the maximum structure loss factor η_{max} were also independent of frequency. In general, however, β and hence X_{op} and η_{max} will vary with frequency.

The automated design procedure outlined in Section 3 of the report may be applied by introducing into the digital computer program the values of the geometrical parameter $Y = 3.54$, shear parameter coefficient $C = 0.327$, loss factor $\beta = 1.4$, and appropriate values of the ratio G'/f for each frequency selected for analysis. The output from the computer is presented in the chart below. The difference in the value of η and f_o shown in

DIGITAL COMPUTER OUTPUT FOR DESIGN EXAMPLE					
G'/f	β	X	f_o	η	$f=f_r$
4.65000	1.40000	3.08354	4.91610	0.10463	10
3.40000	1.40000	2.20986	10.03142	0.13894	20
2.80000	1.40000	1.78965	15.30129	0.16448	30
2.20000	1.40000	1.36884	26.19738	0.20105	50
1.86000	1.40000	1.13029	37.55250	0.22944	70
1.60000	1.40000	0.94814	55.01309	0.25648	100
1.20000	1.40000	0.66996	116.78366	0.30930	200
1.00000	1.40000	0.53348	183.32575	0.34012	300
0.78000	1.40000	0.38832	327.40796	0.37205	500
0.67100	1.40000	0.31978	478.83544	0.38268	700
0.56500	1.40000	0.25635	718.51302	0.38506	1000

Figure 4.3 and in the chart of the digital computer output indicate the degree of accuracy that can be expected using the manual design procedure. For this particular structural composite design, a comparison of the predicted and experimentally determined values of the structure loss factor η is presented in Figure 4.6(C). The difference between the theoretical prediction and the experimental measurements indicated by Figure 4.6(C) is considered typical of that which can generally be expected.

For a free-free beam of length L , the natural frequency equation is given by [Ref. 9]

$$(f_o)_n = \frac{\alpha_n \sqrt{g}}{2\pi L^2} \sqrt{\frac{(EI)_o}{w}} \quad (52)$$

where $\alpha_n = 22.4, 61.7, 121$ and 200 for the first four modes of vibration. Using this equation and the values of $(EI)_o$ and w given above for a beam length $L = 30$ inches, the values of the uncoupled natural frequency f_o for the first four modes of vibration are 14.6, 40, 78.5 and 130 Hz, respectively. By use of the graphical presentation of the resonant frequency f_r versus the uncoupled natural frequency f_o shown in Figure 4.4(a), the resonant frequency for the first four modes of vibration are determined and presented in the chart below. For purposes of comparison, the experimentally determined resonant

Mode	Theoretical f_r (Hz)	Experimental f_r (Hz)
1	28	24
2	74	61
3	140	127
4	220	175

frequencies for the first four modes of vibration of the free-free beams are also presented. The agreement is reasonably good in view of the fact that the accelerometer and counter weight placed on the beam, as shown in Figure 4.5, would cause a reduction in the experimental resonant frequency because of the additional mass loading.

The automated design procedure was employed to predict the structure loss factor as a function of frequency for 27 different two-elastic-element structural composite beam specimens in a manner similar to that outlined in the design example. A discussion of the method employed to experimentally determine the structure loss factor versus frequency follows.

Measurement of Structure Loss Factor

The decay rate method was selected to measure the loss factor of the viscoelastic shear-damped beam specimens since the measurements can be made with considerable speed and the method is generally accepted by researchers in the field of structural damping [Ref. 13-15]. Repeated measurements of vibration decay can be made on a structural member under the same conditions in rapid sequence thereby providing an accurate measurement of damping through averaging of data. If the rate of decay is measured in terms of the reverberation time T_{60} , the structure loss factor η is given by

$$\eta = \frac{2.2}{f_r T_{60}} = \frac{2.2\tau_r}{T_{60}} \quad (53)$$

where T_{60} is the time required for the amplitude of free vibration to be attenuated by 60 db (corresponding to a factor of 1000), f_r is the resonant frequency of the decaying vibration for the particular mode of vibration being evaluated, and $\tau_r = 1/f_r$ is the period of the vibration at each particular resonance.

The experimental system for measuring the loss factor of the viscoelastic shear-damped beam specimens is shown in Figure 4.5; the instrumentation for the experimental system is identified in the chart presented below.

INSTRUMENTATION FOR MEASUREMENT OF STRUCTURE LOSS FACTOR		
Instrumentation	Manufacturer	Model Number
Electrodynamic Exciter (Magnetic Housing and Driver Coil)	Acoustic Research, Inc.	12W-0808(modified) and 12W-0114
Accelerometer	Endevco	2233
Cathode Follower Amplifier	Columbia Research Lab.	6003
High-Pass Filter	Krohn-Hite	330-M
Decay Rate Meter	Spencer-Kennedy Lab.	507
Power Amplifier	Dynaco	Mark III
Oscilloscope	Tektronix	564/2867/3A3
Harmonic Oscillator	Hewlett-Packard	200CDR

The structural specimen is supported vertically by a string suspension. A small driver coil is cemented to the specimen in a manner which will add a minimum amount of stiffness or weight and allow centering of the driver coil within the magnetic housing of the electrodynamic exciter, which provides a linear magnetic field for the driver coil. The electrodynamic exciter, which is driven by the harmonic oscillator through a power amplifier, is capable of delivering 25 watts of power to a beam specimen for an extended period of time at a maximum linear peak-to-peak displacement of one half inch.

The response of the beam specimen is detected by the accelerometer which is mounted near the end of the beam with a counter weight of equal magnitude mounted on the opposite end of the beam for purposes of balance. The high-pass filter is used to reject all frequencies less than the particular resonant frequency at which the loss factor is being measured. The decay rate meter provides electronic switching between two alternating functions: (1) processing the signal from the high-pass filter through a logarithmic amplifier, and (2) generating a calibrated logarithmic decay signal. The oscilloscope provides alternate displays of the logarithmic decay signal representing the beam vibration and the calibrated logarithmic decay signal.

The experimental procedure for the measurement of structure loss factor is as follows. The structural specimen is excited by harmonic vibration and, when a resonant frequency is located, allowed to attain a steady-state vibration condition. The cut-off frequency of the high-pass filter is set approximately at the resonant frequency. As part of the electronic switching function performed by the decay rate meter, the excitation vibration is abruptly removed from the structure and the ensuing vibration decay is sensed by the accelerometer. The accelerometer signal is processed through the cathode follower amplifier, high-pass filter and decay rate meter. The decay rate meter processes the signal through a logarithmic amplifier and generates a separate calibrated logarithmic decay signal. The structure vibration decay signal and the calibrated decay signal are alternately displayed on the oscilloscope on a repetitive basis thereby allowing adjustment of the calibrated decay signal to match the vibration

decay signal. When the calibrated decay signal is adjusted to match the structure vibration decay signal, the value of the reverberation time T_{60} is read from the decay rate meter and the structure loss factor is calculated from Equation (53).

Loss factor measurements are made at the various resonances of the structure and, therefore, data is obtained at discrete frequencies. However, a curve may be passed through the discrete loss factor data points to generate a description of loss factor as a continuous function of frequency. The connotation is that if the structure were to resonate at an intermediate frequency, the continuous curve of loss factor versus frequency indicates the loss factor which exists for that particular mode of vibration.

The filter in the experimental system places a limitation on the maximum value of structure loss factor which can be measured accurately. Because of its "ringing" characteristic, the filter itself exhibits a decay rate characteristic and, hence, the experimental system may be employed only to measure vibration decay rates which are less than that of the filter. The active high-pass filter was selected because of its high rejection rate (24 db/octave) below the cut-off frequency and its favorable ringing characteristic. Based on the fact that the effective loss factor of the filter was generally greater than 0.5 over the frequency range of interest (10 Hz to 1000 Hz), data can confidently be obtained for structure loss factor measurements as high as 0.4. Actually, even if the range of loss factor measurement was not limited by the filter ringing characteristic, there would be another limitation imposed by the physical difficulty encountered in interpreting the decay of a signal having a few cycles of oscillation, which would be the case for values of loss factor greater than 0.4. It is concluded that the experimental system is capable of measuring maximum values of structure loss factor equal to 0.4 with a high degree of confidence; however, a sharp decrease in confidence exists for measurements between 0.4 and 0.5.

Theoretical and Experimental Structure Loss Factor Data

Theoretically predicted and experimentally determined values of structure loss factor are shown graphically in Figures 4.6 to 4.10 for 27 different viscoelastic shear-damped composite structural beams having cross-sections illustrated in Figure 4.1. The relevant modulus and dimension data are presented with each graph as well as the value of the geometrical parameter Y . Theoretical predictions are presented as a continuous curve and the results of measurements are indicated by discrete data points.

Structure loss factor data for 12 composite structural beams comprised of a lamination of two solid sheets are shown in Figure 4.6 for the following structural material combinations: (A)-(F) both solid sheets aluminum; (G)-(J) one solid sheet steel and one solid sheet aluminum; (K), (L) one solid sheet fibre-glass and one solid sheet aluminum. In addition to the different modulus combinations, data are provided for a range of elastic element thickness ratios. In general, the experimental values of structure loss factor are greater than the theoretical values for the aluminum-aluminum combinations; the experimental values are extremely close to the theoretical values for the steel-aluminum combinations; finally, the experimental values are less than the theoretical values for the fibre-glass-aluminum combinations.

Structure loss factor data for 8 composite structural beams comprised of a lamination of a solid and a honeycomb sheet are shown in Figure 4.7 for the following structural material combinations: (A)-(F) both solid and honeycomb sheets aluminum; (G) solid sheet steel and honeycomb sheet aluminum; (H) solid sheet fibre-glass and honeycomb sheet aluminum. For the aluminum-aluminum combinations, data are provided for a range of elastic element thickness ratios. In general, the experimental values of structure loss factor are less than the theoretical values for the aluminum-aluminum and fibre-glass-aluminum combinations, whereas the experimental values are greater than the theoretical values for the steel-aluminum combination.

Structure loss factor data for 3 composite structural beams comprised of a lamination of aluminum honeycomb sheets having various combinations of skin thicknesses are shown in Figure 4.8 (A-C). The experimental values of structure loss factor are less than the theoretical values in all cases.

Structure loss factor data for 3 composite structural beams comprised of a lamination of an aluminum or steel solid sheet and an aluminum channel section are shown in Figure 4.9. For the aluminum-aluminum combinations represented in Figure 4.9(A,B), the experimental values of structure loss factor are equal to or greater than the theoretical values whereas, for the steel-aluminum combination represented in Figure 4.9(C), the experimental values are equal to or less than the theoretical values.

Structure loss factor data for one composite structural beam comprised of a back-to-back lamination of two aluminum channel sections is shown in Figure 4.10. The experimental values of the structure loss factor are greater than the theoretical values.

Sources of errors. - The difference between the predicted and measured values of structure loss factor indicated in Figures 4.6 to 4.10 provide specific guidelines for anticipated discrepancies between theory and measurement for the various cross-section design configurations. No general rule for correcting theoretical predictions of loss factor for two-elastic-element structural composites is immediately apparent. However, all experimental data for structure loss factor consistently exhibits the same trend with frequency as predicted by the theory. Furthermore, structural composite designs having larger values of the geometrical parameter Y consistently exhibit higher values of the structure loss factor.

An obvious source of error is the energy dissipation which is introduced by damping mechanisms other than that involving the viscoelastic damping material; these would include air, structural material, and specimen support damping mechanisms. The theory assumes that the viscoelastic shear-damping mechanism is the only one present. This assumption appears to be justified since the degree of damping obtained from properly designed viscoelastic shear-damping mechanisms is substantially greater than that available from other damping mechanisms. Also, there will be errors due to the fact that a particular structural composite will not, in general, satisfy all of the basic assumptions enumerated on page 36.

The errors involved in experimentally determining the structure loss factor η can be separated into two categories. The first category

encompasses those errors involved with not having a beam with the dimensions and physical properties that were assumed. In the second category are those errors involved with not measuring the loss factor exactly.

The errors in the first category can be divided into those involved with the parameters Y , X , and β . The geometrical parameter Y is a straightforward calculation depending on the dimensions of the cross-section and the modulus of elasticity of the structural material used. For most structural materials, the modulus of elasticity can be (or has been) accurately determined. One source of error in calculating Y is in not knowing the dimensions exactly (e.g., honeycomb structures). Also, the effects of the core are usually neglected when dealing with honeycomb structures. Another possible source of error in determining Y is to read the design graphs incorrectly and/or make mistakes in the mathematical calculations.

The shear parameter X is a function of the width B_v and thickness H_v of the viscoelastic damping layer, the distance between the neutral axis of the two elastic elements d , the geometrical parameter Y , the static flexural rigidity $(EI)_0$, the weight per unit length of the beam w , the frequency of vibration f , the viscoelastic material loss factor β , and the storage modulus of the viscoelastic material G' . The width of viscoelastic damping layer B_v in most cases can be determined with good accuracy. The thickness H_v , however, is more difficult to determine accurately, with unfortunate consequences. For a nominal thickness $H_v = 0.005$ in., an error in measurement of 0.001 in. can cause a 20 per cent error in the shear parameter which, in some cases, can cause a 20 per cent error in the structure loss factor. The distance d can be determined with considerable accuracy, except in those cases where it is very small; however, these cases are poor designs with regard to structural damping. The problem of determining $(EI)_0$ is the same as for Y . Since the density of materials generally is accurately determined, the problem of determining w is the same as for Y . The frequency f is assumed given and therefore does not represent a source of error.

There remains the loss factor β and the storage modulus G' of the viscoelastic damping material to consider. These quantities are not easily

determined and they are quite variable, depending on many factors. Frequency and temperature have the biggest effects on the values of β and G' ; the magnitude and history of the shear strain also may affect their values [Ref. 16].

Statistical analysis of experimental data. - The experimentally determined values of structure loss factor η_e are plotted versus their theoretically predicted values η_t in Figure 4.11, where the data point symbols are identified in the chart below. A linear regression of η_e on η_t ,

SYMBOLS FOR EXPERIMENTAL STRUCTURE LOSS FACTOR DATA		
Configuration	Symbol	Structural Material Combination
Laminated Beams	● ○ ⊕	(E ₁) Aluminum (E ₂) Aluminum (E ₁) Steel (E ₂) Aluminum (E ₁) Fibre-glass (E ₂) Aluminum
Constrained Honeycomb	■ □ none	(E ₁) Aluminum (E _H) Aluminum (E ₁) Steel (E _H) Aluminum (E ₁) Fibre-glass (E _H) Aluminum
Laminated Honeycomb	+	(E ₁) Aluminum (E ₂) Aluminum
Constrained Channel	▲ Δ	(E ₁) Aluminum (E ₂) Aluminum (E ₁) Steel (E ₂) Aluminum
Double Channel	×	(E ₁) Aluminum (E ₂) Aluminum

representing a least squares fit for η_e , was obtained for the 118 data points for which the equation is

$$\eta_e = 0.001 + 1.05 \eta_t \quad (53)$$

The regression line indicates that the damping accountable from sources other than the viscoelastic shear-damping mechanism is equivalent to an effective structure loss factor of 0.001; also, the structure loss factor is predicted five per cent too low on the average. However, these numbers are both quite small and it is felt that what is more significant is that the equation for this line is approximately $\eta_e \approx \eta_t$, which supports the theory.

A statistical analysis was made of the 118 values of the loss factor ratio η_e/η_t . The accepted statistical mean for variables which are ratios is the geometrical mean [Ref. 17]. The geometric mean of η_e/η_t for all the experiments is 1.006, indicating excellent agreement between theory and experiment. The statistical distribution of the ratio η_e/η_t is naturally skewed, since about half of the values fall between zero and one, and the other half between one and infinity. Therefore, it is reasonable to determine the statistical distribution of the logarithm of the ratio η_e/η_t . This is in agreement with using the geometric mean since the logarithm of the geometric mean is the arithmetic mean of the logarithms of the values being analyzed.

The standardized probability density of $\ln(\eta_e/\eta_t)$ is shown compared to that of a normal distribution in Figure 4.12, where the standardized value of $\ln(\eta_e/\eta_t)$ is given by the ratio of the difference between the value of $\ln(\eta_e/\eta_t)$ and the mean value to the standard deviation (root-mean-square) of the $\ln(\eta_e/\eta_t)$ values. It is approximately a normal distribution, which would be an expected result if the distribution is caused by many factors, none of which represents a predominant influence. The previous discussion of sources of errors suggests that this is the case for the problem related to the prediction and measurement of structure loss factor.

The standard deviation of $\ln(\eta_e/\eta_t)$ is ± 0.28 . Therefore, using the mean value $\eta_e/\eta_t \approx 1.0$ and assuming a normal distribution, it can be expected that 68 per cent of the values of η_e/η_t will be between 0.76 and 1.32 and 95 per cent will be between 0.57 and 1.75. This value of the standard deviation, while somewhat high, seems reasonable considering the previous discussion on errors. As an alternate statistical measure, the per cent error relative to η_t defined by $100(\eta_e - \eta_t)/\eta_t$ indicates that 68 per cent of the experiments will have an error between +32 per cent and -24.5 per cent. Based on the results of the statistical analysis of the experimental data compared to the theoretical predictions, it is concluded that the existing theory and design procedures for calculating the loss factor of two-elastic-element viscoelastic shear-damped structural composites is satisfactory within accepted engineering accuracy.

CONCLUSIONS

The research investigation has resulted in (1) the generation of extensive design data for the geometrical properties of viscoelastic shear-damped structural composites, (2) the development of manual and automated design procedures for predicting the loss factor of two-elastic-element viscoelastic shear-damped structural composites, and (3) the performance of laboratory experiments which have confirmed the adequacy of the existing theory and design procedures developed. Specific conclusions drawn are:

(1) The "geometrical parameter" determined solely by cross-section geometry and the moduli of the elastic elements comprising the structural composite is a fundamental design parameter which plays a significant role in the performance of all structural composite designs incorporating viscoelastic shear-damping mechanisms.

(2) With regard to predicting the structure loss factor, the assumption that the effective flexural rigidity is the real part of the complex flexural rigidity has been confirmed.

(3) Based on a statistical analysis of the experimentally determined values of structure loss factor, the existing theory and design procedures for calculating the loss factor of two-elastic-element viscoelastic shear-damped structural composites is satisfactory within accepted engineering accuracy.

It is anticipated that the results of the research investigation will prove useful to structural design engineers, especially those concerned with controlling the vibration response of air-borne and aerospace structural assemblies.

Recommendations for additional research work on structural composites with shear-damping mechanisms include:

(1) Theoretical analysis and experimental verification of structure loss factor for three-elastic-element viscoelastic shear-damped structural composites.

(2) Evaluation of the accuracy of various methods for predicting the effect of damping on the structural resonant frequencies.

(3) Development of applicable equations and design graphs for the structure loss factor and resonant frequency of structural composites with viscous shear-damping mechanisms.

(4) Application of shear-damping structural design techniques to realistic structural members (prediction and experimental verification) beginning with relatively simple constructions, such as frames and chassis, and concluding with more complex assemblies such as scale models of spacecraft structures.

REFERENCES

1. Ruzicka, J. E., ed.: Structural Damping, ASME, New York, 1959.
2. Oberst, H.; and Schommer, A. : Verbundblechsysteme mit Optimal Eingestellten Schwingungsdämpfenden Kunststoff-Zwichenschichten (Laminated Systems with Optimally Adjusted Vibration Damping Polymers as Intermediate Layers). Kunststoffe, vol. 55, 1965.
3. Kerwin, E. M., Jr. : Damping of Flexural Waves by a Constrained Viscoelastic Layer. J. Acoust. Soc. Am., vol. 31, no. 7, July 1959, pp. 952-962.
4. Ungar, E. E.; and Ross, D.: Damping of Flexural Vibrations By Alternate Visco-Elastic and Elastic Layers. Proceedings of the Fourth Annual Conference on Solid Mechanics, University of Texas, Austin, Texas, Sept. 1959, pp. 468-487.
5. Ungar, E. E.: Loss Factors of Viscoelastically Damped Beam Structures. J. Acoust. Soc. Am., vol. 34, no. 8, Aug. 1962, pp. 1082-1089.
6. Ungar, E. E.: Highly Damped Structures. Machine Design, Feb. 14, 1963, pp. 162-168.
7. Ruzicka, J. E.: Damping Structural Resonances Using Viscoelastic Shear-Damping Mechanisms. J. Eng. Industry, (Series B of Trans. ASME), vol. 81, no. 4, Nov. 1961, pp. 403-424.
8. Ruzicka, J. E.: Vibration Response Characteristics of Viscoelastic-Damped Structures. The shock and Vibration Bulletin, No. 34, Part 5, Feb. 1965, pp. 155-175.
9. Young, D.; and Felgar, R. P.: Tables of Characteristic Functions Representing Normal Modes of Vibration of a Beam. University of Texas Publication No. 4913, 1949.
10. Macduff, J. N.; and Felgar, R. P.: Vibration Design Charts. Trans. ASME, vol. 79, 1957, pp. 1459-1475 (also available in Machine Design, vol. 29, no. 3, 1957, p. 109).
11. Linhardt, F.; and Oberst, H.: Über die Temperaturabhängigkeit Schwingungsdämpfender Kunststoffe (The Effect of Temperature on the Vibration Damping Characteristics of Plastics). Acustica, vol. 11, 1961, pp. 255-264.
12. Oberst, H.; Bohn, L; and Linhardt, F.: Schwingungsdämpfende Kunststoffe in der Lärmbekämpfung (Vibration Damping Plastics for Noise Reduction). Kunststoffe, vol. 51, 1961, pp. 495-502.

13. Plunkett, R.: Measurement of Damping. Section 5 of Reference 1, pp. 117-131.
14. Kerwin, E. M., Jr.: Mechanisms and Measurement of Structural Damping. Ship Silencing Symposium, Groton, Conn., May 1963, pp. 1021-1048.
15. Ungar, E. E.: Energy Dissipation at Structural Joints; Mechanisms and Magnitudes. FDL-TDR-64-98, August 1964.
16. Whittier, J. S.: Rheological Properties of Adhesives Considered for Interface Damping. WADD TR-60-280, June 1960.
17. Kenney, J. F.; and Keeping, E. S.: Mathematics of Statistics. D. Van Nostrand Co., Inc., 1954, pp. 54-55.

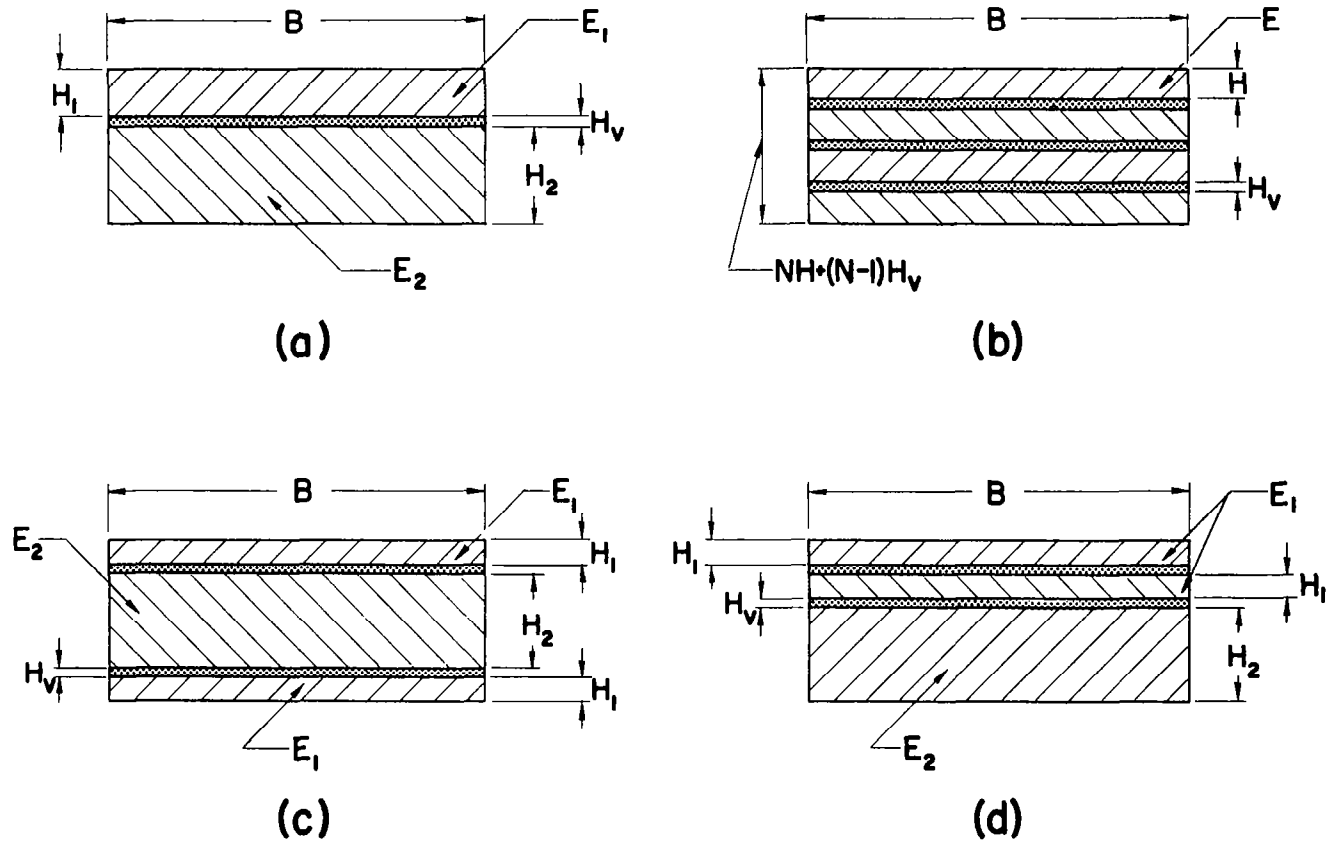


Figure 2.1 Cross-sections of viscoelastic shear-damped plates consisting of laminated solid structural sheets:
 (a) two sheets, (b) N identical sheets, (c) three sheets (symmetrical) and (d) three sheets (unsymmetrical)

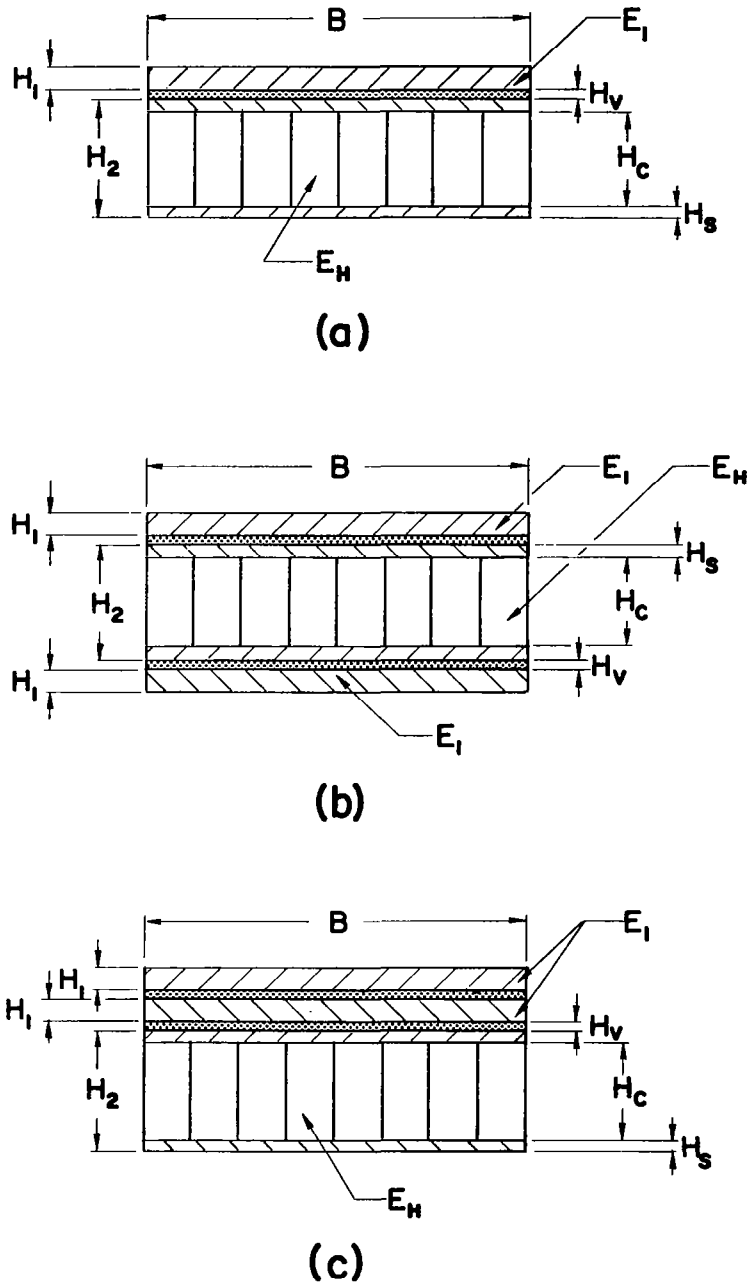


Figure 2.2 Cross-sections of viscoelastic shear-damped plates consisting of laminated honeycomb and solid structural sheets: (a) single-constrained, (b) double-constrained (symmetrical) and (c) double-constrained (unsymmetrical).

Figure 2.3 Cross-sections of viscoelastic shear-damped plates consisting of laminated honeycomb structural sheets: (a) two sneets, (b) N identical sheets, (c) three sneets (symmetrical) and (d) three sheets (unsymmetrical)

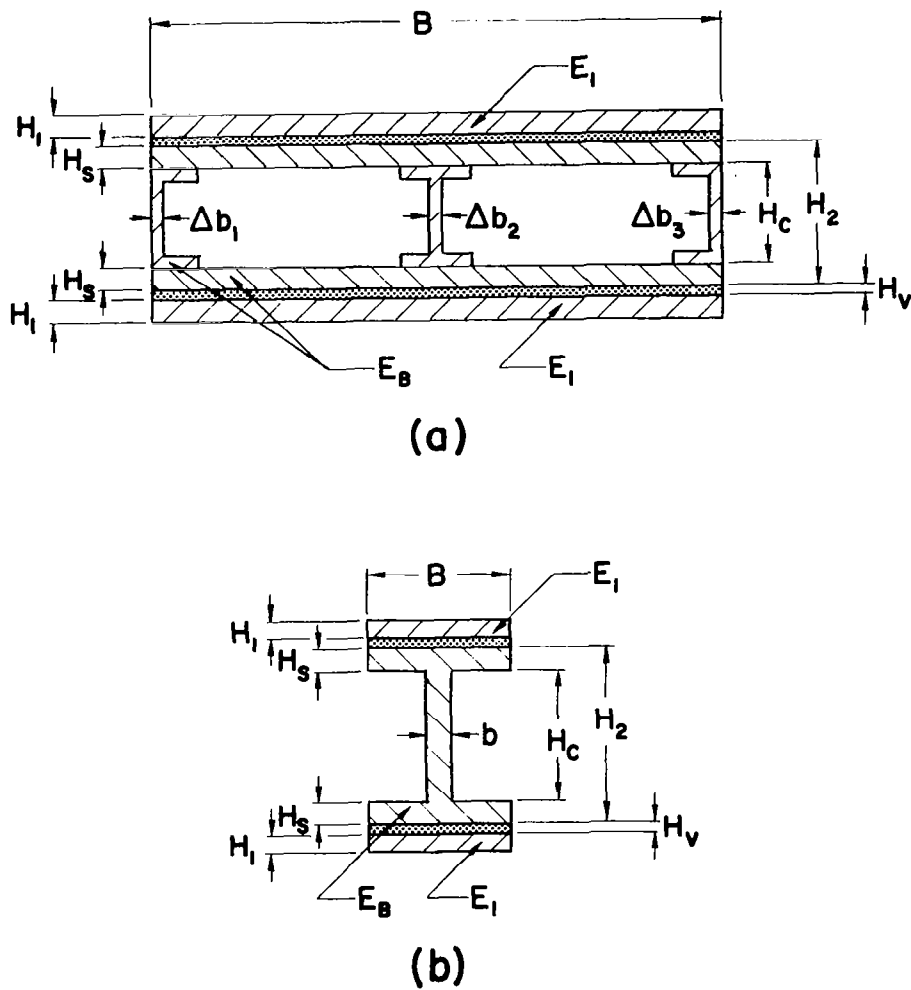


Figure 2.4 Cross-sections of viscoelastic shear-damped double-constrained structural plates and beams incorporating (a) box-beam and (b) I-beam constructions where $b = \sum \Delta b$

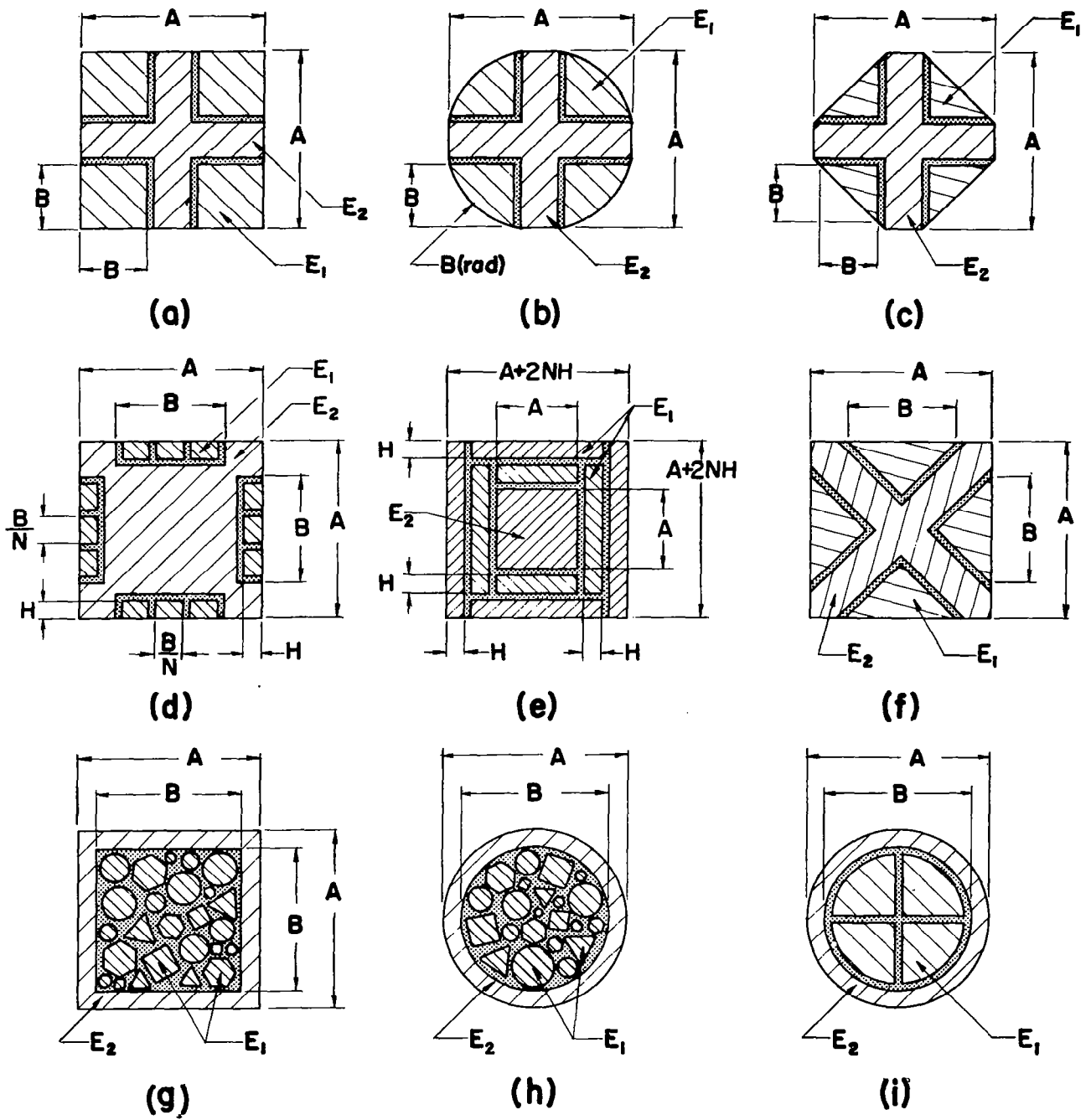


Figure 2.5 Cross-sections of viscoelastic shear-damped structural bar designs.

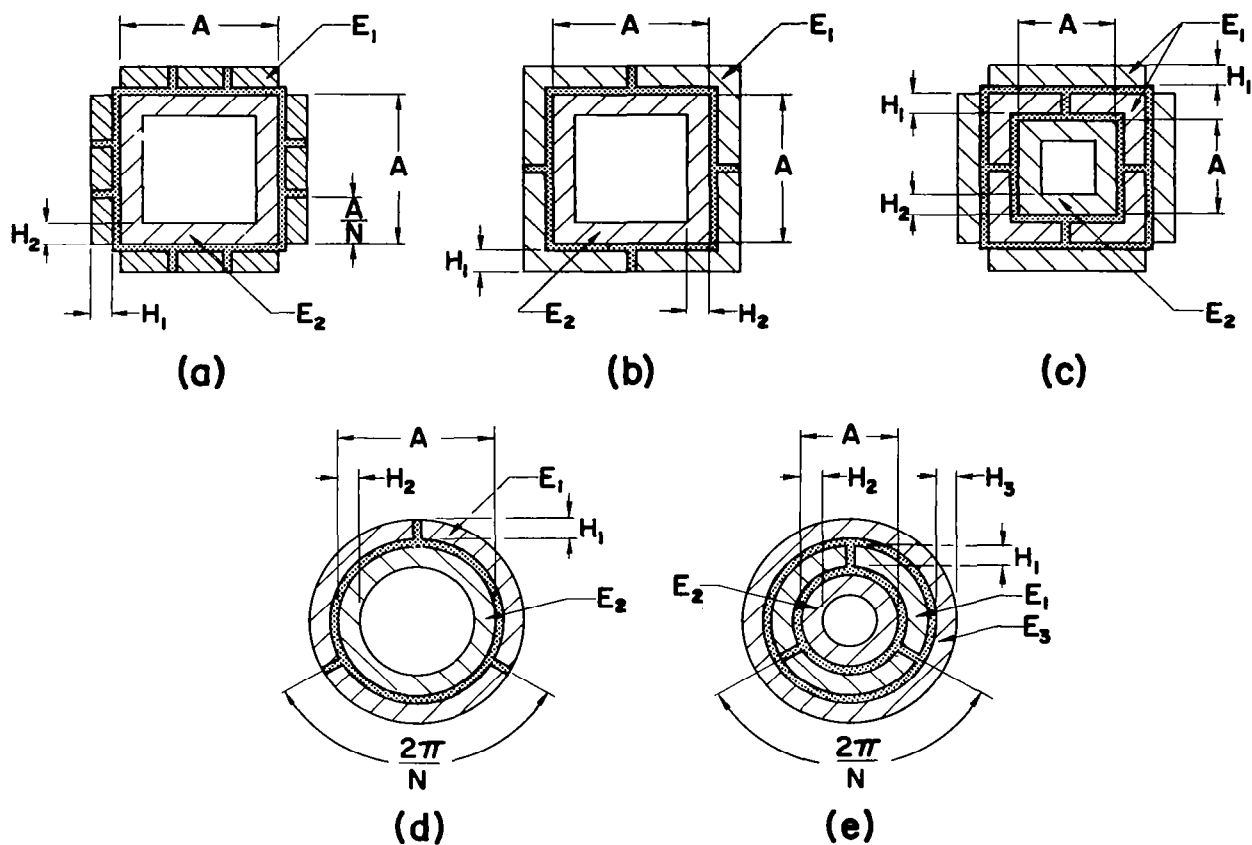
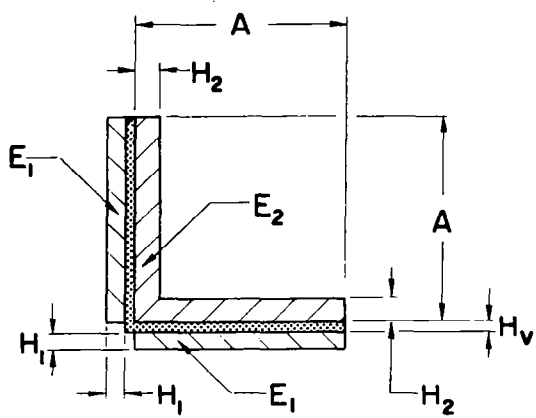
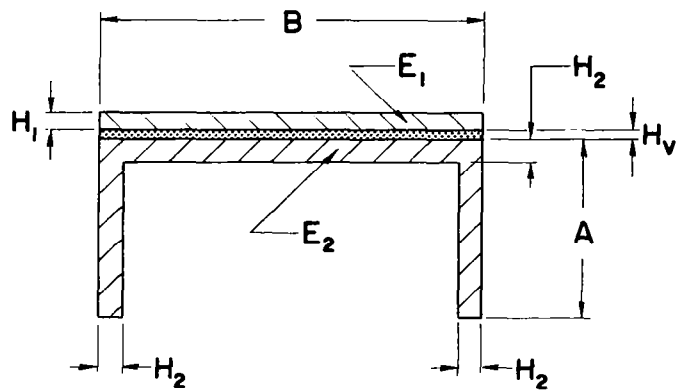


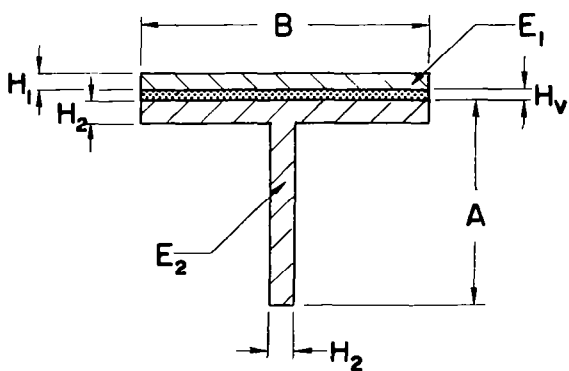
Figure 2.6 Cross-sections of viscoelastic shear-damped structural tube designs



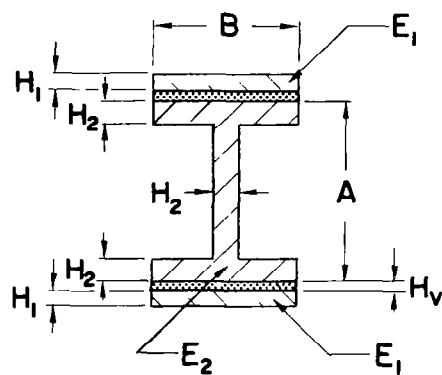
(a)



(b)



(c)



(d)

Figure 2.7 Cross-sections of viscoelastic shear-damped structural shape beams: (a) angle, (b) channel, (c) T-section and (d) I-section, where the basic structural shapes are of constant thickness H_2

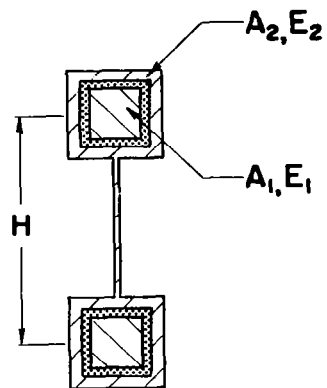


Figure 2.8 Cross-section of a viscoelastic shear-damped dumbbell model where areas A_1 and A_2 may be of any shape

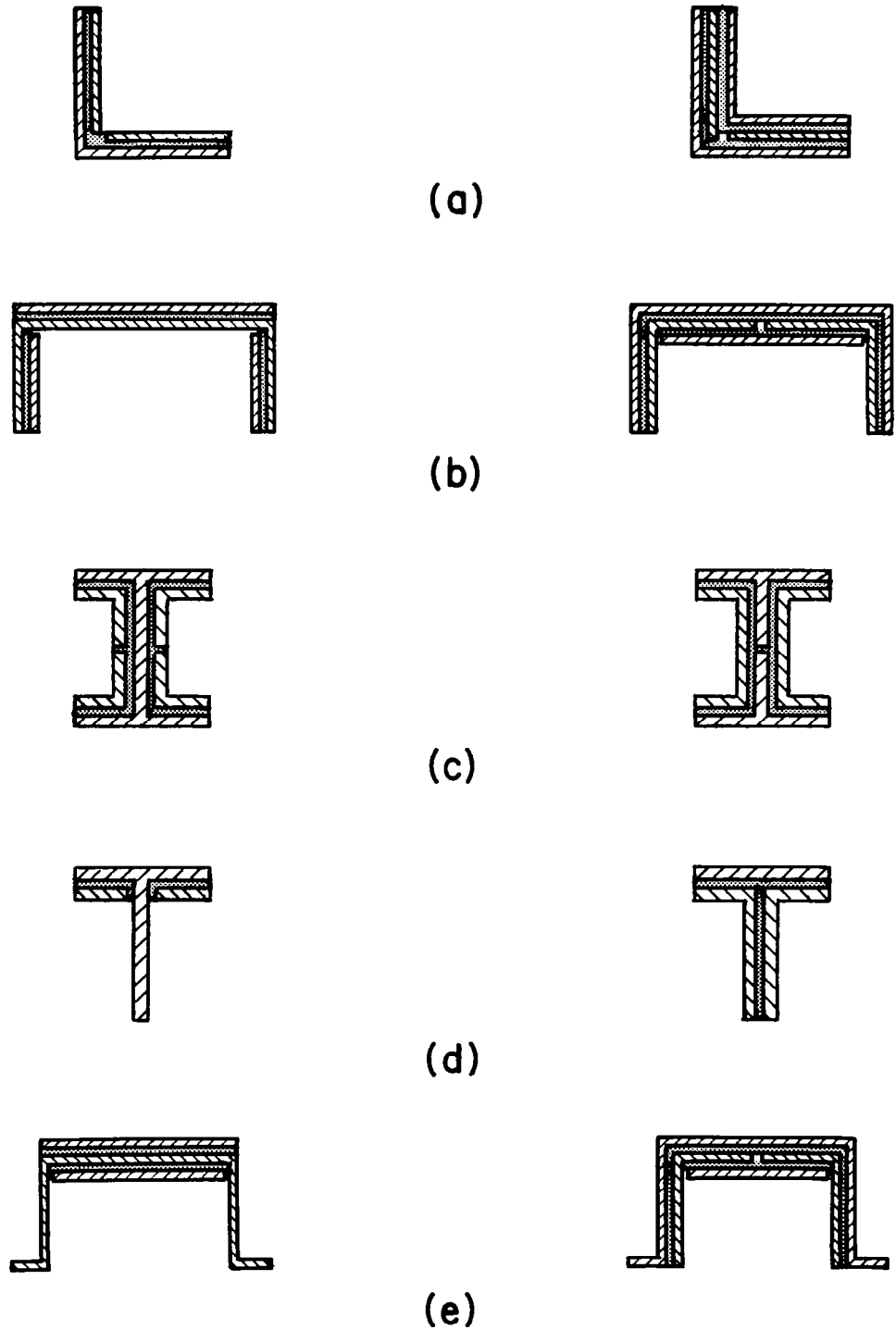


Figure 2.9 Cross-sections of viscoelastic shear-damped composite structural beams of multilaminate construction: (a) angle, (b) channel, (c) I-section, (d) T-section, and (e) hat-section designs

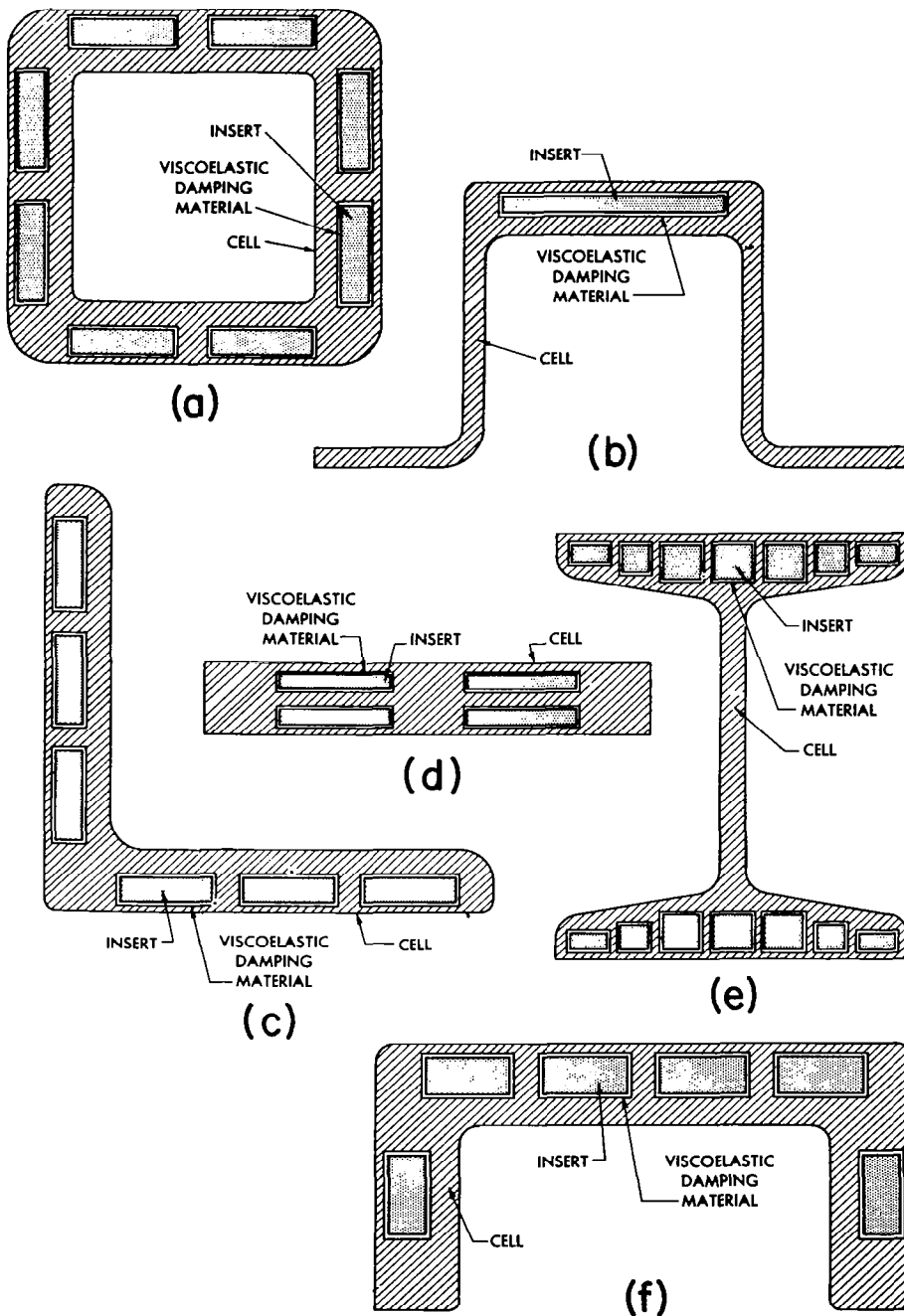


Figure 2.10 Cross-sections of viscoelastic shear-damped composite structural beams of cell-insert construction: (a) square tube, (b) hat-section, (c) angle, (d) flat bar, (e) I-section and (f) channel designs

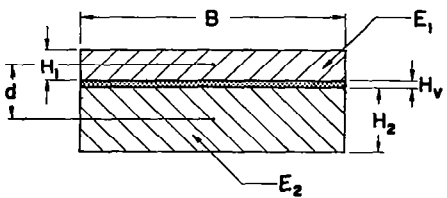
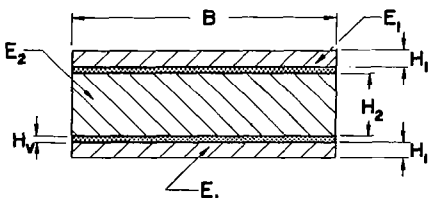
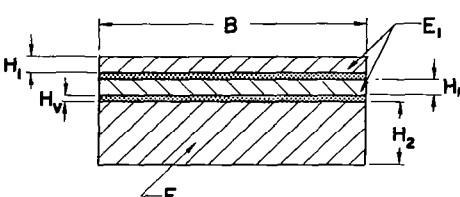
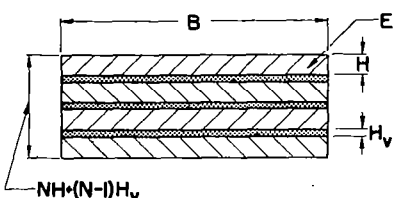
 $M = \frac{E_1}{E_2} \quad R = \frac{H_1}{H_2} \quad V = \frac{H_V}{H_1 + H_2}$	$Y_0 = \frac{3MR(R+1)^2}{(MR^3+1)(MR+1)}$ $\frac{Y}{Y_0} = (1+2V)^2$ $(EI)_0 = \frac{E_2 B H_2^3}{12} (MR^3+1)$ $\omega = B(\gamma_1 H_1 + \gamma_2 H_2)$ $d = \frac{1}{2}(H_1 + H_2) + H_V$ $B_V = B$
 $M = \frac{E_1}{E_2} \quad R = \frac{H_1}{H_2} \quad V = \frac{H_V}{H_1 + H_2}$	$Y_0 = \frac{6MR(R+1)^2}{2MR^3+1}$ $\frac{Y}{Y_0} = (1+2V)^2$ $(EI)_0 = \frac{E_2 B H_2^3}{12} (2MR^3+1)$ $\omega = B(2\gamma_1 H_1 + \gamma_2 H_2)$
 $M = \frac{E_1}{E_2} \quad R = \frac{H_1}{H_2} \quad V = \frac{H_V}{H_1 + H_2}$	$Y_0 = \frac{6MR(2MR^3+5R^2+4R+1)}{(2MR^3+1)(2MR+1)}$ $\frac{Y}{Y_0} \geq (1+2V)^2 \quad (R \leq 1.0)$ $\frac{Y}{Y_0} \leq (1+2V)^2 \quad (R \geq 1.0)$ $(EI)_0 = \frac{E_2 B H_2^3}{12} (2MR^3+1)$ $\omega = B(2\gamma_1 H_1 + \gamma_2 H_2)$
 $V = \frac{H_V}{2H}$	$Y_0 = N^2 - 1$ $\frac{Y}{Y_0} = (1+2V)^2$ $(EI)_0 = \frac{E B N H^3}{12}$ $\omega = \gamma N B H$

Figure 2.11(A) Design equations for geometrical properties of viscoelastic shear-damped plates consisting of laminated solid structural sheets.

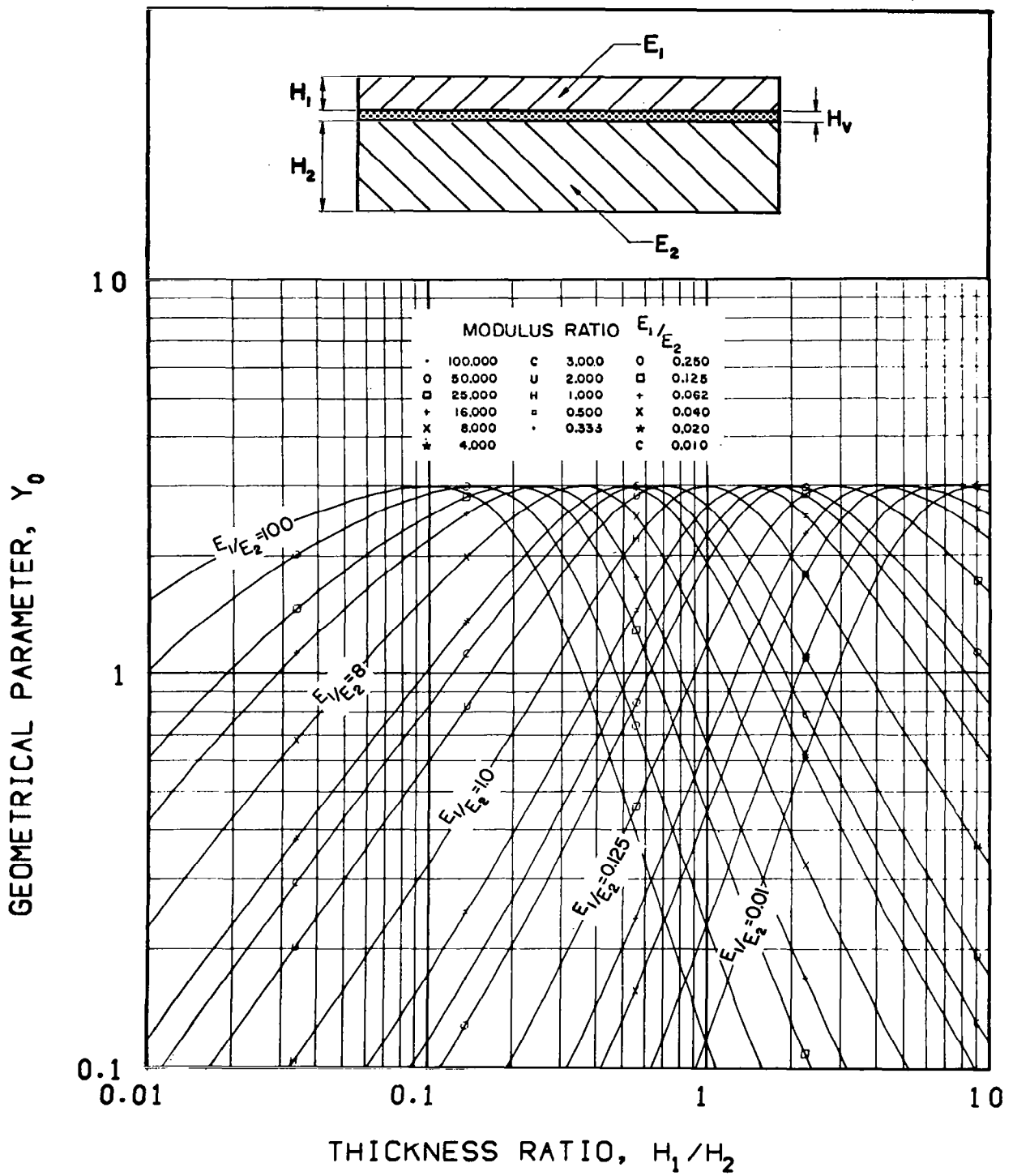


Figure 2.11 (B) Geometrical parameter of composite structural plate comprised of two solid sheets

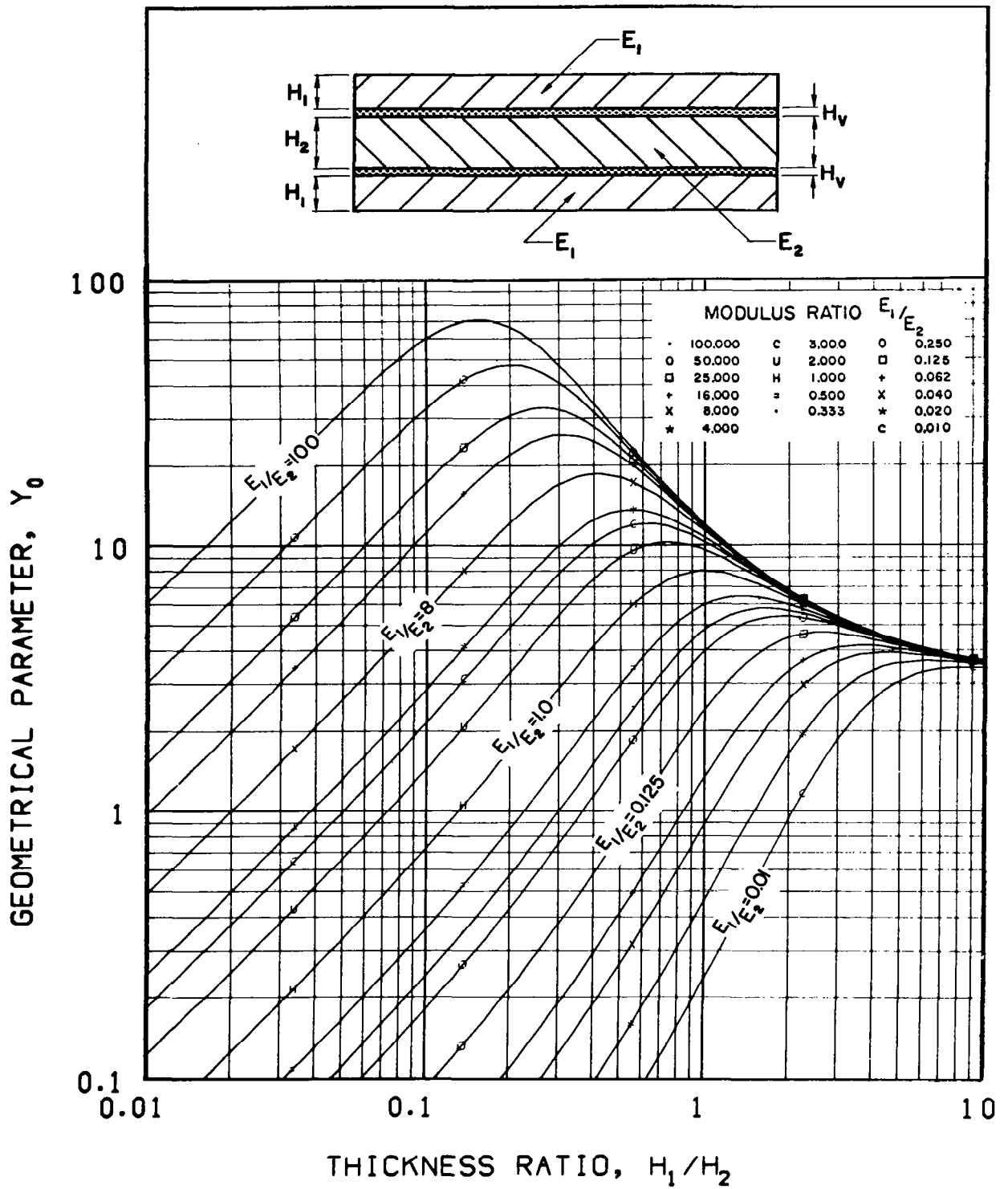


Figure 2.11(C) Geometrical parameter of symmetrical composite structural plate comprised of three solid sheets

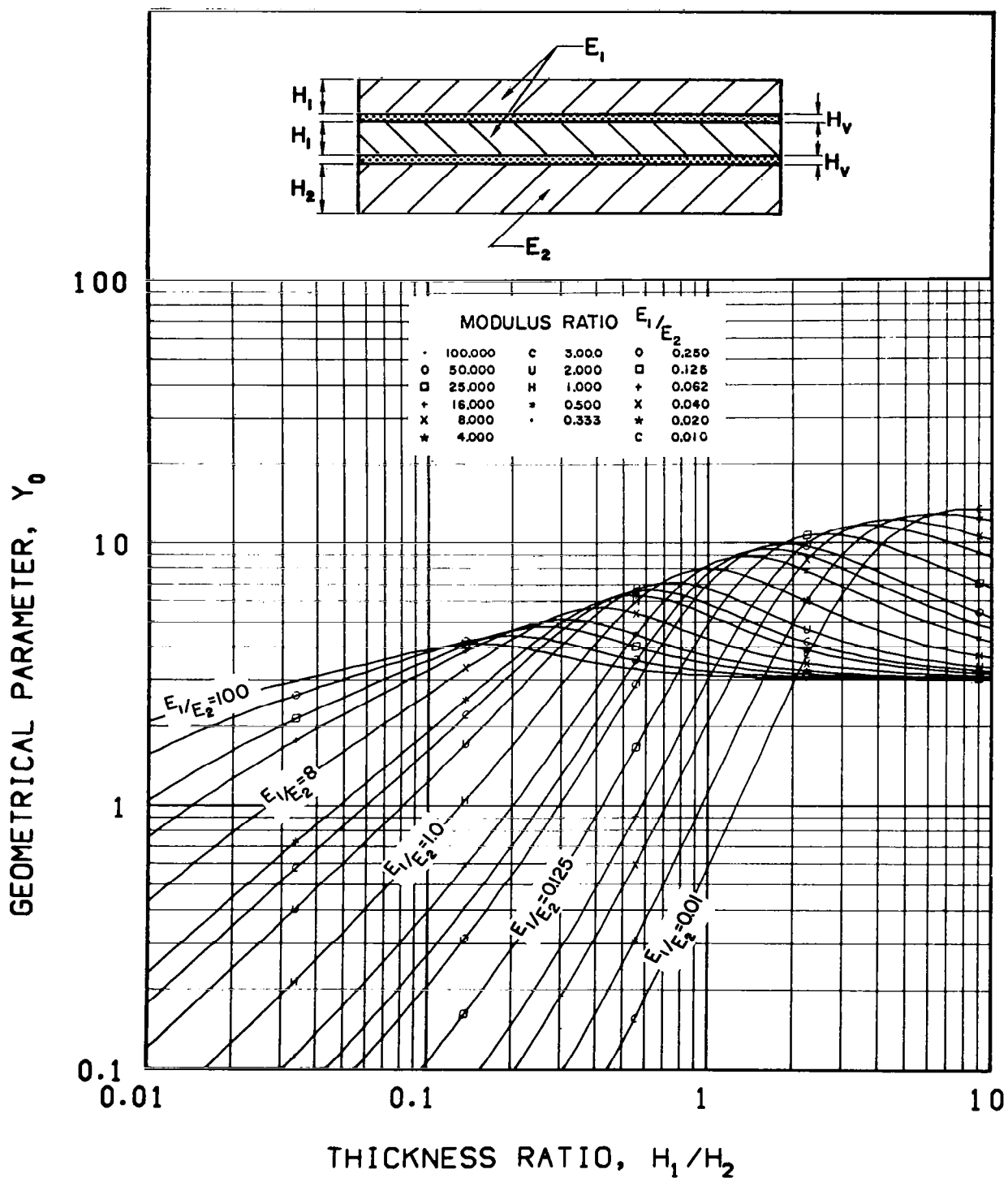
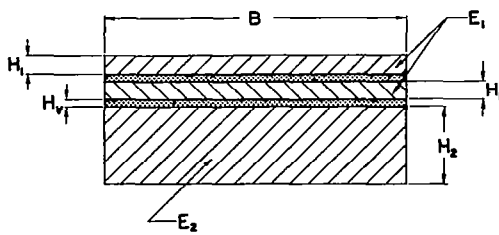
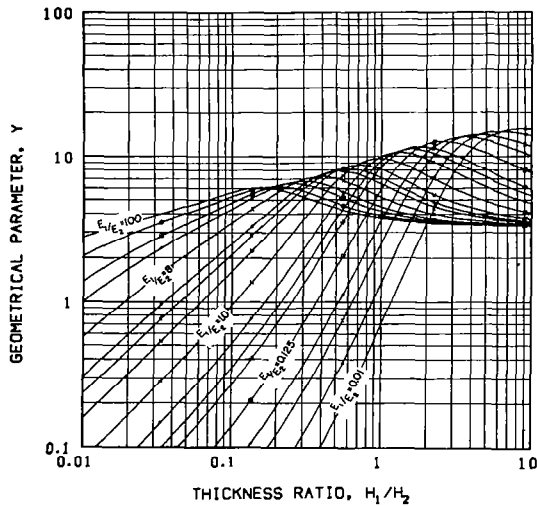


Figure 2.11(D) Geometrical parameter of unsymmetrical composite structural plate comprised of three solid sheets.

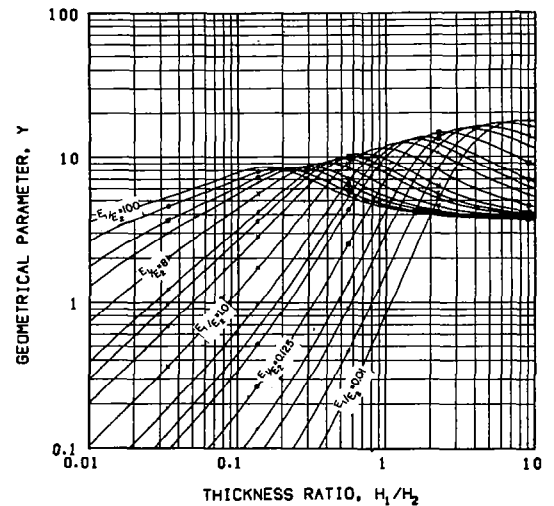


MODULUS RATIO, E_1/E_2

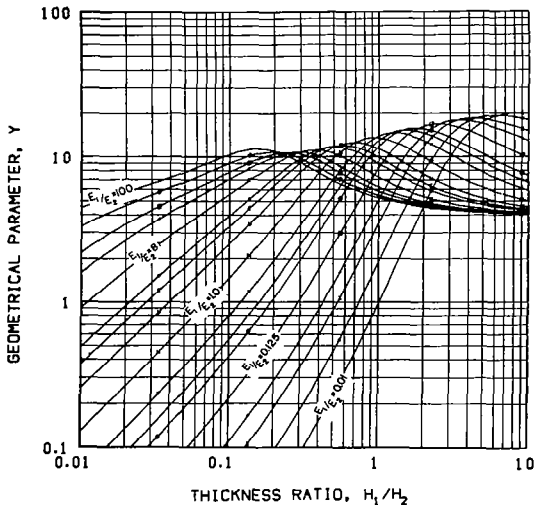
•	100.000	C	3.000	O	0.250
O	50.000	U	2.000	□	0.125
□	25.000	H	1.000	+	0.062
+	16.000	*	0.500	X	0.040
X	8.000	•	0.333	*	0.020
*	4.000			C	0.010



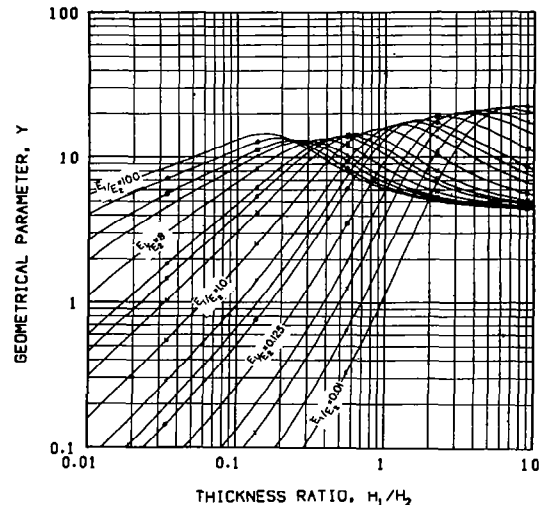
(a) $V = 0.05$



(b) $V = 0.10$



(c) $V = 0.15$



(d) $V = 0.20$

Figure 2.11(E) Geometrical parameter of unsymmetrical composite structural plate comprised of three solid sheets for various values of the viscoelastic thickness parameter $V = H_v / (H_1 + H_2)$

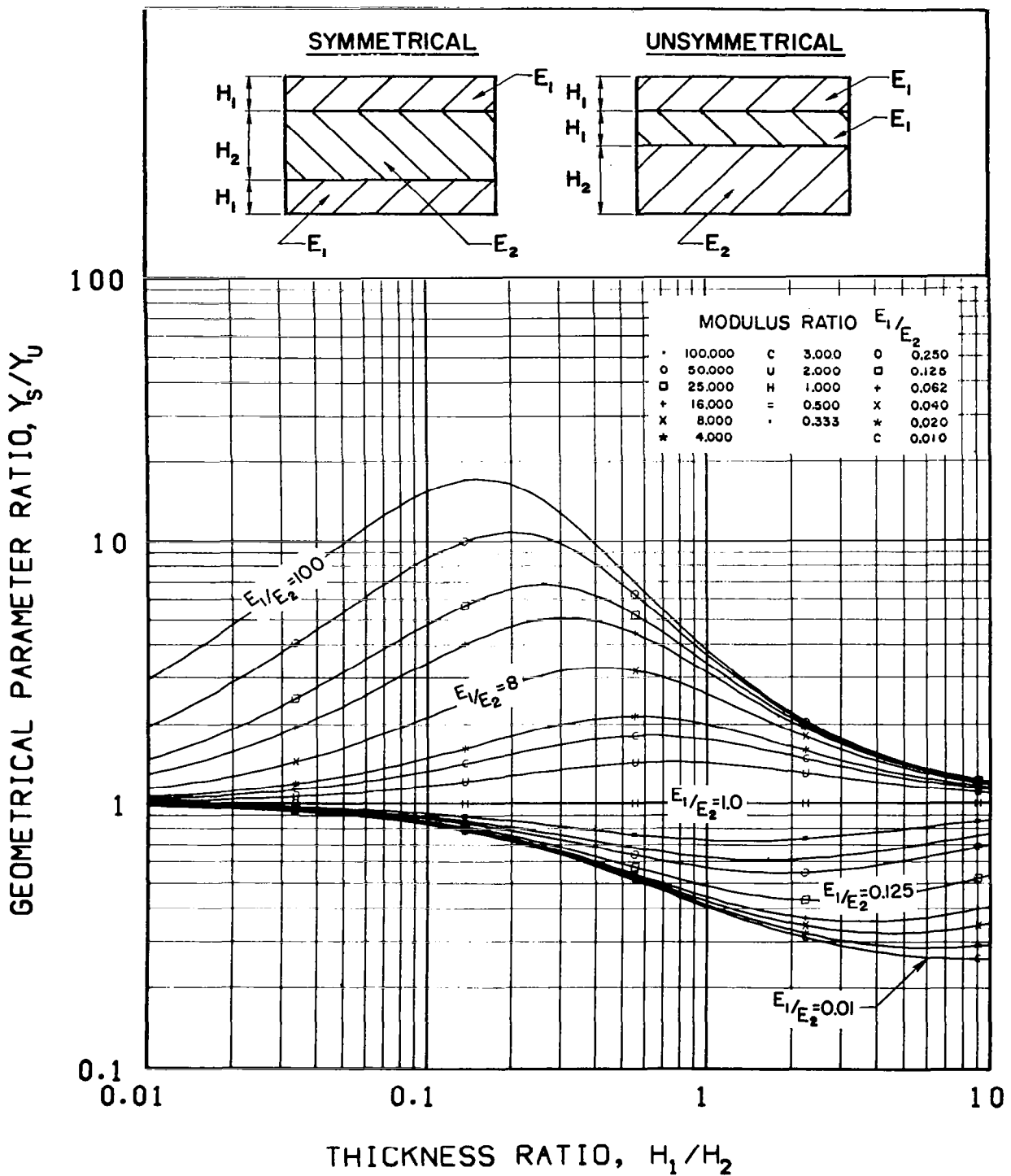
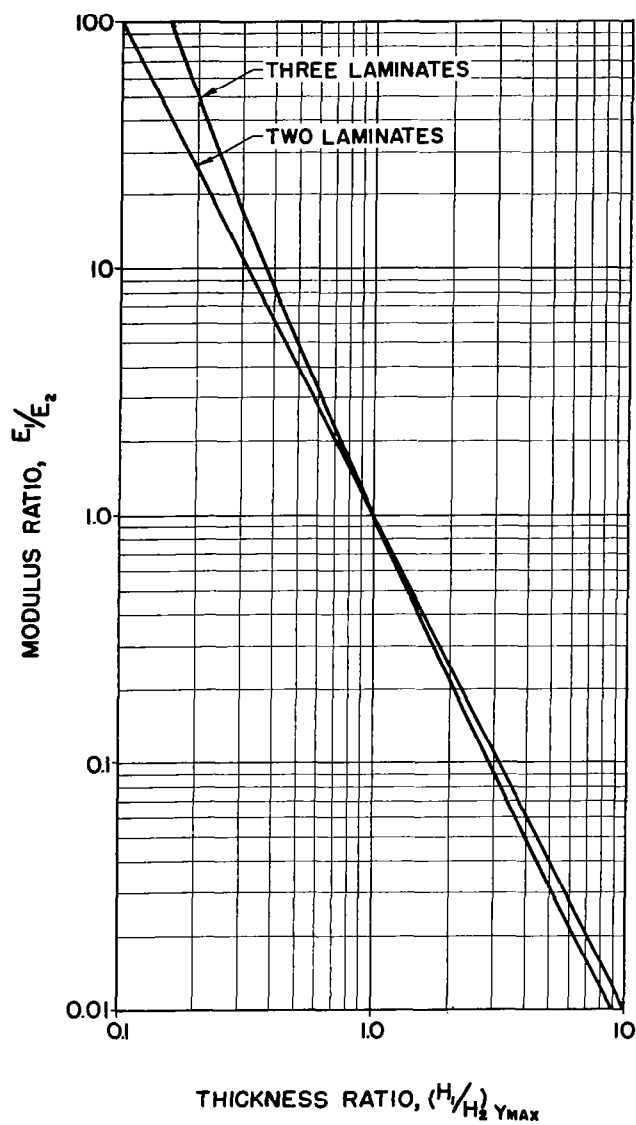
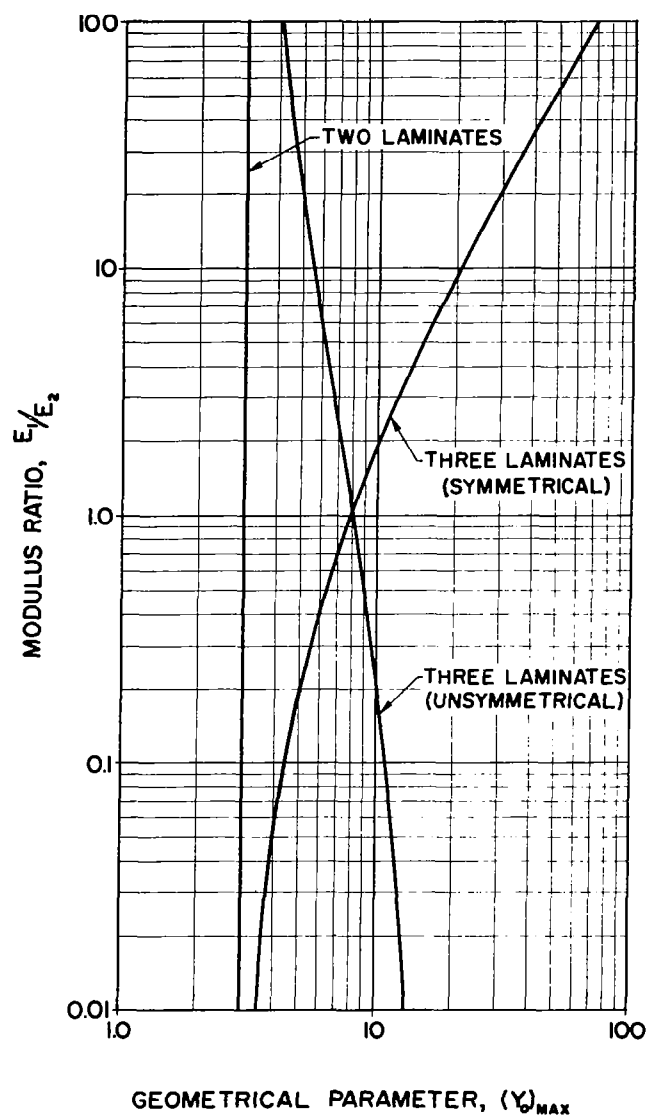


Figure 2.11(F) Comparison of the geometrical parameters Y_s and Y_u of the symmetrical and unsymmetrical three-elastic-element composite structural plates.



(a)



(b)

Figure 2.11 (G) Relationship between the modulus ratio E_1/E_2 and thickness ratio H_1/H_2 to provide the indicated maximum value of geometrical parameter $(Y_0)_{MAX}$ for viscoelastic shear-damped plates consisting of two and three solid structural sheets

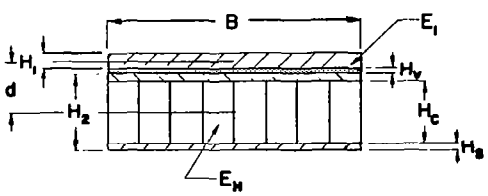
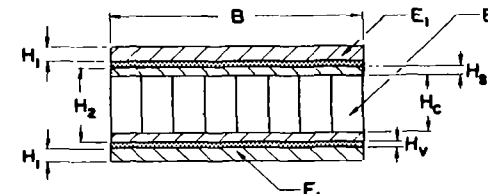
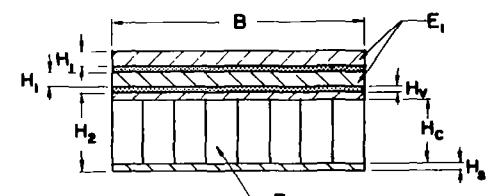
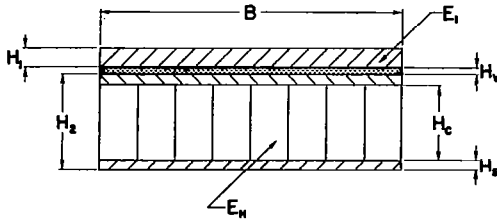
 $M = \frac{E_1}{E_N} \quad R = \frac{H_1}{H_2} \quad T = \frac{H_3}{H_2} \quad V = \frac{H_3}{H_1 + H_2}$	$Y_0 = \frac{6MRT(1+2T)^3(1+R)^2}{[MR(1+2T)+2T]\{MR^3(1+2T)^3+2T[T^3+3(1+T)^2]\}}$ $\frac{Y}{Y_0} = (1+2V)^2$ $(EI)_0 = \frac{E_N B H_2^3}{12} [MR^3 + \frac{2T}{(1+2T)^3} \{T^3 + 3(1+T)^2\}]$ $\omega = 2\delta_N B H_1 + 2\delta_N B H_3$ $d = \frac{1}{2} (H_1 + H_2) + H_3$ $B_V = B$
 $M = \frac{E_1}{E_N} \quad R = \frac{H_1}{H_2} \quad T = \frac{H_3}{H_2} \quad V = \frac{H_3}{H_1 + H_2}$	$Y_0 = \frac{6MR(1+2T)^3(1+R)^2}{(1+2T)^3(2MR^3+1)-1}$ $\frac{Y}{Y_0} = (1+2V)^2$ $(EI)_0 = \frac{E_N B H_2^3}{12} [2MR^3 + \frac{(1+2T)^3-1}{(1+2T)^3}]$ $\omega = 2\delta_N B H_1 + 2\delta_N B H_3$
 $M = \frac{E_1}{E_N} \quad R = \frac{H_1}{H_2} \quad T = \frac{H_3}{H_2} \quad V = \frac{H_3}{H_1 + H_2}$	$Y_0 = \frac{3MR(1+2T)^3[2MR^3(1+2T)+T\{(1+R)^2+(1+3R)^2\}]}{[MR(1+2T)+T][(2MR^3+1)(1+2T)^3-1]}$ $\frac{Y}{Y_0} \geq (1+2V)^2 \quad (R \leq 1.0)$ $\frac{Y}{Y_0} \leq (1+2V)^2 \quad (R \geq 1.0)$ $(EI)_0 = \frac{E_N B H_2^3}{12} [2MR^3 + \frac{(1+2T)^3-1}{(1+2T)^3}]$ $\omega = 2\delta_N B H_1 + 2\delta_N B H_3$

Figure 2. 12 (A) Design equations for geometrical properties of viscoelastic shear-damped plates consisting of laminated honeycomb and solid structural sheets



THICKNESS RATIO, H_1/H_c

•	0.001	*	0.010	o	0.200
o	0.002	c	0.020	□	0.300
□	0.003	U	0.030	+	0.500
+	0.005	H	0.050	X	0.700
X	0.007	=	0.070	*	1.000
				•	0.100

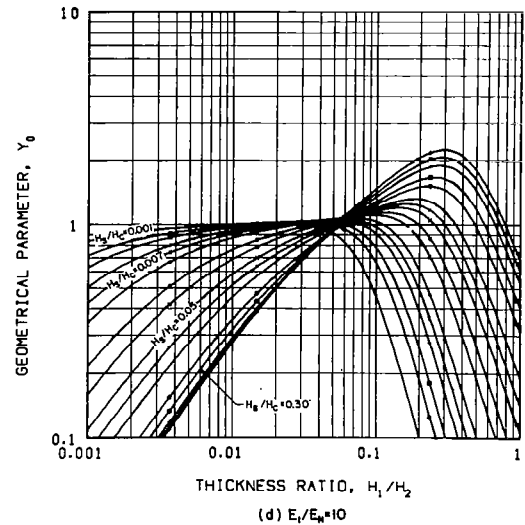
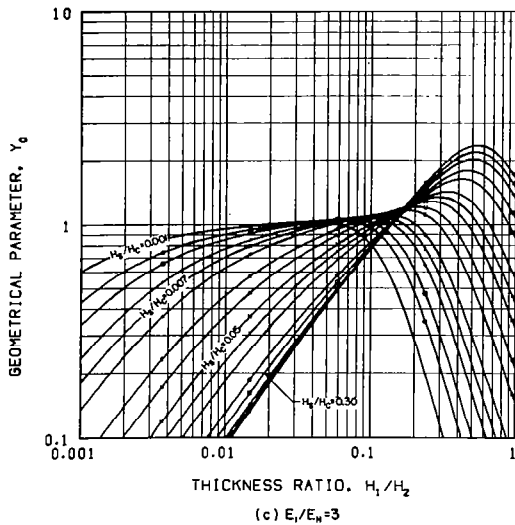
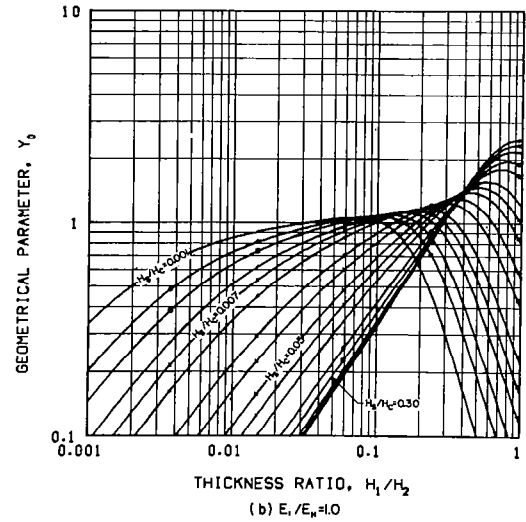
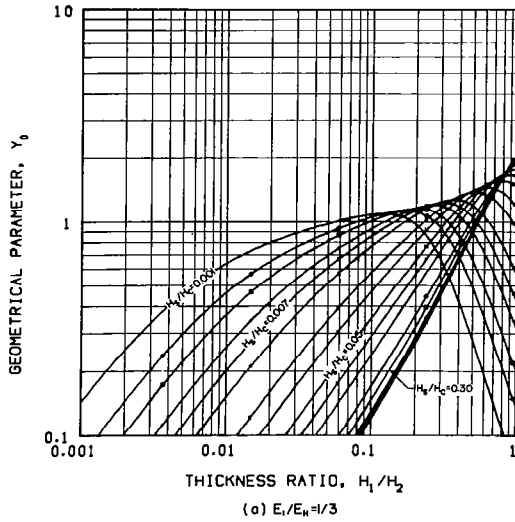


Figure 2.12(B) Geometrical parameter of single-constrained honeycomb structural plate comprised of one honeycomb and one solid sheet for various values of the modulus ratio E_1/E_H

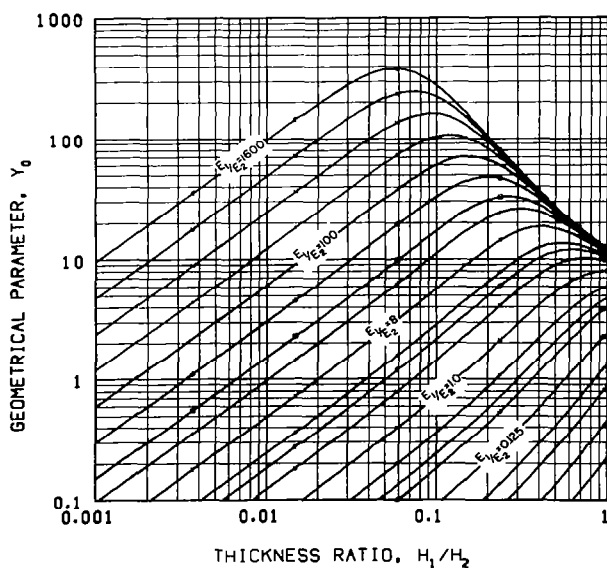
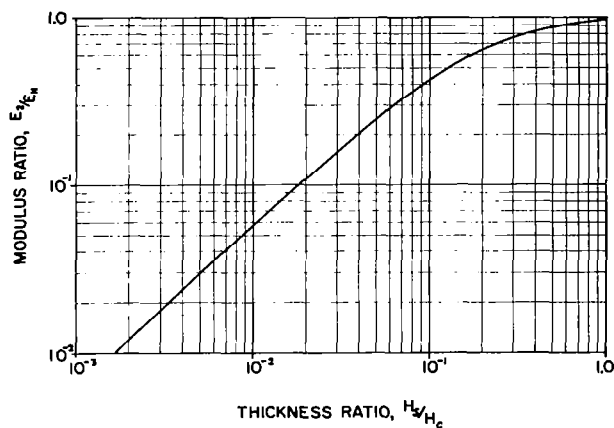
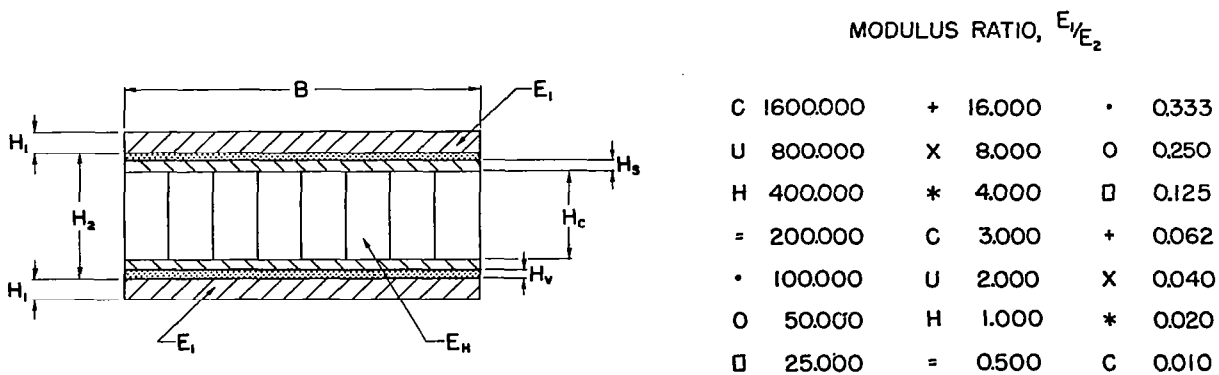
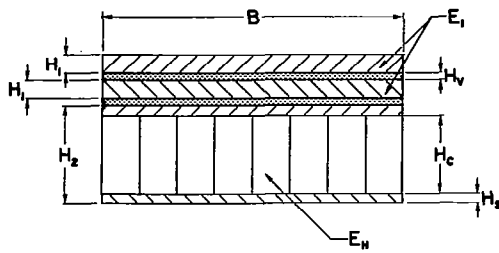


Figure 2.12 (C) Geometrical parameter of symmetrical double-constrained honeycomb structural plate comprised of one honeycomb and two solid sheets



THICKNESS RATIO, H_3/H_2

• 0.001	* 0.010	o 0.200
o 0.002	c 0.020	□ 0.300
□ 0.003	u 0.030	+ 0.500
+ 0.005	h 0.050	x 0.700
x 0.007	= 0.070	* 1.000
	• 0.100	

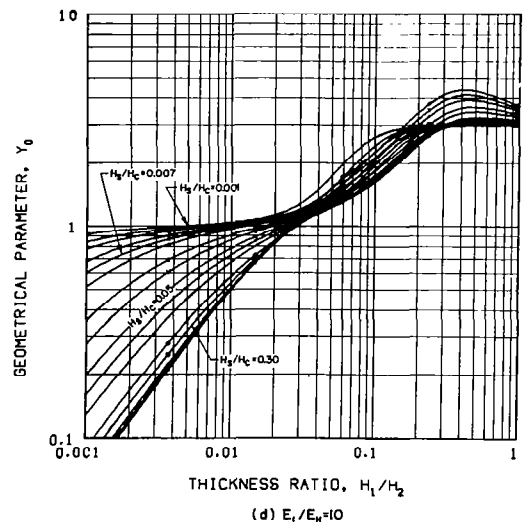
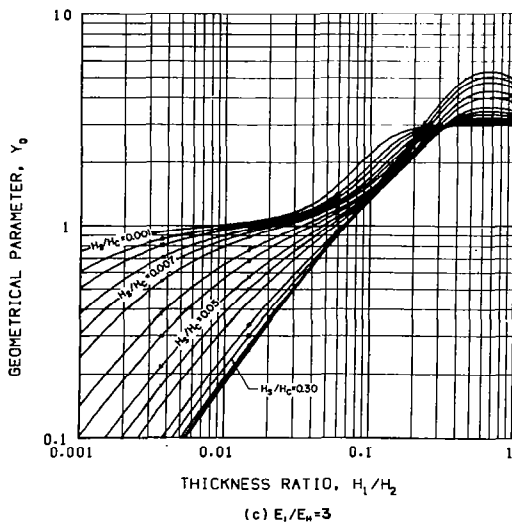
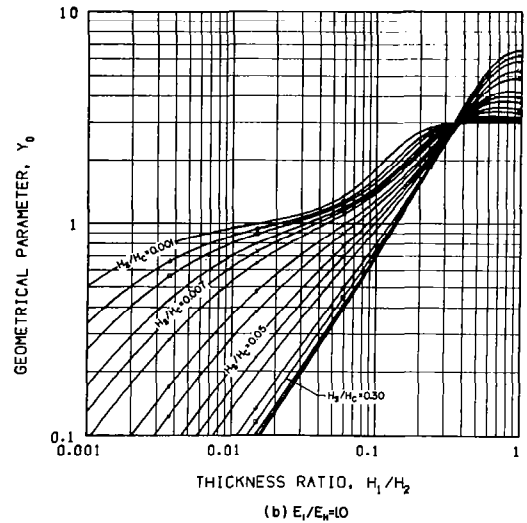
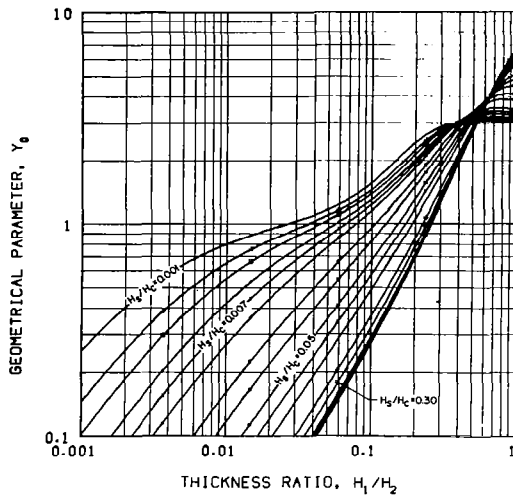


Figure 2.12(D) Geometrical parameter of unsymmetrical double-constrained honeycomb structural plate comprised of one honeycomb and two solid sheets for various values of the modulus ratio E_1/E_H

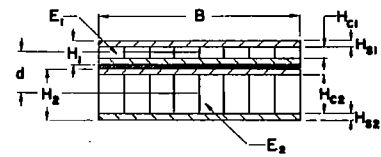
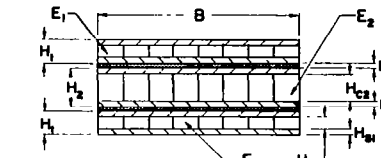
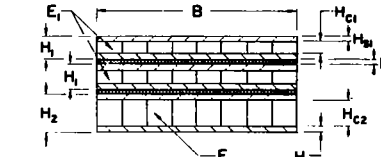
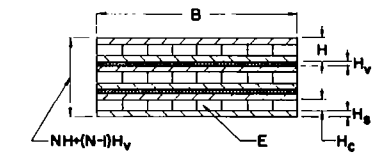
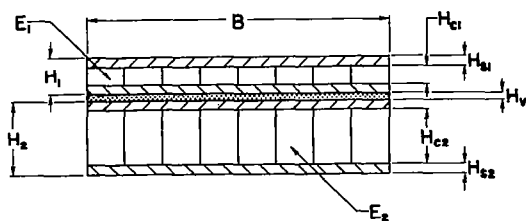
 $M = \frac{E_1}{E_2} \quad R = \frac{H_1}{H_2} \quad T_1 = \frac{H_{c1}}{H_{c2}} \quad T_2 = \frac{H_{c1}}{H_{c2}} \quad V = \frac{H_V}{H_1 + H_2}$	$Y_0 = \frac{6MRT_1 T_2 (1+2T_1)^3 (1+2T_2)^3 (1+R)^2}{[MRT_1 (1+2T_2) + T_2 (1+2T_1)] [MR^3 (1+2T_2)^3 \{(1+2T_1)^3 - 1\} + (1+2T_1)^3 \{(1+2T_2)^3 - 1\}]}$ $\frac{Y}{Y_0} = (1+2V)^2$ $(EI)_0 = \frac{E_2 B H_2^3}{12} \left\{ MR^3 \frac{(1+2T_1)^3 - 1}{(1+2T_1)^3} + \frac{(1+2T_2)^3 - 1}{(1+2T_2)^3} \right\}$ $\omega = 2 \delta_1 B H_{s1} + 2 \delta_2 B H_{s2}$ $d = \frac{1}{2} (H_1 + H_2) + H_V$ $B_V = B$
 $M = \frac{E_1}{E_2} \quad R = \frac{H_1}{H_2} \quad T_1 = \frac{H_{c1}}{H_{c2}} \quad T_2 = \frac{H_{c1}}{H_{c2}} \quad V = \frac{H_V}{H_1 + H_2}$	$Y_0 = \frac{12MRT_1 (1+2T_1)^3 (1+2T_2)^3 (1+R)^2}{2MR^3 (1+2T_2)^3 [(1+2T_1)^3 - 1] + (1+2T_1)^3 [(1+2T_2)^3 - 1]}$ $\frac{Y}{Y_0} = (1+2V)^2$ $(EI)_0 = \frac{E_2 B H_2^3}{12} \left\{ 2MR^3 \frac{(1+2T_1)^3 - 1}{(1+2T_1)^3} + \frac{(1+2T_2)^3 - 1}{(1+2T_2)^3} \right\}$ $\omega = 4 \delta_1 B H_{s1} + 2 \delta_2 B H_{s2}$
 $M = \frac{E_1}{E_2} \quad R = \frac{H_1}{H_2} \quad T_1 = \frac{H_{c1}}{H_{c2}} \quad T_2 = \frac{H_{c1}}{H_{c2}} \quad V = \frac{H_V}{H_1 + H_2}$	$Y_0 = \frac{6MRT_1 (1+2T_1)^3 (1+2T_2)^3 [4MR^3 T_1 (1+2T_2) + T_2 (1+2T_1) \{(1+R)^2 + (1+3R)^2\}]}{[2MRT_1 (1+2T_2) + T_2 (1+2T_1)] [2MR^3 (1+2T_2)^3 \{(1+2T_1)^3 - 1\} + (1+2T_1)^3 \{(1+2T_2)^3 - 1\}]}$ $\frac{Y}{Y_0} \geq (1+2V)^2 \quad (R \leq 1.0)$ $\frac{Y}{Y_0} \leq (1+2V)^2 \quad (R \geq 1.0)$ $(EI)_0 = \frac{E_2 B H_2^3}{12} \left\{ 2MR^3 \frac{(1+2T_1)^3 - 1}{(1+2T_1)^3} + \frac{(1+2T_2)^3 - 1}{(1+2T_2)^3} \right\}$ $\omega = 4 \delta_1 B H_{s1} + 2 \delta_2 B H_{s2}$
 $T = \frac{H_2}{H_c} \quad V = \frac{H_V}{2H}$	$Y_0 = \frac{(1+2T)^2}{T^2 + 3(1+T)^2} (N^2 - 1)$ $\frac{Y}{Y_0} = (1+2V)^2$ $(EI)_0 = \frac{NEBH_c^3}{12} [(1+2T)^3 - 1]$ $\omega = 2 \delta NBH_s$

Figure 2.13(A) Design equations for geometrical properties of viscoelastic shear-damped plates consisting of laminated honeycomb structural sheets.



THICKNESS RATIO, H_{s2}/H_{c2}

•	0.001	*	0.010	0	0.200
0	0.002	C	0.020	□	0.300
□	0.003	U	0.030	+	0.500
+	0.005	H	0.050	X	0.700
X	0.007	=	0.070	*	1.000
			•	0.100	

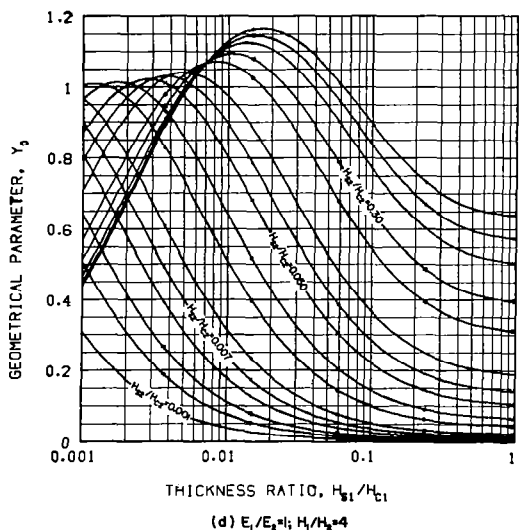
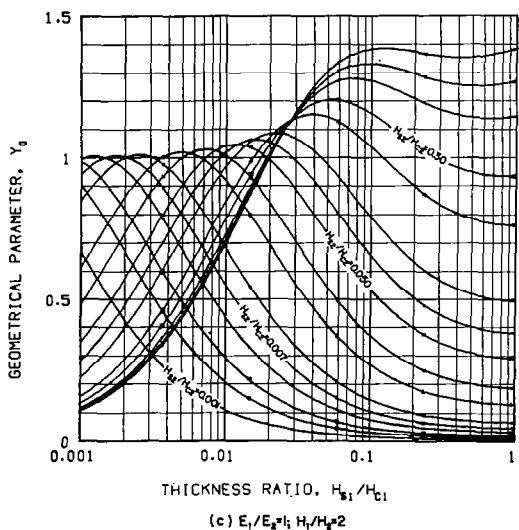
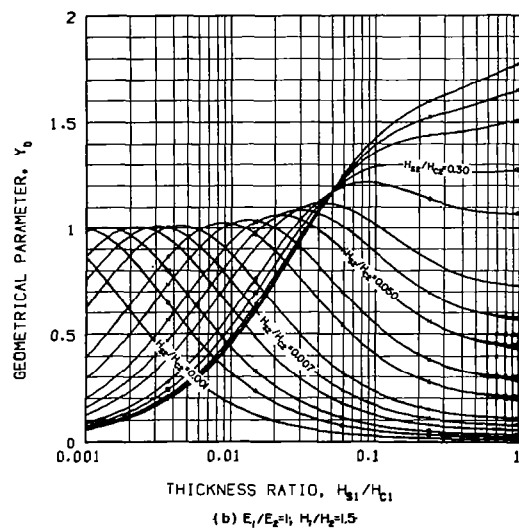
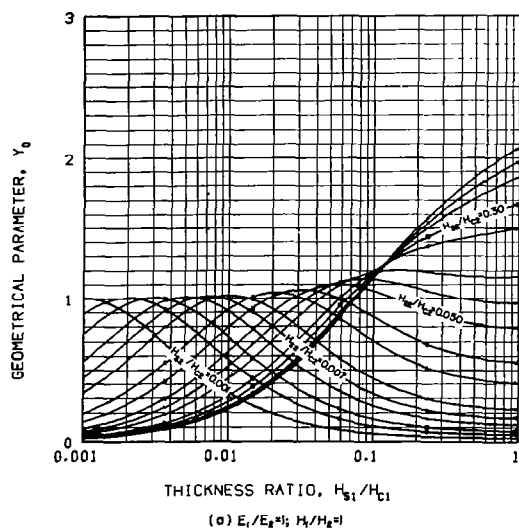
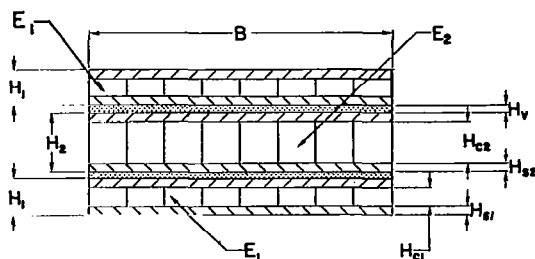
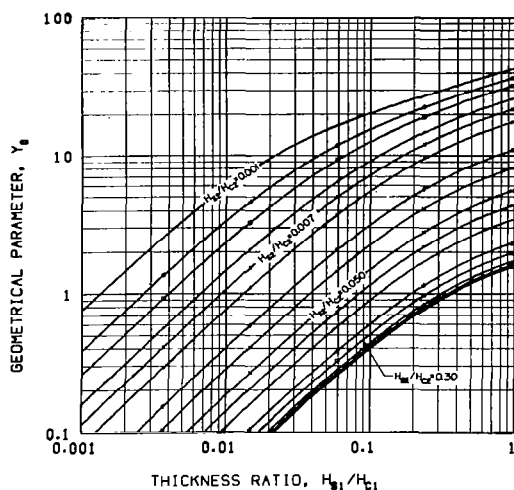


Figure 2.13(B) Geometrical parameter of composite structural plate comprised of two honeycomb sheets for a modulus ratio $E_1/E_2 = 1$ and various values of the thickness ratio H_1/H_2

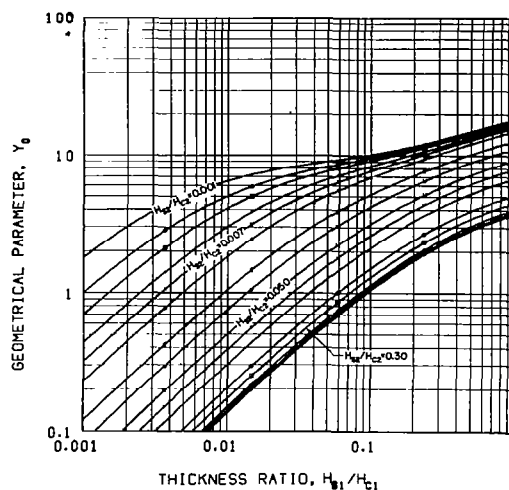


THICKNESS RATIO H_{s2}/H_{c2}

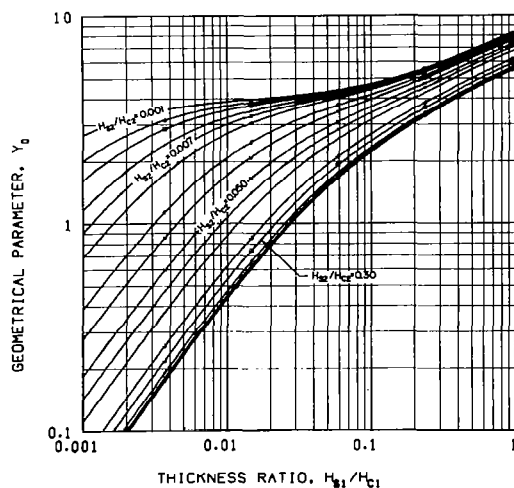
• 0.001	* 0.010	o 0.200
o 0.002	c 0.020	□ 0.300
□ 0.003	u 0.030	+ 0.500
+ 0.005	h 0.050	x 0.700
x 0.007	• 0.070	* 1.000
	• 0.100	



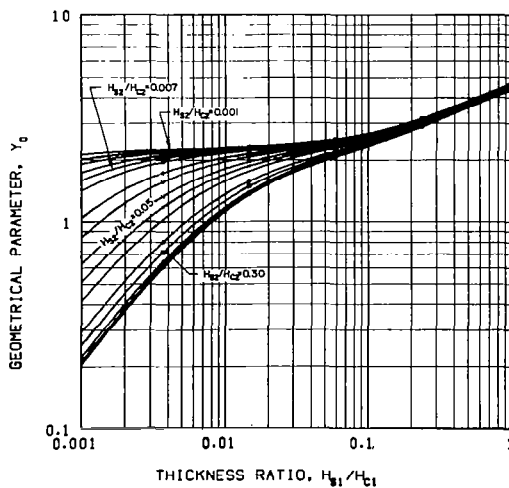
(a) $E_1/E_2=1$; $H_1/H_2=0.25$



(b) $E_1/E_2=1$; $H_1/H_2=0.5$

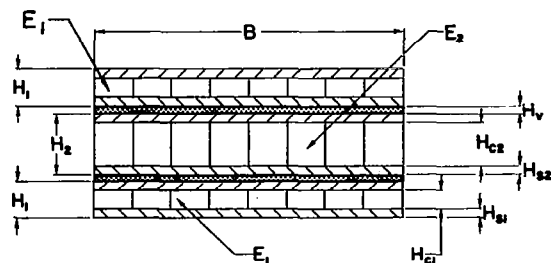


(c) $E_1/E_2=1$; $H_1/H_2=1$



(d) $E_1/E_2=1$; $H_1/H_2=2$

Figure 2.13(C) Geometrical parameter of symmetrical composite structural plate comprised of three honeycomb sheets for a modulus ratio $E_1/E_2 = 1$ and various values of the thickness ratio H_1/H_2



THICKNESS RATIO, H_{s2}/H_{c2}

• 0.001	* 0.010	o 0.200
o 0.002	c 0.020	□ 0.300
□ 0.003	u 0.030	+ 0.500
+ 0.005	h 0.050	x 0.700
x 0.007	= 0.070	* 1.000
	• 0.100	

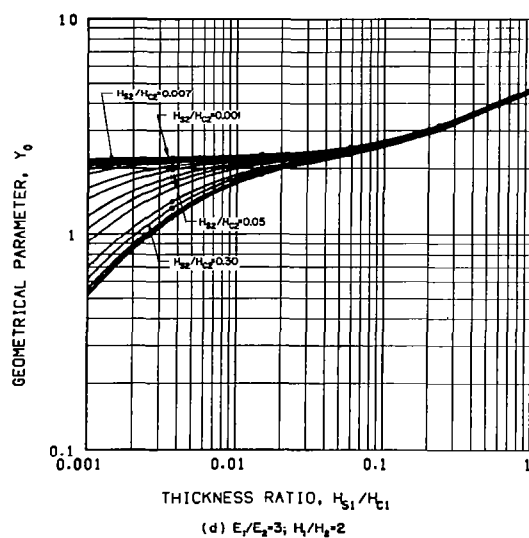
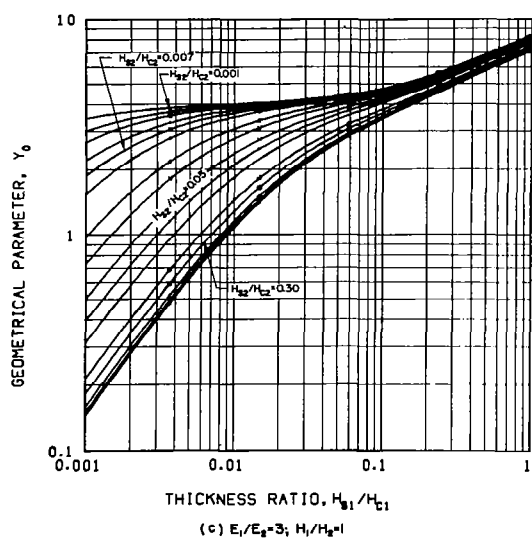
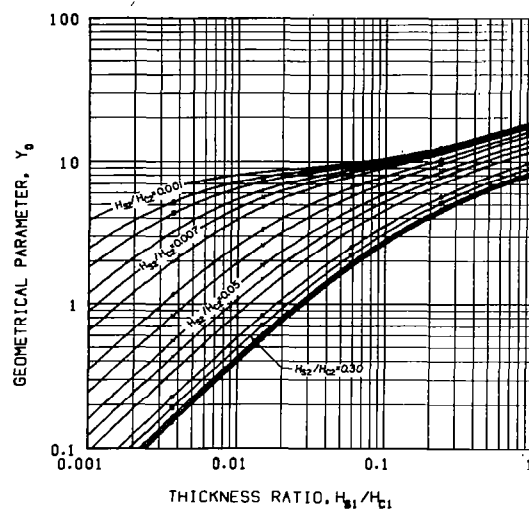
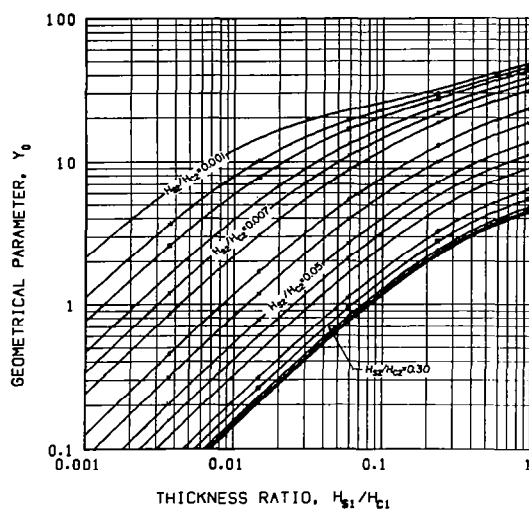
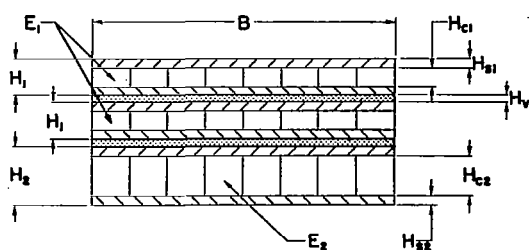
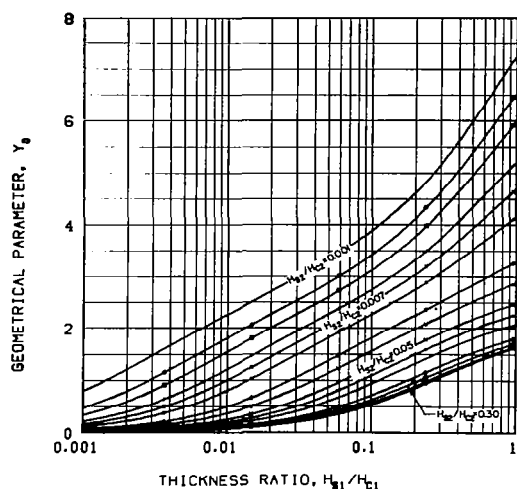


Figure 2.13(D) Geometrical parameter of symmetrical composite structural plate comprised of three honeycomb sheets for a modulus ratio $E_1/E_2 = 3$ and various values of the thickness ratio H_1/H_2

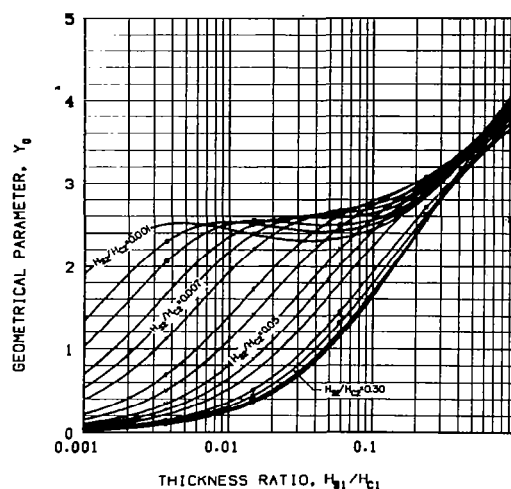


THICKNESS RATIO, H_{s2}/H_{c2}

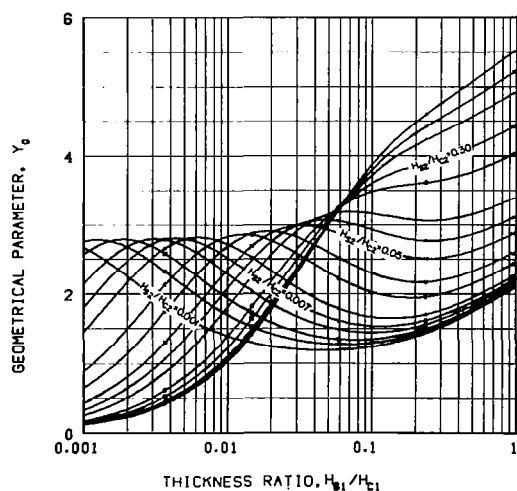
• 0.001	* 0.010	o 0.200
o 0.002	c 0.020	□ 0.300
□ 0.003	u 0.030	+ 0.500
+ 0.005	h 0.050	x 0.700
x 0.007	= 0.070	* 1.000
	• 0.100	



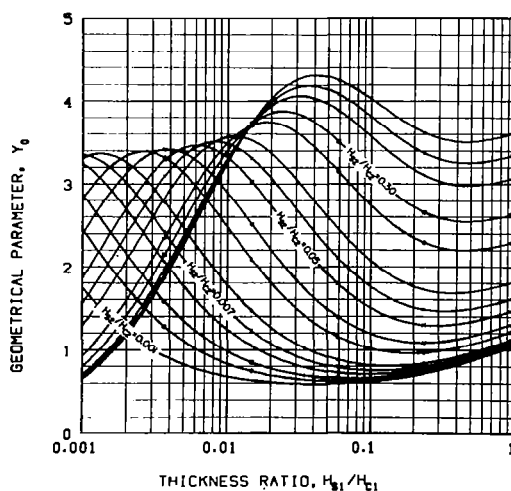
(a) $E_1/E_2=1$; $H_1/H_2=0.25$



(b) $E_1/E_2=1$; $H_1/H_2=0.5$

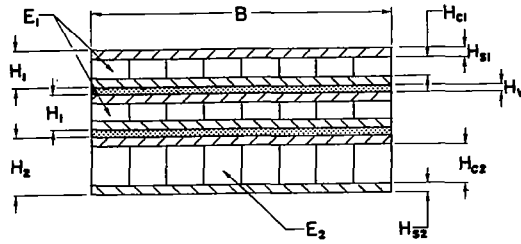


(c) $E_1/E_2=4$; $H_1/H_2=1$



(d) $E_1/E_2=1$; $H_1/H_2=2$

Figure 2.13(E) Geometrical parameter of unsymmetrical composite structural plate comprised of three honeycomb sheets for a modulus ratio $E_1/E_2 = 1$ and various values of the thickness ratio H_1/H_2



THICKNESS RATIO, H_{s2}/H_{c2}

• 0.001	* 0.010	○ 0.200
○ 0.002	c 0.020	□ 0.300
□ 0.003	U 0.030	+ 0.500
+ 0.005	H 0.050	X 0.700
X 0.007	= 0.070	* 1.000
	• 0.100	

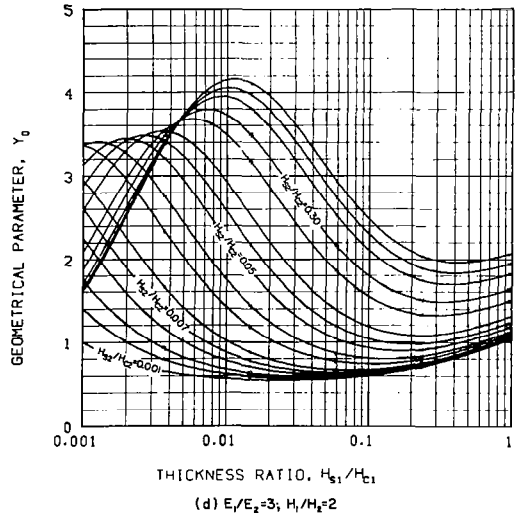
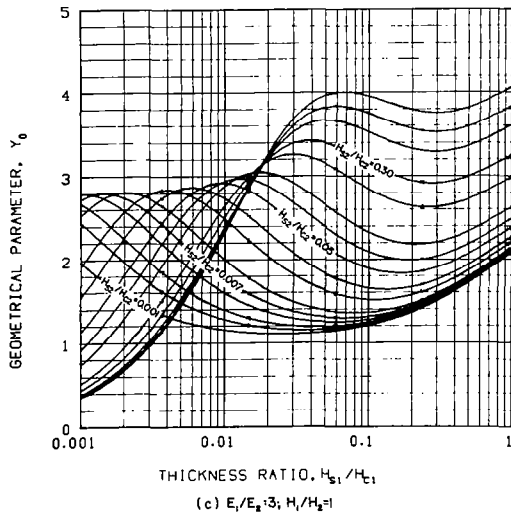
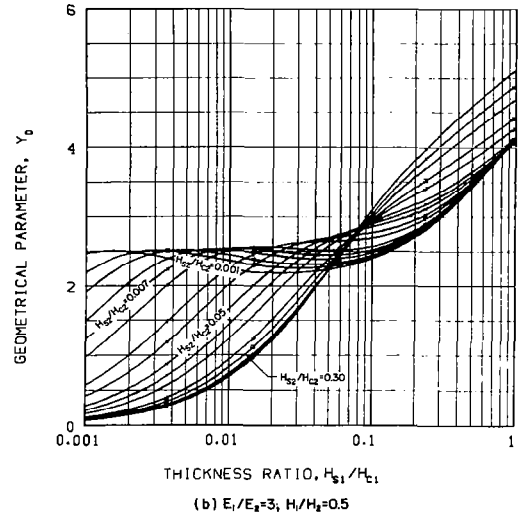
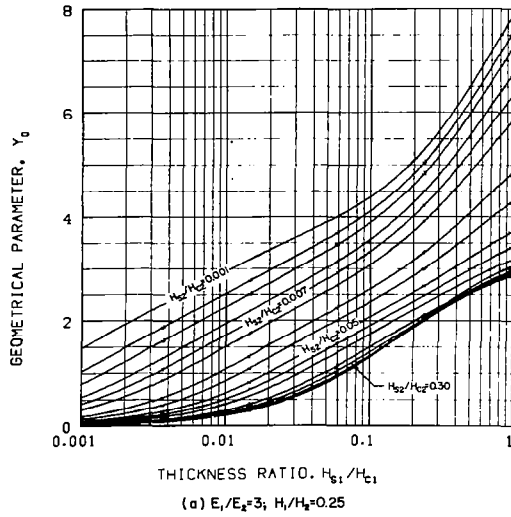


Figure 2.13(F) Geometrical parameter of unsymmetrical composite structural plate comprised of three honeycomb sheets for a modulus ratio $E_1/E_2 = 3$ and various values of the thickness ratio H_1/H_2

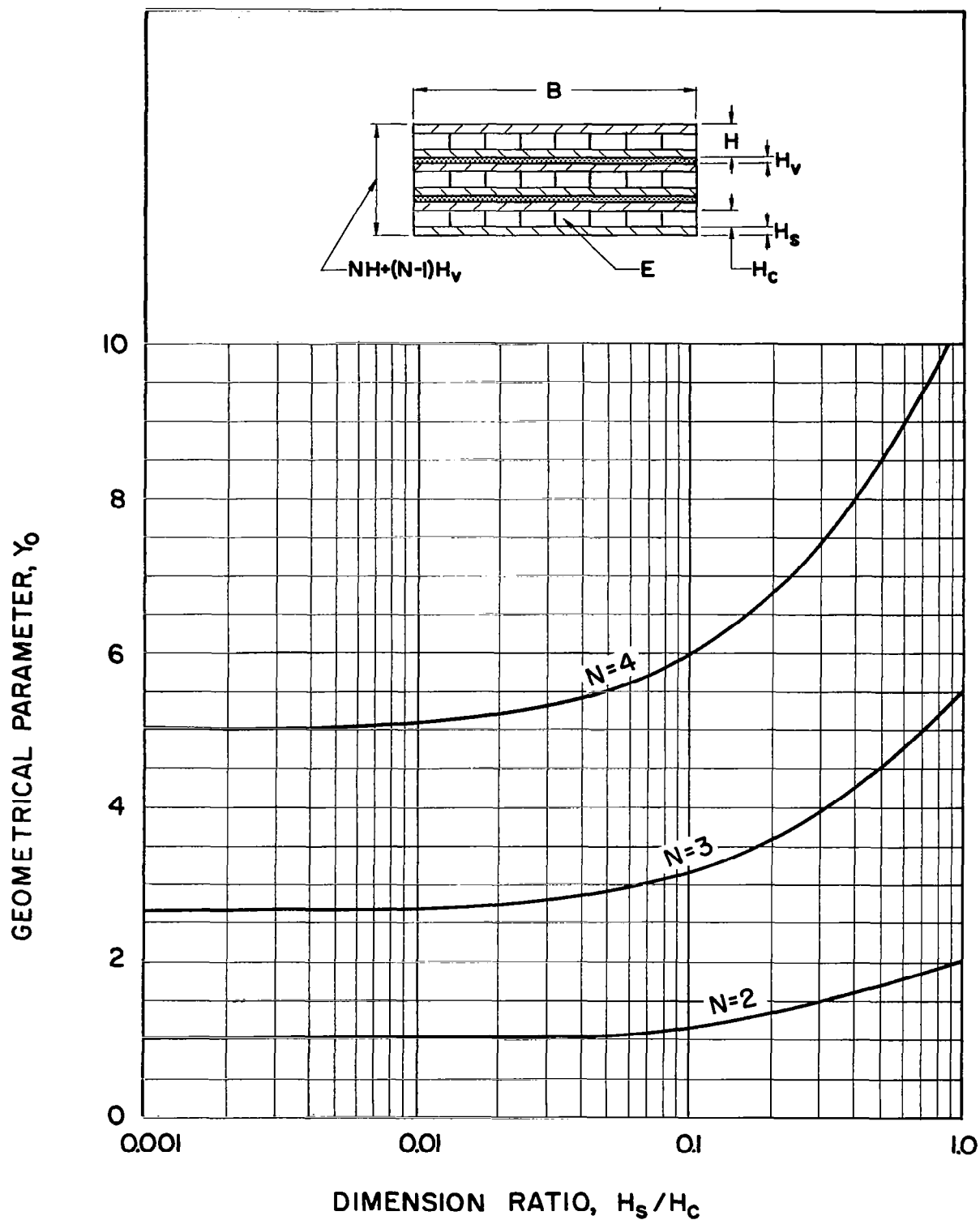
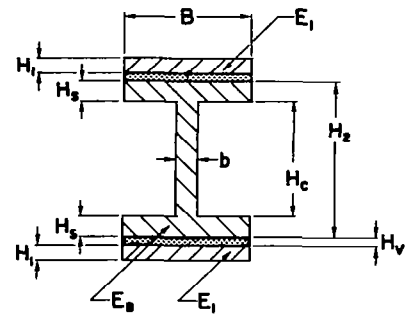
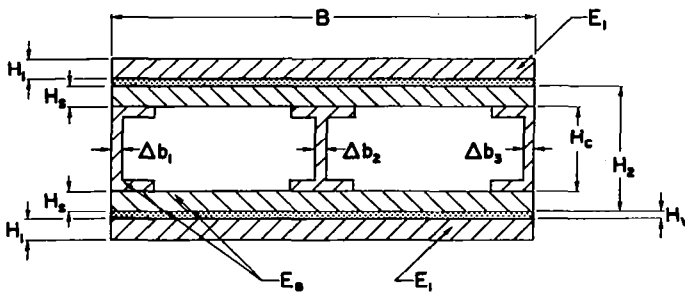


Figure 2.13(G) Geometrical parameter of composite structural plate comprised of N identical honeycomb sheets



$$M = \frac{E_1}{E_2} \quad \frac{E_2}{E_1} = \frac{(2T+1)^3 + b/B - 1}{(2T+1)^3}$$

$$T = \frac{H_1}{H_c} \quad R = \frac{H_1}{H_2} \quad V = \frac{H_1}{H_1 + H_2}$$

$$Y_0 = \frac{6MR(R+1)^2}{2MR^3+1}$$

$$\frac{Y}{Y_0} = (1+2V)^2$$

$$(EI)_0 = \frac{E_2 B H_2^3}{12} (2MR^3+1)$$

$$\omega = B(2\alpha_1 H_1 + 2\alpha_2 H_2) + \alpha_3 b H_c$$

MODULUS RATIO, E_1/E_2

C 1600.000	+	16.000	•	0.333
U 800.000	X	8.000	O	0.250
H 400.000	*	4.000	□	0.125
= 200.000	C	3.000	+	0.062
• 100.000	U	2.000	X	0.040
O 50.000	H	1.000	*	0.020
□ 25.000	=	0.500	C	0.010

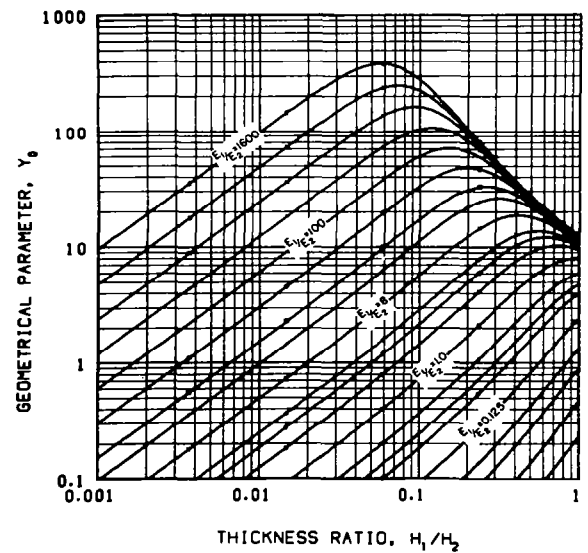
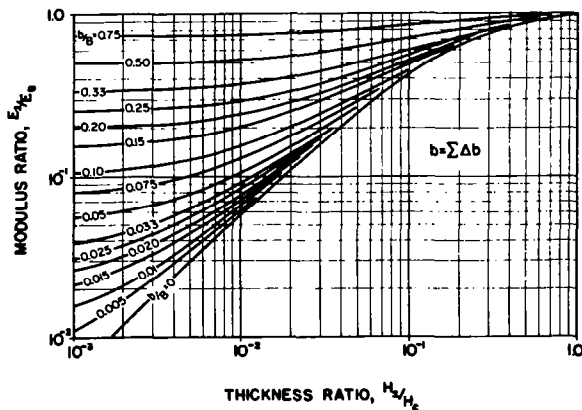


Figure 2.14 Design equations and geometrical parameter of viscoelastic shear-damped plates consisting of double-constrained box-beam and I-beam constructions

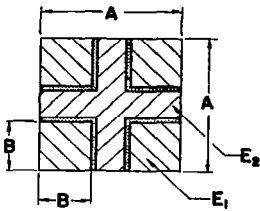
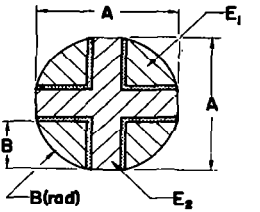
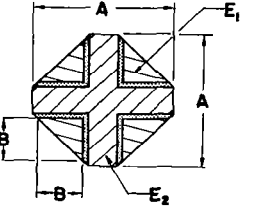
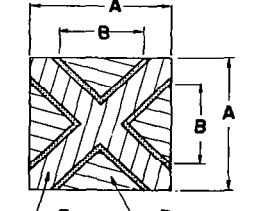
 <p> $M = \frac{E_1}{E_2}$ $D = \frac{B}{A}$ </p>	$Y_0 = \frac{12MD^2(1-D)^2}{4MD^4 + (1-2D)[1+2D(1-2D)^2]}$ $\frac{Y}{Y_0} \approx 1$ $(EI)_0 = E_2 A^4 \left[\frac{1}{12}(1-2D) + \frac{1}{6}D(1-2D)^2 + \frac{1}{3}MD^4 \right]$ $\omega = 4B^2(\gamma_1 - \gamma_2) + \gamma_2 A^2$
 <p> $M = \frac{E_1}{E_2}$ $D = \frac{B}{A}$ </p>	$Y_0 = \frac{1.19MD^2(1.735-2D)^2}{MD^4 + 0.38(1-2D)[1+2D(1-2D)^2]}$ $\frac{Y}{Y_0} \approx 1$ $(EI)_0 = E_2 A^4 \left\{ \frac{(1-2D)}{12} [1+2D(1-2D)^2] + 0.2MD^4 \right\}$ $\omega = \gamma_1 \pi B^2 + \gamma_2 (A^2 - 4B^2)$
 <p> $M = \frac{E_1}{E_2}$ $D = \frac{B}{A}$ </p>	$Y_0 = \frac{2MD^2(3-4D)^2}{4MD^4 + 3(1-2D)[1+2D(1-2D)^2]}$ $\frac{Y}{Y_0} \approx 1$ $(EI)_0 = E_2 A^4 \left\{ \frac{(1-2D)}{12} [1+2D(1-2D)^2] + \frac{MD^4}{9} \right\}$ $\omega = 2\gamma_1 B^2 + \gamma_2 (A^2 - 4B^2)$
 <p> $M = \frac{E_1}{E_2}$ $D = \frac{B}{A}$ </p>	$Y_0 = \frac{MD^2(3-D)^2}{6+2(M-1)D^4-D^2(3-D)^2}$ $\frac{Y}{Y_0} \approx 1$ $(EI)_0 = \frac{E_2 A^4}{72} [6+2D^4(M-1)-D^2(3-D)^2]$ $\omega = \gamma_1 B^2 + \gamma_2 (A^2 - B^2)$

Figure 2.15(A) Design equations for geometrical properties of viscoelastic shear-damped bars consisting of a multiplicity of longitudinal elastic elements arranged to produce various cross-section shapes

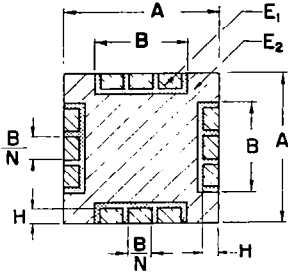
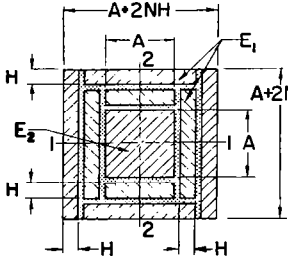
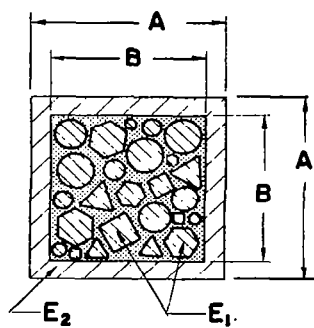
 <p> $M = \frac{E_1}{E_2}$ $D = \frac{B}{A}$ $S = \frac{H}{A}$ </p>	$Y_o = \frac{6MSD(1-S)^2 + 2MSD^3(1-1/N^2)}{1+2(M-1)DS^3+2SD^3(M/N^2-1)-6SD(1-S)^2}$ $\frac{Y}{Y_o} \approx 1$ $(EI)_o = E_2 A^4 \left\{ \frac{1}{12} + \frac{1}{6}(M-1)DS^3 + \frac{1}{6} \left(\frac{M}{N^2} - 1 \right) SD^3 - \frac{SD}{2}(1-S)^2 \right\}$ $\omega = 4\gamma_1 BH + \gamma_2 (A^2 - 4BH)$
 <p> $M = \frac{E_1}{E_2}$ $S = \frac{H}{A}$ </p>	$Y_{o1} = \frac{2MNS[3+3(3N-1)S+3(4N^2-2N-1)S^2+(6N^3-4N^2-3N+1)S^3]}{2MNS[1+3(N+1)S+(4N^2+6N+3)S^2+(2N^3+4N^2+3N-1)S^3]+1}$ $Y_{o2} = \frac{2MNS[3+3(3N+1)S+3(4N^2+2N-1)S^2+(6N^3+4N^2-3N-1)S^3]}{2MNS[1+3(N-1)S+(4N^2-6N+3)S^2+(2N^3-4N^2+3N+1)S^3]+1}$ $\frac{Y}{Y_o} \approx 1$ $(EI)_{o1} = \frac{E_2 A^4}{12} \left\{ 1 + 2MNS[1+3(N+1)S+(4N^2+6N+3)S^2+(2N^3+4N^2+3N-1)S^3] \right\}$ $(EI)_{o2} = \frac{E_2 A^4}{12} \left\{ 1 + 2MNS[1+3(N-1)S+(4N^2-6N+3)S^2+(2N^3-4N^2+3N+1)S^3] \right\}$ $\omega = \gamma_2 A^2 + 4\gamma_1 NH(A+NH)$

Figure 2.15(A) Continued



$$M = \frac{E_1}{E_2} \quad D = \frac{B}{A}$$

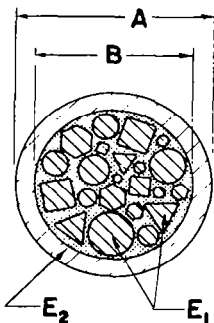
A_i = TOTAL AREA OF INSERTS

$$Y_o = \frac{A_i}{B^2} \left(\frac{MD^4}{1-D^4} \right)$$

$$\frac{Y}{Y_o} \approx 1$$

$$(EI)_o = \frac{E_2 A^4}{12} (1-D^4)$$

$$\omega = \gamma_1 A_i + \gamma_2 (A^2 - B^2)$$



$$M = \frac{E_1}{E_2} \quad D = \frac{B}{A}$$

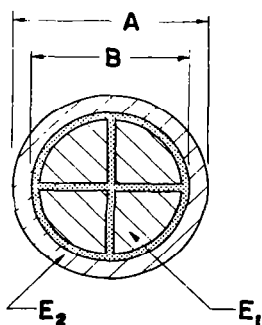
A_i = TOTAL AREA OF INSERTS

$$Y_o = \frac{4A_i}{\pi B^2} \left(\frac{MD^4}{1-D^4} \right)$$

$$\frac{Y}{Y_o} \approx 1$$

$$(EI)_o = \frac{\pi E_2 A^4}{64} (1-D^4)$$

$$\omega = \gamma_1 A_i + \gamma_2 \frac{\pi}{4} (A^2 - B^2)$$



$$M = \frac{E_1}{E_2} \quad D = \frac{B}{A}$$

$$Y_o = \frac{2.57MD^4}{MD^4 + 3.58(1-D^4)}$$

$$\frac{Y}{Y_o} \approx 1$$

$$(EI)_o = E_2 A^4 \left\{ \frac{\pi}{64} (1-D^4) + 0.014 MD^4 \right\}$$

$$\omega = \gamma_1 \frac{\pi}{4} B^2 + \gamma_2 \frac{\pi}{4} (A^2 - B^2)$$

Figure 2.15 (A) Concluded

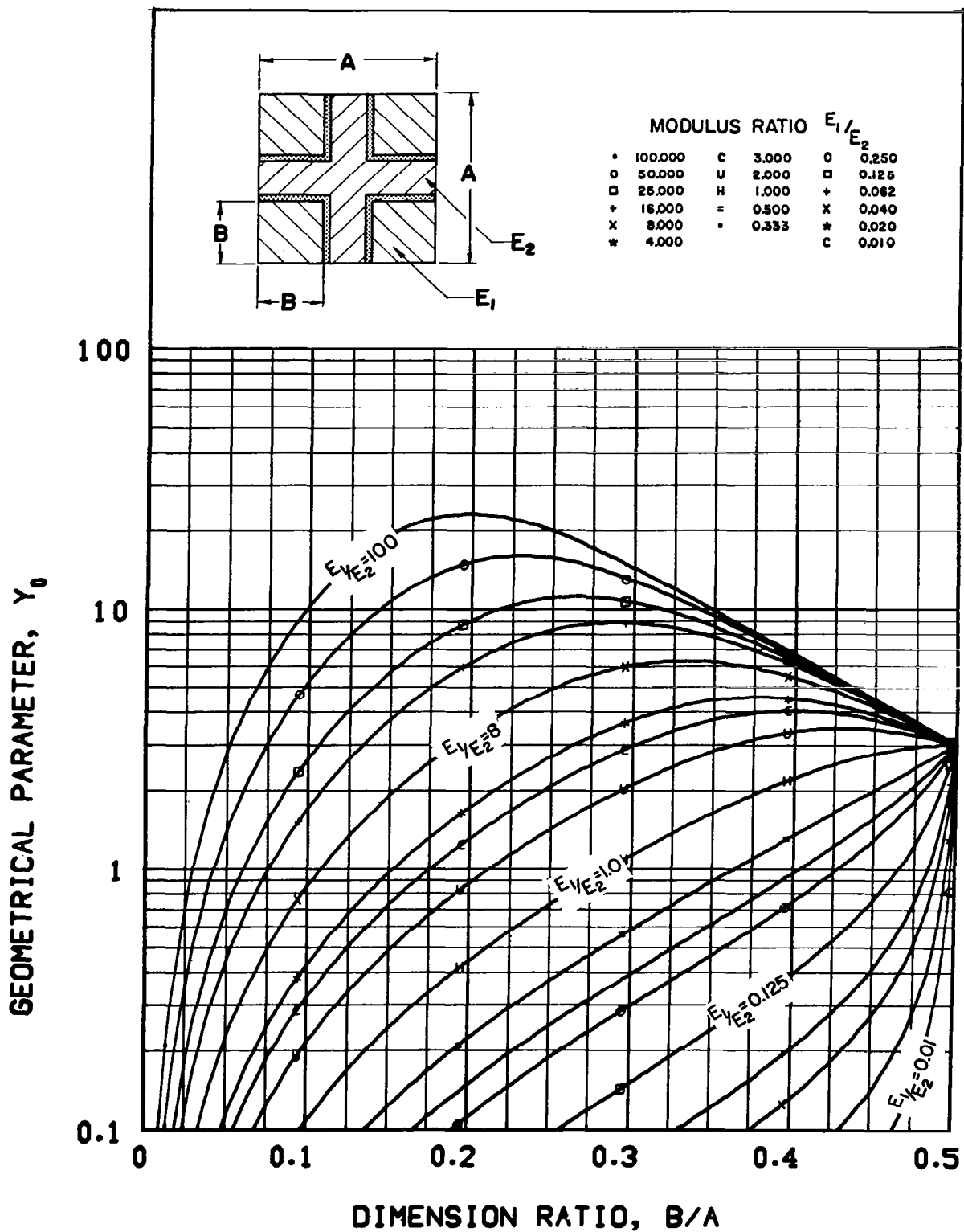


Figure 2.15(B) Geometrical parameter of composite structural bar having a square cross-section shape

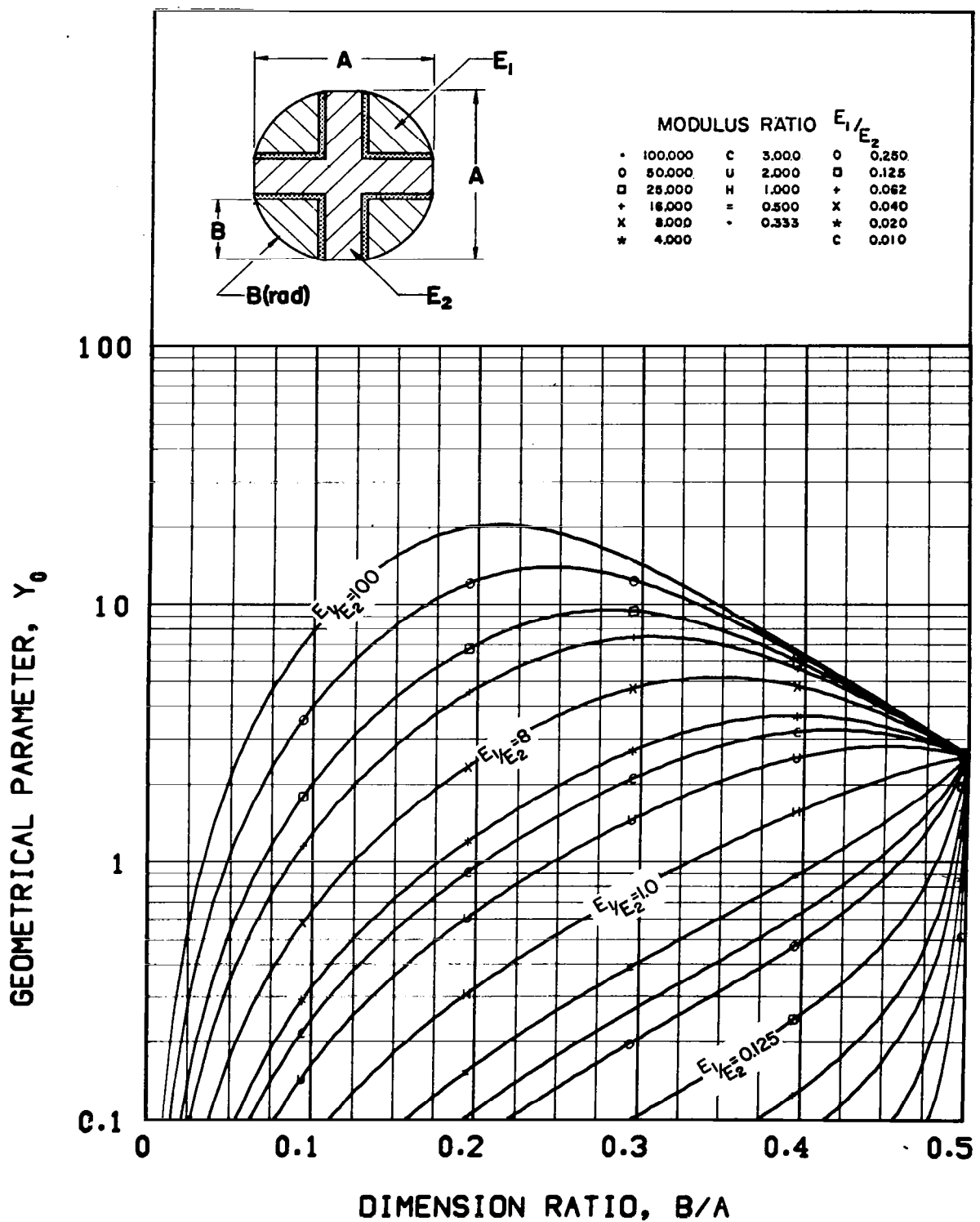


Figure 2.15(C) Geometrical parameter of composite structural bar having a cross-section capable of ranging from a square to a circular shape

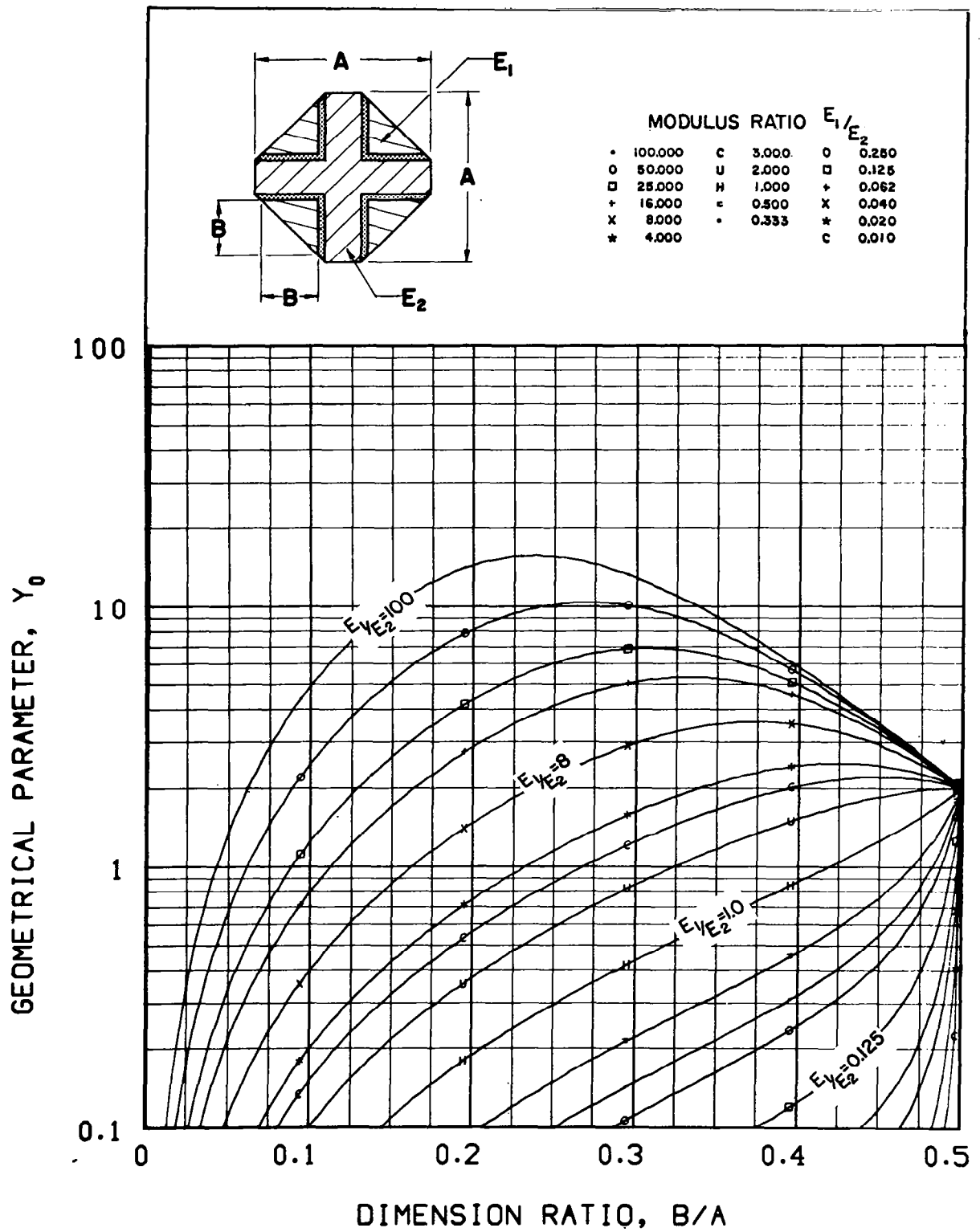


Figure 2.15(D) Geometrical parameter of composite structural bar having a cross-section capable of ranging from a square to an octagonal shape

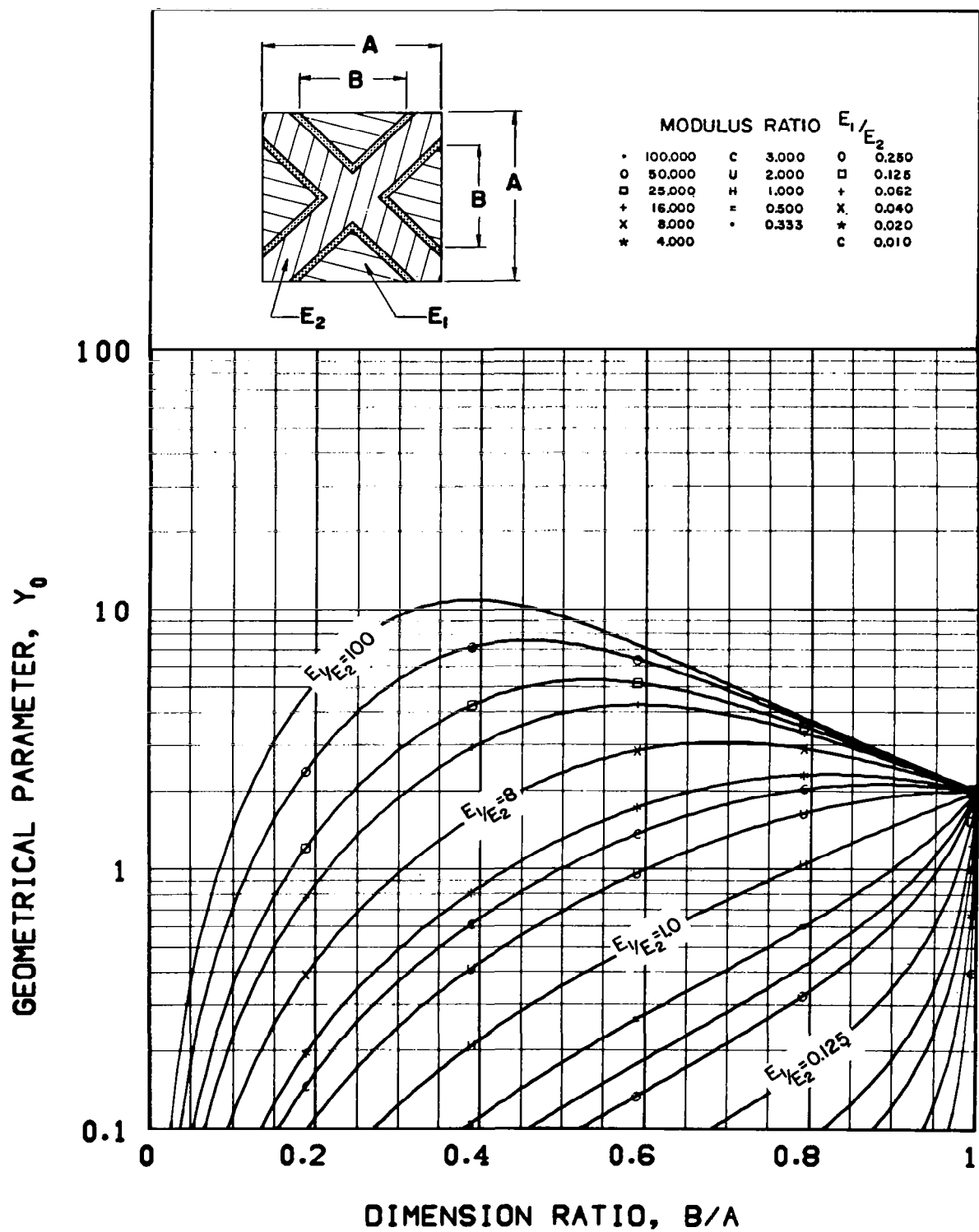
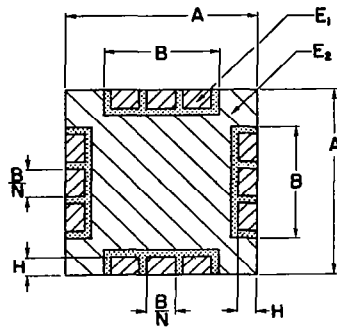


Figure 2.15(E) Geometrical parameter of composite structural bar having square cross-section shape



MODULUS RATIO, E_1/E_2

	100.000	C	3.000	O	0.250
O	50.000	U	2.000	□	0.125
□	25.000	H	1.000	+	0.062
+	16.000	=	0.500	X	0.040
X	8.000	•	0.333	*	0.020
*	4.000			C	0.010

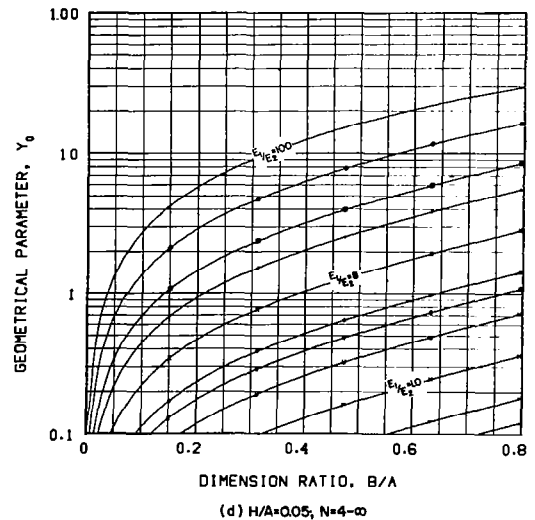
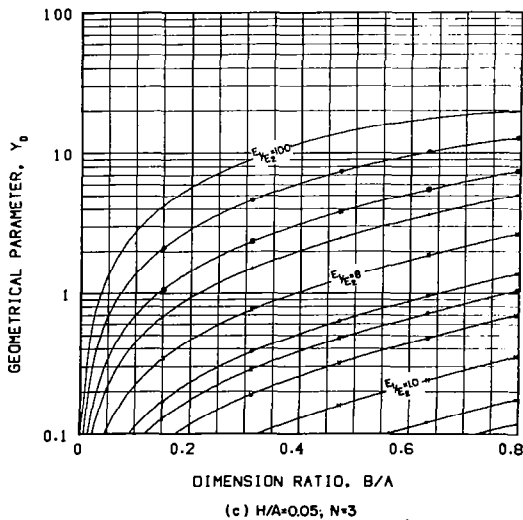
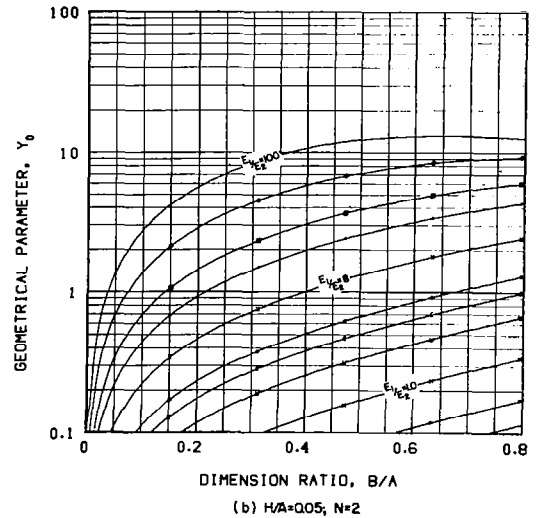
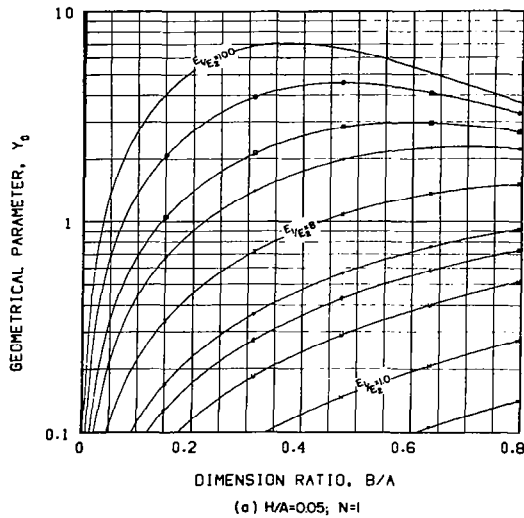
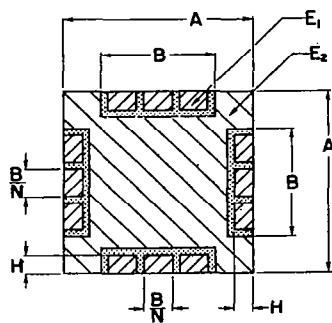


Figure 2.15 (F) Geometrical parameter of composite structural bar having a square cross-section shape for a dimension ratio $H/A = 0.05$ and number of insert elements N ranging from one to infinity



MODULUS RATIO, E_1/E_2

•	100.000	C	3.000	O	0.250
o	50.000	U	2.000	□	0.125
□	25.000	H	1.000	+	0.062
+	16.000	•	0.500	X	0.040
X	8.000	*	0.333	*	0.020
*	4.000			C	0.010

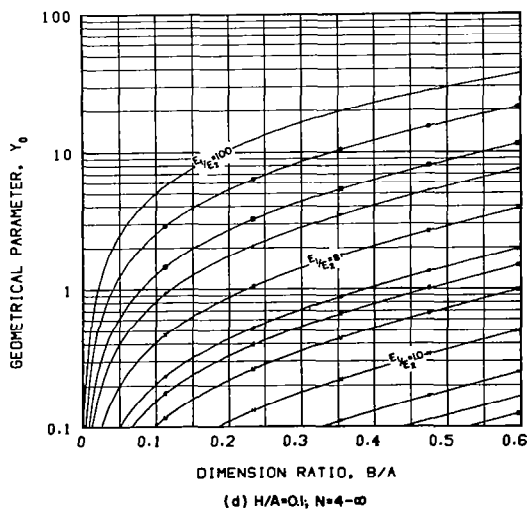
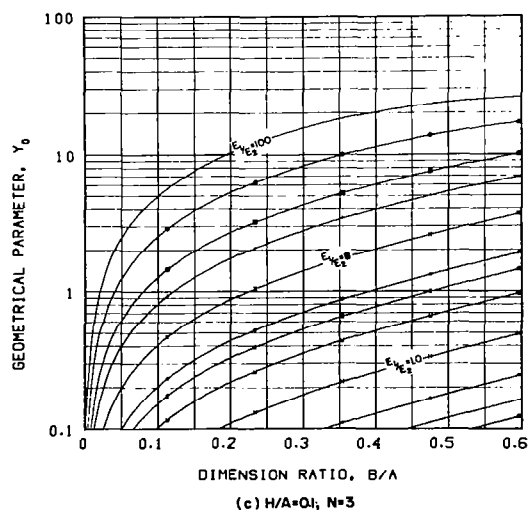
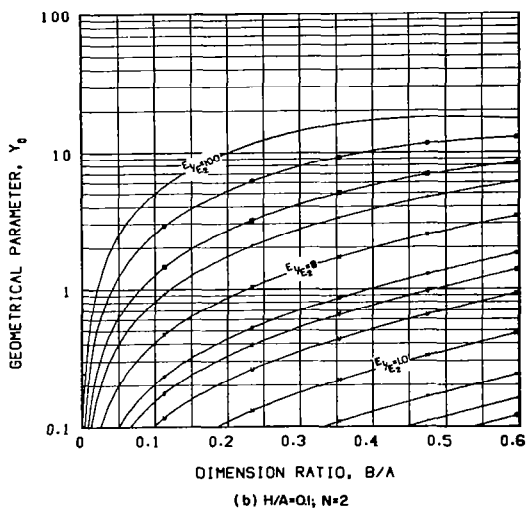
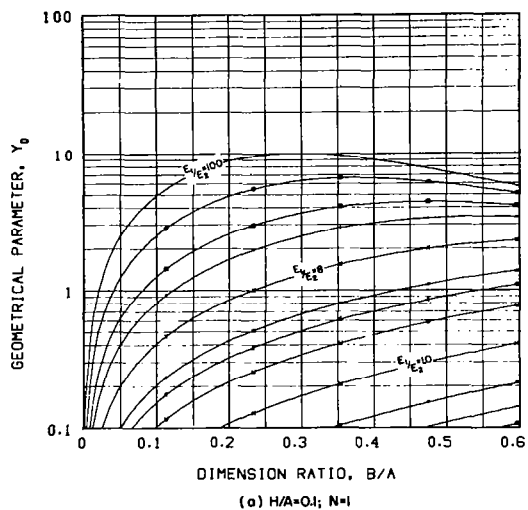
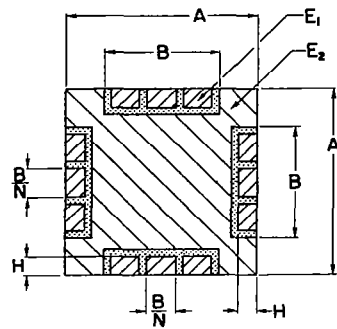


Figure 2.15 (G) Geometrical parameter of composite structural bar having a square cross-section shape for a dimension ratio $H/A = 0.1$ and number of insert elements N ranging from one to infinity



MODULUS RATIO, E_1/E_2

•	100.000	C	3.000	o	0.250
o	50.000	U	2.000	□	0.125
□	25.000	H	1.000	+	0.062
+	16.000	=	0.500	x	0.040
x	8.000	•	0.333	*	0.020
*	4.000			C	0.010

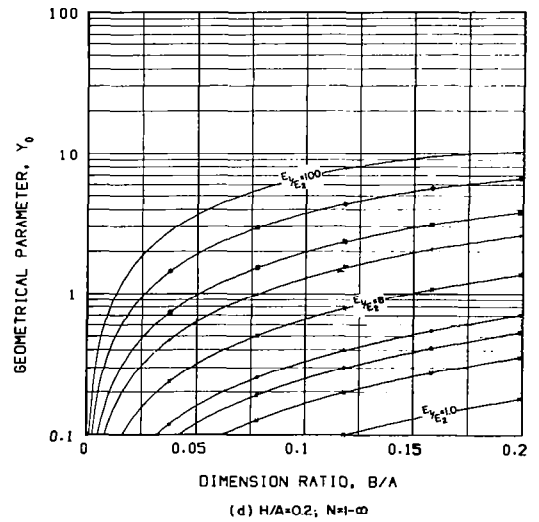
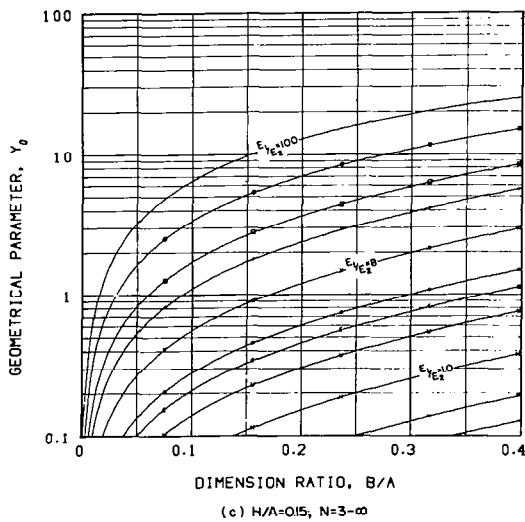
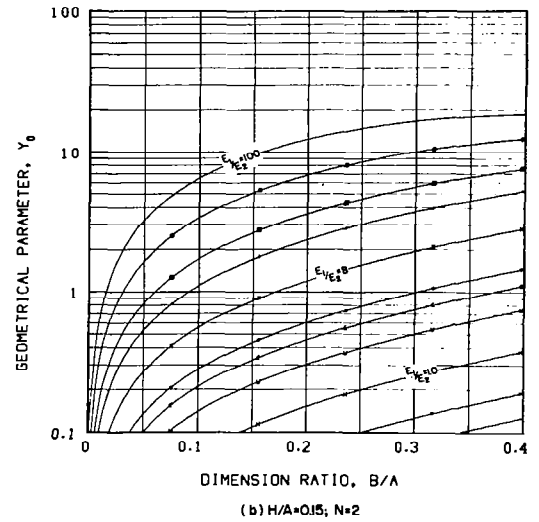
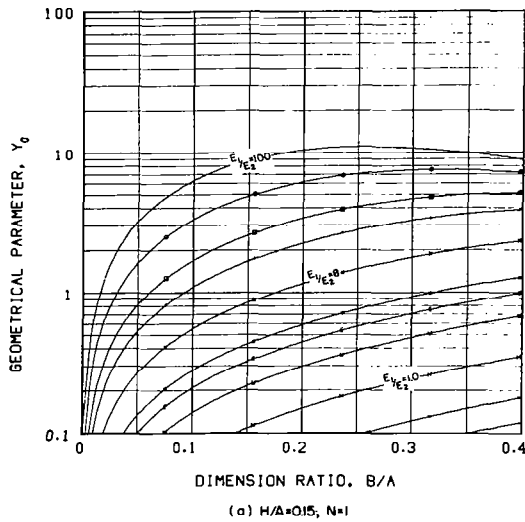
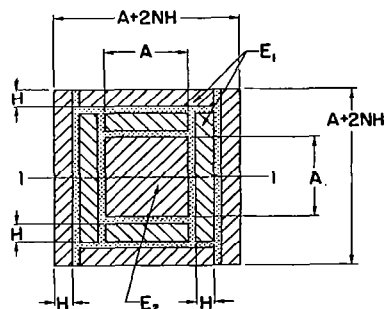
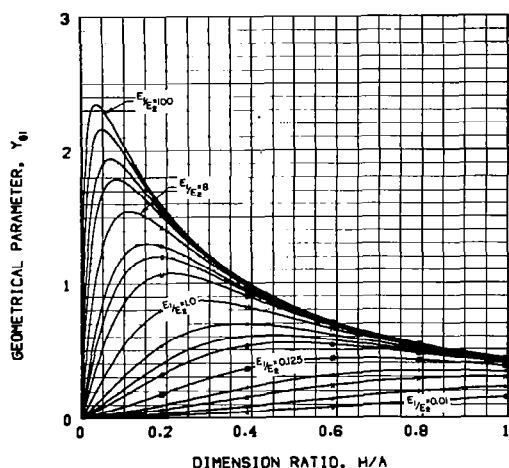


Figure 2.15 (H) Geometrical parameter of composite structural bar having a square cross-section shape for dimension ratios $H/A = 0.15$ and 0.2 and number of insert elements N ranging from one to infinity

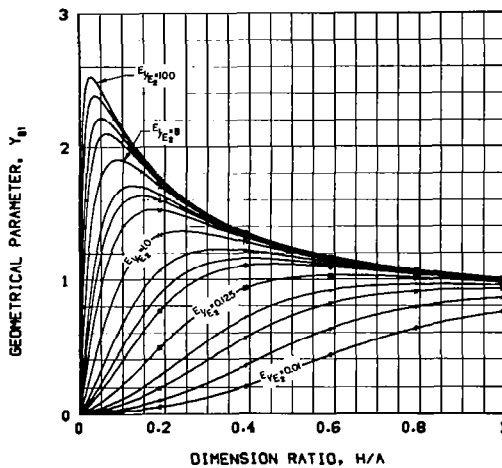


MODULUS RATIO, E_1/E_2

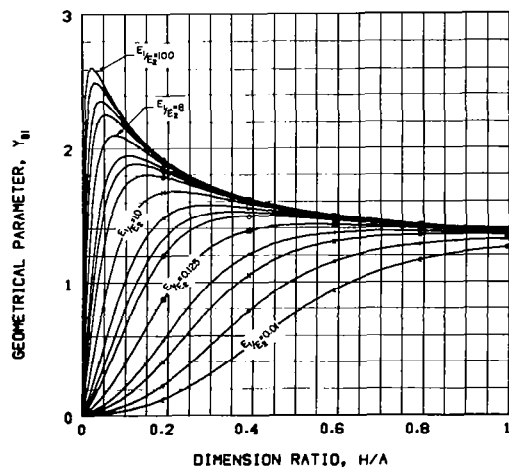
•	100.000	C	3.000	O	0.250
O	50.000	U	2.000	□	0.125
□	25.000	H	1.000	+	0.062
+	16.000	=	0.500	X	0.040
X	8.000	•	0.333	*	0.020
*	4.000			C	0.010



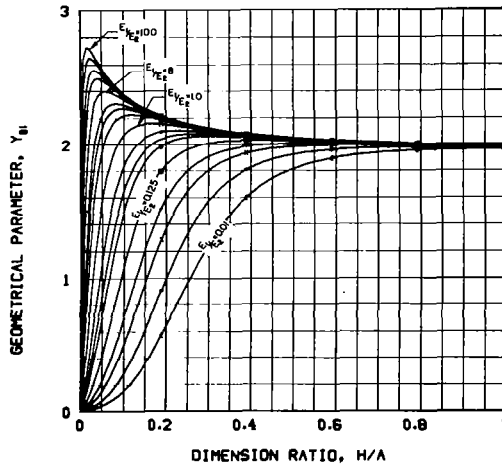
(a) N=1



(b) N=2



(c) N=3



(d) N=6

Figure 2.15(I) Geometrical parameter for neutral axis 1-1 of composite structural bar having a square cross-section shape for various values of the number of solid sheet elements N

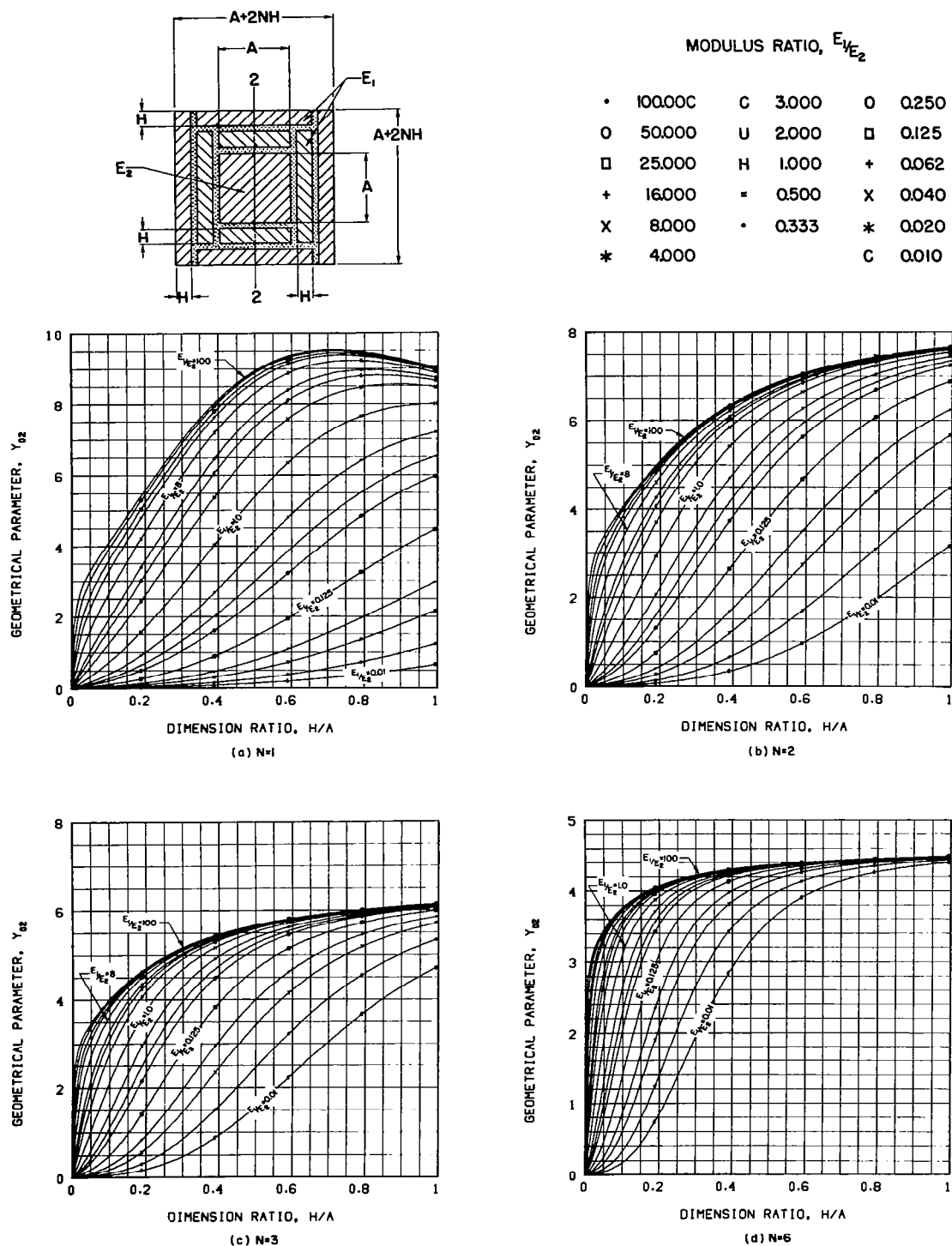


Figure 2.15(J) Geometrical parameter for neutral axis 2-2 of composite structural bar having a square cross-section shape for various values of the number of solid sheet elements N

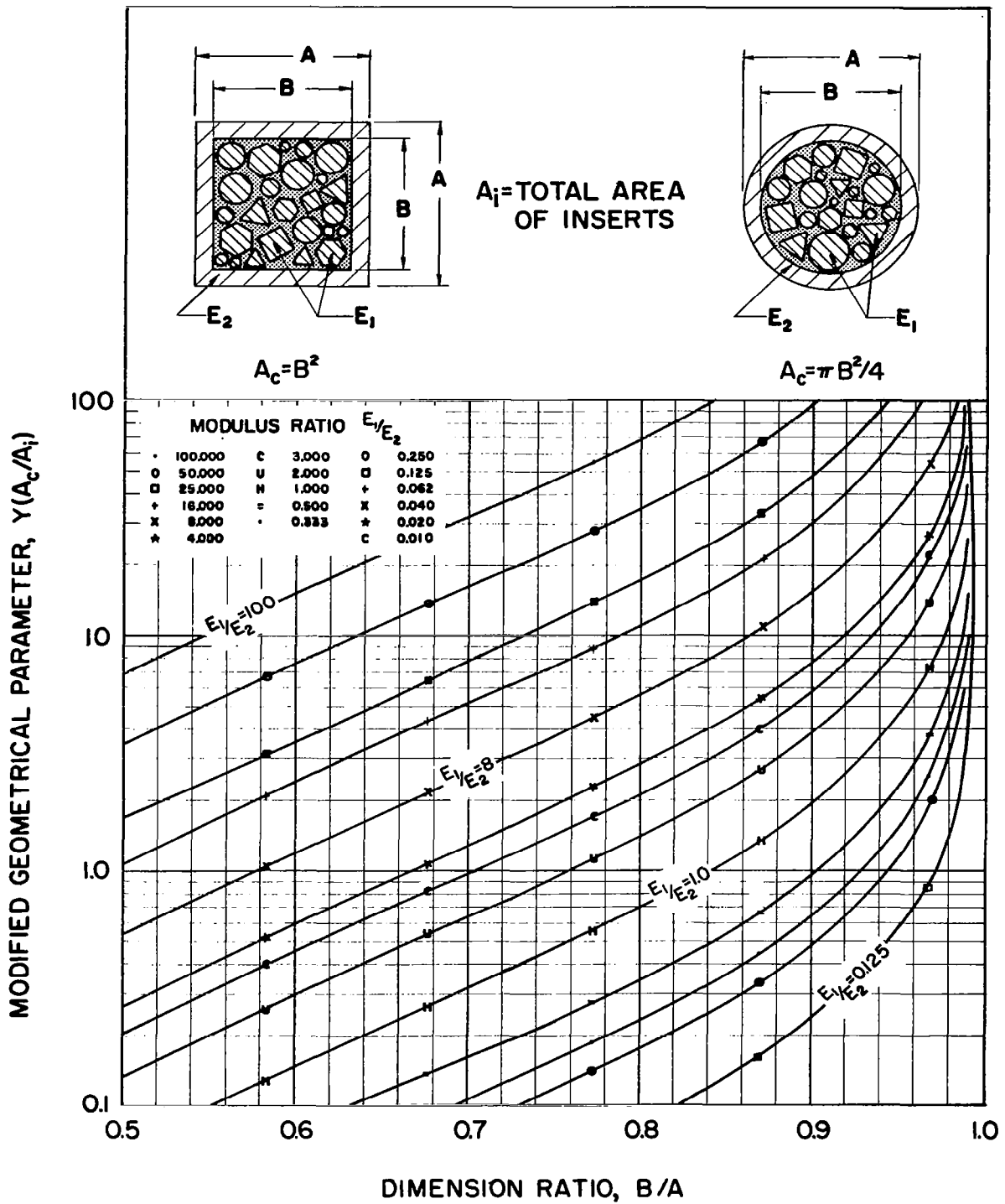


Figure 2.15 (K) Modified geometrical parameter of composite structural bar having a square or round cross-section shape

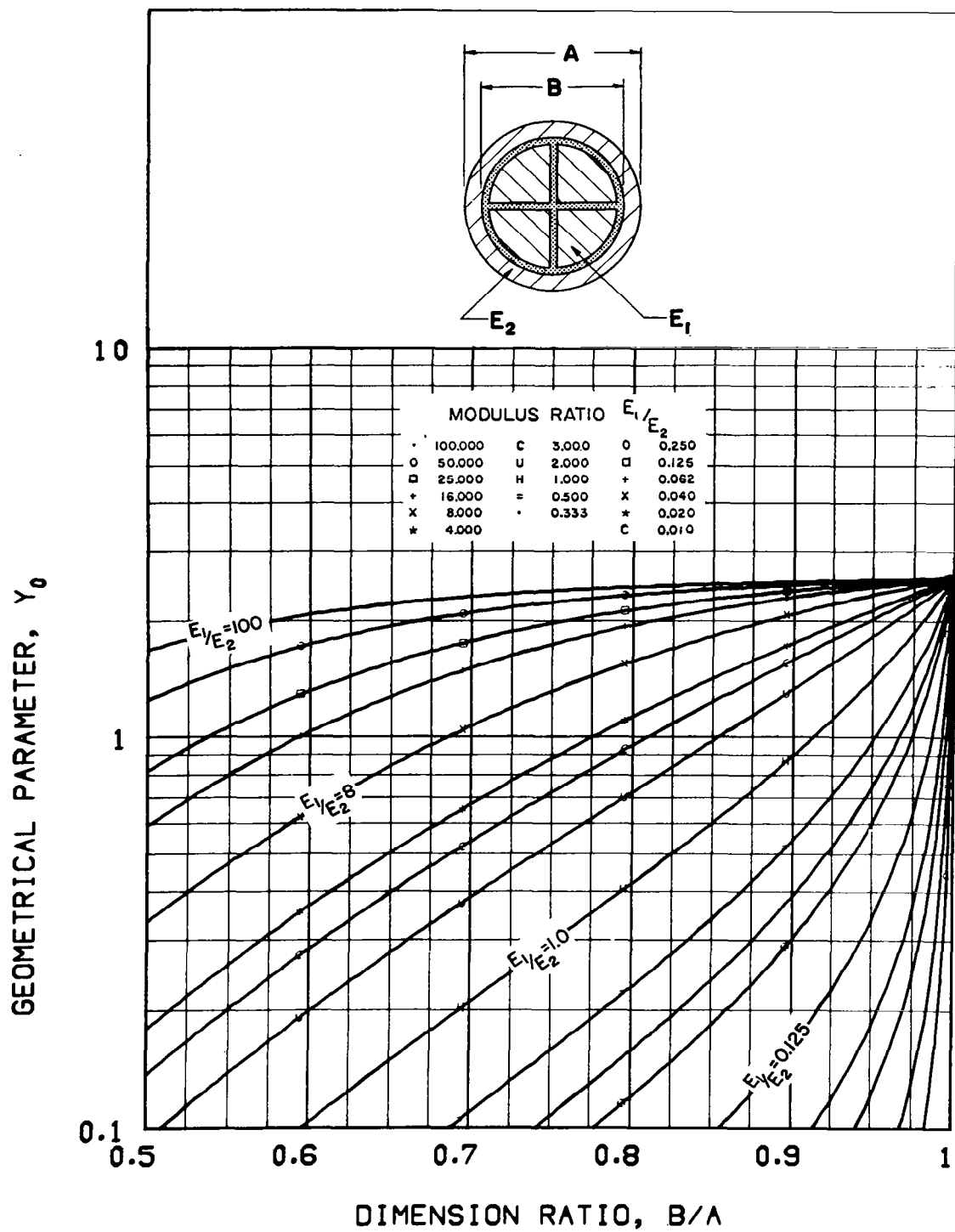


Figure 2.15(I) Geometrical parameter of composite structural bar having a round cross-section shape

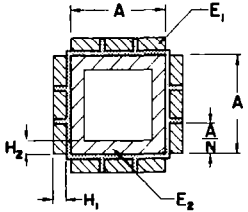
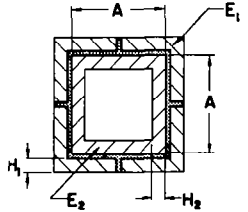
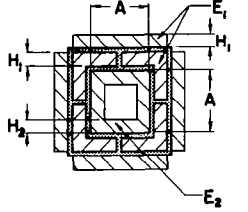
 <p> $M = \frac{E_1}{E_2}$ $R = \frac{H_1}{H_2}$ $S = \frac{H_2}{A}$ </p>	$\gamma_0 = \frac{2MRS[3(1+RS)^2 + 1 - 1/N^2]}{1 - (1-2S)^4 + 2MRS(R^2S^2 + 1/N^2)}$ $\frac{\gamma}{\gamma_0} \approx 1$ $(EI)_0 = \frac{E_2 A^4}{12} \left\{ 2MRS[R^2S^2 + \frac{1}{N^2}] + 1 - (1-2S)^4 \right\}$ $\omega = 4\gamma_1 H_1 A + \gamma_2 [A^2 - (A - 2H_2)^2]$
 <p> $M = \frac{E_1}{E_2}$ $R = \frac{H_1}{H_2}$ $S = \frac{H_2}{A}$ </p>	$\gamma_0 = \frac{3MRS(3+6RS+4R^2S^2)^2}{4(1+RS)[1-(1-2S)^4] + MRS\{(1+2RS)^4 + 4[(1+RS)^3 + 2R^2S^2 + 3R^2S^3]\}}$ $\frac{\gamma}{\gamma_0} \approx 1$ $(EI)_0 = \frac{E_2 A^4}{48} \left\{ 4[1-(1-2S)^4] + \frac{MRS}{(1+RS)} \left\{ (1+2RS)^4 + 4[(1+RS)^3 + 2R^2S^2 + 3R^2S^3] \right\} \right\}$ $\omega = \gamma_1 H_1 (2A + H_1) + \gamma_2 H_2 (2A - H_2)$
 <p> $M = \frac{E_1}{E_2}$ $R = \frac{H_1}{H_2}$ $S = \frac{H_2}{A}$ </p>	$\gamma_0 = \frac{3MRS(3+6RS+4R^2S^2)^2 + 24M(1+RS)(1+2RS)(1+3RS)^2RS}{4(1+RS)[1-(1-2S)^4] + MRS\{(1+2RS)^4 + 4[(1+RS)^3 + 2R^2S^2 + 3R^2S^3]\} + 8(1+RS)(1+2RS)[R^2S^2 + (1+2RS)^2]}$ $\frac{\gamma}{\gamma_0} \approx 1$ $(EI)_0 = \frac{E_2 A^4}{48} \left\{ 4[1-(1-2S)^4] + \frac{MRS}{(1+RS)} \left\{ (1+2RS)^4 + 4[(1+RS)^3 + 2R^2S^2 + 3R^2S^3] \right\} + 8MRS(1+2RS)[R^2S^2 + (1+2RS)^2] \right\}$ $\omega = 4\gamma_1 H_1 (2A + 3H_1) + \gamma_2 4H_2 (A - H_2)$

Figure 2.16(A) Design equation for geometrical properties of viscoelastic shear-damped tubes consisting of a combination of solid structural tubes and longitudinal elastic constraining elements

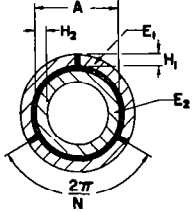
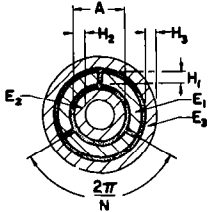
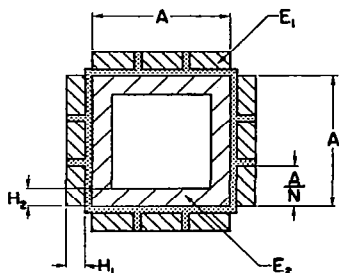
 <p> $M = \frac{E_1}{E_2}$ $R = \frac{H_1}{H_2}$ $S = \frac{H_2}{A}$ </p>	$Y_0 = \frac{8MN^2[(1+2RS)^3-1]^2 \sin^2(\pi/N)}{9\pi^2[(1+2RS)^3-1]\{[1-(1-2S)^4] + M[(1+2RS)^4-1]\} - 8MN^2[(1+2RS)^3-1]^2 \sin^2(\pi/N)}$ $\frac{Y}{Y_0} \approx 1$ $(EI)_0 = E_2 A^4 \left\{ \frac{\pi}{64} [1-(1-2S)^4] + \frac{\pi}{64} M [(1+2RS)^4-1] - \frac{MN^2 [(1+2RS)^3-1]^2}{72\pi [(1+2RS)^3-1]} \sin^2\left(\frac{\pi}{N}\right) \right\}$ $\omega = \gamma, \frac{\pi}{4} [(A+2H_1)^2 - A^2] + \gamma_2 \frac{\pi}{4} [A^2 - (A-2H_2)^2]$
 <p> $M_1 = \frac{E_1}{E_2}$ $R_1 = \frac{H_1}{H_2}$ $S = \frac{H_2}{A}$ $M_2 = \frac{E_3}{E_2}$ $R_2 = \frac{H_3}{H_2}$ </p>	$Y_0 = \frac{8M_1 N^2 [(1+2R_1 S)^3-1]^2 \sin^2(\pi/N)}{9\pi^2 [(1+2R_1 S)^3-1] \{ [1-(1-2S)^4] + M_1 [(1+2R_1 S)^4-1] \} - 8M_1 N^2 [(1+2R_1 S)^3-1]^2 \sin^2(\pi/N) + 8\pi^2 M_2 [(1+2R_1 S)^3-1] [(1+2R_1 S+2SR_2)^4 - (1+2R_1 S)^4]}$ $\frac{Y}{Y_0} \approx 1$ $(EI)_0 = E_2 A^4 \left\{ \frac{\pi}{64} [1-(1-2S)^4] + \frac{\pi}{64} M_1 [(1+2R_1 S)^4-1] + \frac{\pi}{64} M_2 [(1+2R_1 S+2SR_2)^4 - (1+2R_1 S)^4] - \frac{1}{72\pi} M_1 N^2 [(1+2R_1 S)^3-1]^2 \sin^2\left(\frac{\pi}{N}\right) \left[\frac{1}{(1+2R_1 S)^3-1} \right] \right\}$ $\omega = \gamma, \frac{\pi}{4} [(A+2H_1)^2 - A^2] + \gamma_2 \frac{\pi}{4} [A^2 - (A-2H_2)^2] + \gamma_3 \frac{\pi}{4} [(A+2H_1+2H_3)^2 - (A+2H_1)^2]$

Figure 2.16 (A) Concluded



MODULUS RATIO, E_1/E_2

•	100.000	C	3.000	O	0.250
O	50.000	U	2.000	□	0.125
□	25.000	H	1.000	+	0.062
+	16.000	▪	0.500	X	0.040
X	8.000	•	0.333	*	0.020
*	4.000			C	0.010

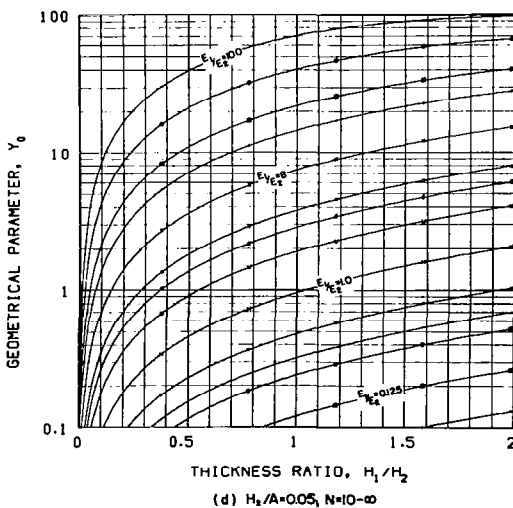
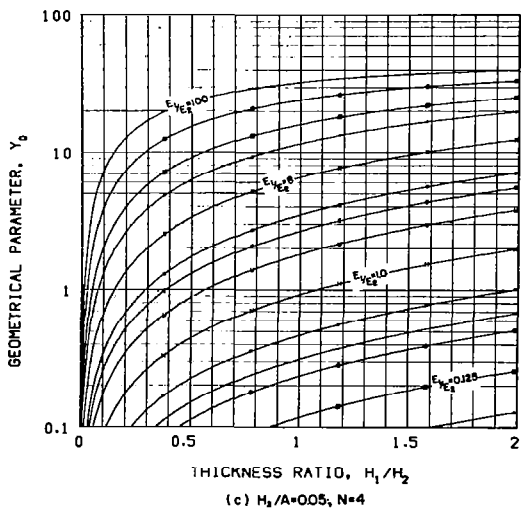
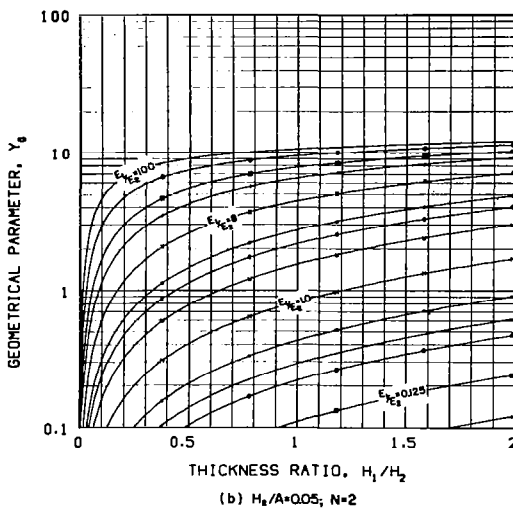
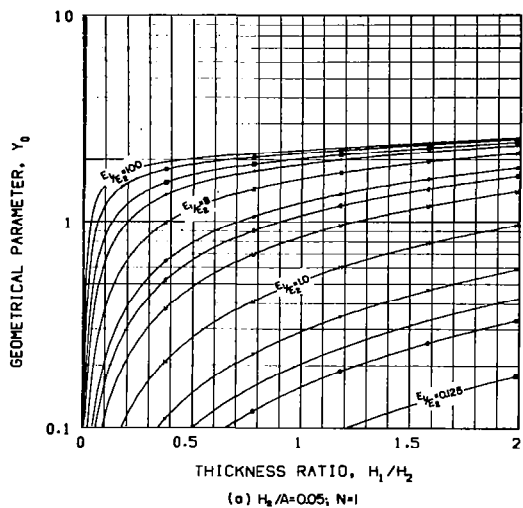
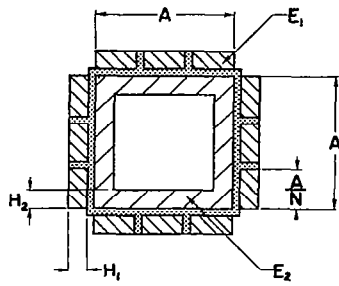


Figure 2.16(B) Geometrical parameter of composite structural tube having a square cross-section shape for a dimension ratio $H_2/A = 0.05$ and number of constraining strips N ranging from one to infinity



MODULUS RATIO, E_1/E_2

•	100.000	C	3.000	O	0.250
O	50.000	U	2.000	□	0.125
□	25.000	H	1.000	+	0.062
+	16.000	•	0.500	X	0.040
X	8.000	•	0.333	*	0.020
*	4.000			C	0.010

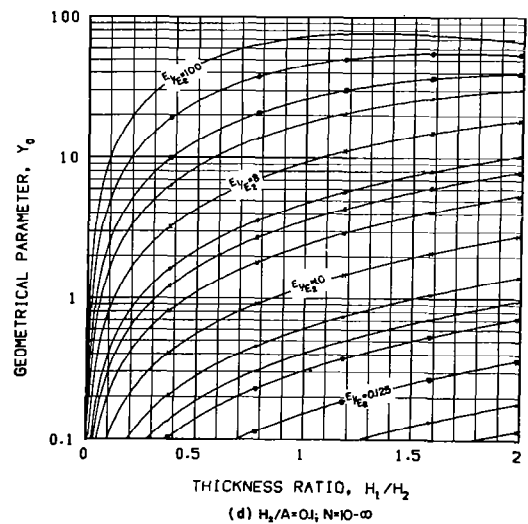
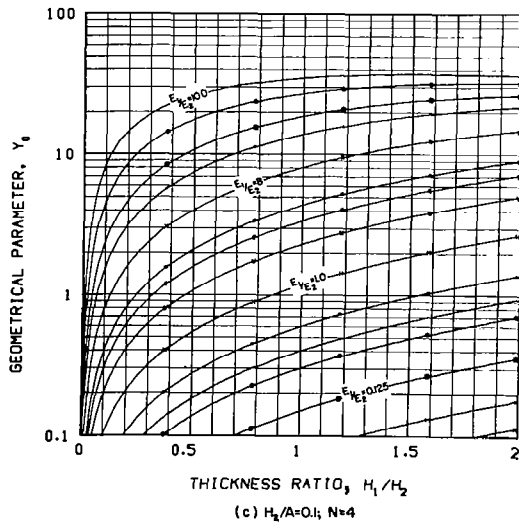
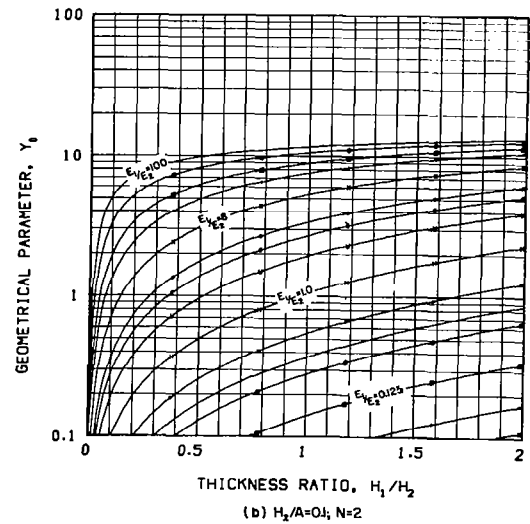
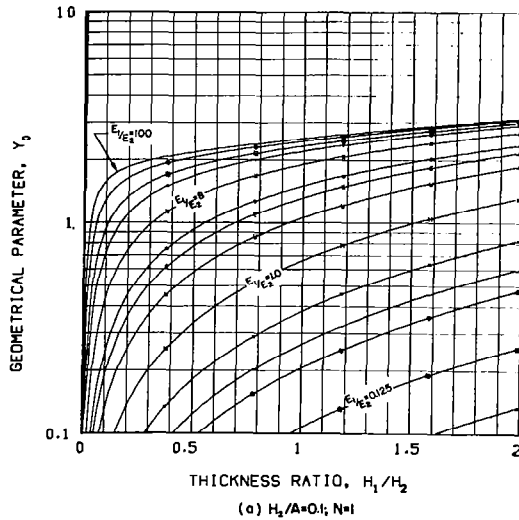
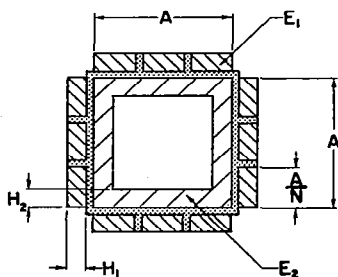


Figure 2.16(C) Geometrical parameter of composite structural tube having a square cross-section shape for a dimension ratio $H_2/A = 0.1$ and number of constraining strips N ranging from one to infinity



MODULUS RATIO, E_1/E_2

•	100.000	C	3.000	O	0.250
O	50.000	U	2.000	□	0.125
□	25.000	H	1.000	+	0.062
+	16.000	▪	0.500	X	0.040
X	8.000	•	0.333	*	0.020
*	4.000			C	0.010

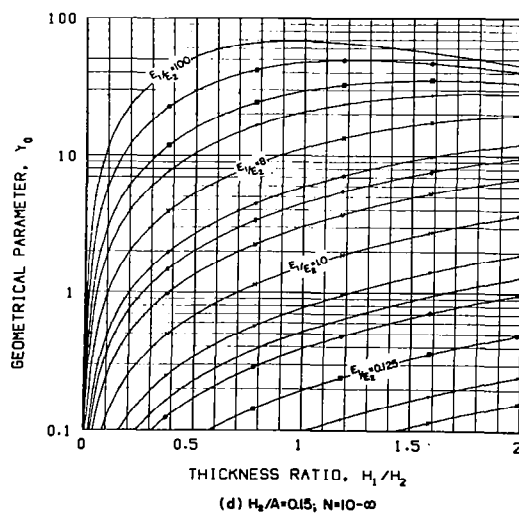
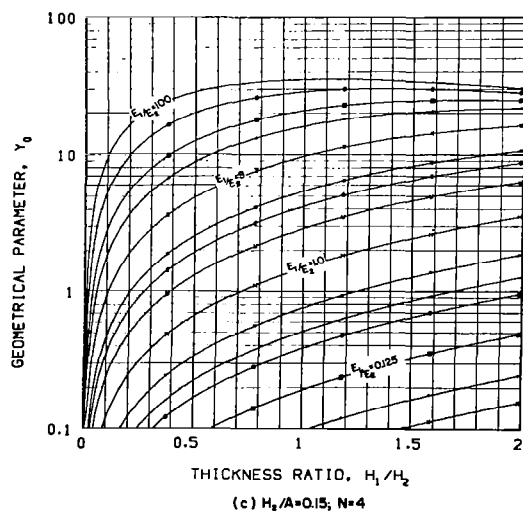
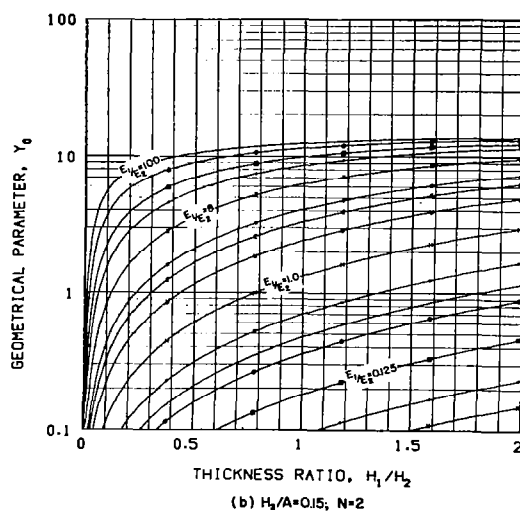
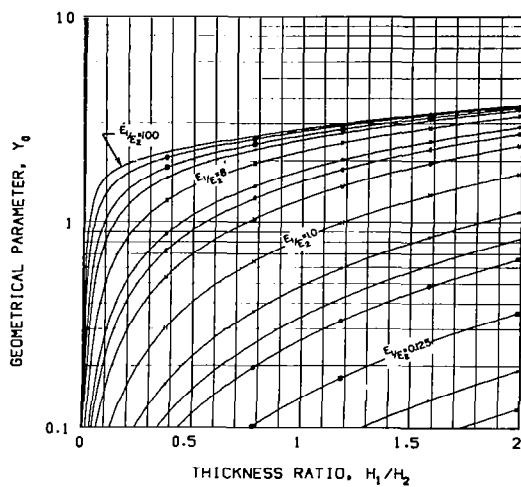
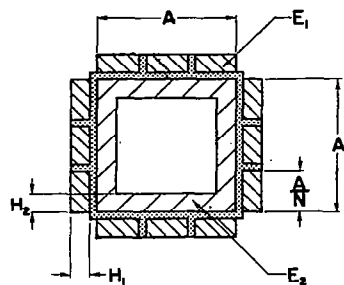


Figure 2.16(D) Geometrical parameter of composite structural tube having a square cross-section shape for a dimension ratio $H_2/A = 0.15$ and number of constraining strips N ranging from one to infinity



MODULUS RATIO, E_1/E_2

•	100.000	C	3.000	O	0.250
O	50.000	U	2.000	□	0.125
□	25.000	H	1.000	+	0.062
+	16.000	=	0.500	X	0.040
X	8.000	•	0.333	*	0.020
*	4.000			C	0.010

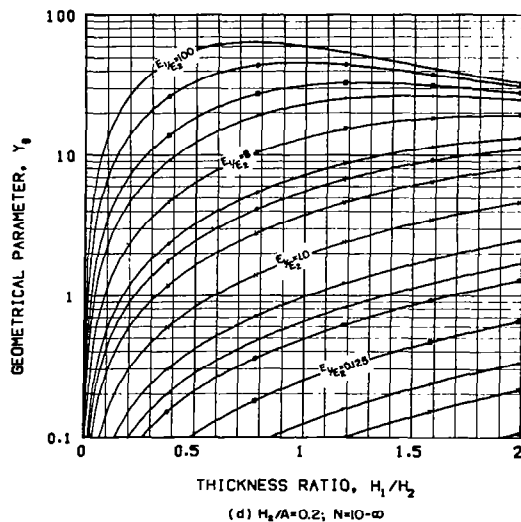
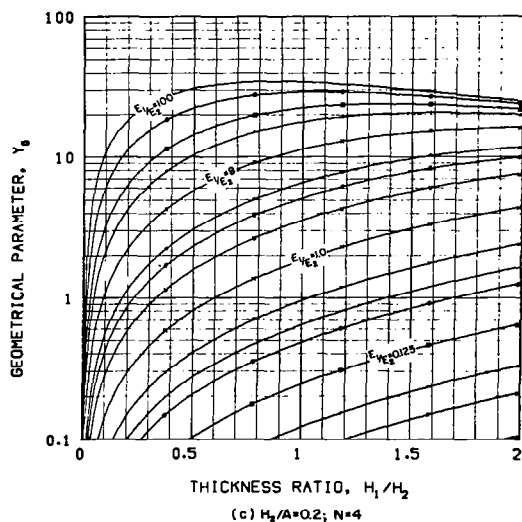
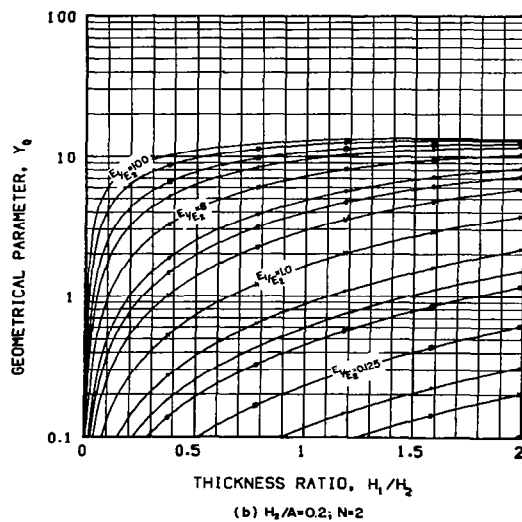
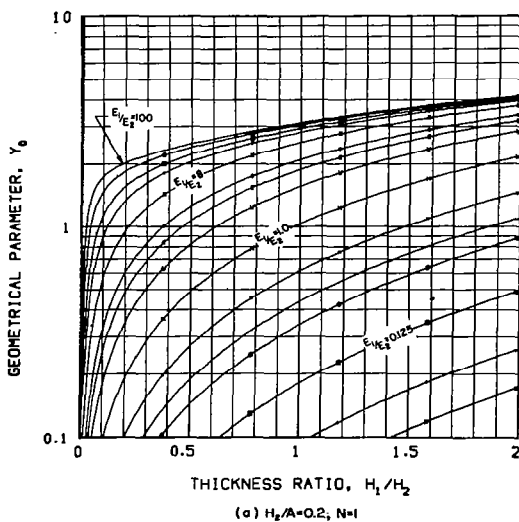
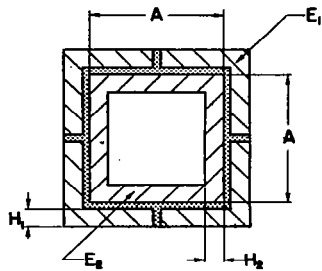


Figure 2.16(E) Geometrical parameter of composite structural tube having a square cross-section shape for a dimension ratio $H_2/A = 0.2$ and number of constraining strips N ranging from one to infinity



MODULUS RATIO, E_1/E_2

•	100.000	C	3.000	O	0.250
O	50.000	U	2.000	□	0.125
□	25.000	H	1.000	+	0.062
+	16.000	▪	0.500	X	0.040
X	8.000	•	0.333	*	0.020
*	4.000			C	0.010

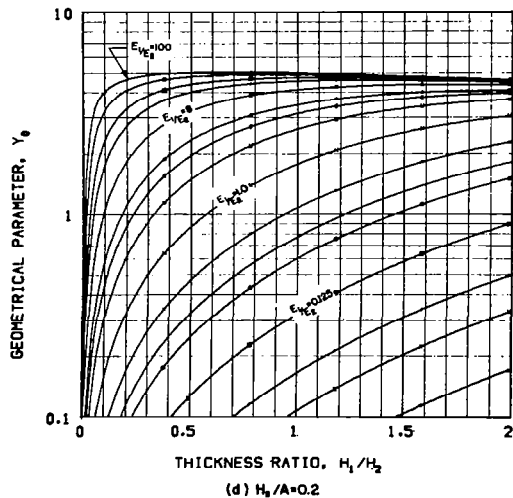
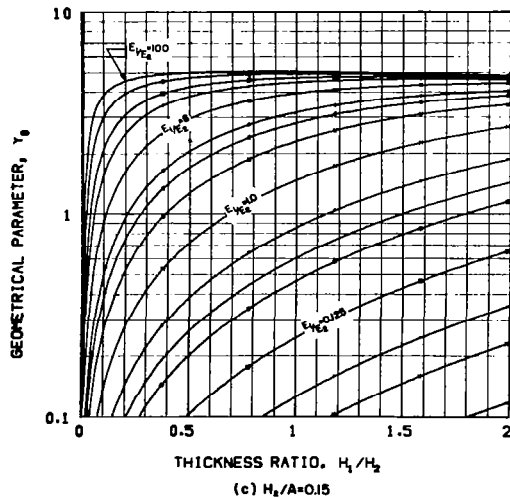
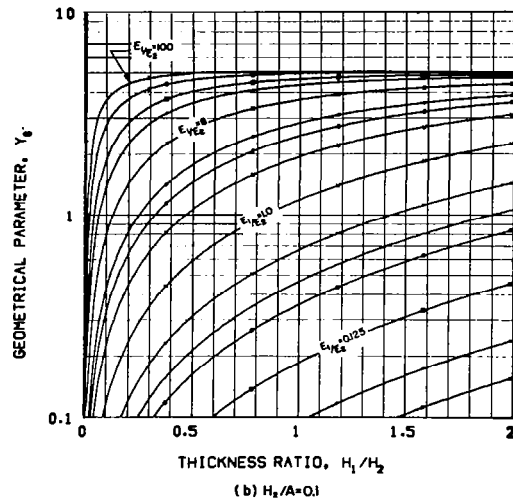
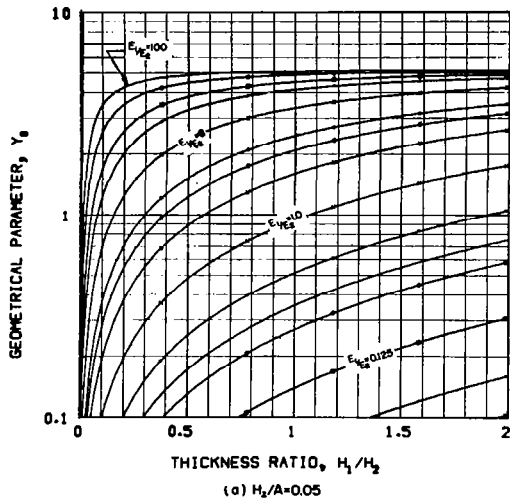
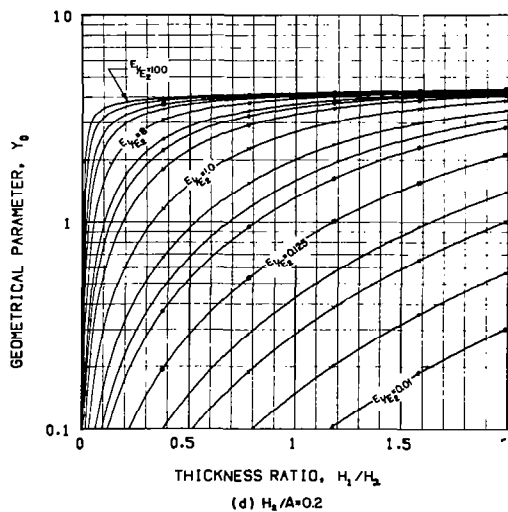
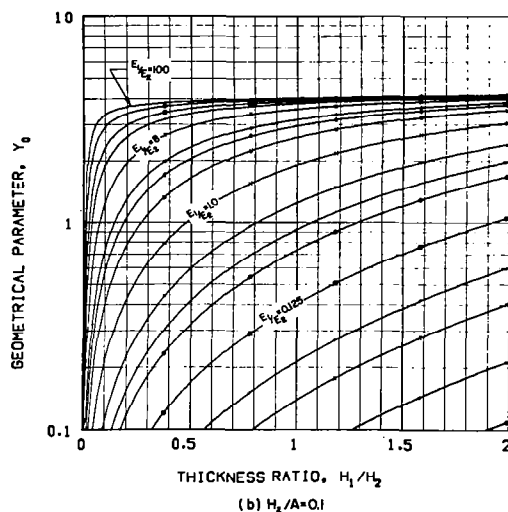


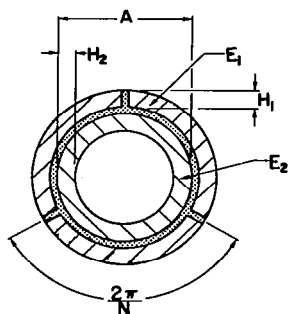
Figure 2.16(F) Geometrical parameter of composite structural tube having a square cross-section shape for various values of the dimension ratio H_2/A



•	100.000	C	3.000	O	0.250
O	50.000	U	2.000	□	0.125
□	25.000	H	1.000	+	0.062
+	16.000	=	0.500	X	0.040
X	8.000	•	0.333	*	0.020
*	4.000			C	0.010



120



MODULUS RATIO, E_1/E_2

•	100.000	C	3.000	○	0.250
○	50.000	U	2.000	□	0.125
□	25.000	H	1.000	+	0.062
+	16.000	▪	0.500	x	0.040
x	8.000	•	0.333	*	0.020
*	4.000			C	0.010

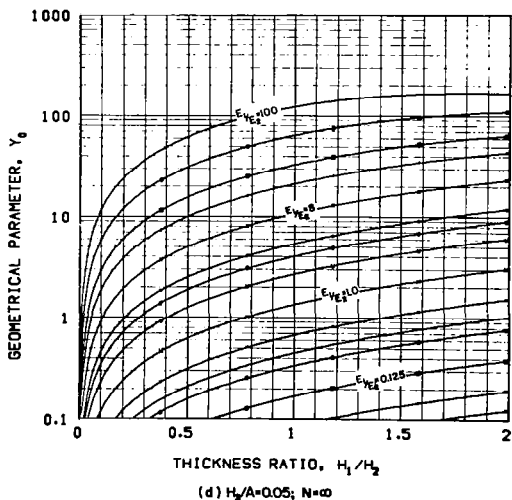
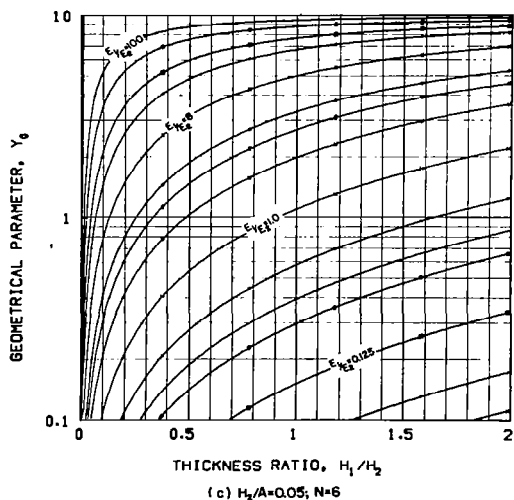
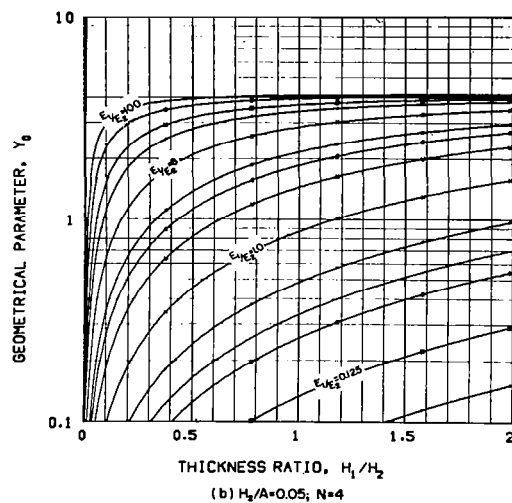
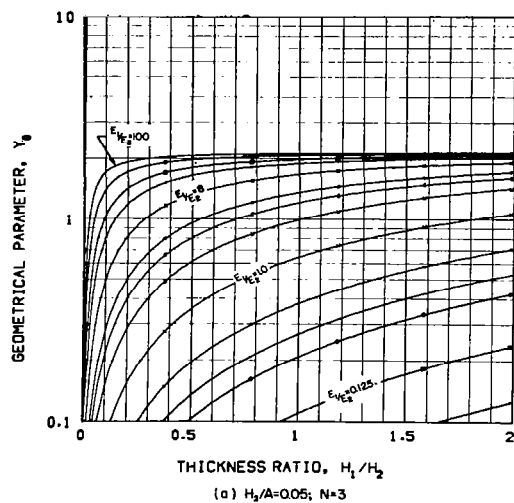
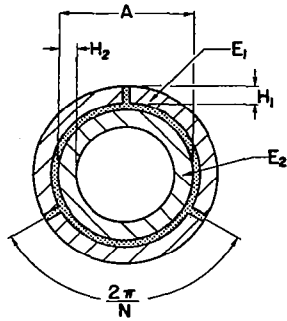


Figure 2.16 (H) Geometrical parameter of composite structural tube having a round cross-section shape for a dimension ratio $H_2/A = 0.05$ and number of tube segments N ranging from three to infinity



MODULUS RATIO, E_1/E_2

•	100.000	C	3.000	O	0.250
O	50.000	U	2.000	□	0.125
□	25.000	H	1.000	+	0.062
+	16.000	▪	0.500	X	0.040
X	8.000	•	0.333	*	0.020
*	4.000			C	0.010

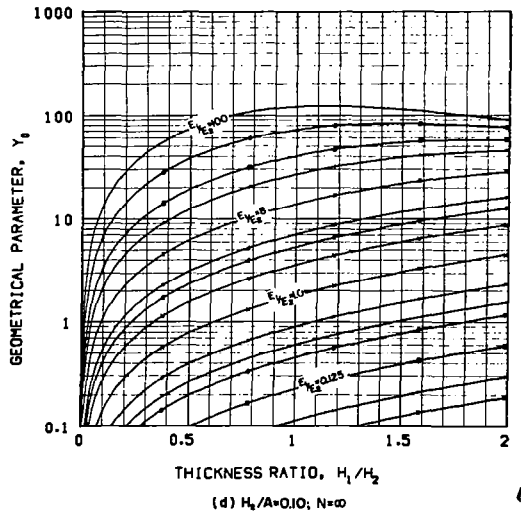
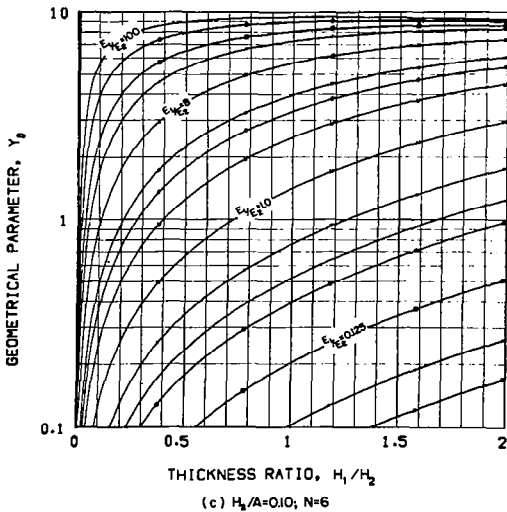
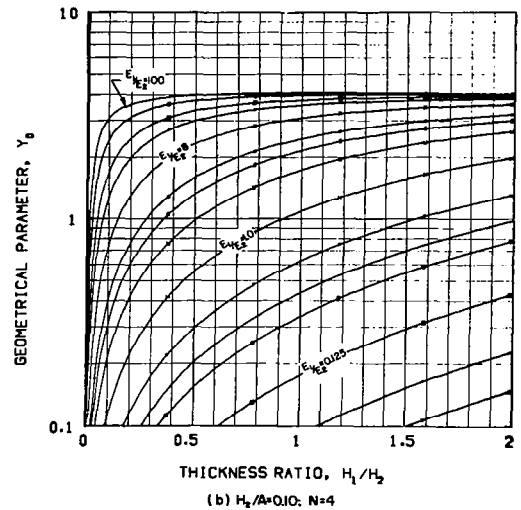
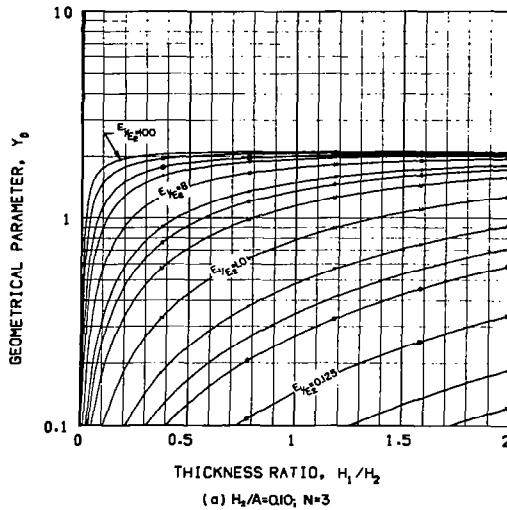
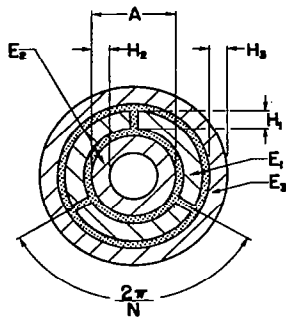


Figure 2.16(I) Geometrical parameter of composite structural tube having a round cross-section shape for a dimension ratio $H_2/A = 0.10$ and number of tube segments N ranging from three to infinity



THICKNESS RATIO, H_1/H_2

• 0.000	+ 0.200	C 0.600
O 0.050	X 0.300	U 0.800
□ 0.100	* 0.400	H 1.000

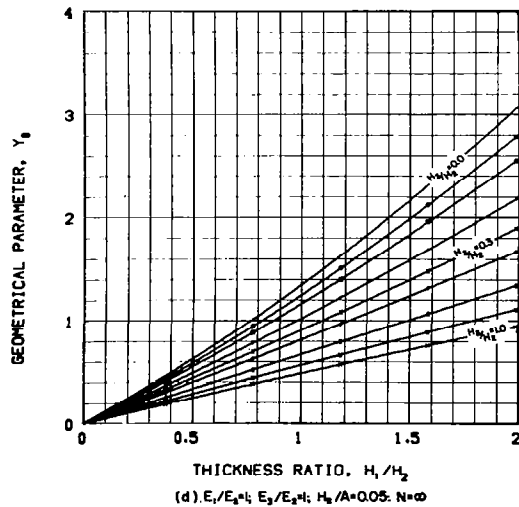
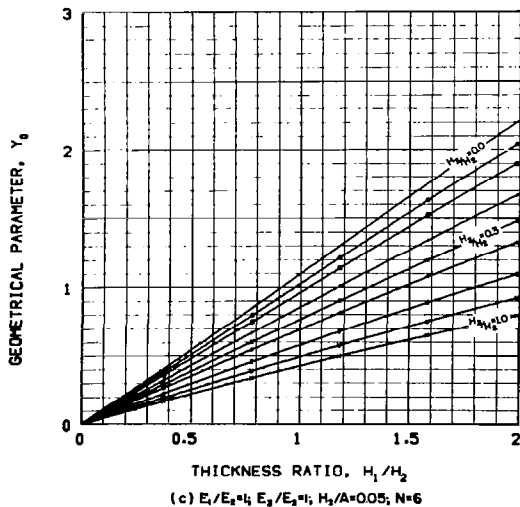
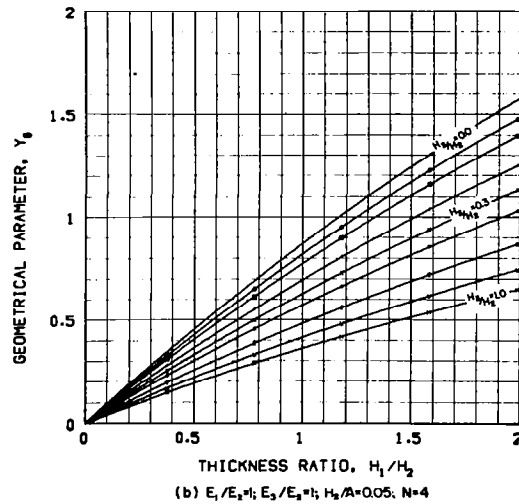
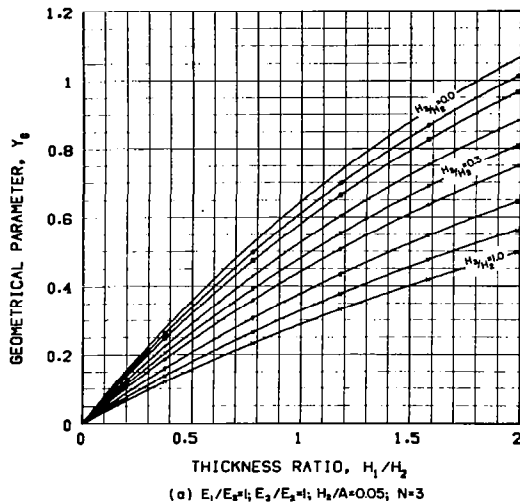
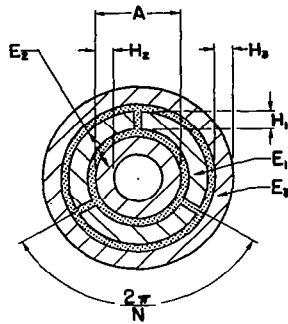
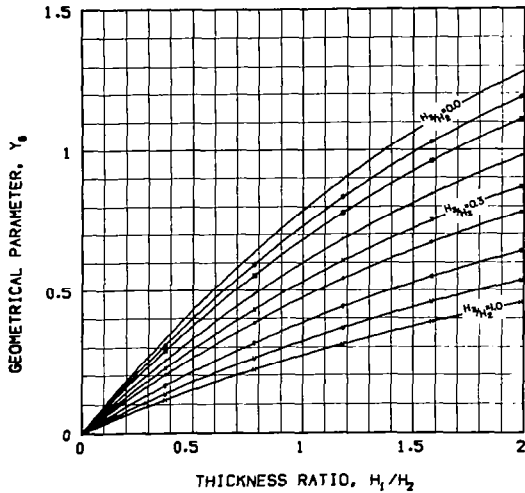


Figure 2.16(J) Geometrical parameter of composite structural tube having a round cross-section shape for modulus ratios $E_1/E_2 = 1$, and $E_3/E_2 = 1$, dimension ratio $H_2/A = 0.05$, and number of tube segments N ranging from three to infinity

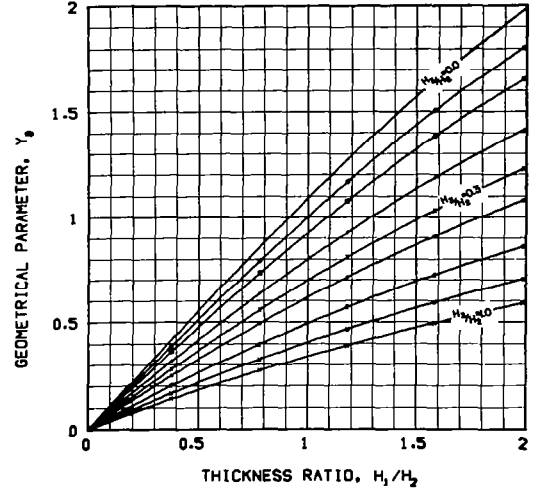


THICKNESS RATIO, H_2/H_3

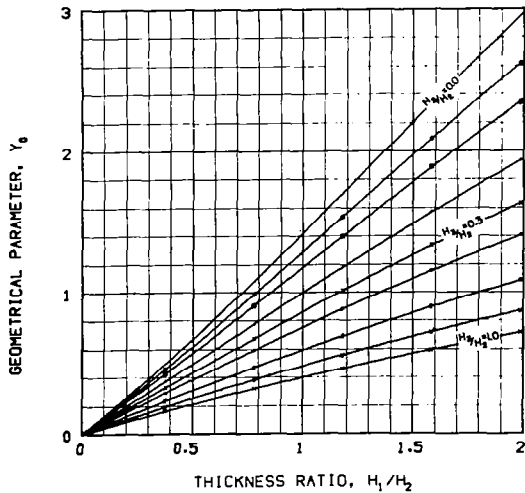
•	0.000	+	0.200	C	0.600
0	0.050	X	0.300	U	0.800
□	0.100	*	0.400	H	1.000



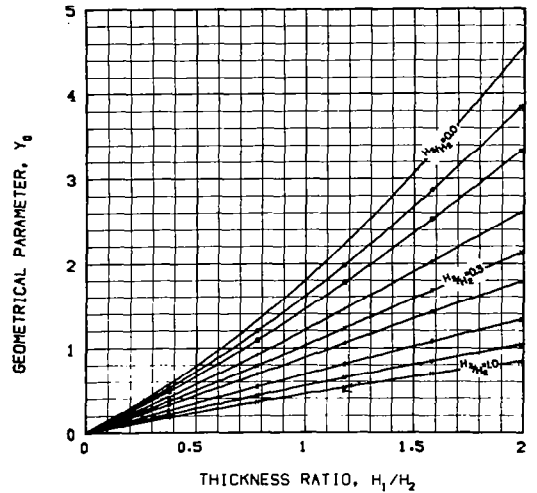
(a) $E_1/E_2=1$; $E_3/E_2=1$; $H_2/A=0.1$; $N=3$



(b) $E_1/E_2=1$; $E_3/E_2=1$; $H_2/A=0.1$; $N=4$

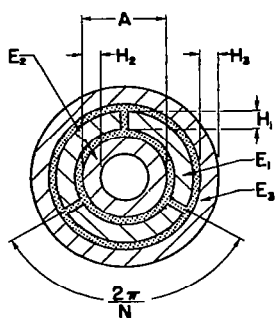


(c) $E_1/E_2=1$; $E_3/E_2=1$; $H_2/A=0.1$; $N=6$



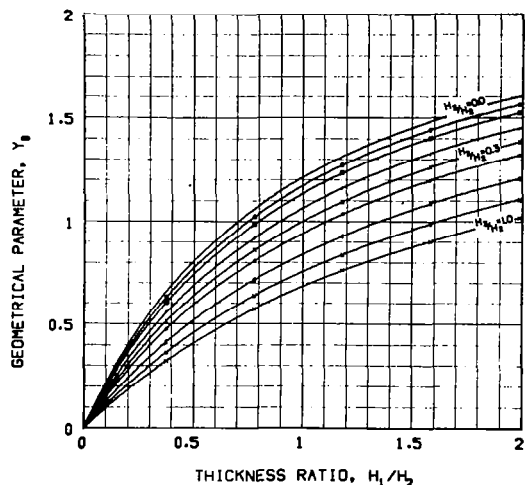
(d) $E_1/E_2=1$; $E_3/E_2=1$; $H_2/A=0.1$; $N=\infty$

Figure 2.16(K) Geometrical parameter of composite structural tube having a round cross-section shape for modulus ratios $E_1/E_2 = 1$ and $E_3/E_2 = 1$, dimension ratio $H_2/A = 0.1$, and number of tube segments N ranging from three to infinity

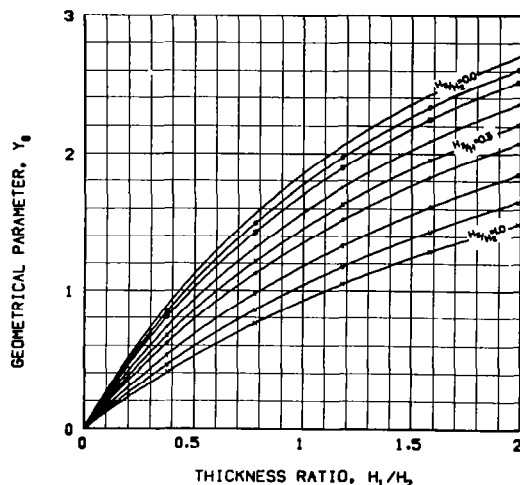


THICKNESS RATIO, H_1/H_2

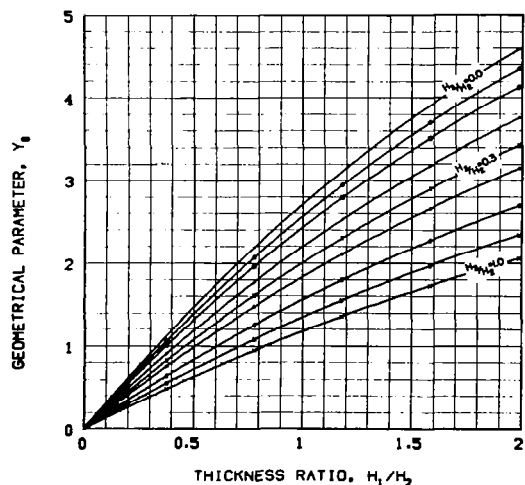
•	0.000	+	0.200	C	0.600
0	0.050	X	0.300	U	0.800
□	0.100	*	0.400	H	1.000



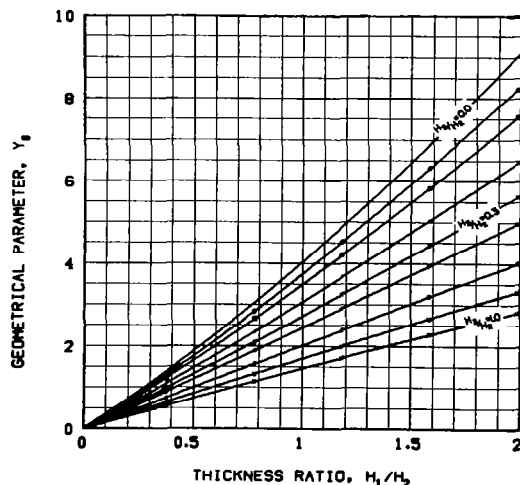
(a) $E_1/E_2=3$; $E_3/E_2=1$; $H_2/A=0.05$; $N=3$



(b) $E_1/E_2=3$; $E_3/E_2=1$; $H_2/A=0.05$; $N=4$

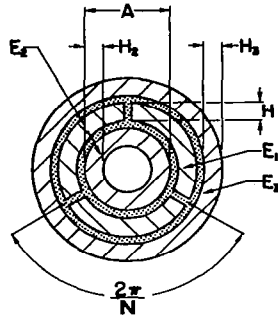


(c) $E_1/E_2=3$; $E_3/E_2=1$; $H_2/A=0.05$; $N=6$



(d) $E_1/E_2=3$; $E_3/E_2=1$; $H_2/A=0.05$; $N=10$

Figure 2.16(L) Geometrical parameter of composite structural tube having a round cross-section shape for modulus ratios $E_1/E_2 = 3$ and $E_3/E_2 = 1$, dimension ratio $H_2/A = 0.05$, and number of tube segments N ranging from three to infinity



THICKNESS RATIO, H_2/H_3

•	0.000	+	0.200	C	0.600
o	0.050	x	0.300	U	0.800
□	0.100	*	0.400	H	1.000

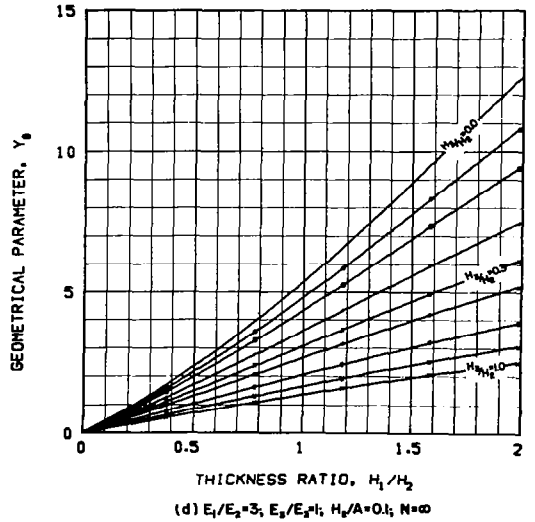
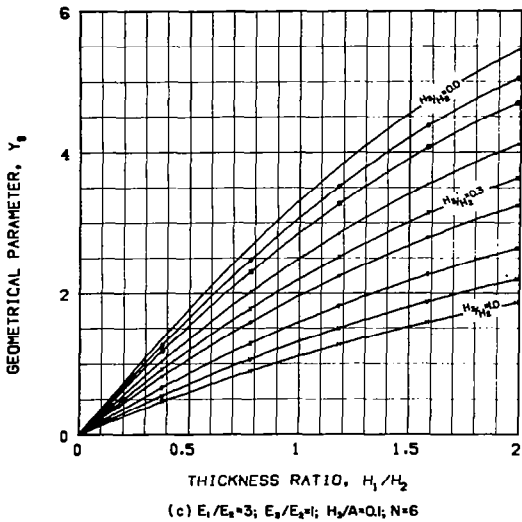
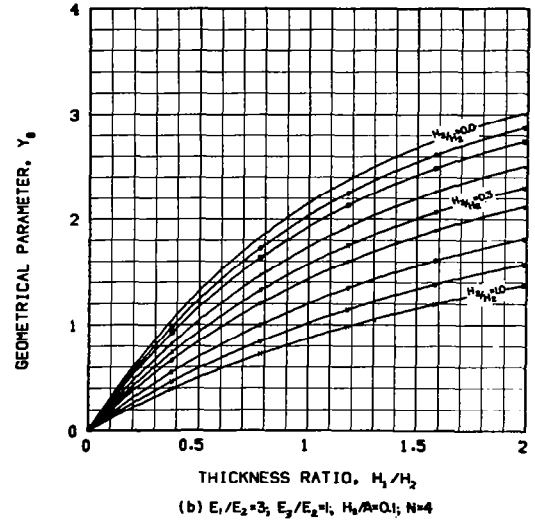
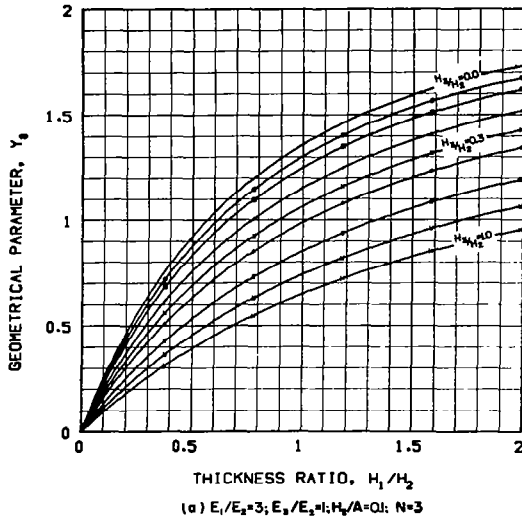


Figure 2.16(M) Geometrical parameter of composite structural tube having a round cross-section shape for modulus ratios $E_1/E_2 = 3$ and $E_3/E_2 = 1$, dimension ratio $H_2/A = 0.1$, and number of tube segments N ranging from three to infinity

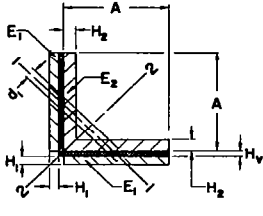
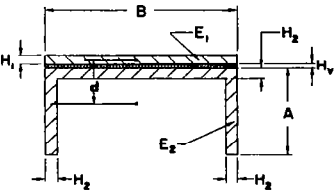
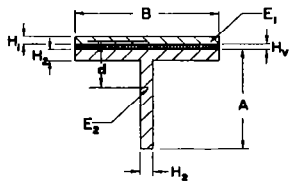
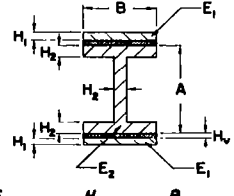
 $M = \frac{E_1}{E_2} \quad R = \frac{H_1}{H_2} \quad S = \frac{H_2}{A}$ $V = \frac{H_v}{H_1 + \lambda H_2} \quad \lambda = \frac{3 + S^2}{2 - S} \quad \lambda_2 = \frac{1}{S}$	$Y_1 = \frac{3MR S^2 [(2-S)\{R+2(R+1)V+1\} + 1-S]^2}{[2RM + (2-S)]\{(2-S)[M(R^2 S^2 + R) + S^2 + (1-S)^3] + 3S(1-S)\}}$ $Y_2 = \frac{3MR[1+2S(R+1)V+RS]^2}{M(R^2 S^2 + R) + S^2 + (1-S)^3 + 3(1-S)}$ $\frac{Y}{Y_0} = (1+2V)^2$ $(EI)_{01} = \frac{E_1 A^4 S}{12} \left\{ M(R^2 S^2 + R) + S^2 + (1-S)^3 + \frac{3S(1-S)}{(2-S)} \right\}$ $(EI)_{02} = \frac{E_2 A^4 S}{12} \left\{ M(R^2 S^2 + R) + S^2 + (1-S)^3 + 3(1-S) \right\}$ $\omega = 2\bar{x}_1 H_1 + \bar{x}_2 H_2 (2A - H_2)$ $d = \frac{1}{2} (H_1 + \lambda H_2) + H_v$ $B_v = 2A$
 $M = \frac{E_1}{E_2} \quad R = \frac{H_1}{H_2} \quad D = \frac{B}{A} \quad S = \frac{H_2}{A}$ $V = \frac{H_v}{H_1 + \lambda H_2} \quad \lambda = \frac{SD + 2(1-S^2)}{S[D + 2(1-S)]}$	$Y = \frac{3MRD[S[D+2(1-S)][R+2(R+1)V] - SD + 2-2S^2]^2}{[D(MR+1) + 2(1-S)]\{[D+2(1-S)][MDR^2 S^2 + DS^2 + 2(1-S)^3] + 6(1-S)D\}}$ $\frac{Y}{Y_0} = (1+2V)^2$ $(EI)_0 = \frac{E_2 A^4 S}{12} \left\{ MDR^2 S^2 + DS^2 + 2(1-S)^3 + \frac{6D(1-S)}{D+2(1-S)} \right\}$ $\omega = \bar{x}_1 B H_1 + \bar{x}_2 H_2 [B + 2(A - H_2)]$ $d = \frac{1}{2} (H_1 + \lambda H_2) + H_v$ $B_v = B$
 $M = \frac{E_1}{E_2} \quad R = \frac{H_1}{H_2} \quad D = \frac{B}{A} \quad S = \frac{H_2}{A}$ $V = \frac{H_v}{H_1 + \lambda H_2} \quad \lambda = \frac{DS + (1-S^2)}{S[D + (1-S)]}$	$Y = \frac{3MDR\{(D+1-S)[RS+2S(R+1)V+S] + (1-S)\}^2}{[MDR + (D+1-S)]\{(D+1-S)[MDR^2 S^2 + DS^2 + (1-S)^3] + 3D(1-S)\}}$ $\frac{Y}{Y_0} = (1+2V)^2$ $(EI)_0 = \frac{E_2 A^4 S}{12} \left\{ MR^2 S^2 D + DS^2 + (1-S)^3 + \frac{3D(1-S)}{(D+1-S)} \right\}$ $\omega = \bar{x}_1 B H_1 + \bar{x}_2 H_2 (B + A - H_2)$ $d = \frac{1}{2} (H_1 + \lambda H_2) + H_v$ $B_v = B$
 $M = \frac{E_1}{E_2} \quad R = \frac{H_1}{H_2} \quad D = \frac{B}{A} \quad S = \frac{H_2}{A}$ $V = \frac{H_v}{H_1 + \lambda H_2} \quad \lambda = \frac{1}{S}$	$Y = \frac{6MDR[1+2S(R+1)V+RS]^2}{2MDR^2 S^2 + (1-2S)^3 + 2DS^2 + 6D(1-S)^2}$ $\frac{Y}{Y_0} = (1+2V)^2$ $(EI)_0 = \frac{E_2 A^4 S}{12} \left\{ 2MDR^2 S^2 + (1-2S)^3 + 2DS^2 + 6D(1-S)^2 \right\}$ $\omega = 2\bar{x}_1 B H_1 + \bar{x}_2 H_2 (A + 2B - H_2)$

Figure 2.17 (A) Design equations for geometrical properties of viscoelastic shear-damped beams consisting of solid rectangular sheets laminated to conventional structural shape beams

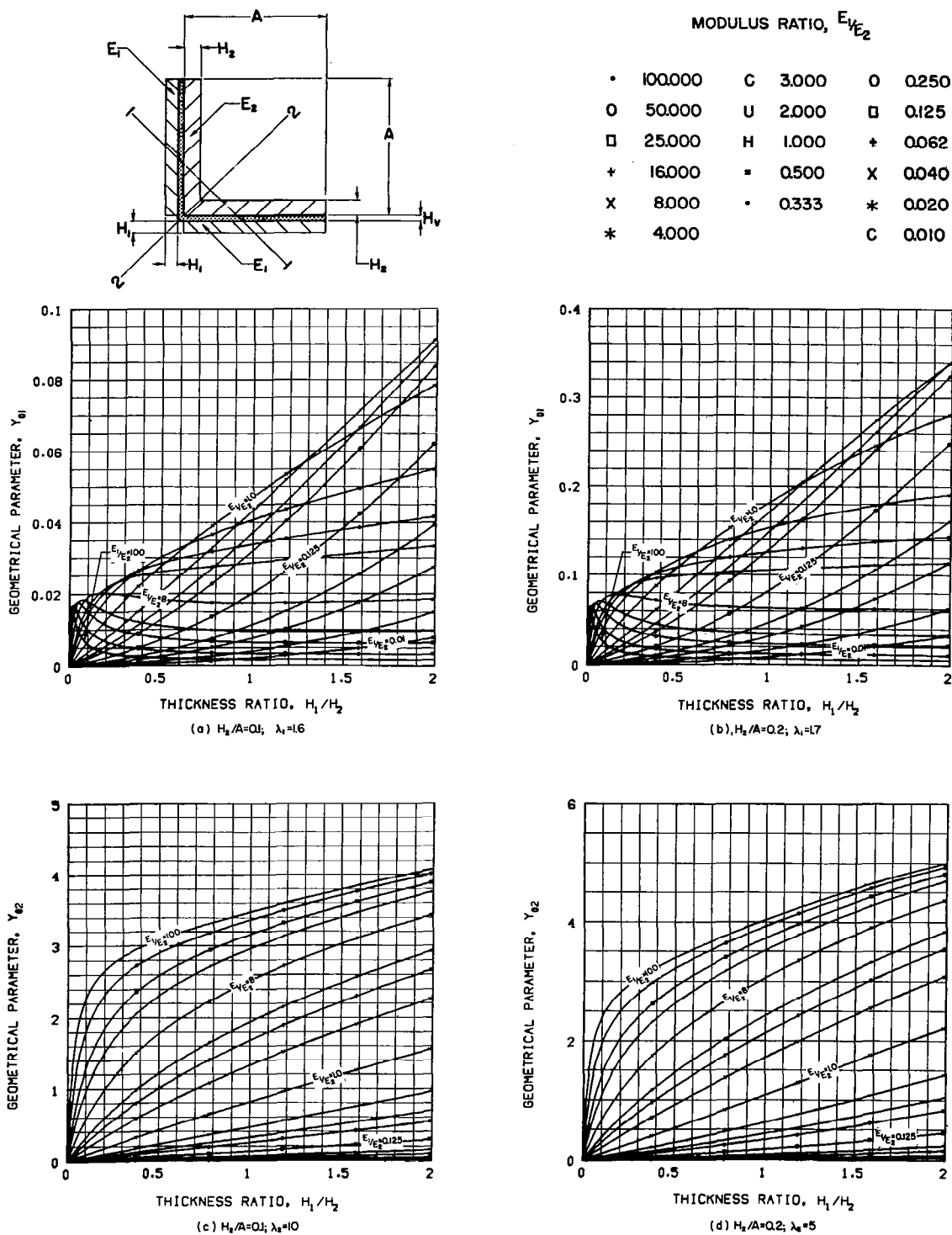
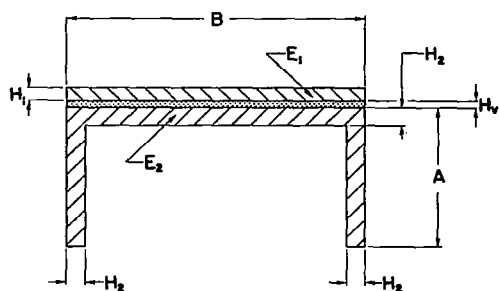


Figure 2.17(B) Geometrical parameter for neutral axes 1-1 and 2-2 of composite structural angle for values of the dimension ratio H_2/A equal to 0.1 and 0.2



MODULUS RATIO, E_1/E_2

•	100.000	C	3.000	O	0.250
O	50.000	U	2.000	□	0.125
□	25.000	H	1.000	+	0.062
+	16.000	▪	0.500	X	0.040
X	8.000	•	0.333	*	0.020
*	4.000			C	0.010

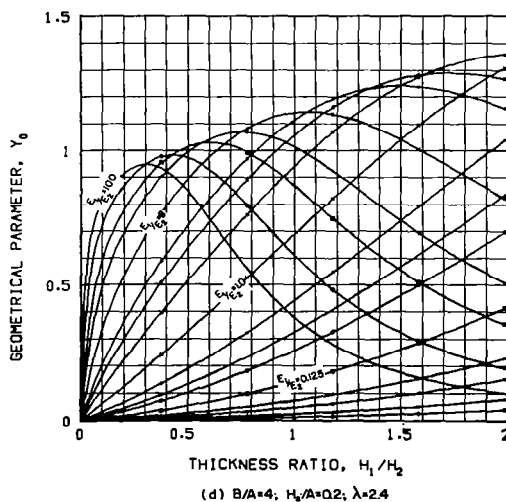
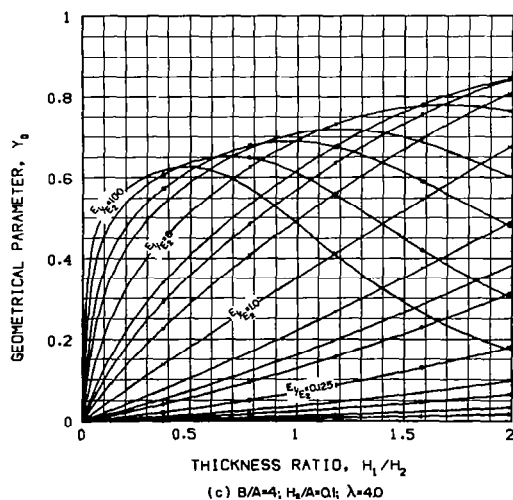
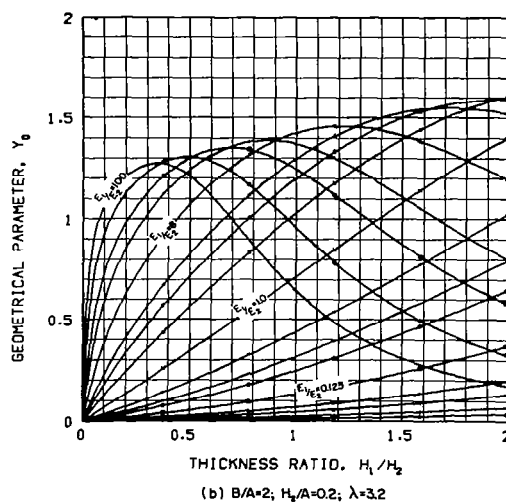
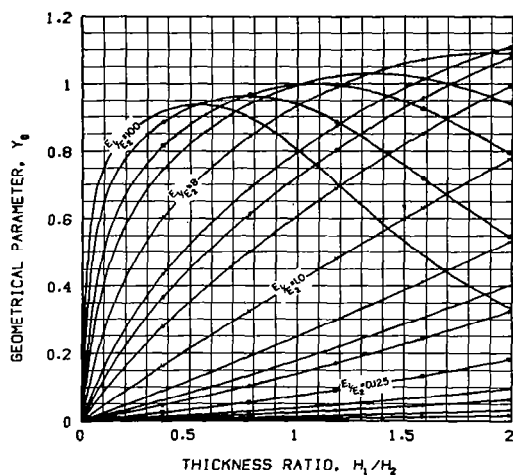
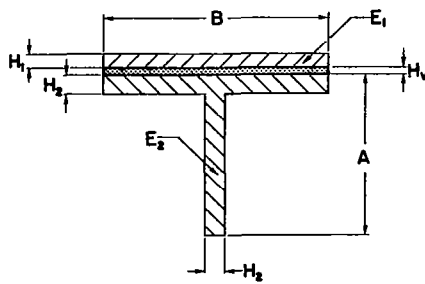


Figure 2.17 (C) Geometrical parameter of composite structural channel for various values of the dimension ratios B/A and H_2/A



MODULUS RATIO, E_1/E_2

•	100.000	C	3.000	O	0.250
O	50.000	U	2.000	□	0.125
□	25.000	H	1.000	+	0.062
+	16.000	=	0.500	X	0.040
X	8.000	•	0.333	*	0.020
*	4.000			C	0.010

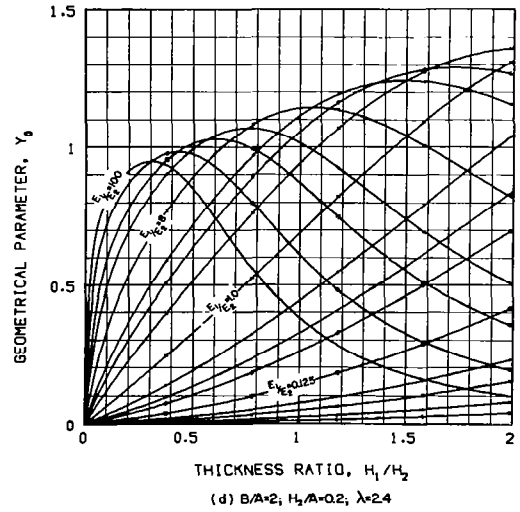
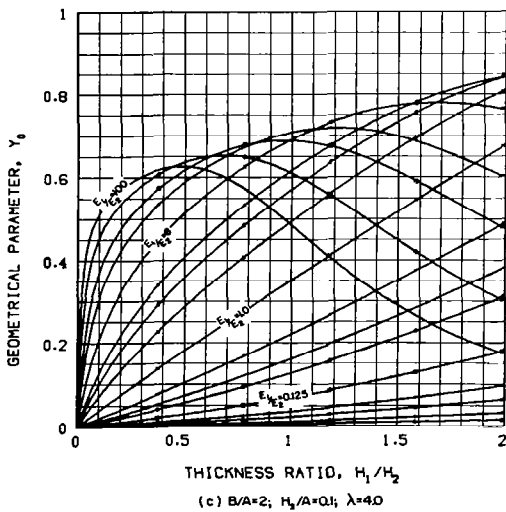
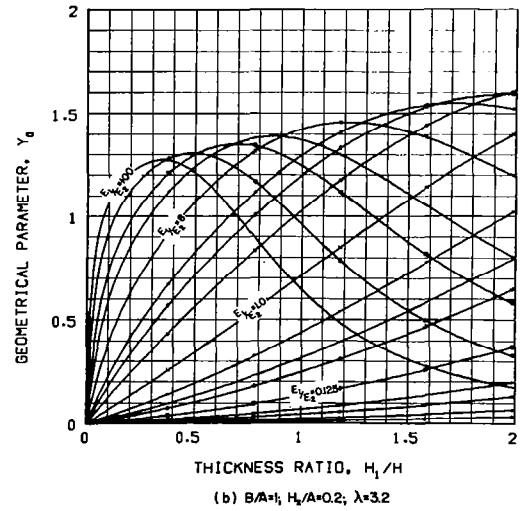
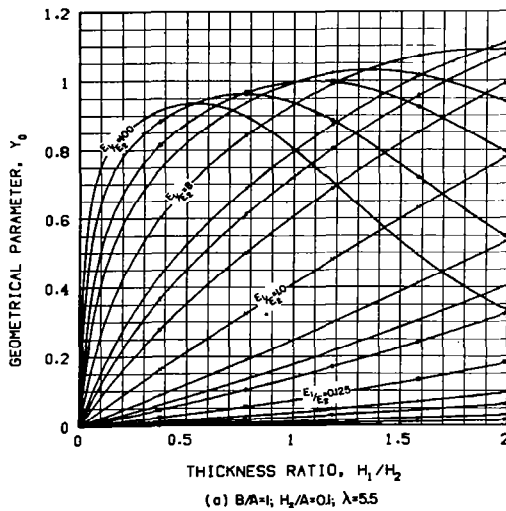
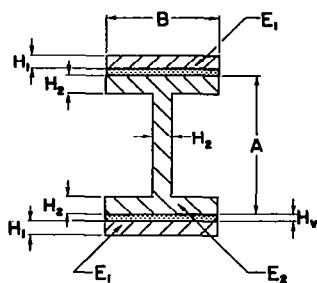


Figure 2.17(D) Geometrical parameter of composite structural T-section for various values of the dimension ratios B/A and H_2/A



MODULUS RATIO, E_1/E_2

•	100.000	C	3.000	O	0.250
O	50.000	U	2.000	□	0.125
□	25.000	H	1.000	+	0.062
+	16.000	=	0.500	X	0.040
X	8.000	•	0.333	*	0.020
*	4.000			C	0.010

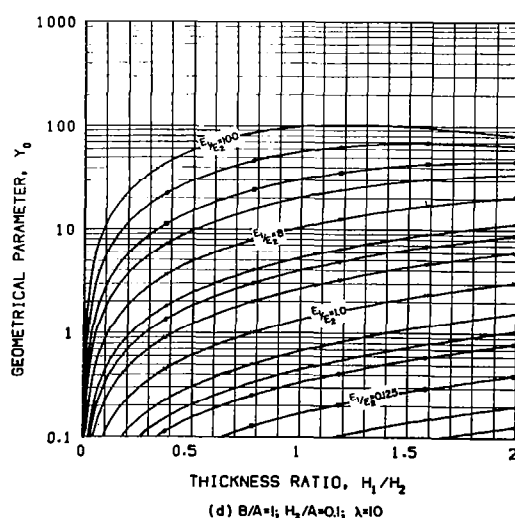
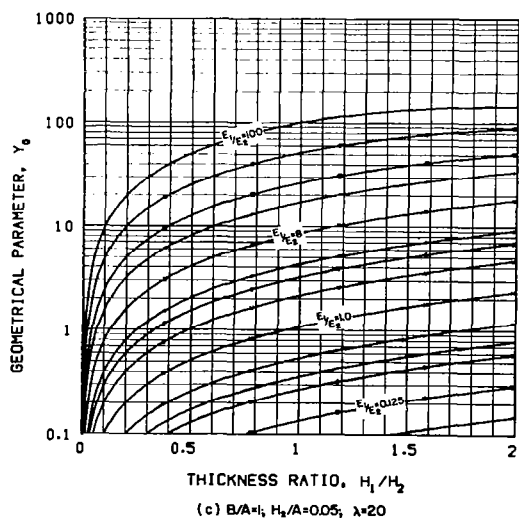
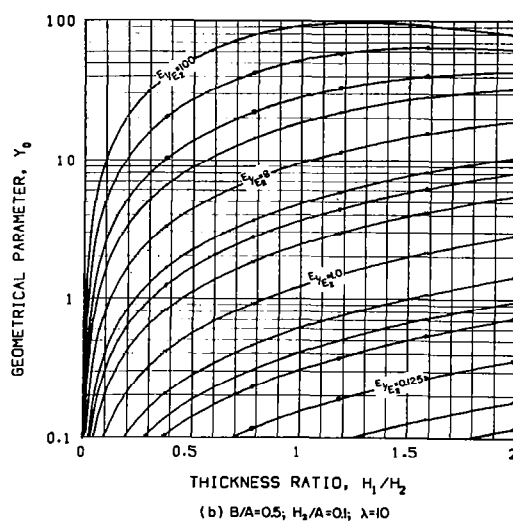
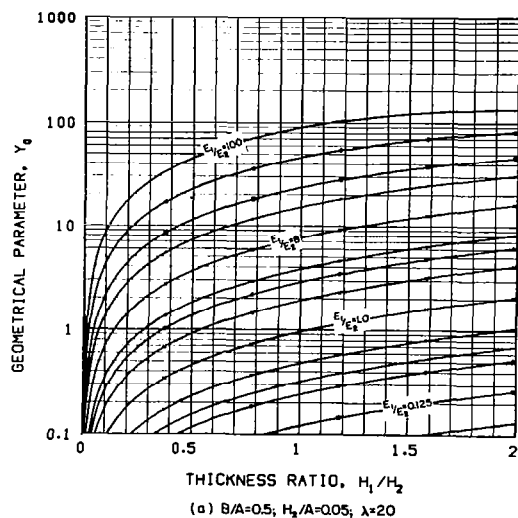


Figure 2.17 (E) Geometrical parameter of composite structural I-section for various values of the dimension ratios B/A and H_2/A

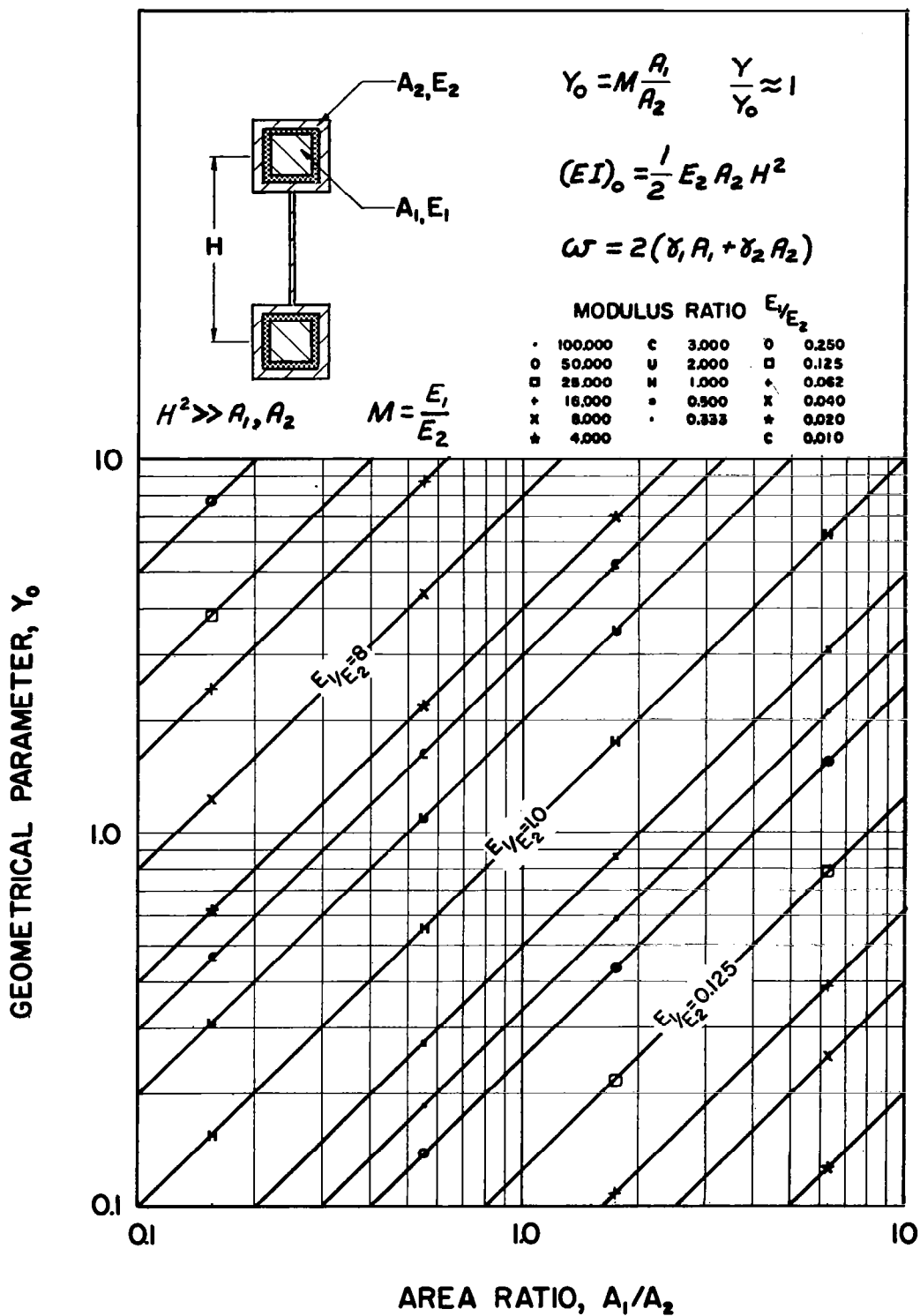


Figure 2.18 Design equations and geometrical parameter of viscoelastic shear-damped dumbbell model

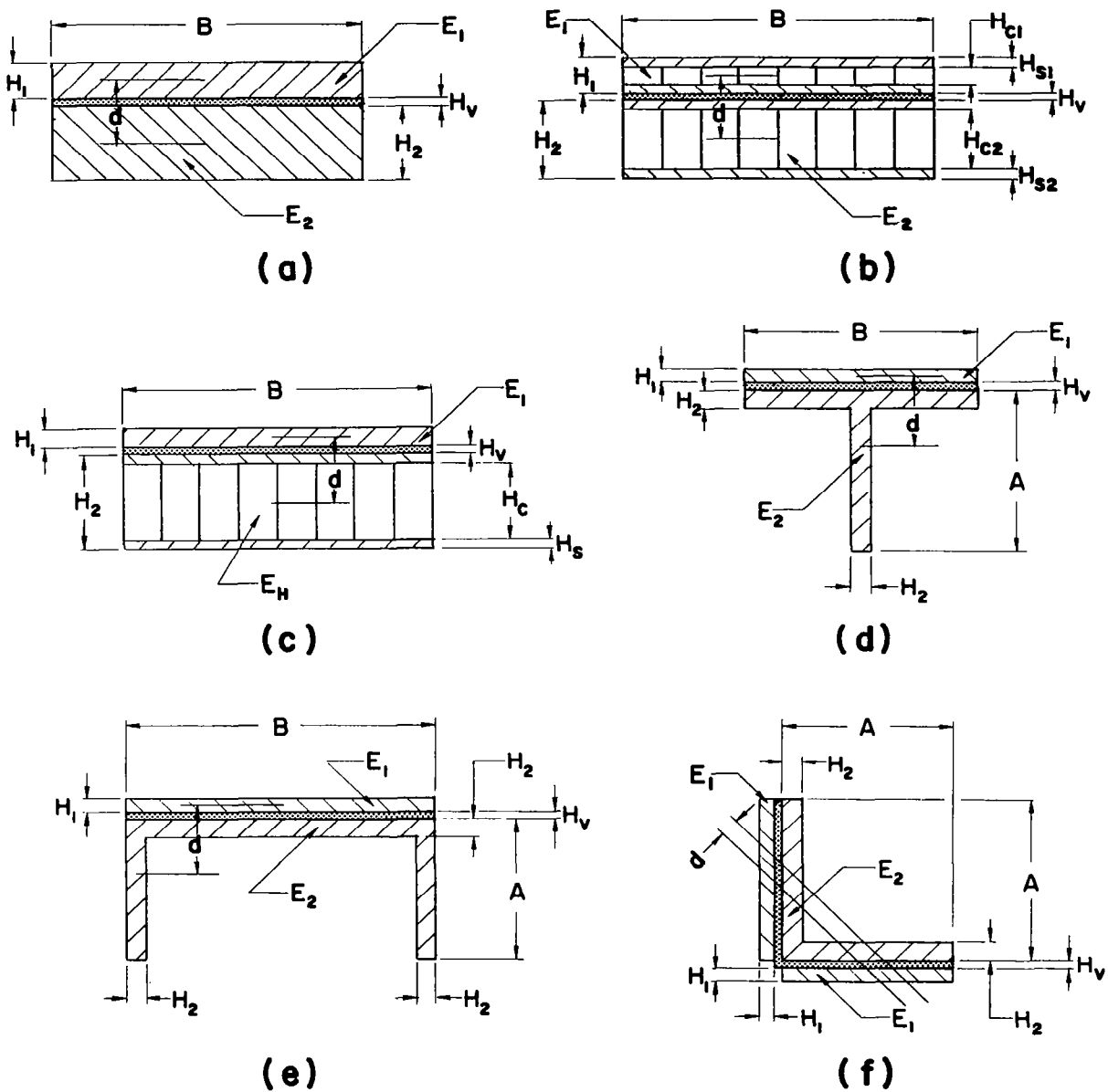


Figure 3.1 Cross-sections of typical two-elastic-element viscoelastic shear-damped structural composites

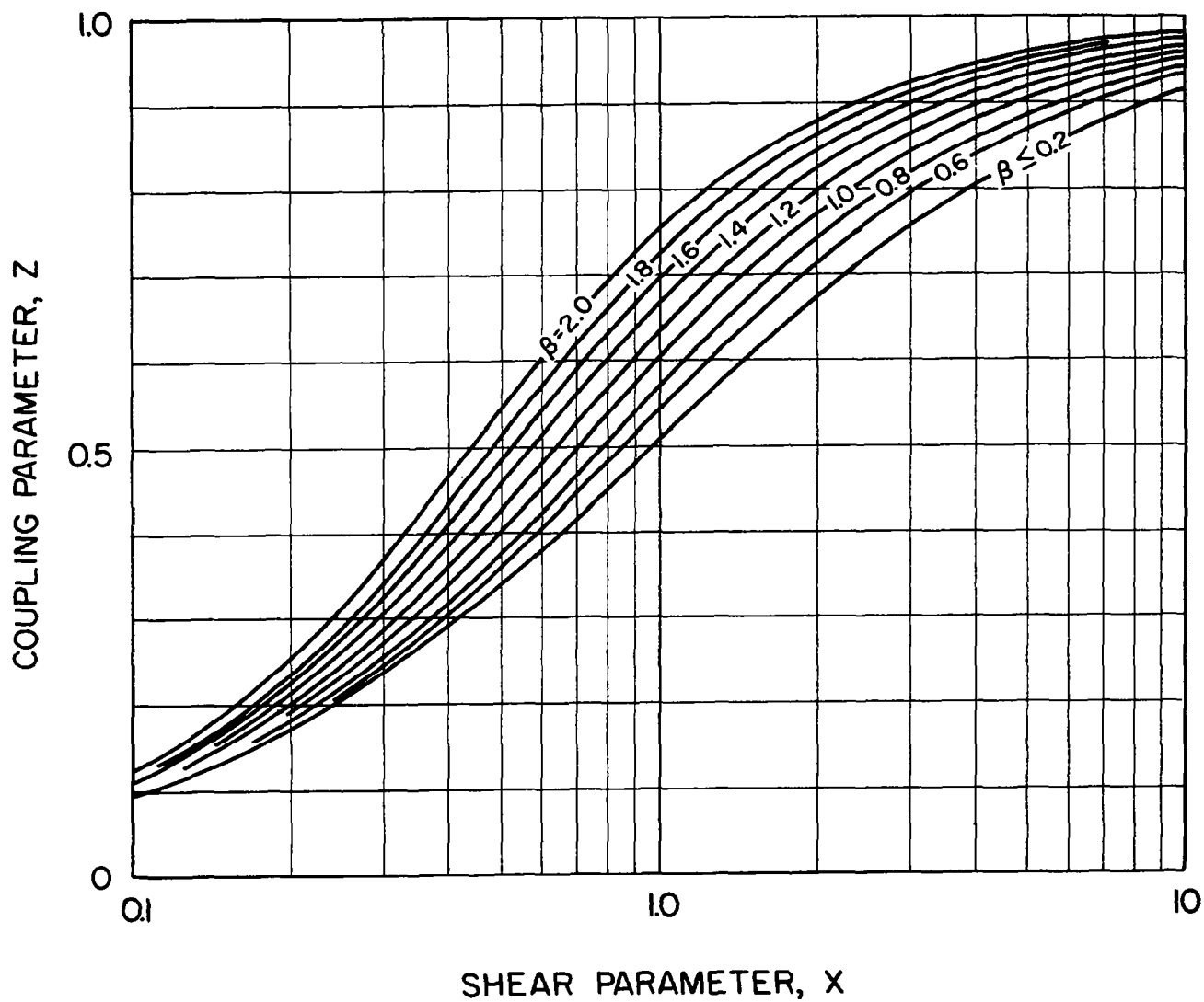


Figure 3.2 Coupling parameter for two-elastic-element viscoelastic shear-damped structural composites

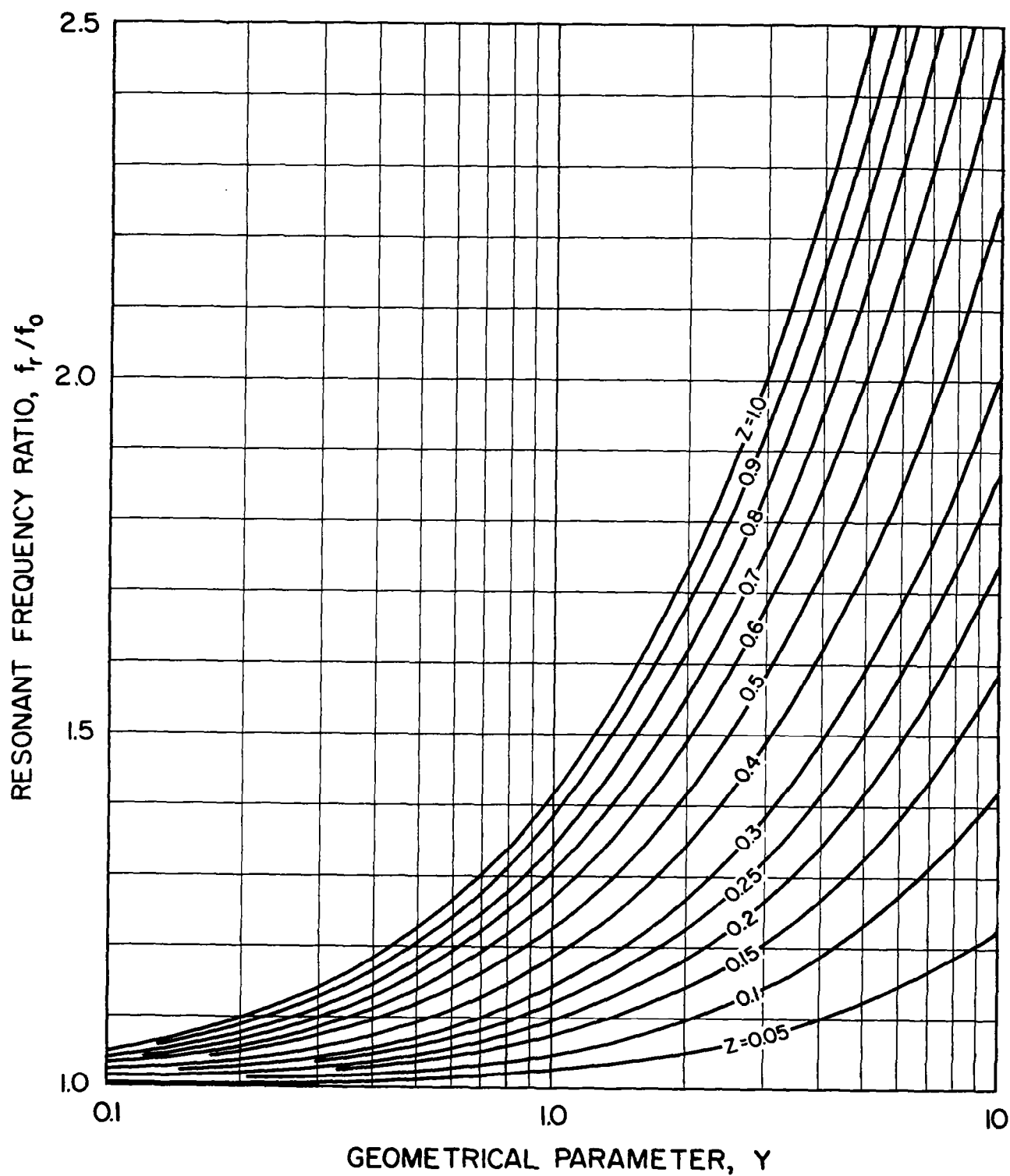


Figure 3.3 Resonant frequency ratio for two-elastic-element viscoelastic shear-damped structural composites

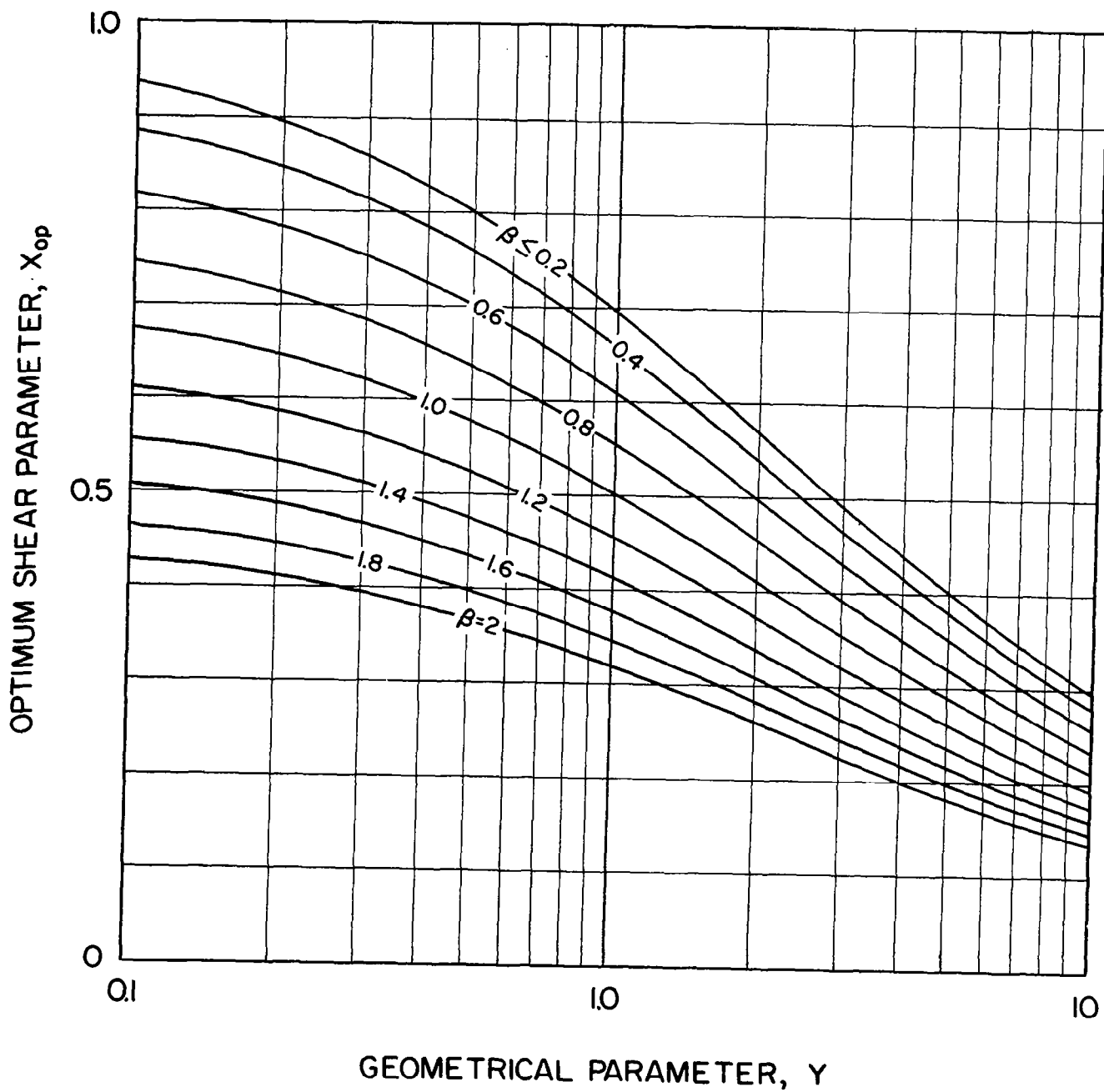


Figure 3.4 Optimum shear parameter for two-elastic-element viscoelastic shear-damped structural composites

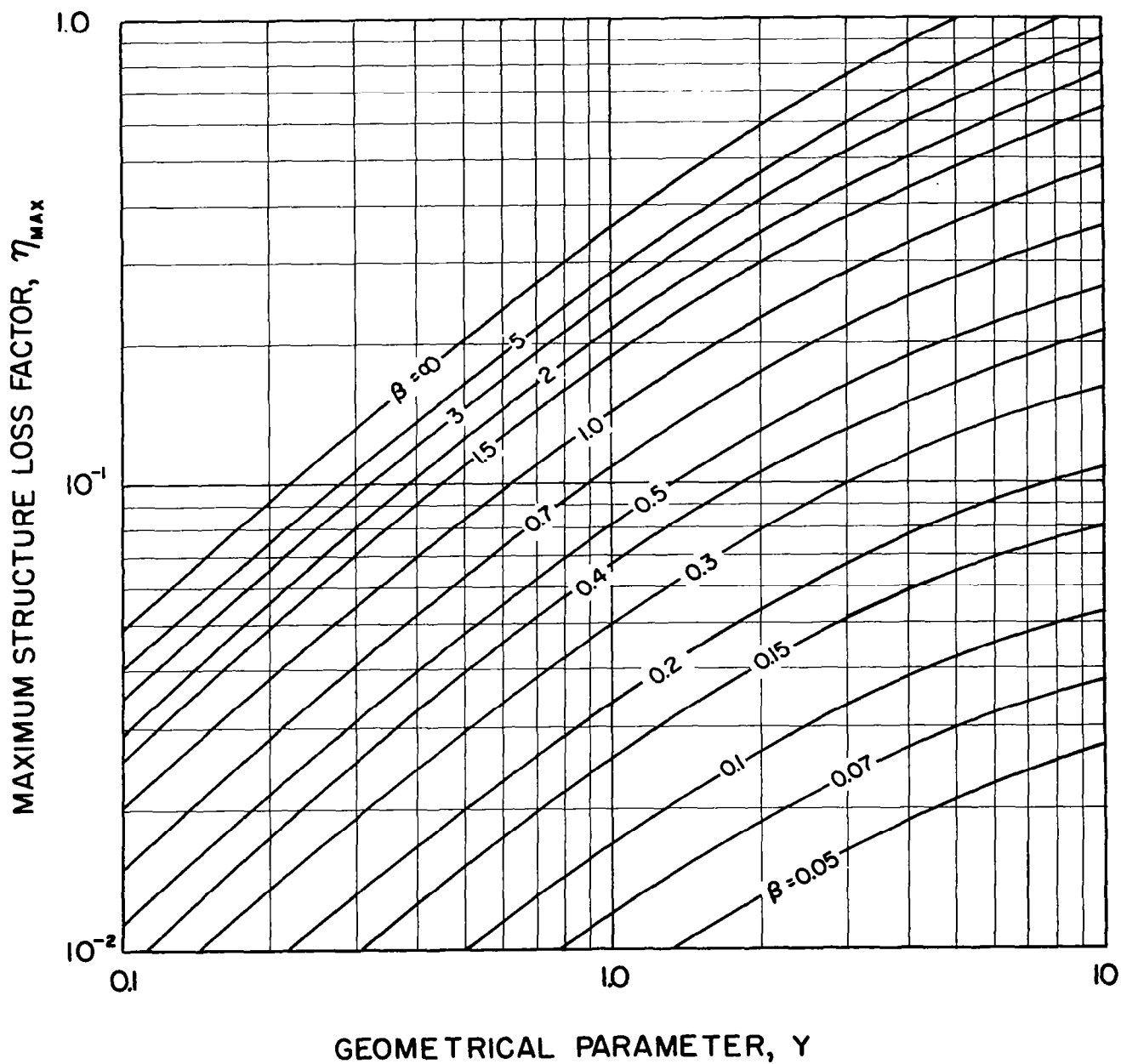


Figure 3.5 Maximum structure loss factor for two-elastic-element viscoelastic shear-damped structural composites for optimum value of the shear parameter

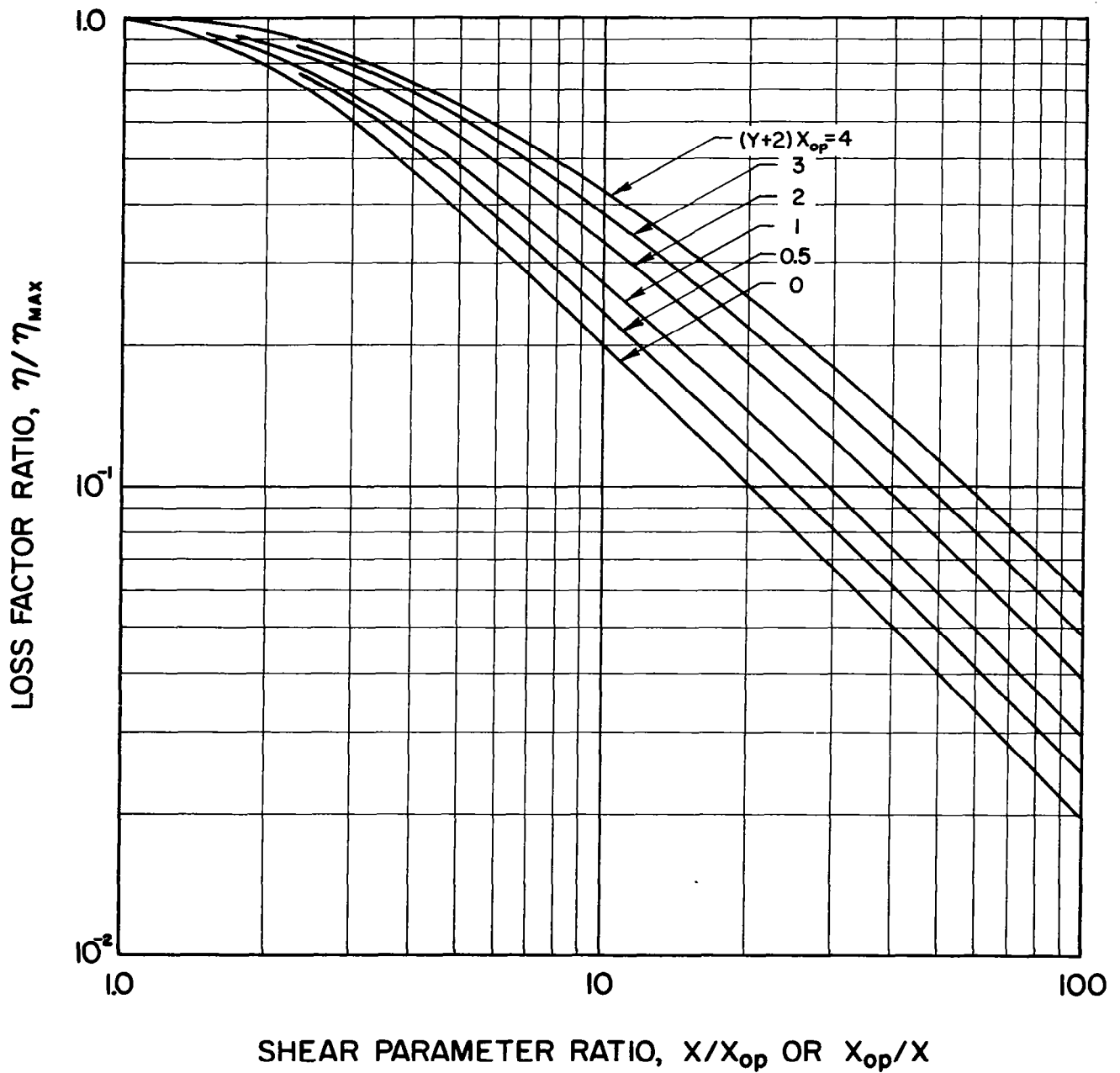


Figure 3.6 Loss factor ratio for two-elastic-element viscoelastic shear-damped structural composites defining the reduction in structure loss factor for non-optimum values of the shear parameter

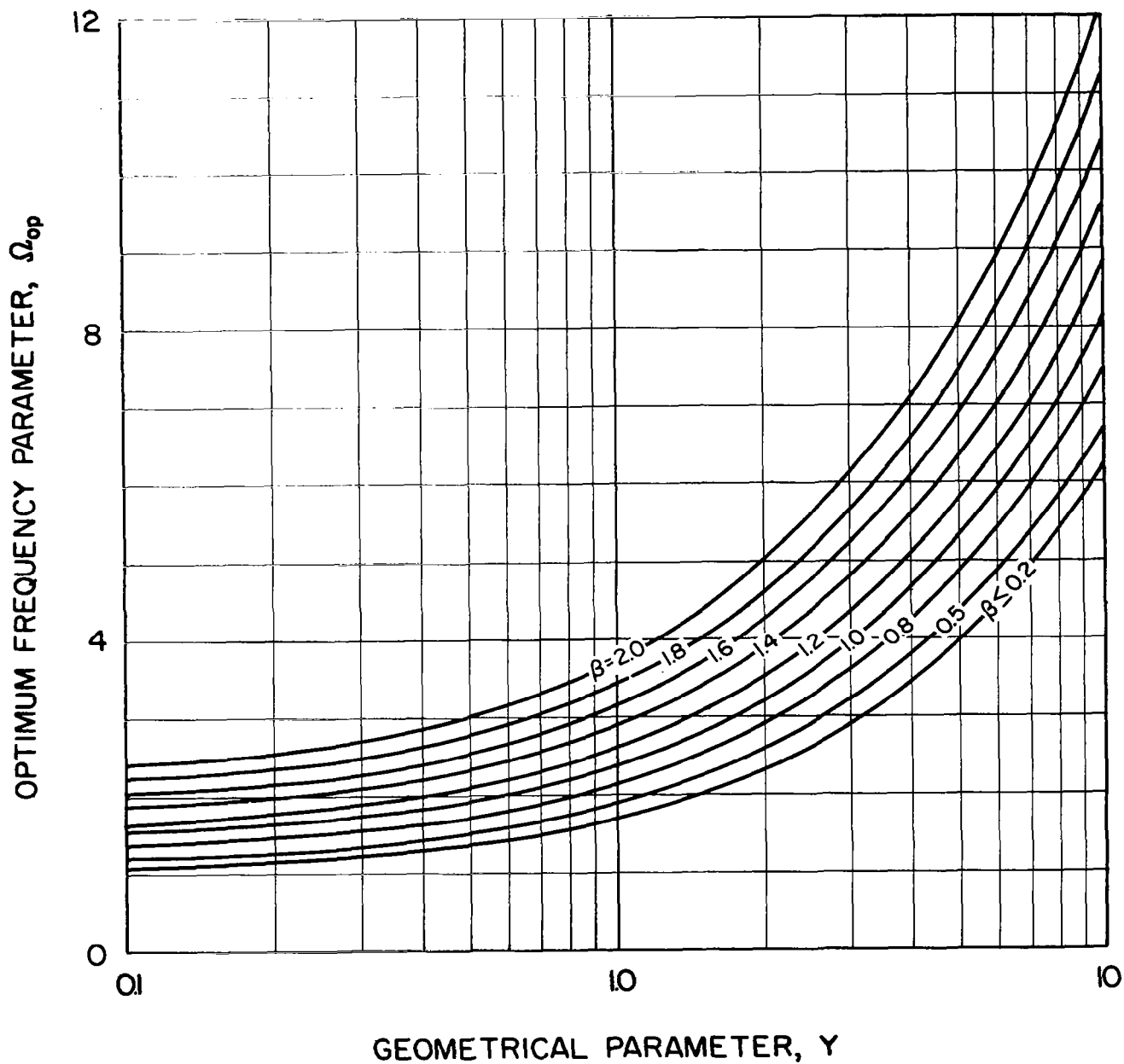


Figure 3.7 Optimum frequency parameter for two-elastic-element viscoelastic shear-damped structural composites

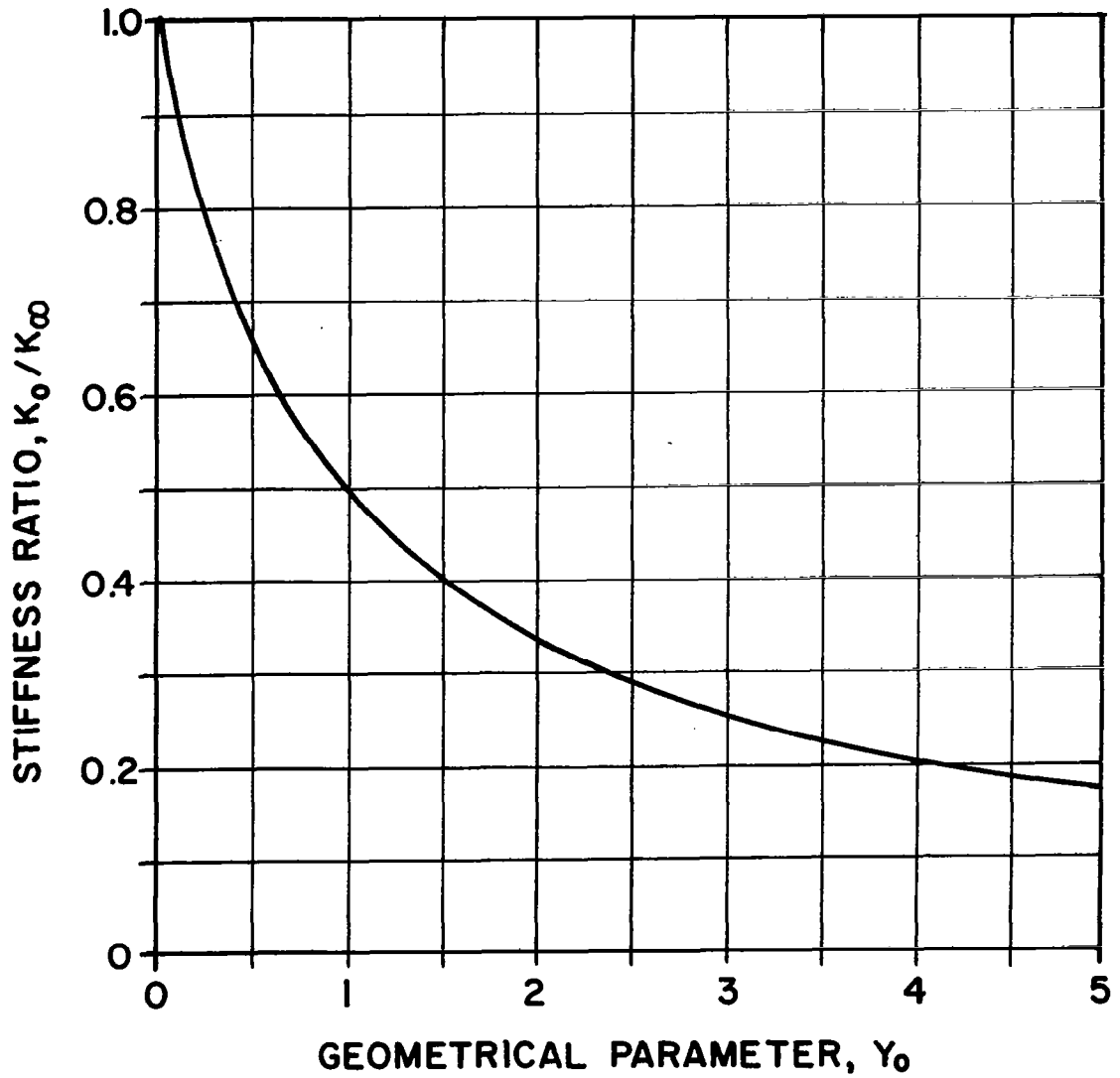


Figure 3.8 Comparison of static stiffness of viscoelastic shear-damped structural composites with that of solid structural members having an equivalent weight

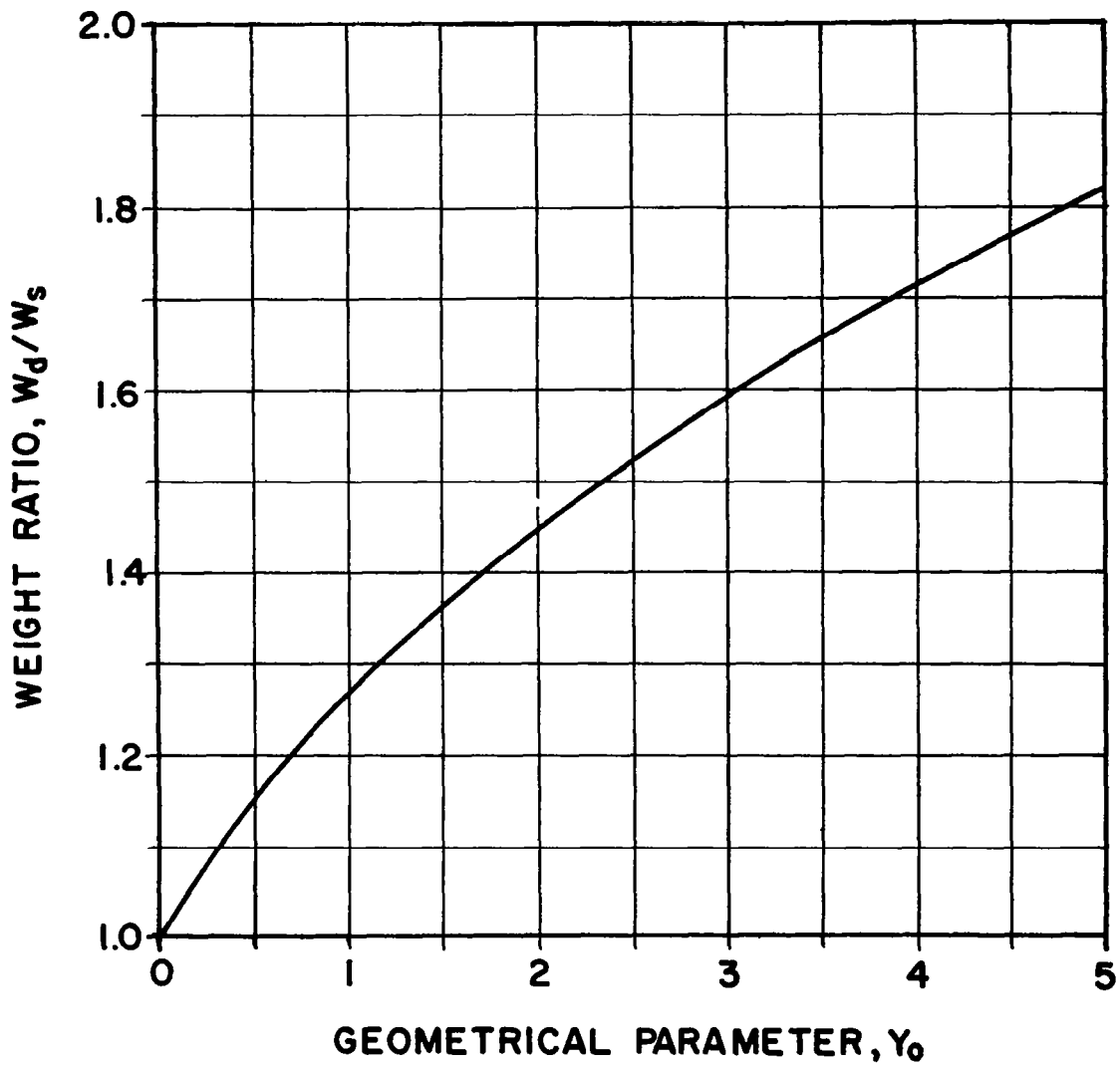


Figure 3.9 Comparison of weight of a viscoelastic shear-damped composite structural plate design comprised of two solid sheets with that of a solid plate having an equivalent static stiffness

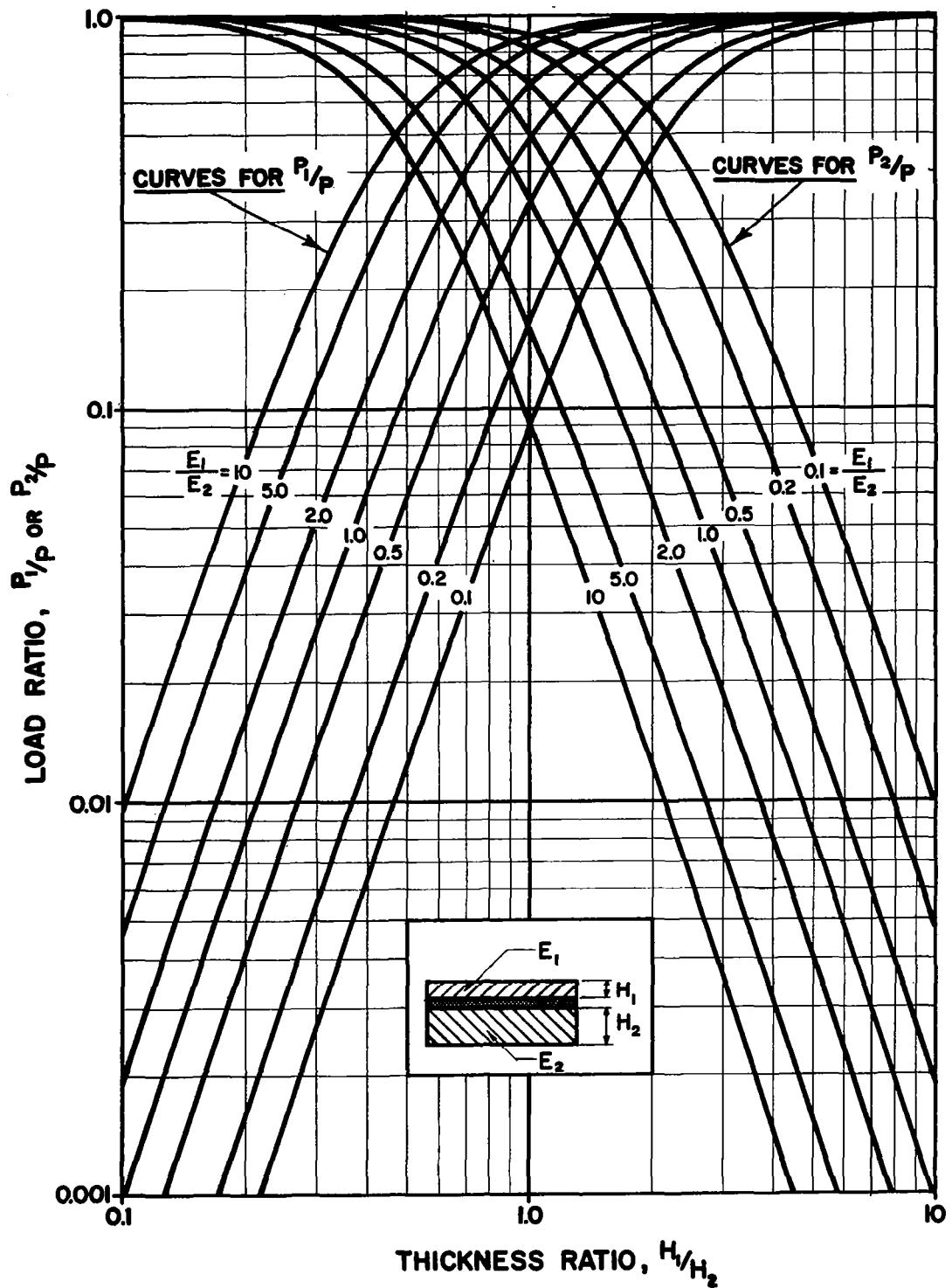


Figure 3.10 Static load distribution curves for viscoelastic shear-damped composite structural plate comprised of two solid structural sheets

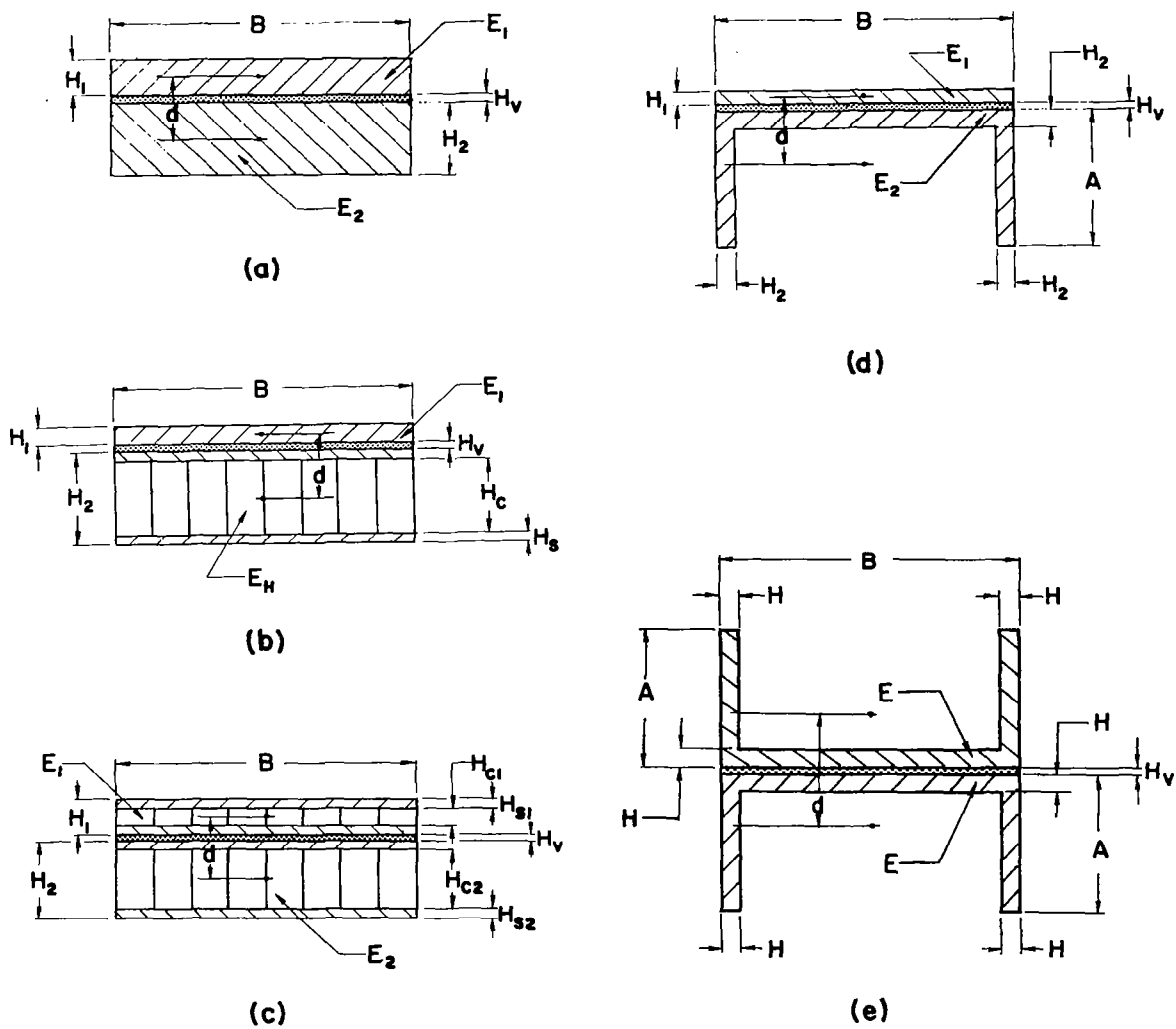


Figure 4.1 Cross-sections of two-elastic-element viscoelastic shear-damped structural composite beams fabricated for experimental evaluation of structure loss factor

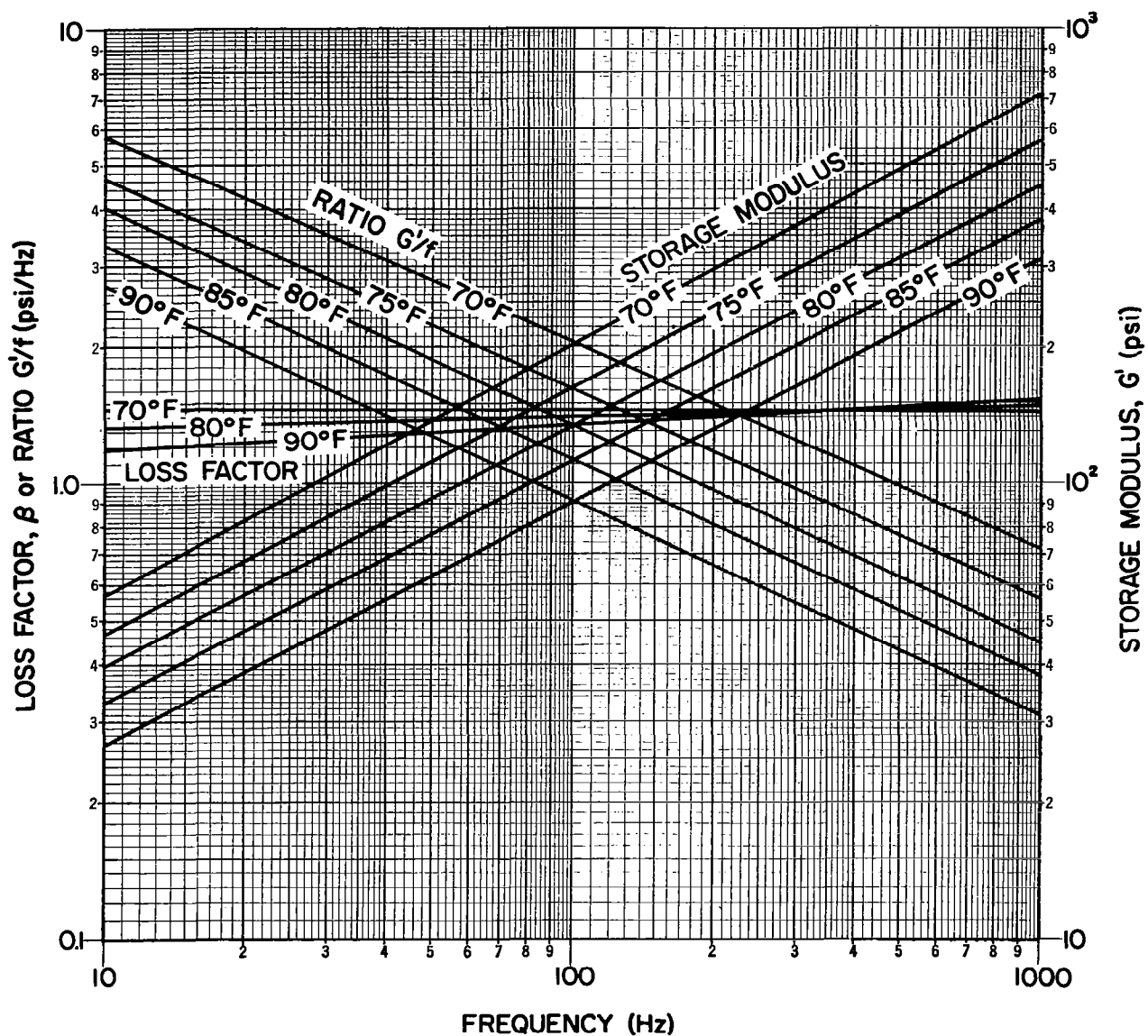


Figure 4.2 Dynamic elastic characteristics of viscoelastic shear-damping material (3M No. 466 tape) used in the structural composite beams evaluated theoretically and experimentally for their structure loss factor characteristics

f	β	G'/f	f_r/f_o	f_o	X	X_{op}	X/X_{op}	r_i/η_{max}	η_{max}	η
10	1.4	4.65	2.03	4.93	3.08	0.27	11.4	0.28	0.385	0.108
20	1.4	3.4	2.00	10.0	2.22	0.27	8.22	0.35	0.385	0.135
30	1.4	2.8	1.95	15.4	1.785	0.27	6.62	0.42	0.385	0.162
50	1.4	2.2	1.91	26.2	1.37	0.27	5.07	0.5	0.385	0.193
70	1.4	1.86	1.86	37.7	1.13	0.27	4.18	0.575	0.385	0.221
100	1.4	1.6	1.84	54.4	0.965	0.27	3.57	0.64	0.385	0.246
200	1.4	1.2	1.73	116	0.678	0.27	2.51	0.8	0.385	0.308
300	1.4	1.0	1.65	182	0.54	0.27	2.0	0.88	0.385	0.339
500	1.4	0.78	1.56	321	0.398	0.27	1.47	0.97	0.385	0.374
700	1.4	0.671	1.48	473	0.324	0.27	1.2	0.99	0.385	0.381
1000	1.4	0.565	1.4	715	0.259	0.27	0.96	1.0	0.385	0.385

Figure 4.3 Manual design procedure calculations for the design example where each discrete frequency f represents a potential resonant frequency f_r of the structural composite beam

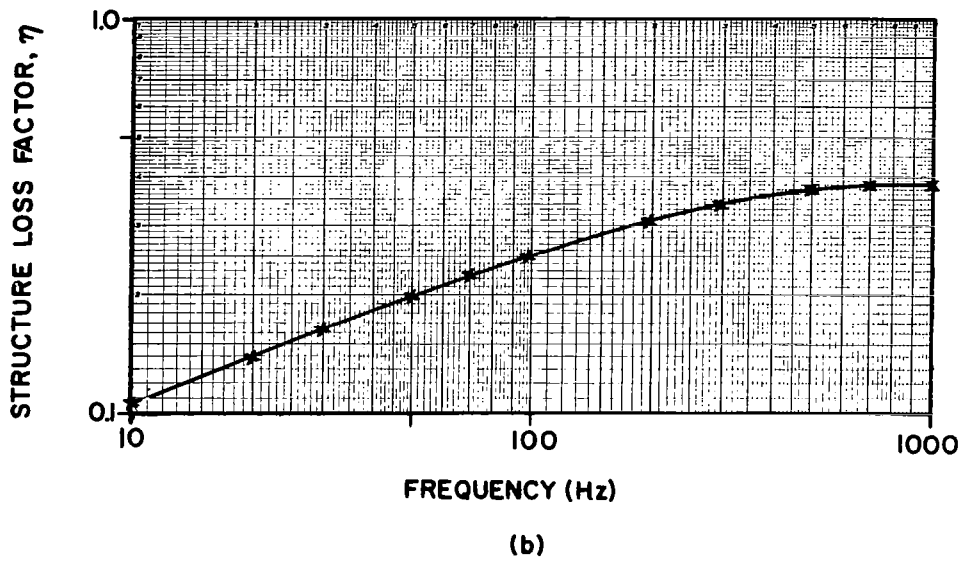
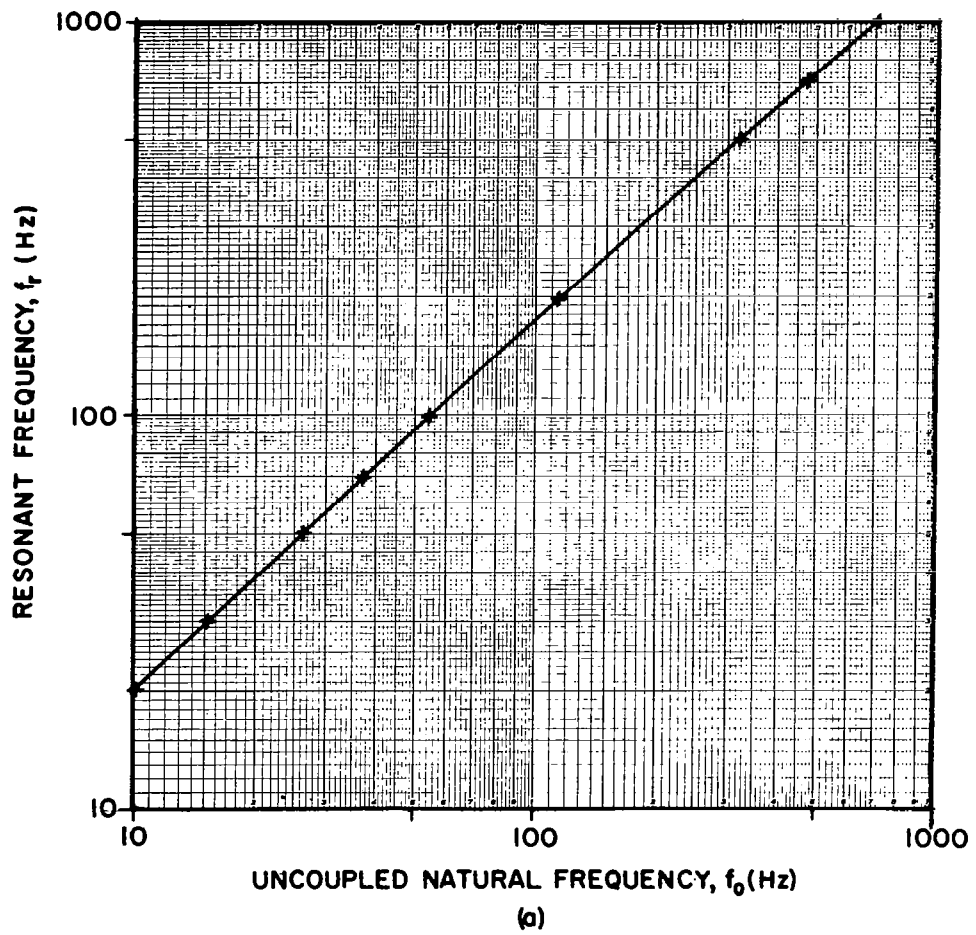


Figure 4.4 Theoretical prediction of (a) resonant frequency and (b) structure loss factor for the design example

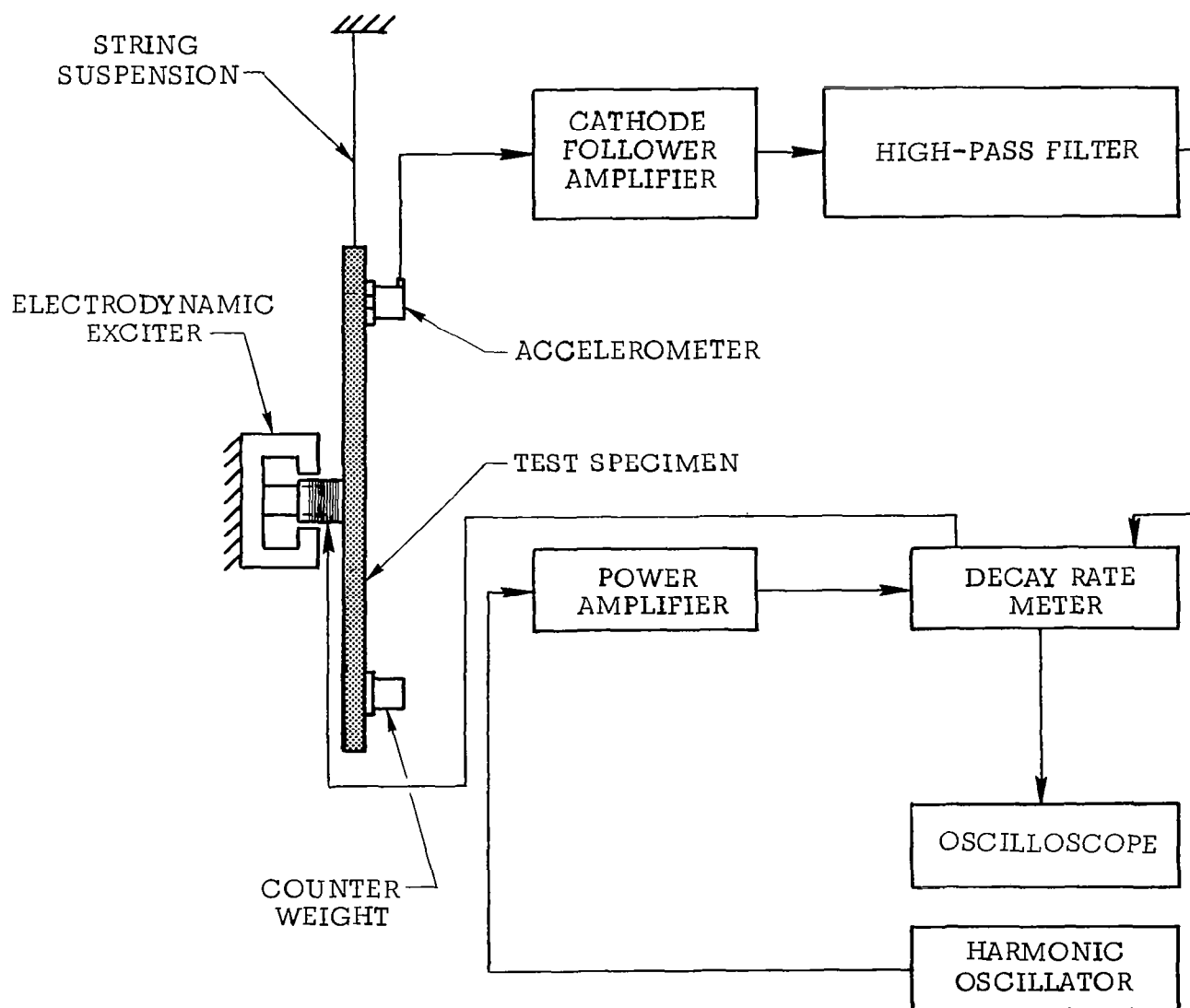


Figure 4.5 Experimental system for measuring the loss factor of viscoelastic shear-damped composite structural beam specimens

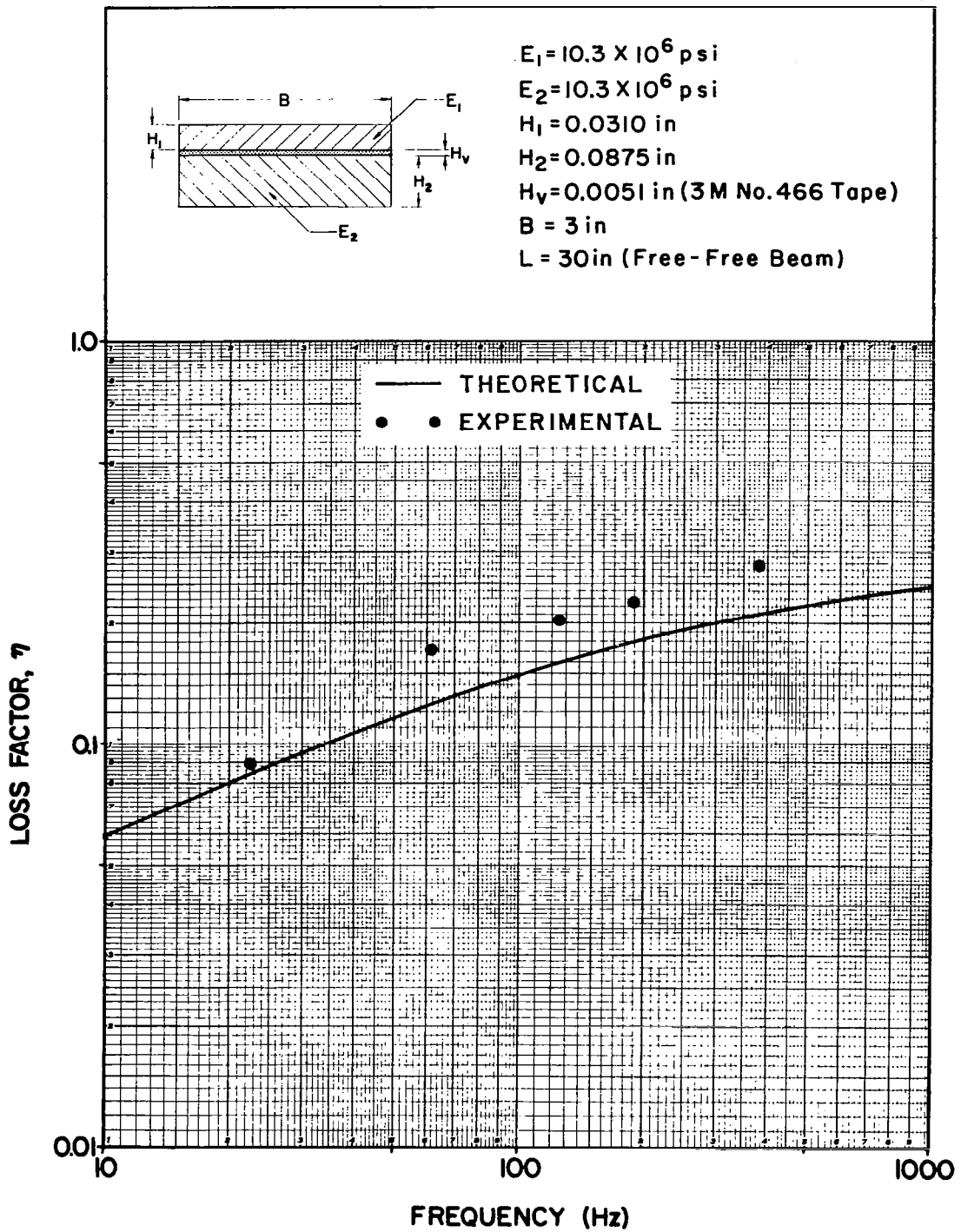


Figure 4.6(A) Theoretically predicted and experimentally determined values of structure loss factor for a viscoelastic shear-damped beam comprised of two solid aluminum sheets for which the geometrical parameter $Y = 1.62$

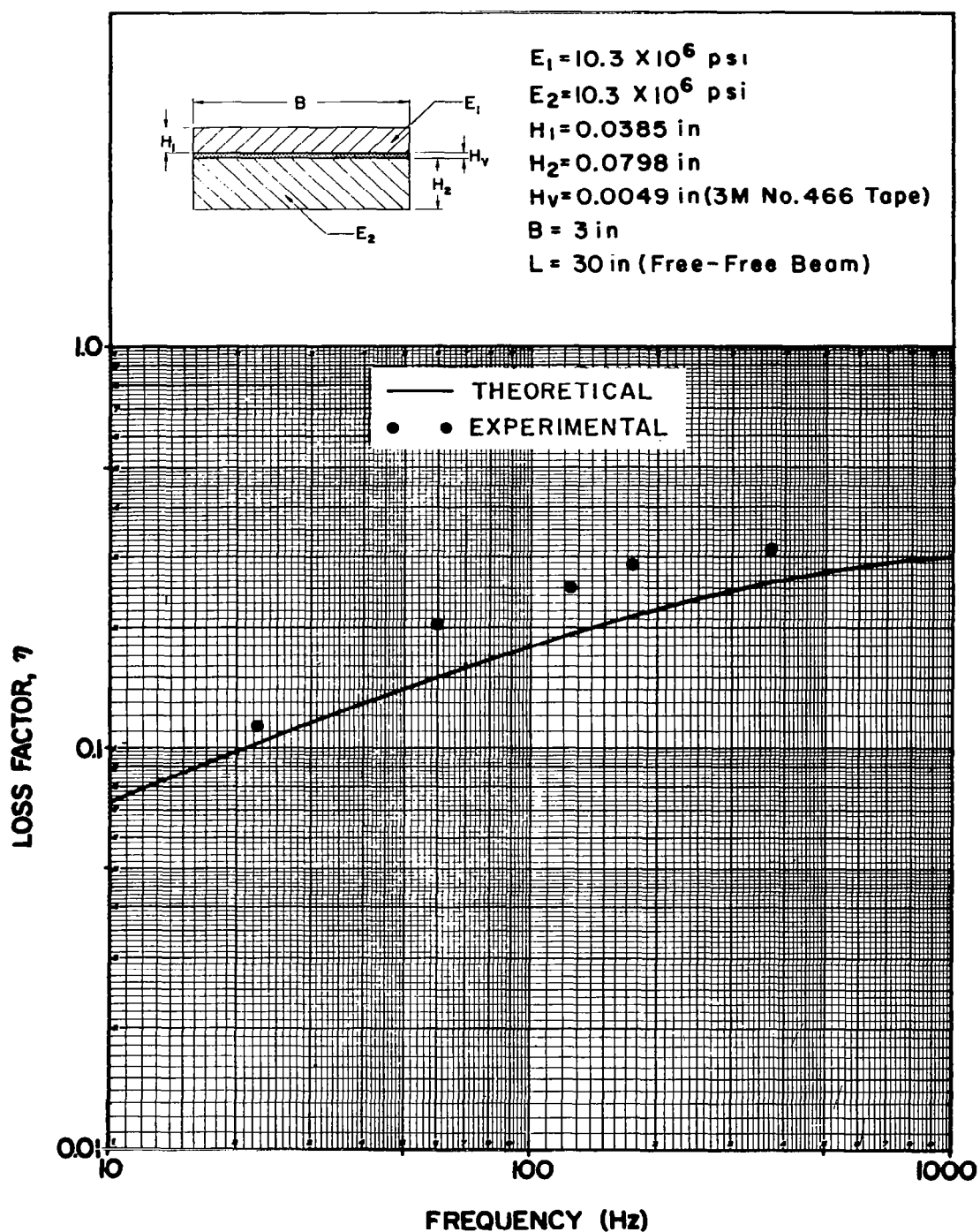


Figure 4.6(B) Theoretically predicted and experimentally determined values of structure loss factor for a viscoelastic shear-damped beam comprised of two solid aluminum sheets for which the geometrical parameter $Y = 2.26$

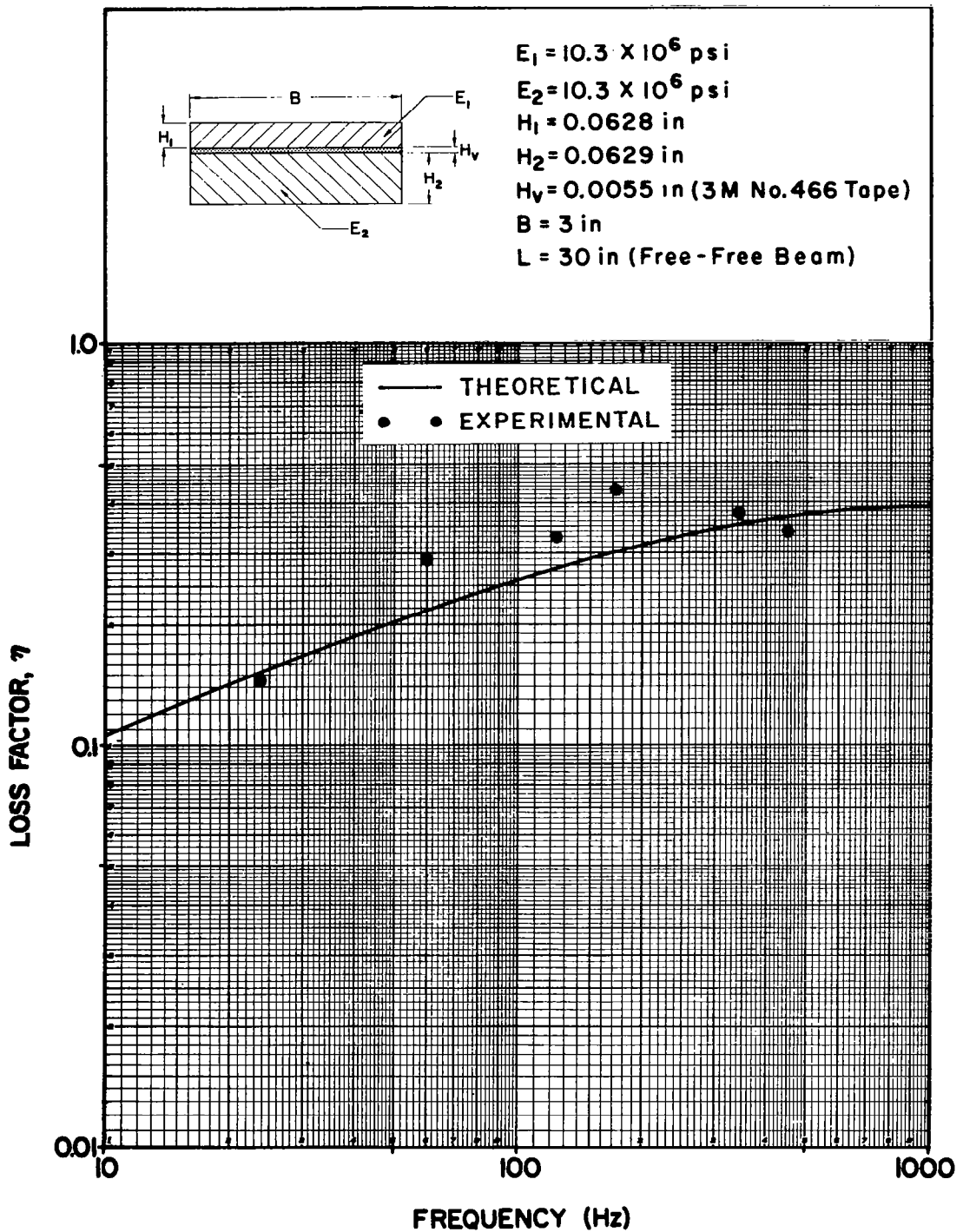


Figure 4.6(C) Theoretically predicted and experimentally determined values of structure loss factor for a viscoelastic shear-damped beam comprised of two solid aluminum sheets for which the geometrical parameter $Y = 3.55$

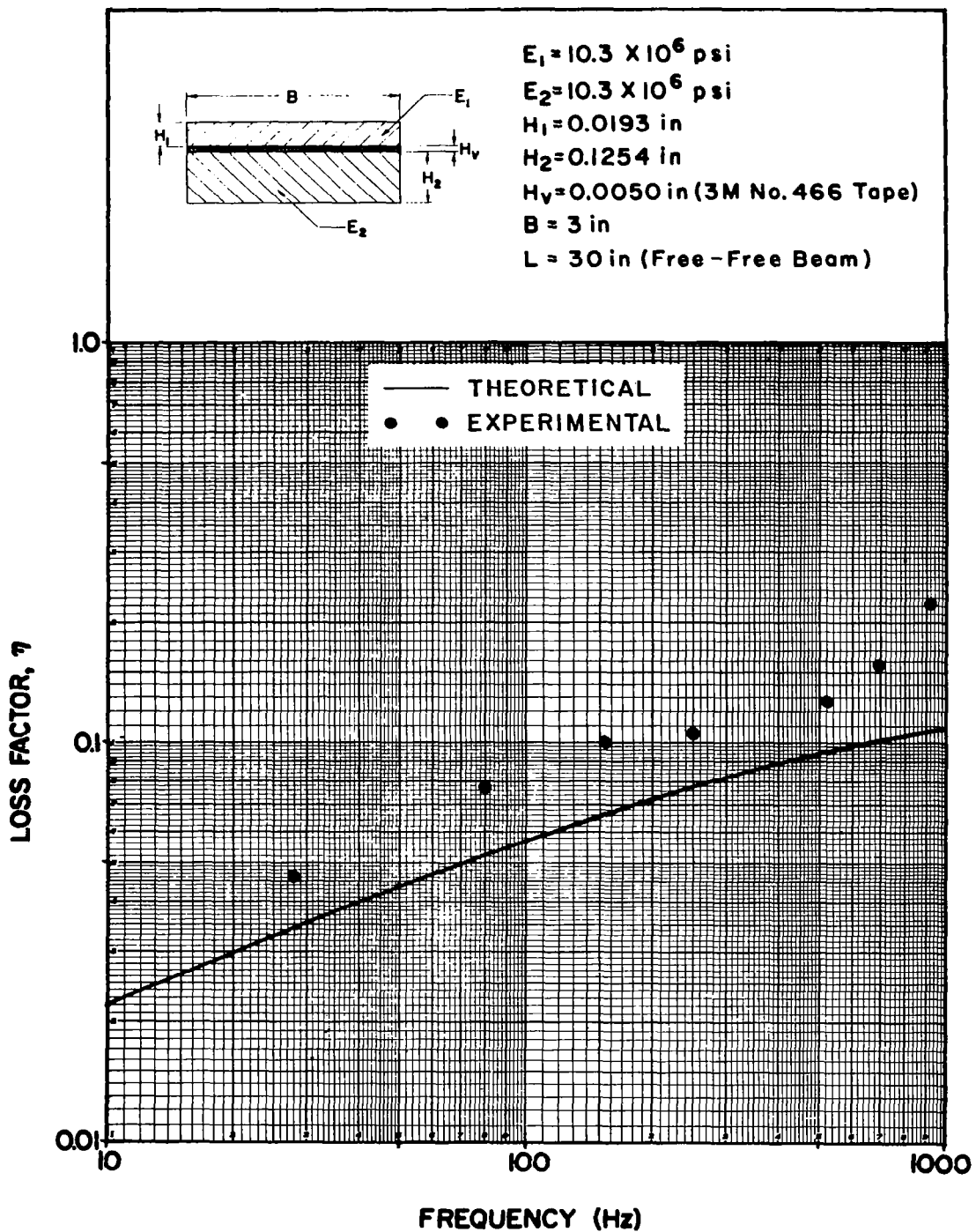


Figure 4.6(D) Theoretically predicted and experimentally determined values of structure loss factor for a viscoelastic shear-damped beam comprised of two solid aluminum sheets for which the geometrical parameter $Y = 0.61$

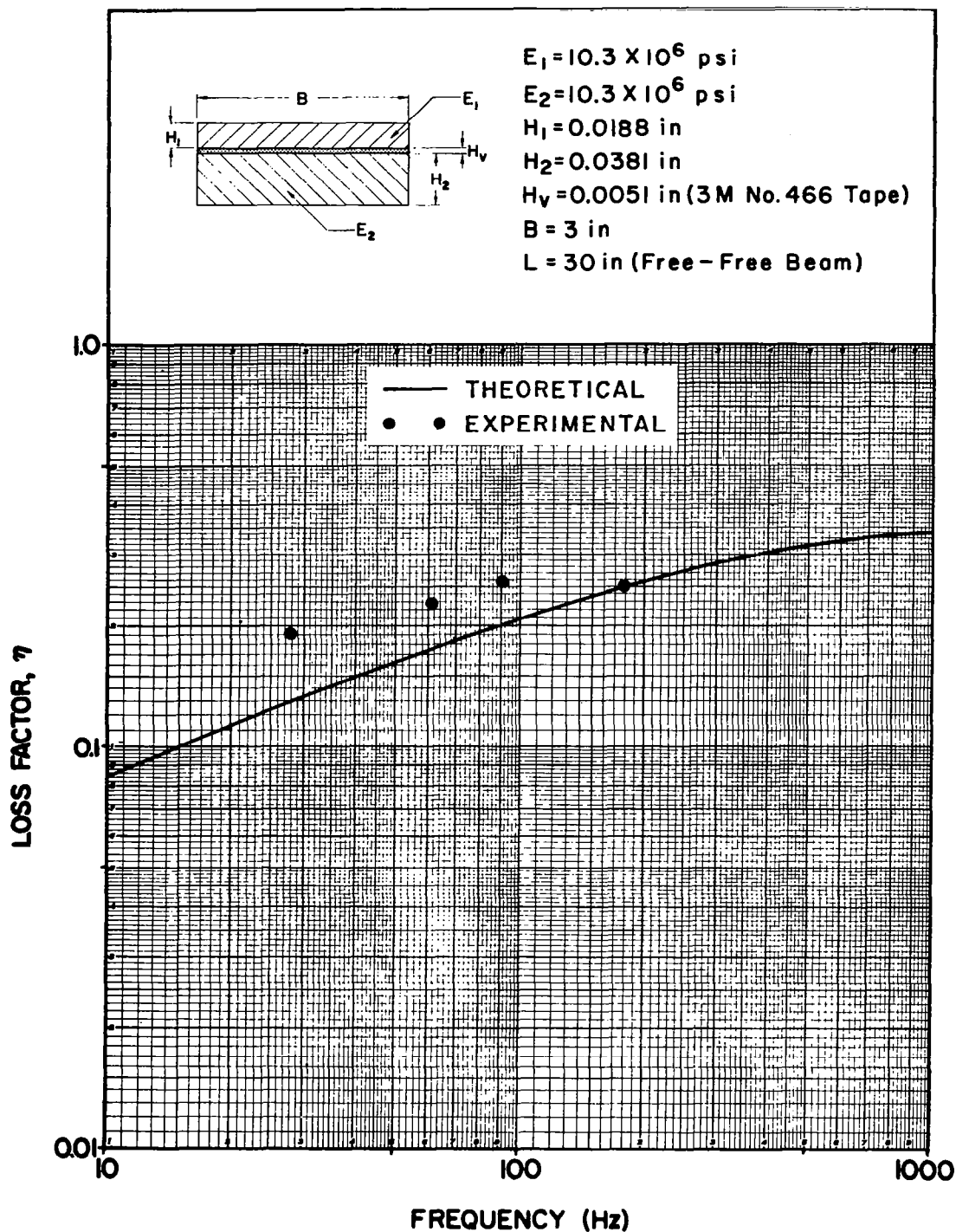


Figure 4.6(E) Theoretically predicted and experimentally determined values of structure loss factor for a viscoelastic shear-damped beam comprised of two solid aluminum sheets for which the geometrical parameter $Y = 2.83$

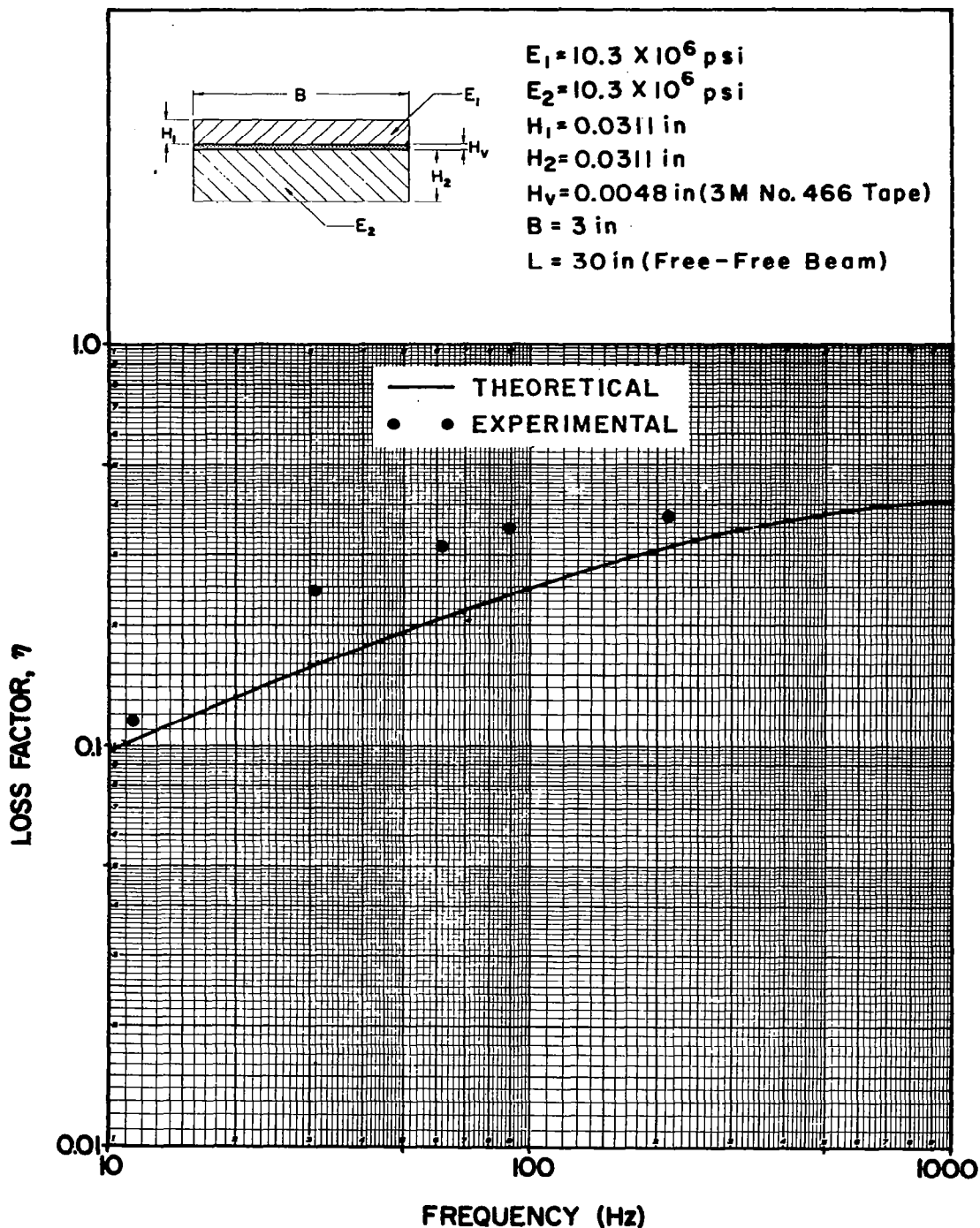


Figure 4.6(F) Theoretically predicted and experimentally determined values of structure loss factor for a viscoelastic shear-damped beam comprised of two solid aluminum sheets for which the geometrical parameter $Y = 4.00$

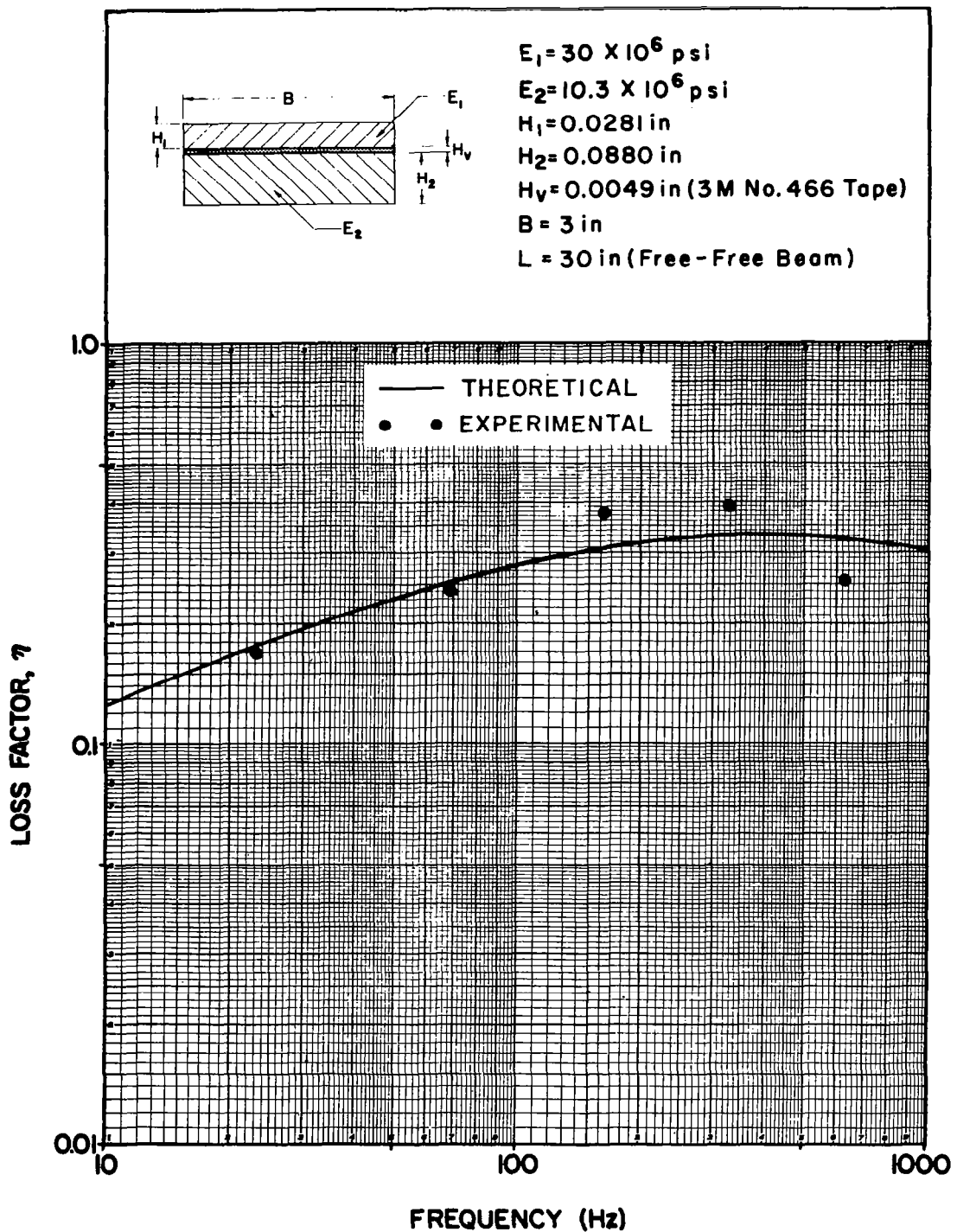


Figure 4.6(G) Theoretically predicted and experimentally determined values of structure loss factor for a viscoelastic shear-damped beam comprised of one steel and one aluminum solid sheet for which the geometrical parameter $Y = 2.69$

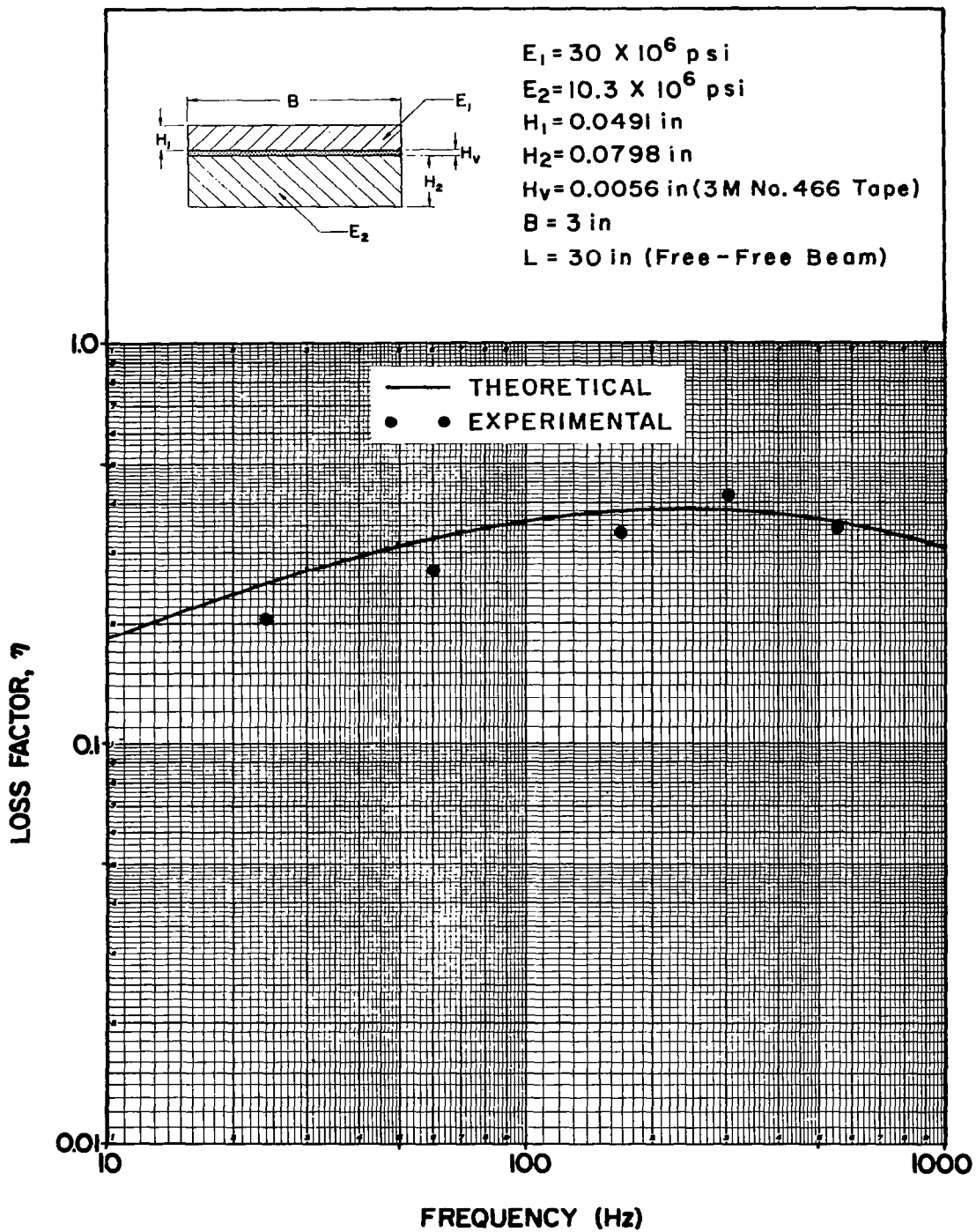


Figure 4.6(H) Theoretically predicted and experimentally determined values of structure loss factor for a viscoelastic shear-damped beam comprised of one steel and one aluminum solid sheet for which the geometrical parameter $\gamma = 3.54$

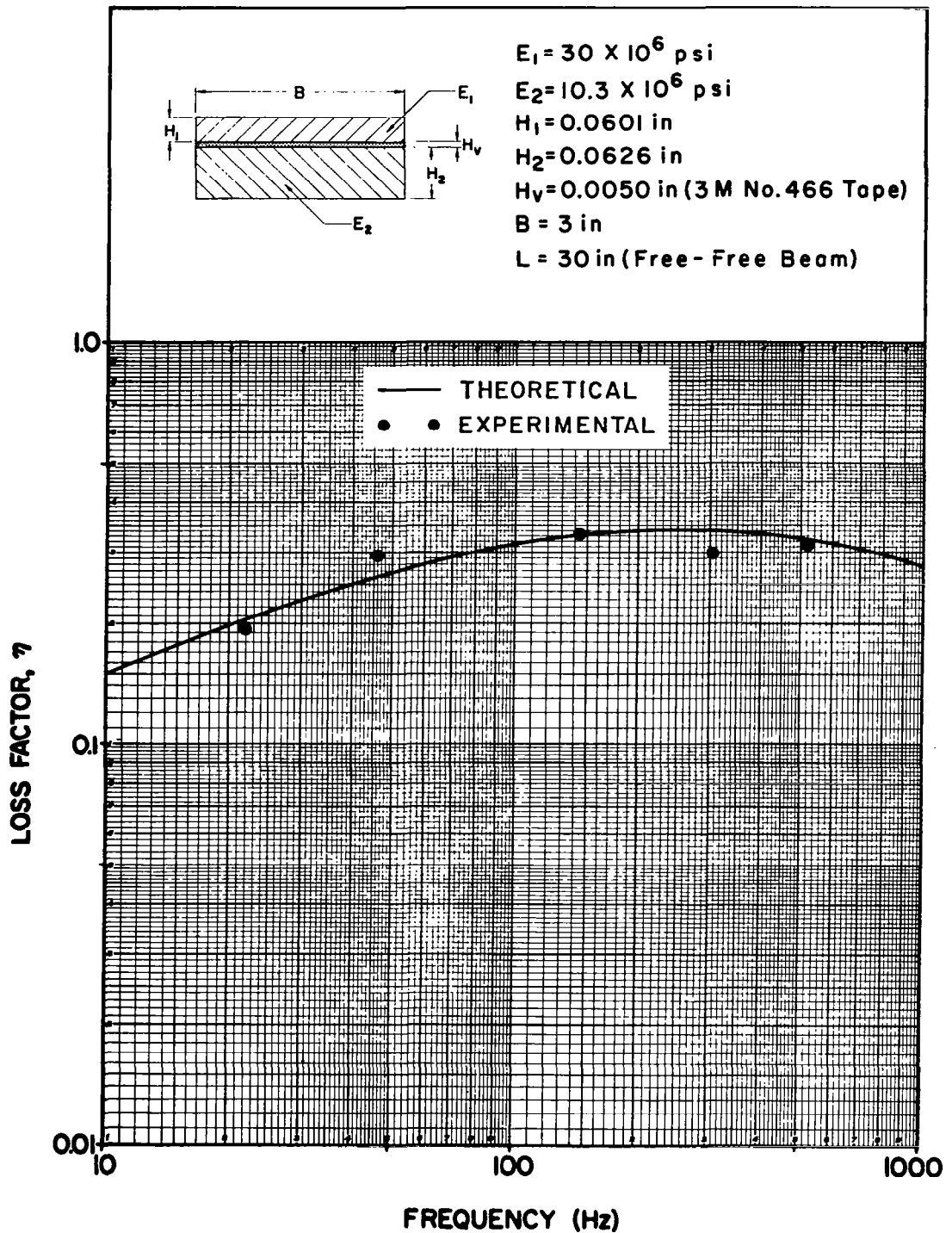


Figure 4.6(I) Theoretically predicted and experimentally determined values of structure loss factor for a viscoelastic shear-damped beam comprised of one steel and one aluminum solid sheet for which the geometrical parameter $\gamma = 2.83$

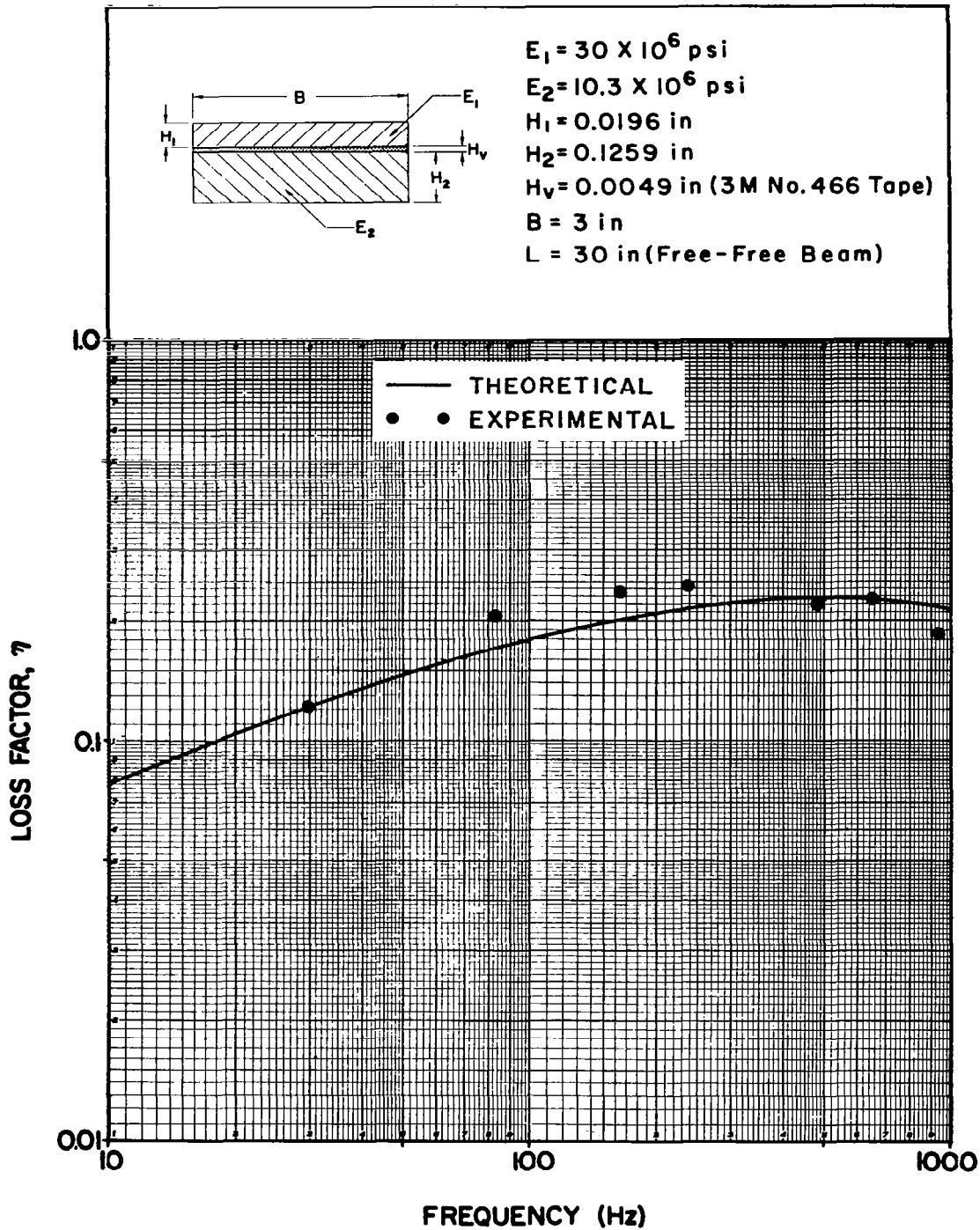


Figure 4.6(J) Theoretically predicted and experimentally determined values of structure loss factor for a viscoelastic shear-damped beam comprised of one steel and one aluminum solid sheet for which the geometrical parameter $Y = 1.41$

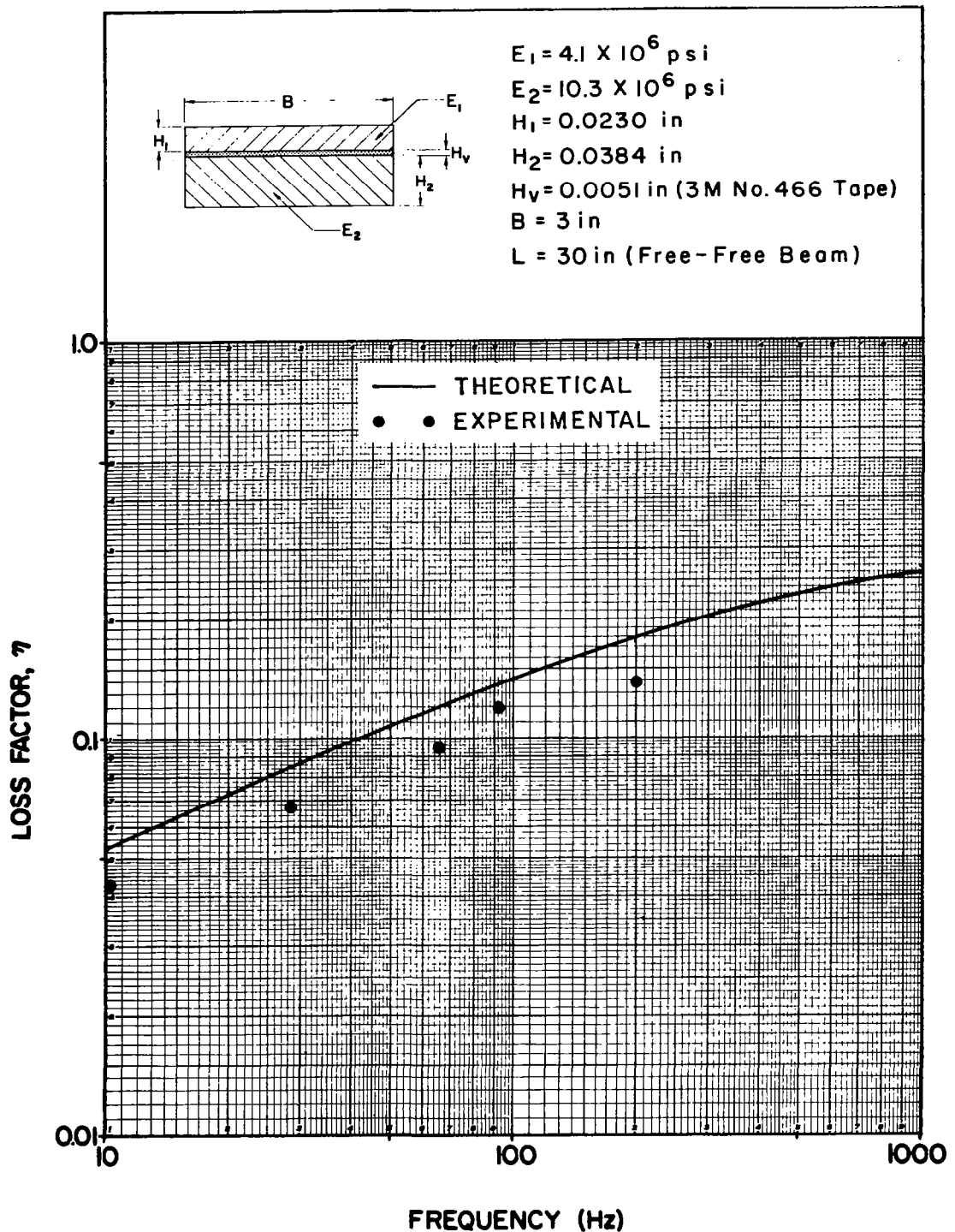


Figure 4.6(K) Theoretically predicted and experimentally determined values of structure loss factor for a viscoelastic shear-damped beam comprised of one fibre-glass and one aluminum solid sheet for which the geometrical parameter $\gamma = 1.84$

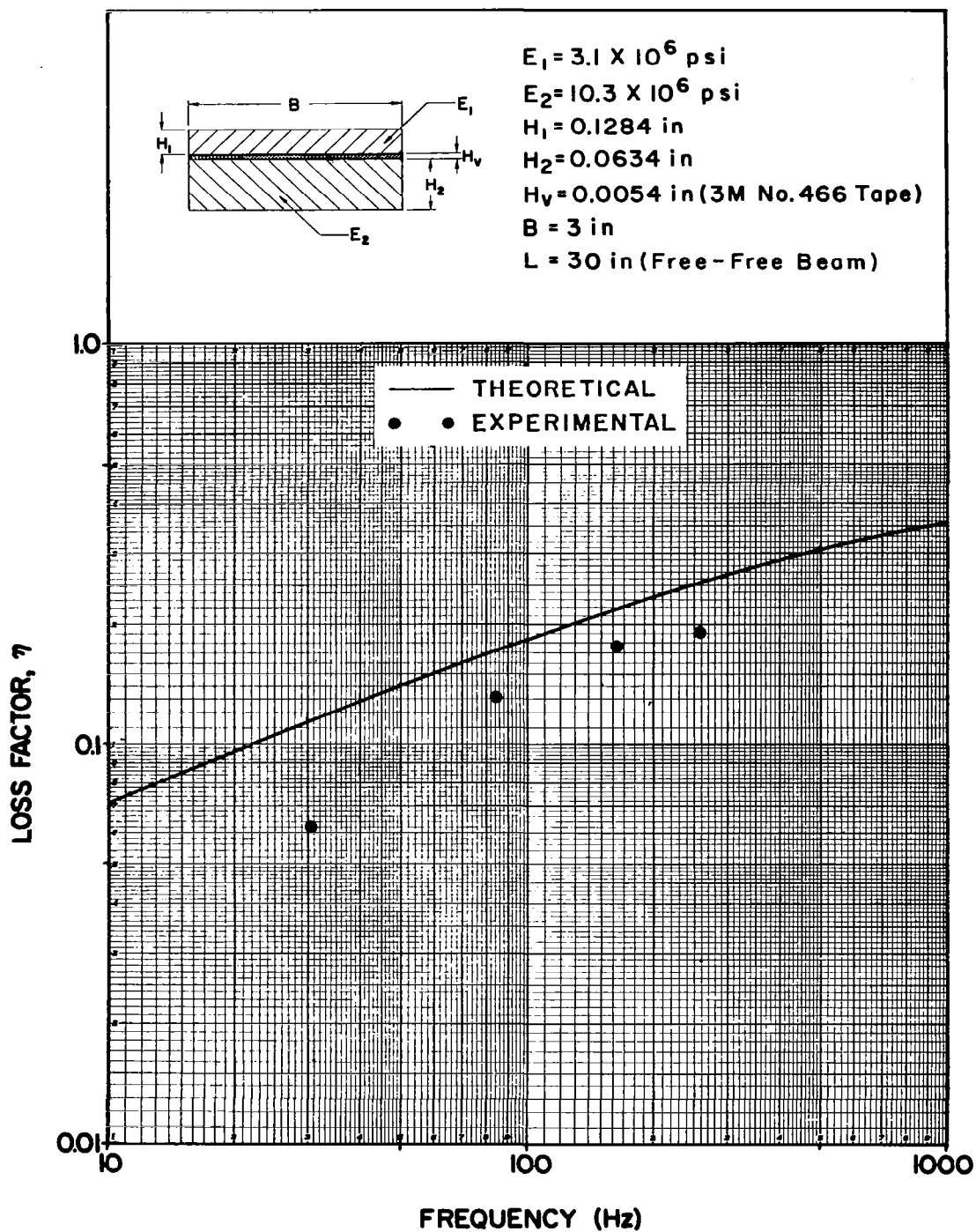


Figure 4.6(L) Theoretically predicted and experimentally determined values of structure loss factor for a viscoelastic shear-damped beam comprised of one fibre-glass and one aluminum solid sheet for which the geometrical parameter $Y = 3.31$

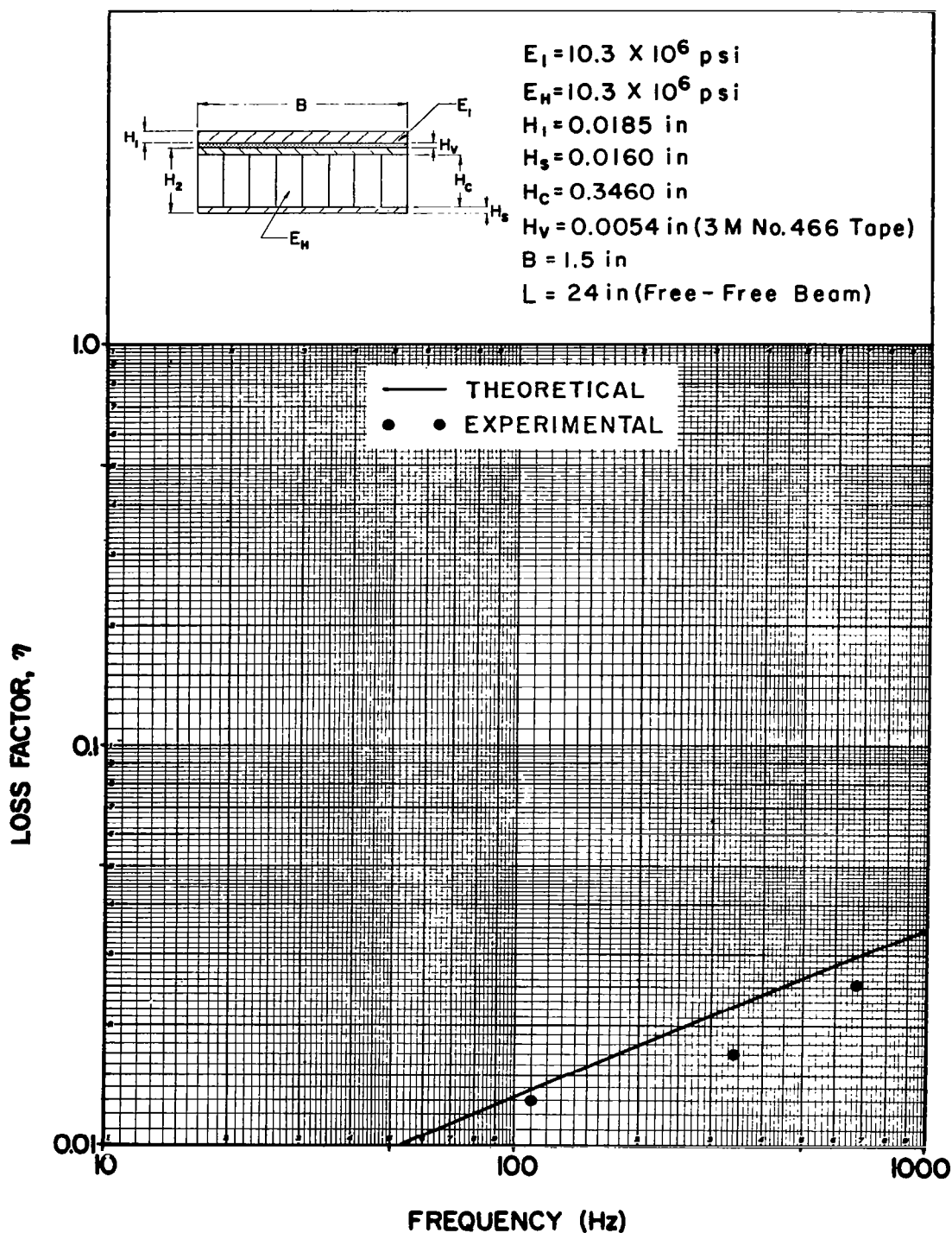


Figure 4.7(A) Theoretically predicted and experimentally determined values of structure loss factor for a viscoelastic shear-damped beam comprised of one solid and one honeycomb aluminum sheet for which the geometrical parameter $Y = 0.46$

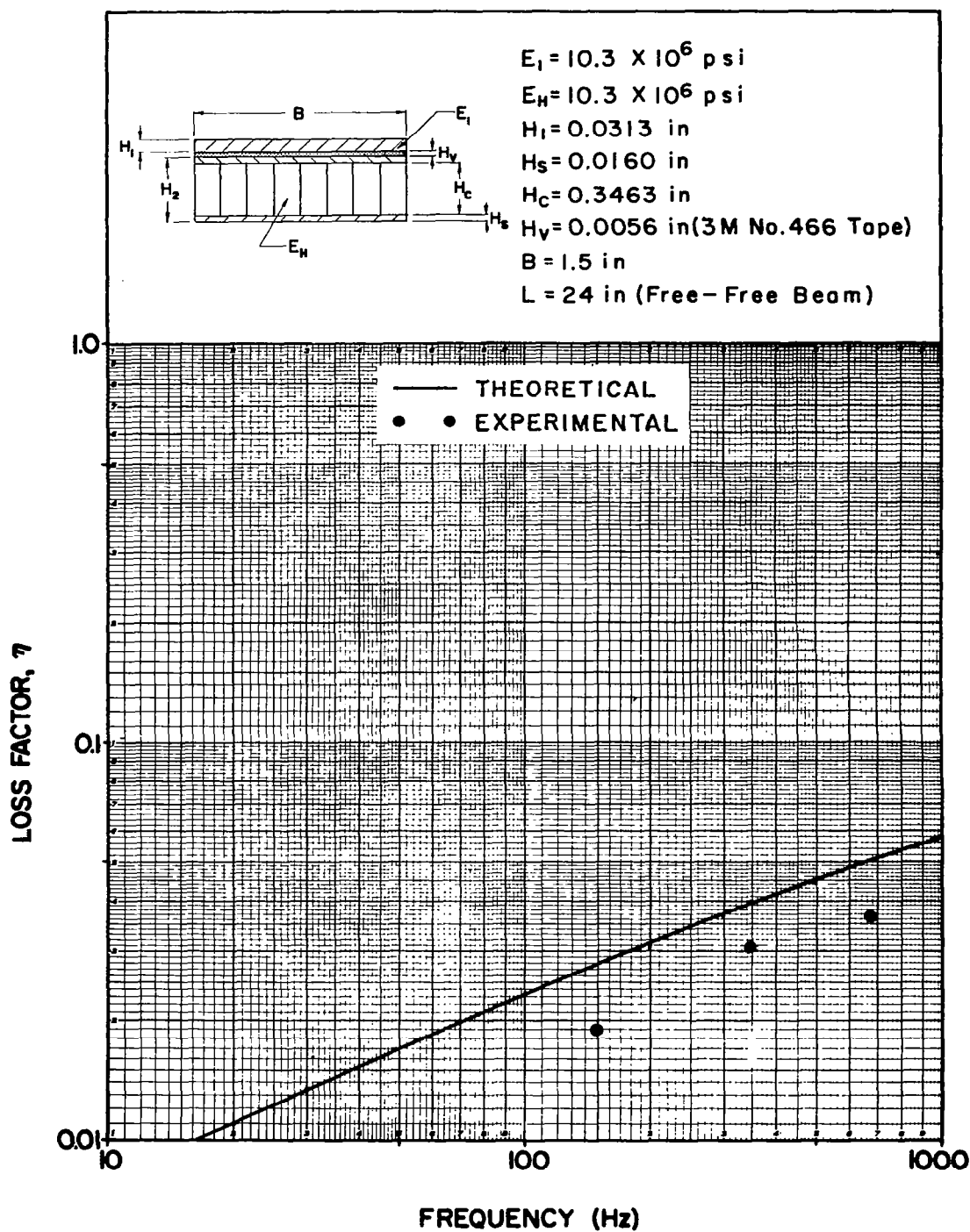


Figure 4.7(B) Theoretically predicted and experimentally determined values of structure loss factor for a viscoelastic shear-damped beam comprised of one solid and one honeycomb aluminum sheet for which the geometrical parameter $Y = 0.68$

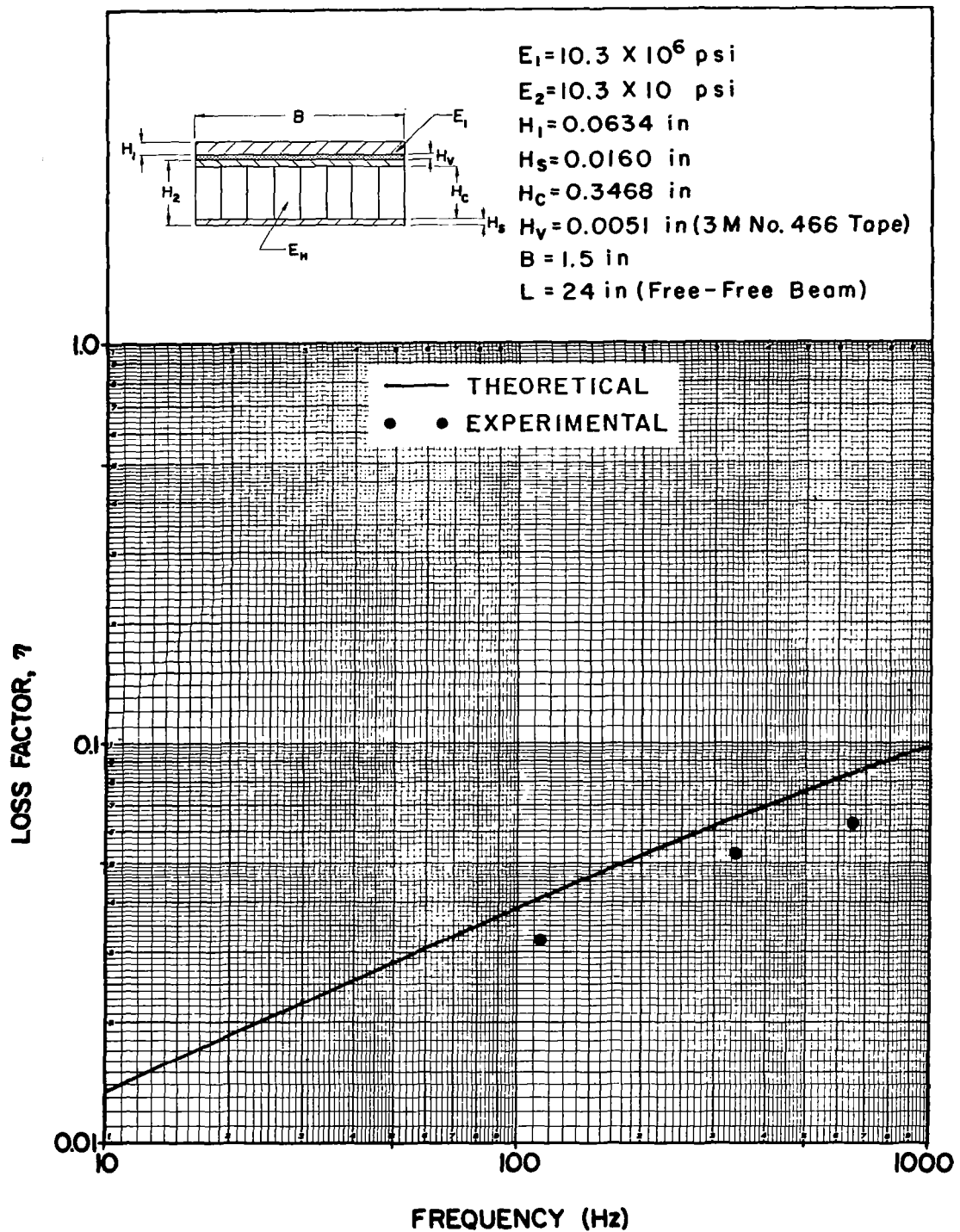


Figure 4.7(C) Theoretically predicted and experimentally determined values of structure loss factor for a viscoelastic shear-damped beam comprised of one solid and one honeycomb aluminum sheet for which the geometrical parameter $Y = 0.99$

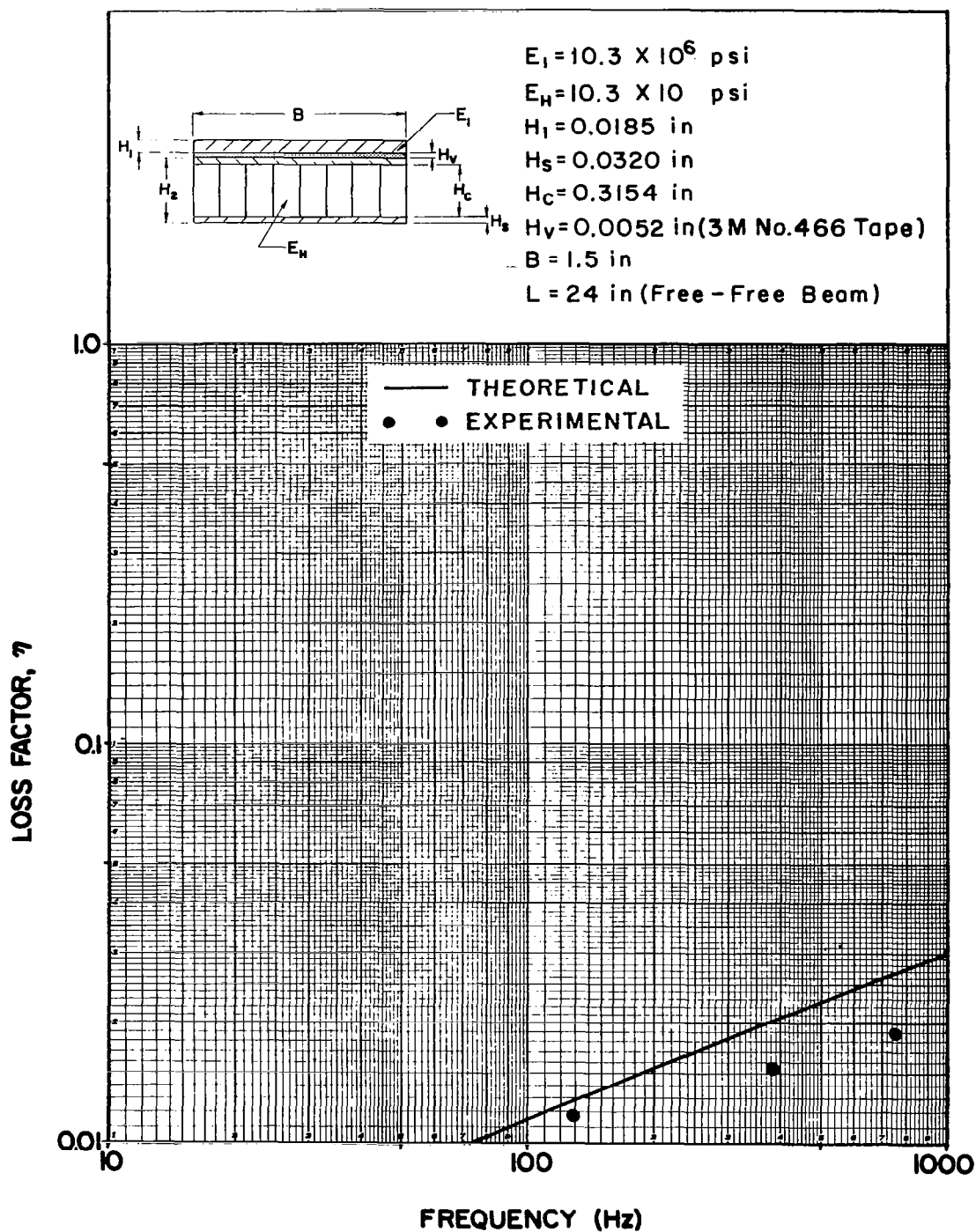


Figure 4.7(D) Theoretically predicted and experimentally determined values of structure loss factor for a viscoelastic shear-damped beam comprised of one solid and one honeycomb aluminum sheet for which the geometrical parameter $Y = 0.32$

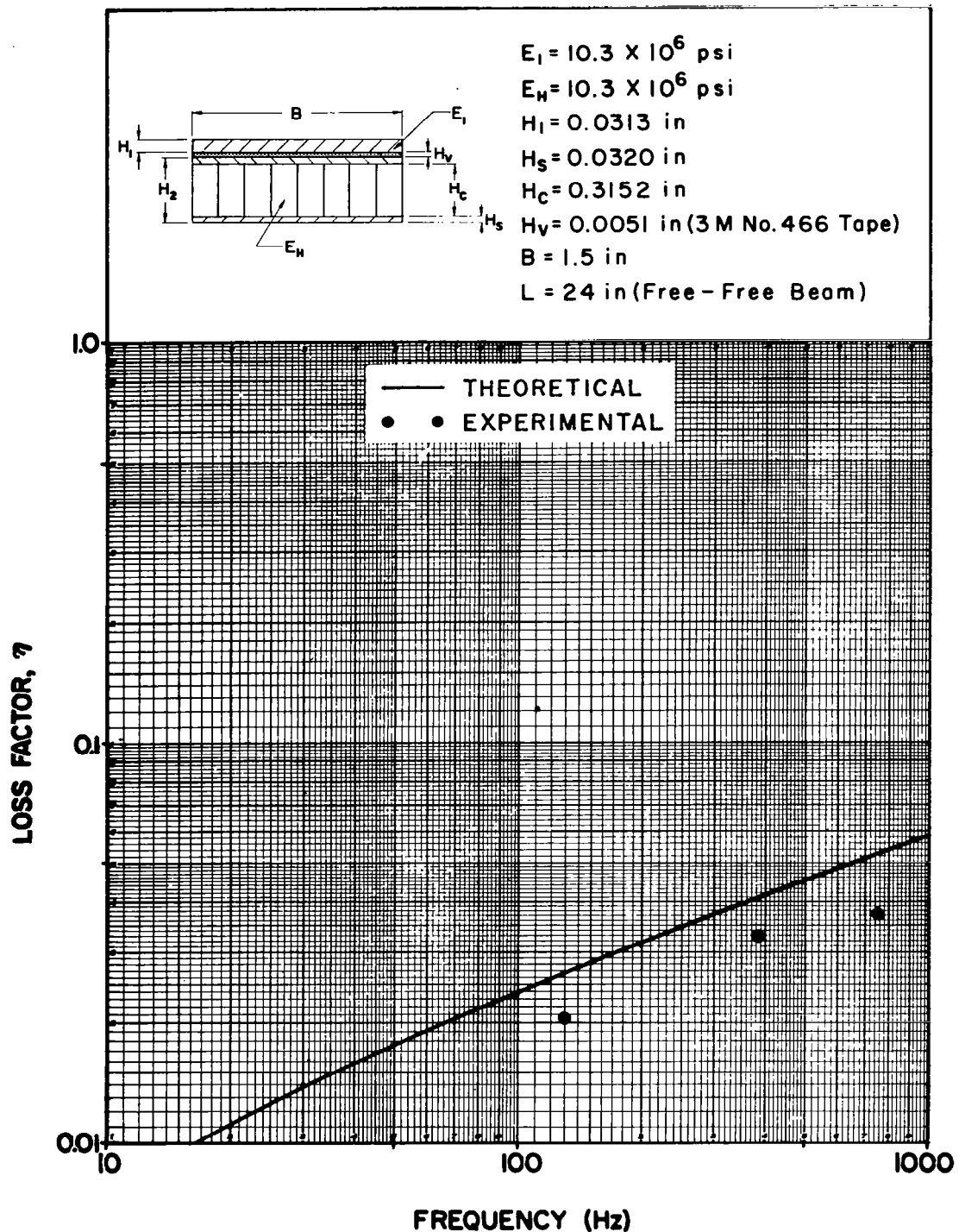


Figure 4.7(E) Theoretically predicted and experimentally determined values of structure loss factor for a viscoelastic shear-damped beam comprised of one solid and one honeycomb aluminum sheet for which the geometrical parameter $Y = 0.48$

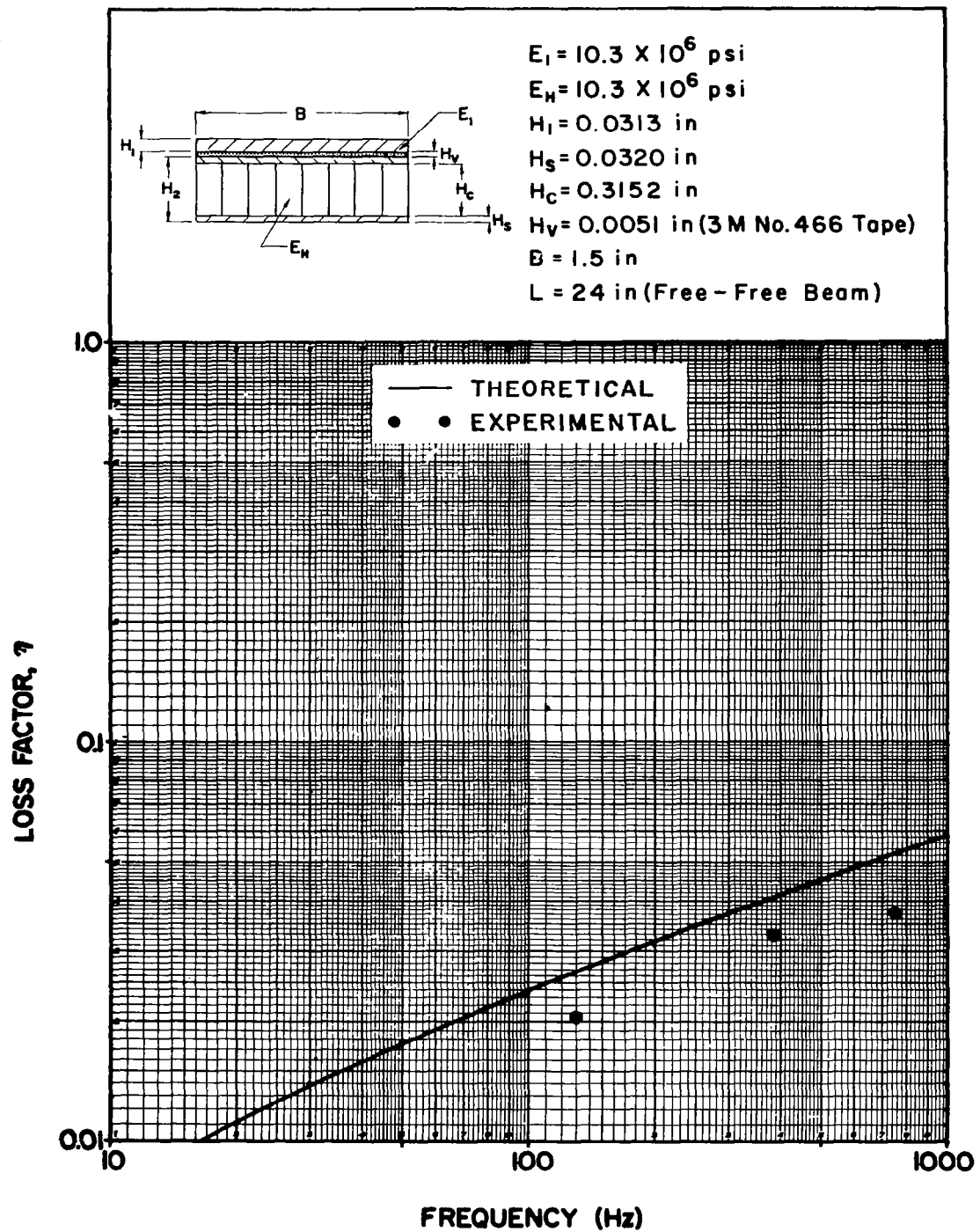


Figure 4.7(F) Theoretically predicted and experimentally determined values of structure loss factor for a viscoelastic shear-damped beam comprised of one solid and one honeycomb aluminum sheet for which the geometrical parameter $Y = 0.84$

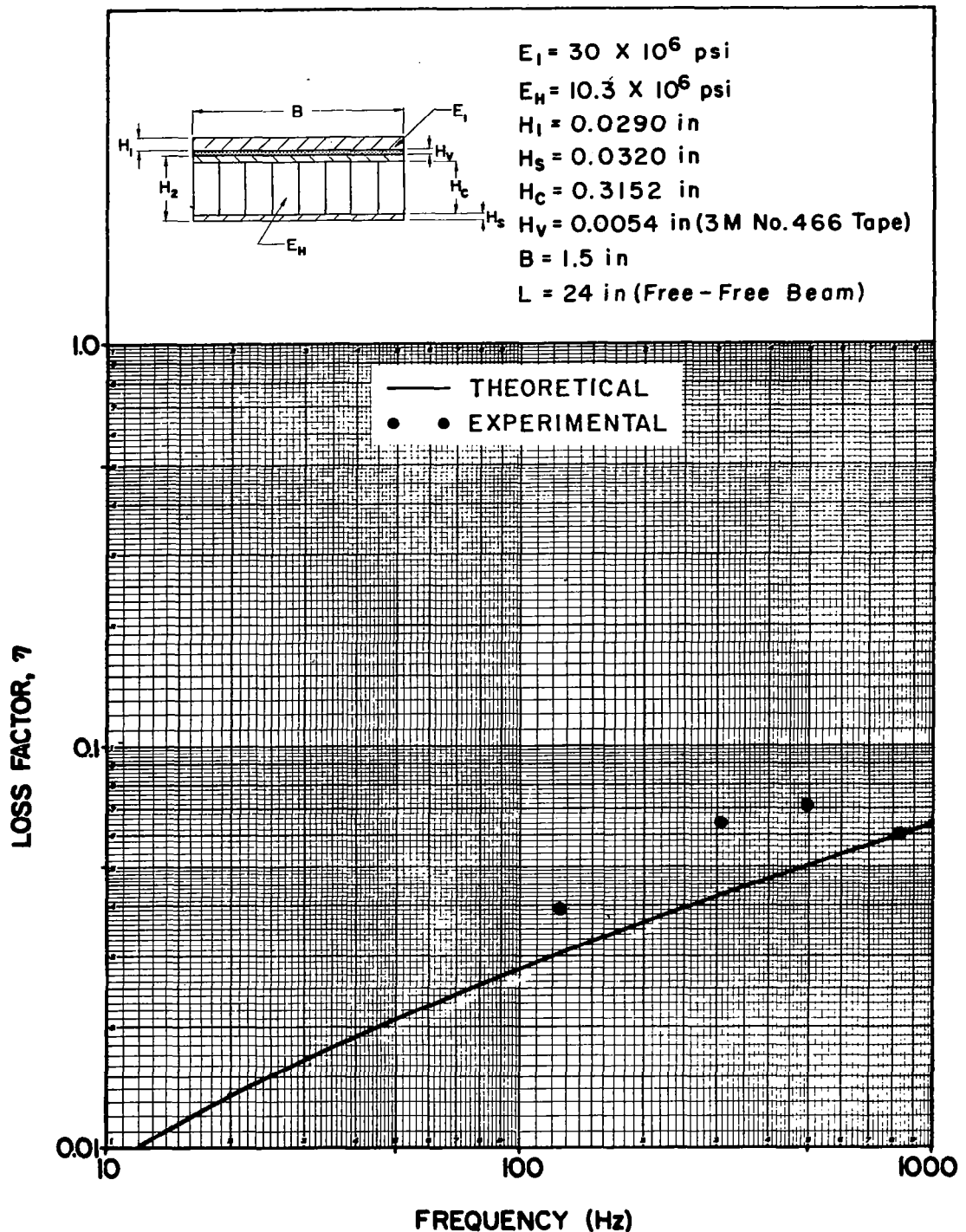


Figure 4.7(G) Theoretically predicted and experimentally determined values of structure loss factor for a viscoelastic shear-damped beam comprised of one solid steel and one aluminum honeycomb sheet for which the geometrical parameter $Y = 0.45$

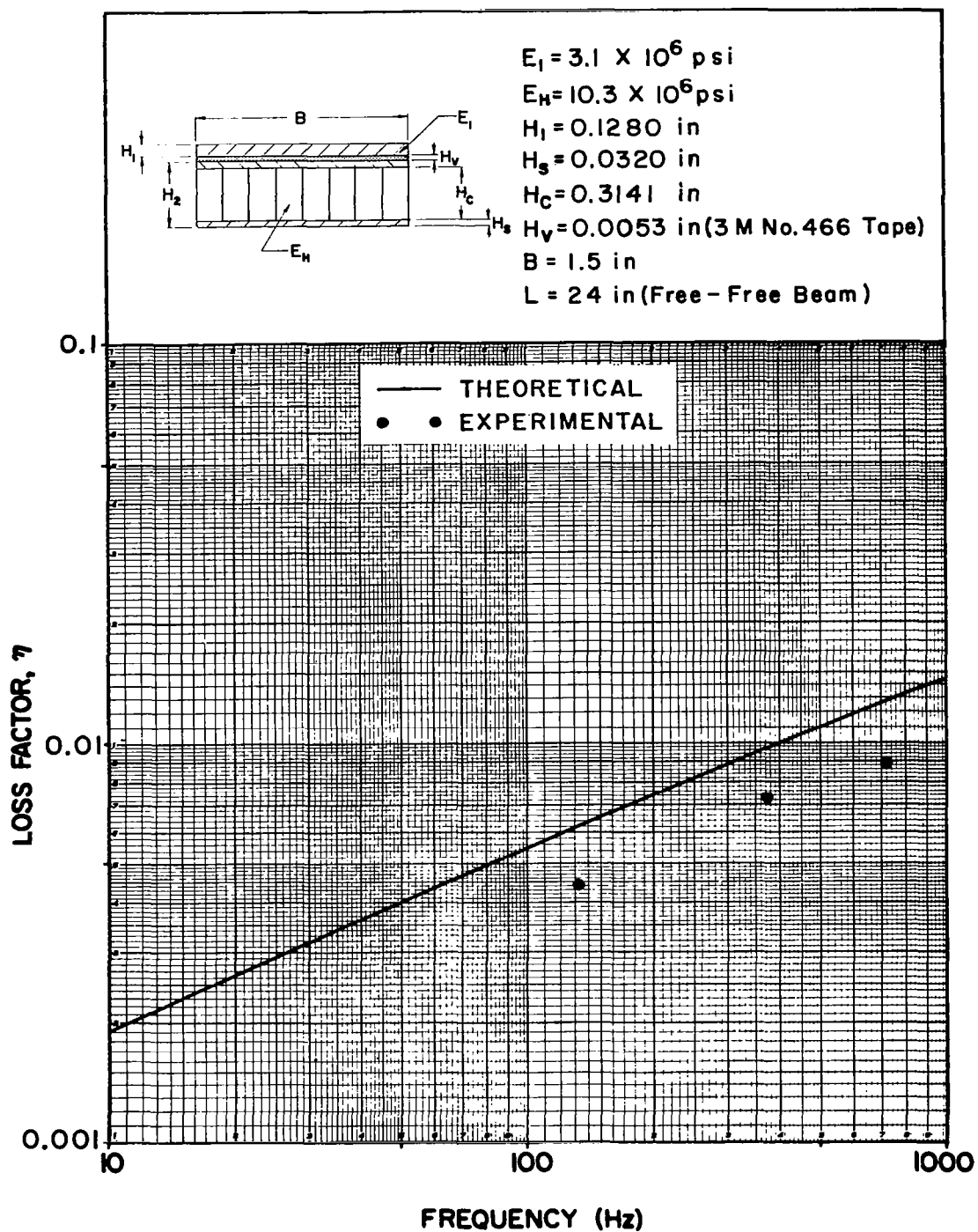


Figure 4.7(H) Theoretically predicted and experimentally determined values of structure loss factor for a viscoelastic shear-damped beam comprised of one solid fibre-glass and one aluminum honeycomb sheet for which the geometrical parameter $Y = 0.27$

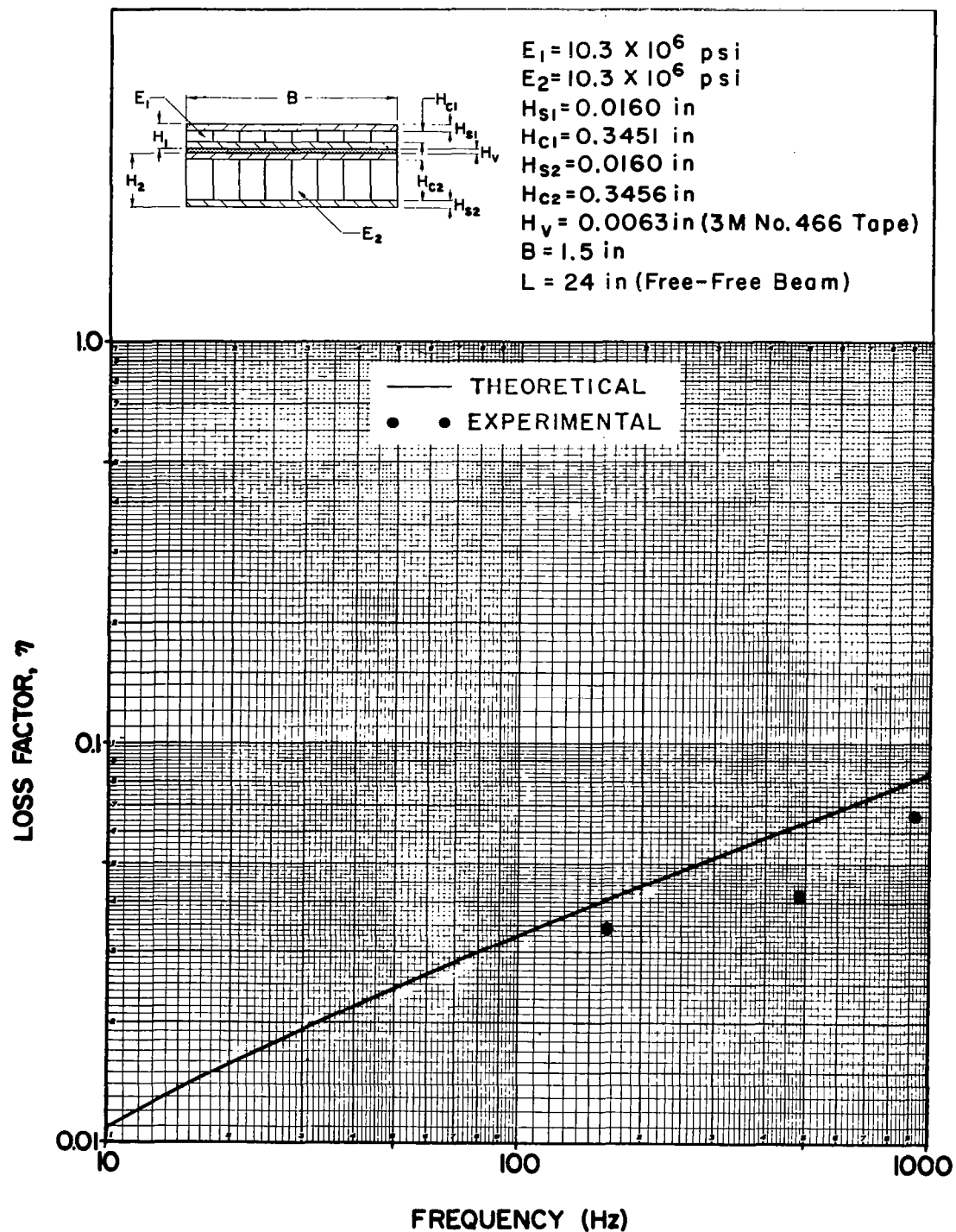


Figure 4.8(A) Theoretically predicted and experimentally determined values of structure loss factor for a viscoelastic shear-damped beam comprised of two aluminum honeycomb sheets for which the geometrical parameter $\gamma = 1.14$

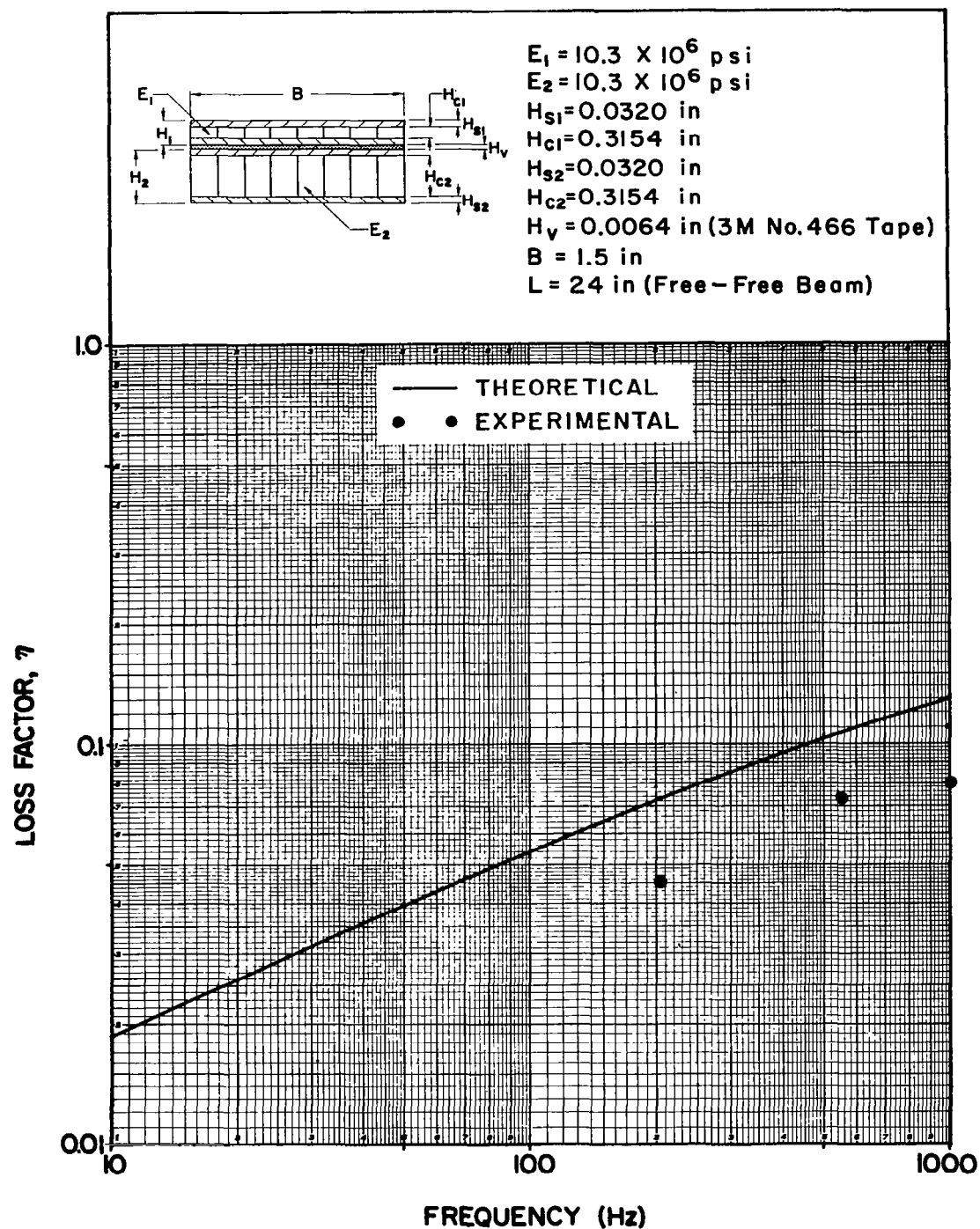


Figure 4.8(B) Theoretically predicted and experimentally determined values of structure loss factor for a viscoelastic shear-damped beam comprised of two aluminum honeycomb sheets for which the geometrical parameter $Y = 1.24$

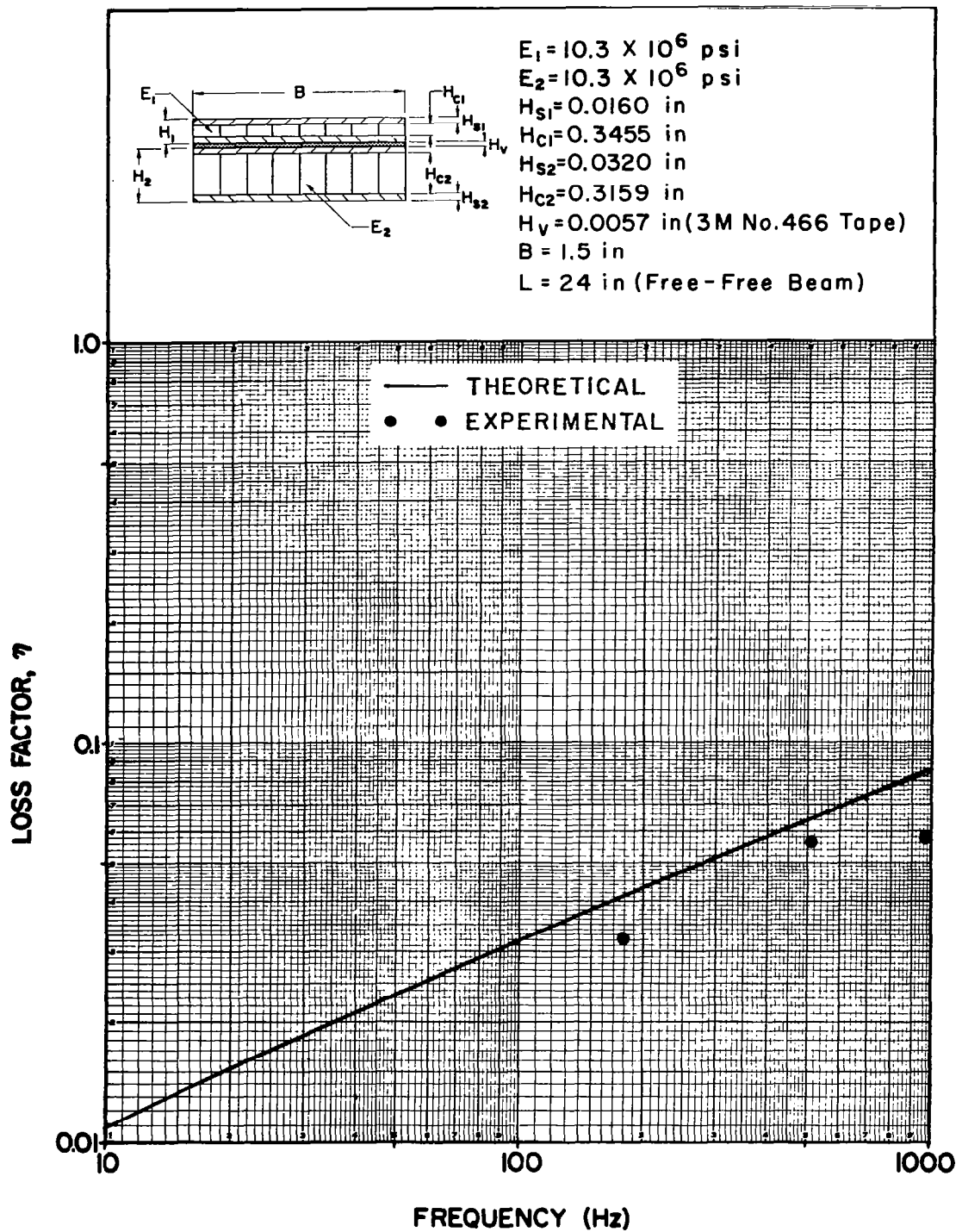


Figure 4.8(C) Theoretically predicted and experimentally determined values of structure loss factor for a viscoelastic shear-damped beam comprised of two aluminum honeycomb sheets for which the geometrical parameter $Y = 1.05$

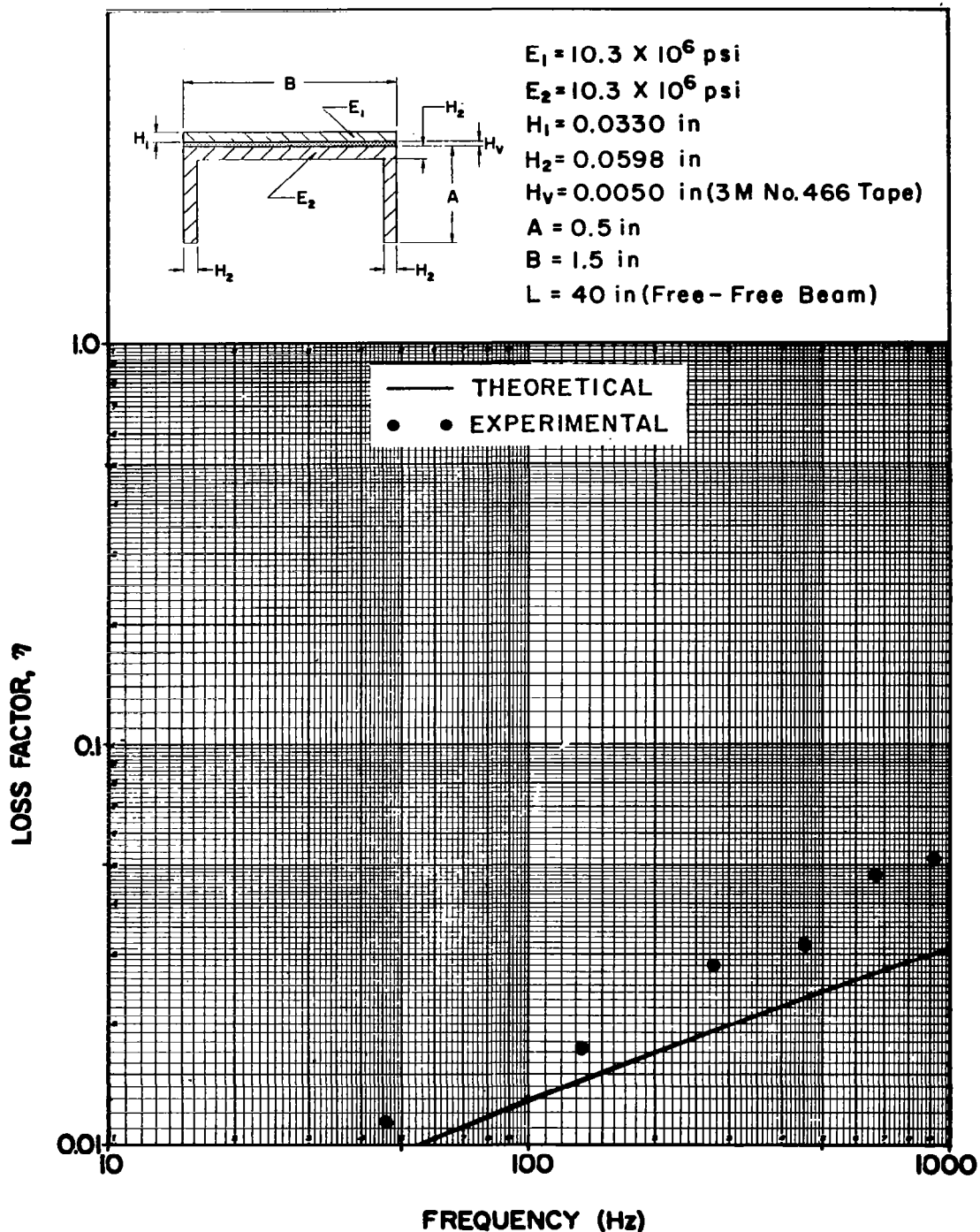


Figure 4.9(A) Theoretically predicted and experimentally determined values of structure loss factor for a viscoelastic shear-damped beam comprised of a solid aluminum sheet and an aluminum channel section for which the geometrical parameter $Y = 0.26$

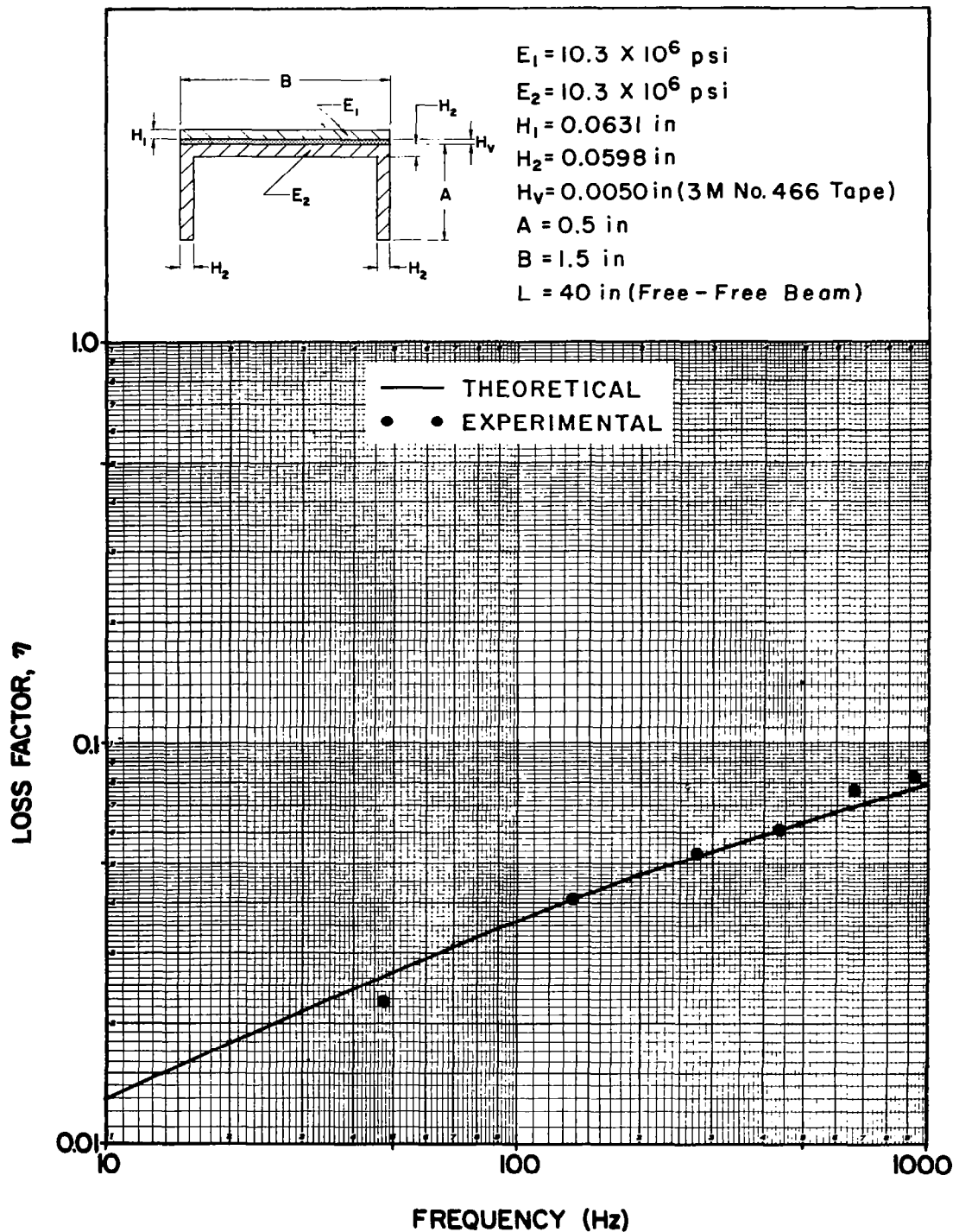


Figure 4.9(B) Theoretically predicted and experimentally determined values of structure loss factor for a viscoelastic shear-damped beam comprised of a solid aluminum sheet and an aluminum channel section for which the geometrical parameter $Y = 0.47$

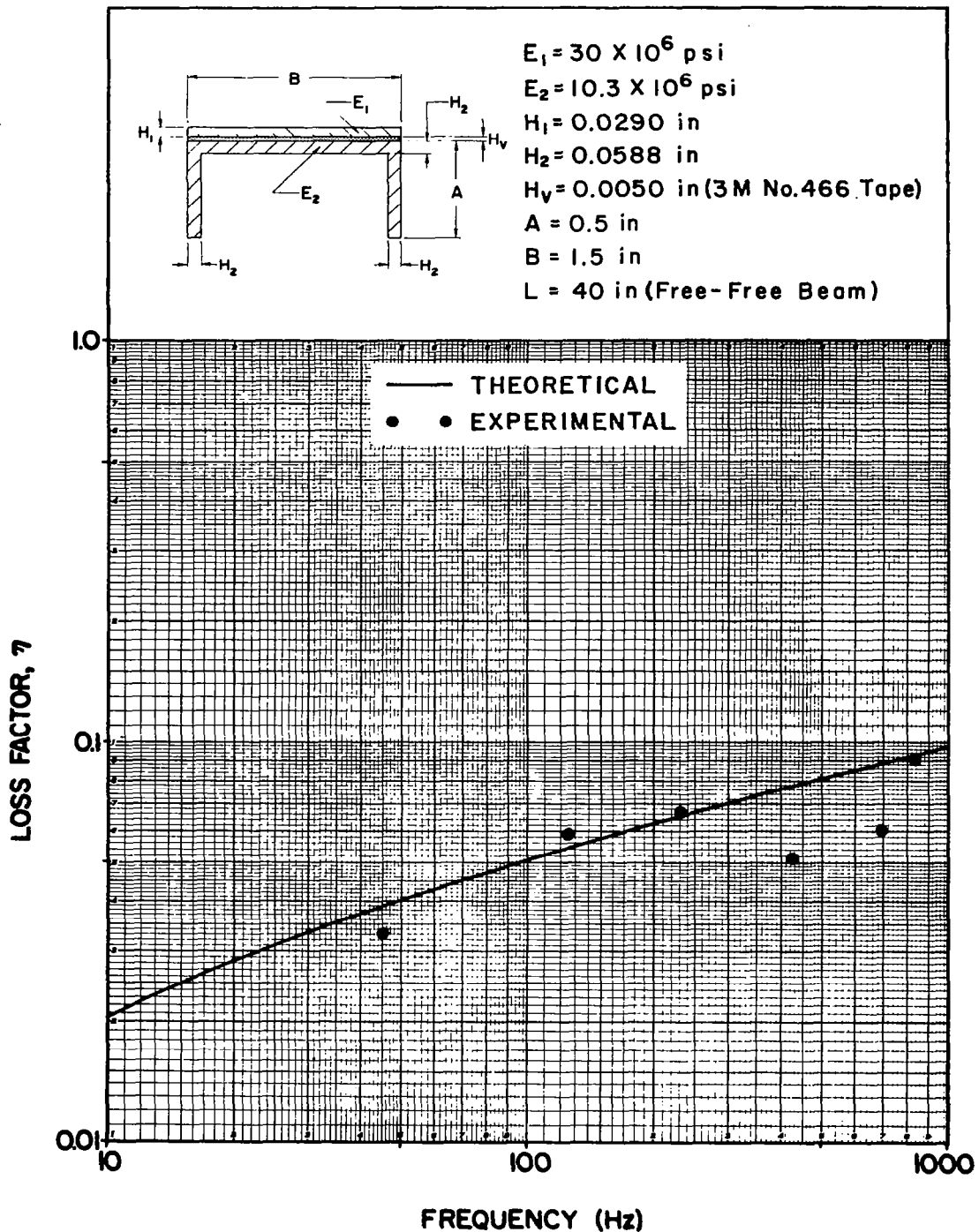


Figure 4.9(C) Theoretically predicted and experimentally determined values of structure loss factor for a viscoelastic shear-damped beam comprised of a solid steel sheet and an aluminum channel section for which the geometrical parameter $Y = 0.49$

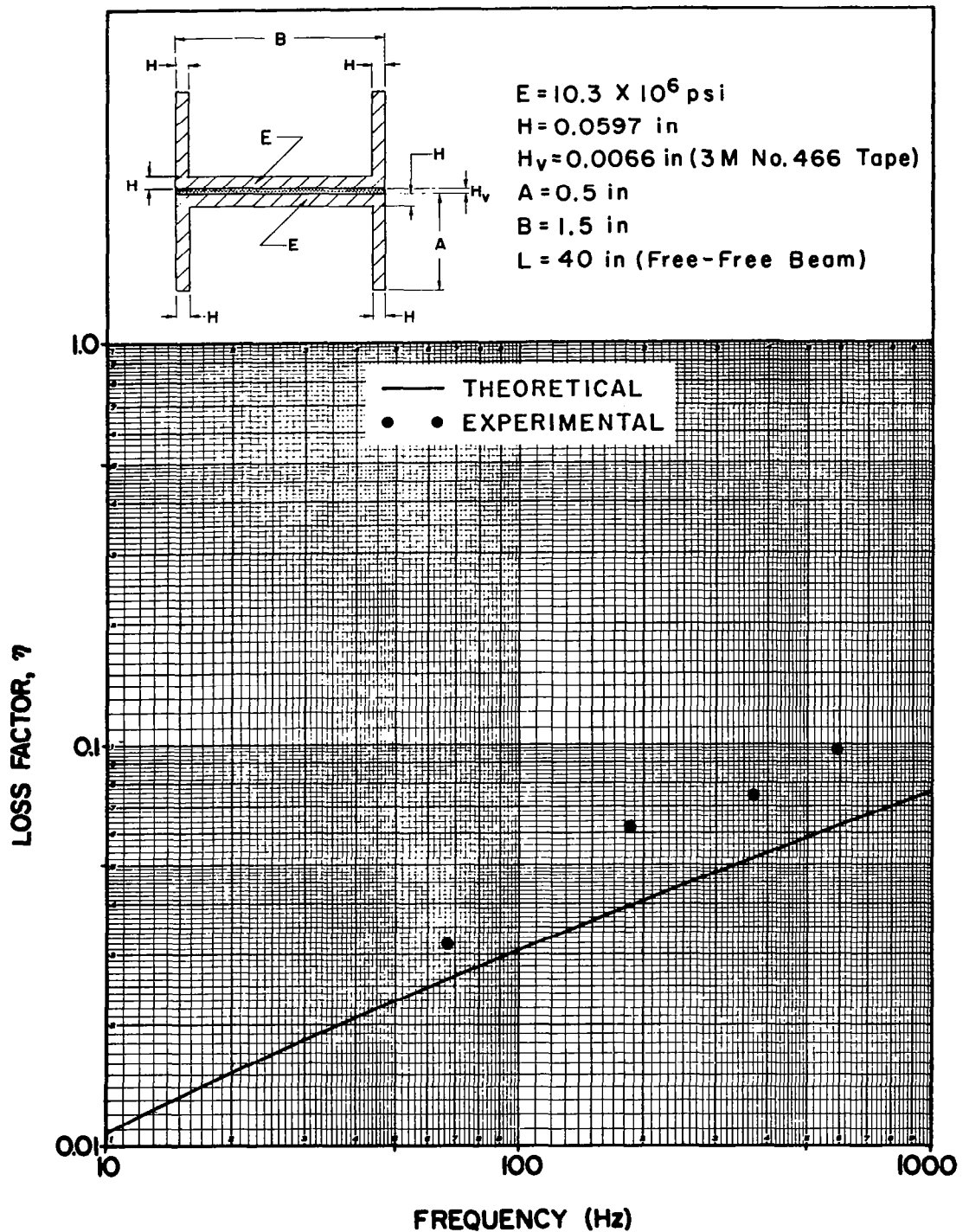


Figure 4.10 Theoretically predicted and experimentally determined values of structure loss factor for a viscoelastic shear-damped beam comprised of two back-to-back aluminum channel sections for which the geometrical parameter $Y = 0.76$

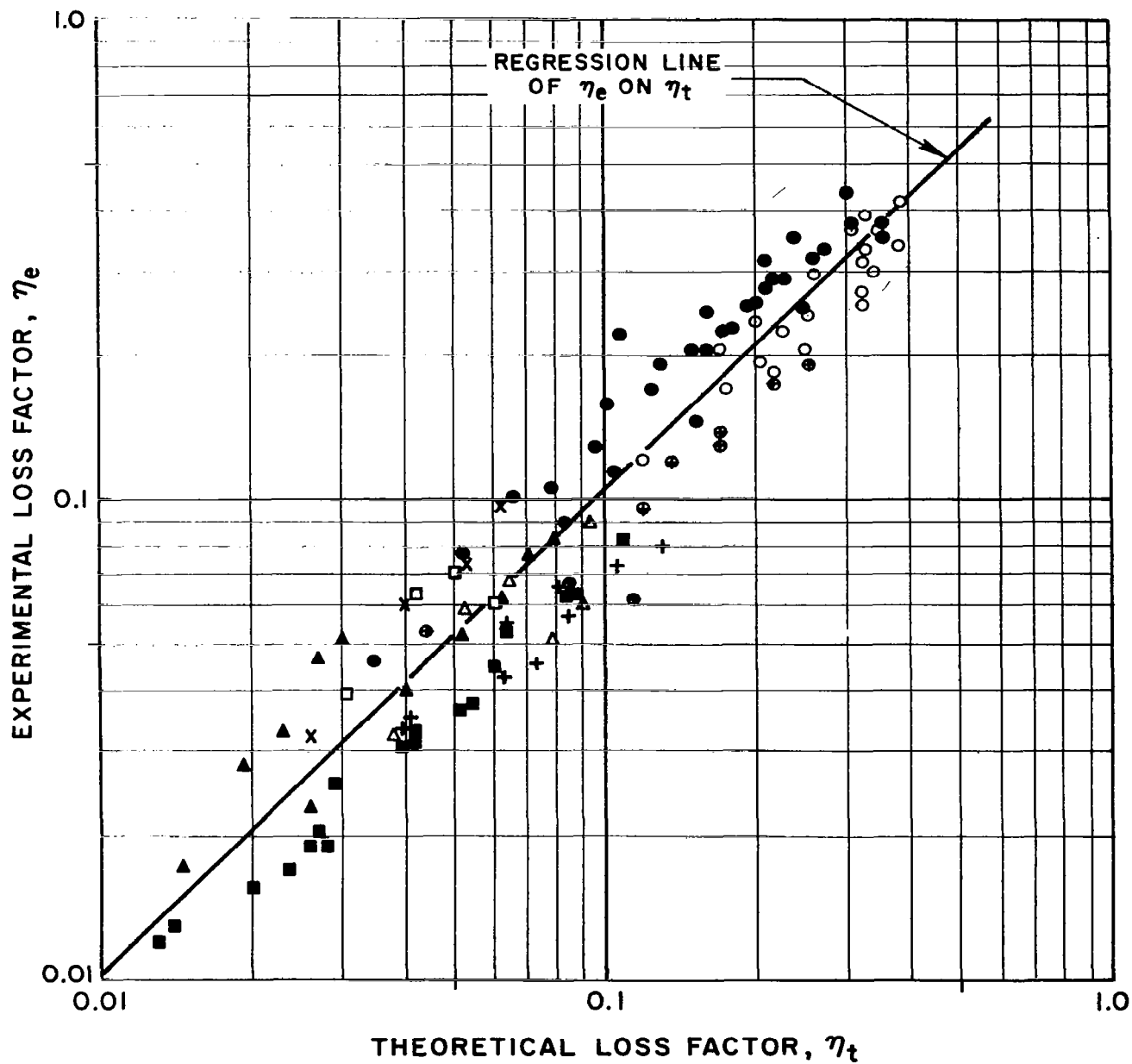


Figure 4.11 Comparison of the experimental and theoretical values of loss factor for the composite structural beam specimens

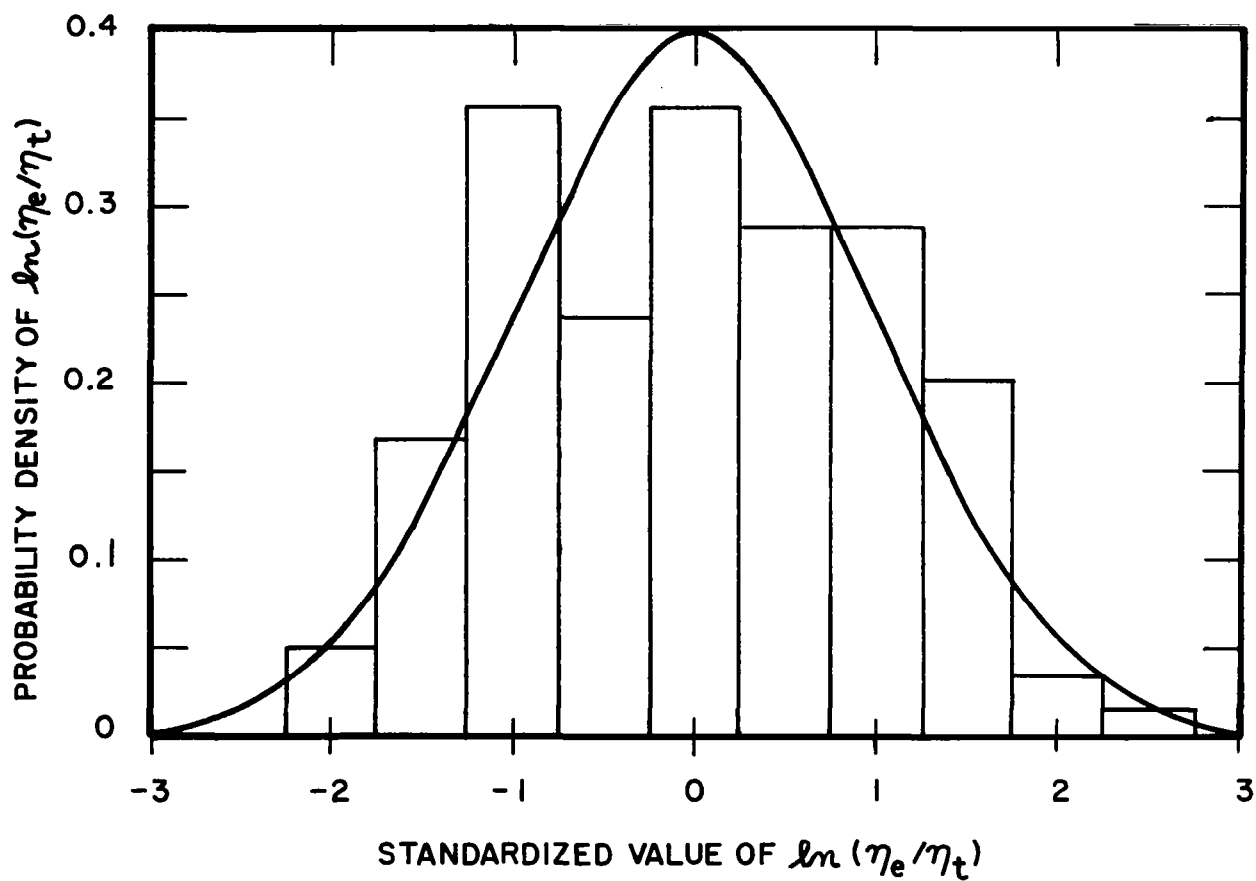


Figure 4.12 Comparison of the standardized probability density of $\ln(\eta_e/\eta_t)$, shown as vertical bars, with that of a normal distribution, shown as the continuous curve